

TRANSPORTATION RESEARCH RECORD 916

Engineering Fabrics in Transportation Construction

TRANSPORTATION RESEARCH BOARD

*NATIONAL RESEARCH COUNCIL
NATIONAL ACADEMY OF SCIENCES*

WASHINGTON, D.C. 1983

Transportation Research Record 916

Price \$12.60

Edited for TRB by Scott C. Herman

modes

- 1 highway transportation
- 3 rail transportation
- 4 air transportation

subject areas

- 22 hydrology and hydraulics
- 24 pavement design and performance
- 31 bituminous materials and mixes
- 33 construction
- 62 soil foundations
- 63 soil and rock mechanics

Library of Congress Cataloging in Publication Data

National Research Council. Transportation Research Board.

Engineering fabrics in transportation construction.

(Transportation research record; 916)

- 1. Road materials—Addresses, essays, lectures.
 - 2. Pavements—Design and construction—Addresses, essays, lectures.
 - 3. Road construction—Addresses, essays, lectures.
 - 4. Textile fabrics—Addresses, essays, lectures.
- I. National Research Council (U.S.). Transportation Board. II. Series.
TE7.H5 no. 916 [TE203] 380.5s [625.7] 83-26864
ISBN 0-309-03559-7 ISSN 0361-1981

Sponsorship of the Papers in This Transportation Research Record

DIVISION A—REGULAR TECHNICAL ACTIVITIES

Lester A. Hoel, University of Virginia, chairman

Committee on Low Volume Roads

*Melvin B. Larsen, Illinois Department of Transportation, chairman
John A. Alexander, Victor C. Barber, Mathew J. Betz, A.S. Brown,
Everett C. Carter, Robert A. Cherveney, Robert C. Esterbrooks,
Martin C. Everitt, Gordon M. Fay, James L. Foley, Jr., Raymond J.
Franklin, Marian T. Hankerd, Clell G. Harral, Raymond H. Hogrefe,
J.M. Hoover, Lynne H. Irwin, Clarkson H. Oglesby, Adrian Pelzner,
George W. Ring, III, Eldo W. Schornhorst, Eugene L. Skok, Jr.,
Eldon J. Yoder, John P. Zedalis*

GROUP 2—DESIGN AND CONSTRUCTION OF TRANSPORTATION FACILITIES

Robert C. Deen, University of Kentucky, chairman

Task Force on Engineering Fabrics

Verne C. McGuffey, New York State Department of Transportation, chairman

*Robert K. Barrett, J.R. Bell, Michael Bozozuk, Robert G. Carroll, Jr.,
Jerry A. DiMaggio, James B. Farris, Gary L. Hoffman, Robert D.
Holtz, Thomas P. Hoover, Thomas C. Kinney, Vaughn Marker,
B. Dan Marks, Willard G. Puffer, Gregory N. Richardson, George W.
Ring, III, John E. Steward, F.W.B. Taylor, J. Allan Tice, Walter C.
Waidelich, William A. Wood, David C. Wyant*

Pavement Management Section

W. Ronald Hudson, University of Texas at Austin, chairman

Committee on Pavement Rehabilitation

*Gordon W. Beecroft, Oregon Department of Transportation,
chairman*

*James F. Shook, The Asphalt Institute, secretary
Edward Aikman, Walter R. Barker, Martin L. Cawley, W.G.
Davison, Paul J. Diethelm, Wade L. Gramling, William Bryan Greene,
W.J. Head, James W. Hill, Ali S. Kemahli, Richard W. May, Carl L.
Monismith, Gene R. Morris, Louis G. O'Brien, Robert G. Packard,
Lawrence L. Smith, Richard L. Stewart, R.N. Stubstad, Reuben S.
Thomas, Harvey J. Treybig, Hugh L. Tyner, Matthew W. Witczak,
Loren M. Womack*

Neil F. Hawks and Lawrence F. Spaine, Transportation Research Board staff

Sponsorship is indicated by a footnote at the end of each report. The organizational units, officers, and members are as of December 31, 1982.

Contents

TREATMENTS FOR REDUCTION OF REFLECTIVE CRACKING OF ASPHALT OVERLAYS ON JOINTED-CONCRETE PAVEMENTS IN GEORGIA Wouter Gulden and Danny Brown	1
LABORATORY TESTING OF FABRIC INTERLAYERS FOR ASPHALT CONCRETE PAVING: INTERIM REPORT Roger D. Smith	6
REFLECTION CRACKING MODELS: REVIEW AND LABORATORY EVALUATION OF ENGINEERING FABRICS Kamran Majidzadeh, George J. Ilves, and Michael S. Luther	18
OPTIMUM-DEPTH METHOD FOR DESIGN OF FABRIC-REINFORCED UNSURFACED ROADS T. Allan Haliburton and John V. Barron	26
DYNAMIC TEST TO PREDICT FIELD BEHAVIOR OF FILTER FABRICS USED IN PAVEMENT SUBDRAINS Donald J. Janssen	32
MECHANISM OF GEOTEXTILE PERFORMANCE IN SOIL-FABRIC SYSTEMS FOR DRAINAGE AND EROSION CONTROL (Abridgment) Richard D. Weimar, Jr.	37
PERMEABILITY TESTS OF SELECTED FILTER FABRICS FOR USE WITH A LOESS-DERIVED ALLUVIUM G.T. Wade, F.W. Klaiber, and R.A. Lohnes	40
GEOTEXTILE FILTER CRITERIA R.G. Carroll, Jr.	46
USE OF FABRICS FOR IMPROVING THE PLACEMENT OF TILL ON PEAT FOUNDATION C. Lupien, G. Lefebvre, P. Rosenberg, J.J. Paré, and J.G. Lavallé	54
GEOTEXTILE EARTH-REINFORCED RETAINING WALL TESTS: GLENWOOD CANYON, COLORADO J.R. Bell, R.K. Barrett, and A.C. Ruckman	59
NEW YORK STATE DEPARTMENT OF TRANSPORTATION'S EXPERIENCE AND GUIDELINES FOR USE OF GEOTEXTILES Anthony Minnitti, L. David Suits, and Todd H. Dickson	70

EVALUATION OF TWO GEOTEXTILE INSTALLATIONS IN EXCESS OF A DECADE OLD	
Barry R. Christopher	79
LONG-TERM IN SITU PROPERTIES OF GEOTEXTILES	
Gary L. Hoffman and Robert Turgeon	89

Authors of the Papers in This Record

- Barrett, R.K., Colorado Division of Highways, 606 South 9th Street, Grand Junction, CO 81591
- Barron, John V., Haliburton Associates, Engineering Consultants, 3602 North Star Drive, Stillwater, OK 74074
- Bell, J.R., Department of Civil Engineering, Oregon State University, Corvallis, OR 97331
- Brown, Danny, Research and Development Bureau, Office of Materials and Research, Georgia Department of Transportation, 15 Kennedy Drive, Forest Park, GA 30050
- Carroll, R.G., Jr., Mirafi, Inc., P.O. Box 240967, Charlotte, NC 28224
- Christopher, Barry R., ST/ Consultants, Ltd., 111 Pfingsten Road, Northbrook, IL 60062
- Dickson, Todd H., Soil Mechanics Bureau, New York State Department of Transportation, 1220 Washington Avenue, State Campus, Albany, NY 12232
- Gulden, Wouter, Research and Development Bureau, Office of Materials and Research, Georgia Department of Transportation, 15 Kennedy Drive, Forest Park, GA 30050
- Haliburton, T. Allan, Haliburton Associates, Engineering Consultants, 3602 North Star Drive, Stillwater, OK 74074
- Hoffman, Gary L., Materials Evaluation Section, Pennsylvania Department of Transportation, P.O. Box 2926, Harrisburg, PA 17120
- Ilves, George J., Resource International, Inc., 130 E. Wilson Bridge Road, Worthington, OH 43085
- Janssen, Donald J., Department of Civil Engineering, Talbot Laboratory, University of Illinois at Urbana-Champaign, Urbana, IL 61081
- Klaiber, F.W., Civil Engineering Department and Engineering Research Institute, Iowa State University, Ames, IA 50011
- Lavallé, J.G., Société d'énergie de la Baie James, 800 boul. de Maisonneuve est, Montréal, Québec, Canada H2L 4M8
- Lefebvre, G., Département de génie civil, Université de Sherbrooke, Sherbrooke, Québec, Canada, J1K 2R1
- Lohnes, R.A., Civil Engineering Department and Engineering Research Institute, Iowa State University, Ames, IA 50011
- Lupien, C., Département de génie civil, Université de Sherbrooke, Sherbrooke, Québec, Canada J1K 2R1
- Luther, Michael S., Resource International, Inc., 130 E. Wilson Bridge Road, Worthington, OH 43085
- Majidzadeh, Kamran, Resource International, Inc., 130 E. Wilson Bridge Road, Worthington, OH 43085
- Minnitti, Anthony, Soil Mechanics Bureau, New York State Department of Transportation, 1220 Washington Avenue, State Campus, Albany, NY 12232
- Paré, J.J., Société d'énergie de la Baie James, 800 boul. de Maisonneuve est, Montréal, Québec, Canada H2L 4M8
- Rosenberg, P., Lupien, Rosenberg, Journeaux et ass, Inc., 960, 24ième avenue, Lachine, Québec, Canada H8S 3W7
- Ruckman, A.C., Corn Construction, Grand Junction, CO 81501
- Smith, Roger D., Office of Transportation Laboratory, California Department of Transportation, 5900 Folsom Boulevard, P.O. Box 19128, Sacramento, CA 95819
- Suits, L. David, Soil Mechanics Bureau, New York State Department of Transportation, 1220 Washington Avenue, State Campus, Albany, NY 12232
- Turgeon, Robert, Materials Evaluation Section, Pennsylvania Department of Transportation, P.O. Box 2926, Harrisburg, PA 17120
- Wade, G.T., Civil Engineering Department and Engineering Research Institute, Iowa State University, Ames, IA 50011
- Weimar, Richard D., Jr., Textile Fibers Department, E.I. du Pont de Nemours & Co., Inc., Christina Laboratory, Wilmington, DE 19898

Treatments for Reduction of Reflective Cracking of Asphalt Overlays On Jointed-Concrete Pavements in Georgia

WOUTER GULDEN AND DANNY BROWN

For the past 6 years, the Georgia Department of Transportation has placed emphasis on the rehabilitation of the concrete pavement sections of the Interstate system. Many of these sections were resurfaced with asphaltic concrete. One of the problems that had to be addressed was that of reflective cracking of the joints into the overlay. A research project began in 1976, which consisted of placing 16 asphalt overlay test sections with various treatments on an existing jointed-concrete pavement on I-85 north of Atlanta. The treatments consisted of two nonwoven fabrics and sections with strips of a waterproofing membrane. The treatments were repeated for each of three overlay thicknesses. The philosophy behind the experiment was that no treatment would completely stop reflective cracking, but it would provide a waterproofing barrier to prevent surface water from entering the pavement system and thereby cause pumping of the concrete pavement. The waterproofing membrane was included in the experiment for this purpose and was placed in strips over the joints and cracks while the fabrics were placed full width. In 1979, additional test sections were placed on I-85 south of Atlanta to evaluate three types of waterproofing membranes and a nonwoven fabric. The fabric material was placed in strips rather than full width in this experiment. Overlay thicknesses of 2 and 4 in. were placed over the test sections. The performance to date indicates that the treatments reduced the rate of reflective cracking for the 4- and 6-in.-thick overlay sections. Some improvement was also obtained with the 2-in. overlay section, and the best performance was obtained with the waterproofing membrane.

The solution to the problem of the reflection of cracks from the existing pavement into an asphaltic-concrete overlay has eluded researchers for many years. Even today, with the existence of new techniques and products such as asphalt rubber and geotextiles, reflective cracking will occur at some time in the life of the overlay.

The mere presence of cracks is not necessarily a detriment to the performance of a pavement. Only when water and repeated applications of heavy loads are added do substantial problems occur. The entrance of water through cracks can lead to loss of subgrade strength under the existing pavement and pumping of base material through the cracks.

Additional problems occur when an asphaltic-concrete surface is placed over a jointed-concrete pavement. The expansion and contraction movement of the joints causes a crack to occur in the overlay. Jointed-concrete pavements also have vertical movements at the joints that are induced by heavy loads. The presence of water and an erodible base causes pumping and a loss of slab support. The eventual result will be faulted joints and slab breakage. These distresses are transferred into the asphaltic-concrete overlay, which behaves as a rigid rather than a flexible pavement.

Treatments of the existing concrete pavement, such as breakage of the slab into smaller pieces and the placement of aggregate layers, have been tried. Fabrics and waterproofing membranes have also been used. Past practice has been to place thick asphaltic-concrete overlays to delay the occurrence of reflective cracks. Many concrete pavements are structurally adequate and will not require thick overlays from that standpoint. It would be economically advantageous if the same effect as a thick overlay could be achieved with the use of a treatment and a thinner overlay to retard reflective cracking. Perhaps even more important than a reduction in reflection cracking for any treatment would

be the prevention of surface water from entering reflective cracks into the base courses and subgrades of the existing pavement systems.

EXPERIMENTAL SECTIONS IN GEORGIA

The Georgia Department of Transportation (DOT) has emphasized the rehabilitation of plain jointed-concrete pavement on the Interstate system during the past 7 years. Many of these sections have been resurfaced with asphaltic concrete. One problem that had to be addressed before starting this resurfacing program was the occurrence of reflective cracking of the portland cement concrete (PCC) pavement joints. The deterioration of the PCC pavements in Georgia was mainly caused by the combination of heavy loads, the infiltration of surface water into the base and subgrade through joints and cracks, and erodible base materials.

A research project began in 1976, which consisted of placing 16 asphaltic-concrete test sections with various treatments over existing plain jointed-concrete pavements on I-85 north of Atlanta. These treatments consisted of placing two fabrics, strips of a waterproofing membrane, and a layer of a coarse stone before resurfacing.

In 1979 additional test sections were placed on I-85 south of Atlanta to evaluate three types of waterproofing membranes and a nonwoven fabric. The fabric material was placed in strips rather than full width. Short asphalt pavement test sections that used fabrics and asphalt-rubber membranes were placed in 1976, but the emphasis in this paper is on the experimental sections placed over the PCC pavements.

DESCRIPTION OF TEST SECTIONS

I-85, Gwinnett County

The test section in Gwinnett County is located approximately 30 miles north of Atlanta on I-85. It carries 23,000 vehicles/day, with 31 percent heavy trucks. The original pavement is a 9-in.-thick plain jointed-concrete pavement that has 30-ft joint spacing and no load-transfer devices in the joint.

The existing pavement was faulted, where 29 percent of the joints had a difference in slab elevation at the joint of 0.25 in. or more and approximately 8 percent of the slabs were cracked. Before placing the asphaltic-concrete overlay, all slabs were test rolled for excessive movement; they were subsequently stabilized with a cement-lime-fly ash mix where needed. The major variables in the test section were three overlay thicknesses of 2, 4, and 6 in. and various treatments before placing the overlay. These treatments consisted of two nonwoven engineering fabrics, the placement of edge drains, and strips of a waterproofing membrane over all joints and cracks. The fabrics used were Petromat, which is a polypropylene material, and Mirafi 140, which consists of a combination of polypropylene

fibers and a polypropylene fiber covered with nylon. The waterproofing membrane was heavy-duty Bituthene, which consisted of a self-adhesive rubberized asphalt with woven fabric reinforcement.

All test sections were repeated for each overlay thickness along with a control section. In addition, a special test section was placed that contained a 3.5-in.-thick Arkansas-type base layer, which was used with a 3.5-in.-thick asphaltic-concrete overlay. The length of the test sections was 1,320 ft for the control, edge drain, Arkansas base, and 4-oz Petromat sections, whereas the Mirafi 140 and waterproofing membrane sections were 660 ft long. The total project was 3.5 miles long, with short transition sections placed where a change in overlay thickness occurred.

I-85, Troup County

Additional test sections were placed in Troup County in 1979, primarily for the evaluation of additional waterproofing membrane materials. A heavier Petromat (8 oz) was also included in the experiment. The control section was Polyguard with 14 percent rubber content, which was used on the construction project as the standard treatment. Placement was also made of Polyguard with 9 percent rubber content, Bituthene, and Protecto-Wrap. All materials, including the Petromat, were placed in 12-in.-wide strips over joints and cracks for a distance of 600 ft/test section. The test sections were repeated for a 2-in.-thick asphaltic-concrete overlay and a 4-in.-thick overlay. The original pavement was a 9-in. undowelled plain jointed-concrete pavement that had 30-ft joint spacing. The construction project represented the first use of Polyguard for this application in Georgia and was selected by the contractor after it was determined that the product met Georgia DOT specifications.

CONSTRUCTION OF TEST SECTIONS: GWINNETT COUNTY

Fabrics

A leveling course of 70 lb/yd² of asphaltic concrete was placed over the entire test area before placement of the fabrics. A tack coat rate of 0.25 gal/yd² of AC-10 was used with the 4-oz Petromat and 0.18 gal/yd² of AC-10 was used with Mirafi 140.

Fabrics were placed by hand on this particular project. Special emphasis was placed on obtaining a wrinkle-free installation to prevent cracks in the overlay caused by wrinkles in the fabric. When wrinkles did occur, they were cut and the ends tacked down. The standard width of the Mirafi 140 was 14 ft 9 in., which allowed for a 2-ft lap onto the shoulder and a 9-in. lap at the centerline of the 12-ft-wide lanes. The Petromat was 13.5-ft wide, which allowed a 1-ft lap onto the shoulder and a 6-in. lap at the center of the roadway. The initial 2-in.-thick lift of the overlay was constructed immediately after the fabric had been placed. Traffic was maintained at all times in the adjacent lane while the material was being placed. No severe problems were encountered with the placement of the fabrics, with the exception of obtaining the required tack rate at all times.

Special attention needs to be given to the operation of the dump trucks; they should not be allowed to make sudden stops or starts or sharp turning movements on the fabrics. An additional caution had to be taken with the Mirafi 140 because the asphalt concrete (AC) tack on the truck tires tended to pick up the top fibers of this fabric. This problem was overcome by not allowing the trucks to park on the fabric before dumping into the asphalt spreader.

One major construction drawback in placing the fabrics was the time and personnel required to place the material. This problem can easily be rectified through the use of placement equipment for the fabrics.

Only minor problems were encountered with the placement of the asphaltic-concrete overlay on the fabrics. Some slippage during rolling was observed where excessive tack coat was placed.

Waterproofing Membrane

The primary application for the waterproofing membrane is as a waterproofing barrier for bridge decks underneath an asphalt overlay. The use of this material on the roadway, therefore, was primarily intended to waterproof the joints and cracks in the concrete pavement. The membrane was placed in 18-in. strips over all transverse and longitudinal, centerline, and shoulder joints. The strips were placed directly on the concrete pavement after the application of a special primer provided by the manufacturer. Initial placement was extremely tedious because the material was 36 in. wide and had to be cut on the roadway and then placed by hand. In addition, the placement of the material for this application was new to the contractor, the state personnel, as well as the manufacturer, and problems in placement and proper use of manpower had to be worked out.

The membrane is self-adhesive, and once placed can only be removed with great difficulty. Traffic was allowed for 1 day on the test sections with the waterproofing membrane before placement of any overlay. The action of the traffic actually improved the installation by securely adhering the material to the pavement and molding it to the faulted joint contours. The leveling course was placed over the strips of membrane followed by the required overlay thickness. Some problems were encountered with shoving of the mix over the membrane in some places, especially when the roller stopped or started on the strips.

Arkansas Base Test Section

A special test section was constructed with an Arkansas base interlayer to prevent reflection cracking. The stone was mixed with 2 percent asphalt at a temperature of 200° to 225°F. Drainage of liquid asphalt from the mix was not a problem at this temperature.

No problems were encountered with placement of the material on the roadway leveling course that had been placed previously. Edge drains had also been installed previously in this test section. The material was placed with two asphalt spreaders working simultaneously in the travel lane and outside shoulder, because the Arkansas base layer extended over both shoulders as well as the roadway.

The Arkansas base course was compacted with only one pass of a 5-ton steel roller to set the stone. Rolling was done immediately behind the spreaders, and there was no excessive shoving in most cases. When shoving did occur, the mix was allowed to cool slightly before rolling. The basic function of the rolling operation was to key-in the stone, not to achieve any kind of compaction. After placement of the base course, 2.5 in. of asphaltic-concrete binder was placed with no apparent problems, although some minor pickup of stone by the asphalt trucks was noted. One possible construction drawback to using the Arkansas-type interlayer was the need for two asphalt plants because the material had to be covered with an asphalt mix before traffic could use the roadway.

In addition to the 2.5-in.-thick binder, a 1-in. surface course was also placed for a total overlay thickness of 3.5 in. Cores obtained after placement of the overlay indicated that the binder penetrated the Arkansas base up to a depth of 1 in., thereby effectively keying-in the Arkansas base layer and providing stability.

Control Sections

The control sections were similar to the test sections for each overlay thickness, but without the fabrics and waterproofing membrane. Two control sections were placed with each overlay thickness. The difference between control sections was the placement of a 3-in. corrugated plastic drain along the pavement edge in the outside shoulder of one of the control sections. The drain rapidly removed any infiltrated surface water from under the slab that may have entered through any reflection cracks over joints in the old pavement.

CONSTRUCTION OF TEST SECTIONS: TROUP COUNTY

Waterproofing Membranes

The waterproofing membranes were placed in 12-in.-wide strips over all joints and cracks by using the primer recommended by each manufacturer. No problems were encountered with the placement of Bituthene, Polyguard, or Protecto-Wrap. All sections were left open to traffic with no apparent detrimental effects.

Severe problems were encountered with the Protecto-Wrap strips during the paving operation. The tack used during the paving operation was AC-20 placed at a rate of approximately 0.05 gal/yd² at 375°F. The construction sequence was such that trucks delivering the mix to the spreader had to back up over the test material, including the Protecto-Wrap. The tack on the truck tires pulled the Protecto-Wrap loose from the concrete in some instances and also caused the material to separate at the fabric interlayer. This problem was especially noted in the 2-in. AC overlay section. It was requested that the trucks not back up over the material; however, the construction sequence and the turnaround locations for the trucks made this impractical.

One possible reason for the problem occurring in the 2-in. AC section, but not to a large extent in the 4-in. AC section, was that the paving operation started in the 4-in. AC test area that was adjacent to the 2-in. AC test area. The distributor would apply the tack to both the 4- and 2-in.-thick AC test sections at one pass; therefore, the tack was still fairly warm and fluid when the 4-in. AC section was being paved, but was cool and sticky as the trucks were continually backing up over the 2-in. AC test area.

The major problem observed on the damaged joints was the delamination of the material at the fabric layer, which was approximately halfway in the material. Another problem that may have affected performance was the poor adhesion of Protecto-Wrap to the asphalt on the shoulder, generally along the entire length of the test section. Apparently the primer was not compatible with the asphalt. The Protecto-Wrap on some joints was damaged to the extent that the material had to be replaced with Polyguard.

Fabric

The fabric used in this test section was 8-oz Petromat placed in 12-in.-wide strips over both the

transverse and longitudinal joints. The desired tack coat was to be 0.40 gal/yd², but the liquid AC had to be sprayed by hand, and it was difficult to estimate the actual application rate.

The placement of the Petromat strips took less time than that required for placement of the other material because there was no paper or plastic film to peel and no cleanup of discarded boxes.

It was initially thought by Georgia DOT personnel that the material would not withstand traffic and, therefore, the plans called for the material to be placed on the same day that the section was to be paved. Ten joints in the 4-in. AC section outside lane were placed 2 days before paving to determine if traffic would damage the strips. These strips held up excellently during 2 days of traffic with no apparent damage. The experience on this project indicated that it would be desirable to have the Petromat strips under traffic for several days.

Some problems were encountered during the paving of the Petromat sections. These problems were related to the fact that some of the material was placed just ahead of the paver, which did not allow time for the AC tack to cure out and be pressed into the fabric. Some of the strips were pulled up slightly as the asphalt trucks backed over them. The application of the tack coat over the material eased the problem somewhat. The strips were paved over within 15 min after they were placed in the inside lane of the 4-in. AC section. No such problems were encountered on the outside lane, where the material had been in place for 2 days or in the 2-in. overlay section where the AC tack had time to cure out for about 2.5 hr before paving. Also, on the 2-in. overlay section, tack was applied to the entire roadway before any of the asphalt trucks backed up over the strips.

METHOD OF EVALUATION

The performance of the test sections is being evaluated through visual observations, mapping of cracks, rutting measurements, and deflection measurements.

Rutting measurements are more an indicator of the stability of the asphalt mix than of the performance of the fabric or waterproofing membrane, and therefore are not discussed in this paper. Deflection measurements also do not necessarily indicate fabric performance, except that excessive deflections at joints may accelerate the reflection cracking. The magnitude of the deflections measured at joints are highly sensitive to the time of year and the time of day that the measurements are made. The main criteria for evaluating the effectiveness of the treatments at this time are the occurrence of reflective cracking and the rate at which this cracking is increasing. Tests to determine waterproofing ability of the materials have not been performed; however, they will be performed before preparation of the final report on the project.

PERFORMANCE

I-85, Gwinnett County

The latest cracking survey of the test sections was made in February 1982. The results of this survey are expressed as a percentage of the joints that have reflected into the overlay (Table 1) and as a percentage of the available joint length that has reflected (Table 2). The data in Table 2 are considered to be a more valid indicator, because the data in Table 1 do not distinguish between a 6-in.-long crack and, for example, an 18-ft-long crack, but merely indicate the number of joints that indicate reflective cracking.

Little difference is noted between the sections in the number of joints that have reflected after 5 years for the 2- and 4-in.-thick overlay. There is a significant difference in the 6-in.-thick overlay section for the heavy-duty Bituthene when compared with the control section or with the other treatments.

The data in Table 2 are more indicative of actual performance, and these reveal a reduction in the amount of reflective cracking for the fabric and waterproofing treatments compared with the control sections for the 4-in. overlay and for the waterproofing treatment for the 6-in. overlay section. Of interest is the unsatisfactory performance of the edge drain section with the 6-in. overlay.

The progression of the accumulative length of cracking on the test sections is shown in Figures

1-3. These figures give a better indication of the effect of the treatments on the occurrence of the reflective cracking. An increase in cracking is always observed after the winter months; a section may show small increases for several winters, and then cracking may begin to increase at a rapid rate.

The amount of cracking for the 2-in. overlay is currently about the same for all treatments. It can be seen from Figure 1 that the fabrics delayed the rapid increase in reflective cracking for about 1 year. The waterproofing membrane showed virtually no reflective cracking for the first 2 years and no significant increases until after the first 4 years.

The performance of the treatments with a 4-in. overlay showed only slight differences between the fabrics and the waterproofing membrane. The control sections showed large increases in cracking lengths

Table 1. Percentage of joints reflected into overlay after 6 years: I-85, Gwinnett County.

Treatment	Joints Reflected (%) by Overlay Thickness		
	2 in.	4 in.	6 in.
Heavy-duty Bituthene	96	82	17
Mirafi 140 fabric	100	95	50
4-oz Petromat fabric	98	86	66
Edge drains	100	100	93
Control	100	100	73

Note: Arkansas base = 70 percent.

Table 2. Percentage of joint length reflected into overlay after 6 years: I-85, Gwinnett County.

Treatment	Joint Length Reflected (%) by Overlay Thickness		
	2 in.	4 in.	6 in.
Heavy-duty Bituthene	83	55	6
Mirafi 140 fabric	97	70	24
4-oz Petromat fabric	91	54	27
Edge drains	98	92	73
Control	100	89	29

Note: Arkansas base = 34 percent.

Figure 1. Crack reflection: 2-in. AC overlay, I-85, Gwinnett County.

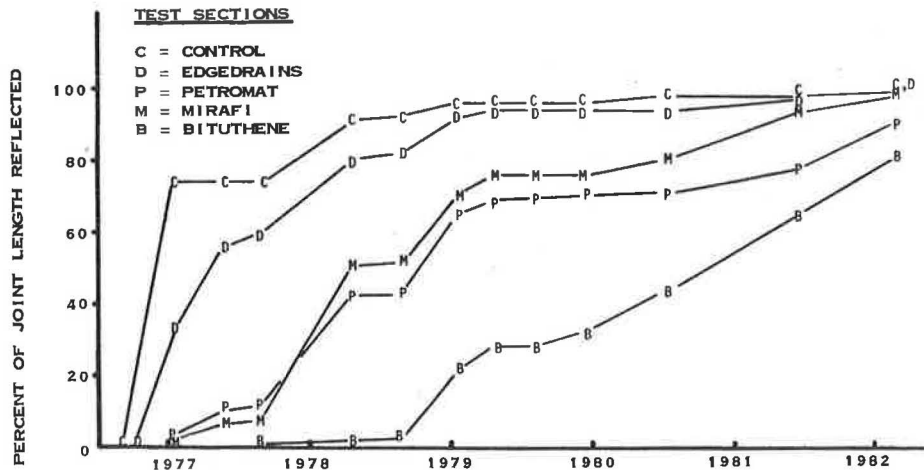


Figure 2. Crack reflection: 4-in AC overlay, I-85, Gwinnett County.

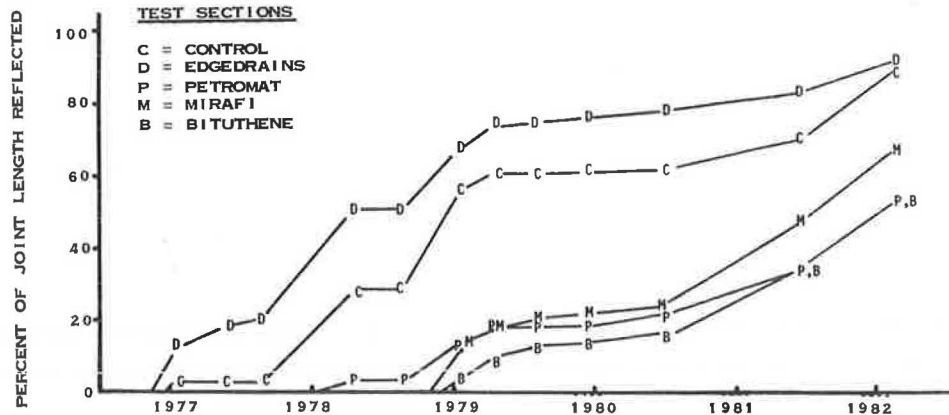


Figure 3. Crack reflection: 6-in. AC overlay, I-85, Gwinnett County.

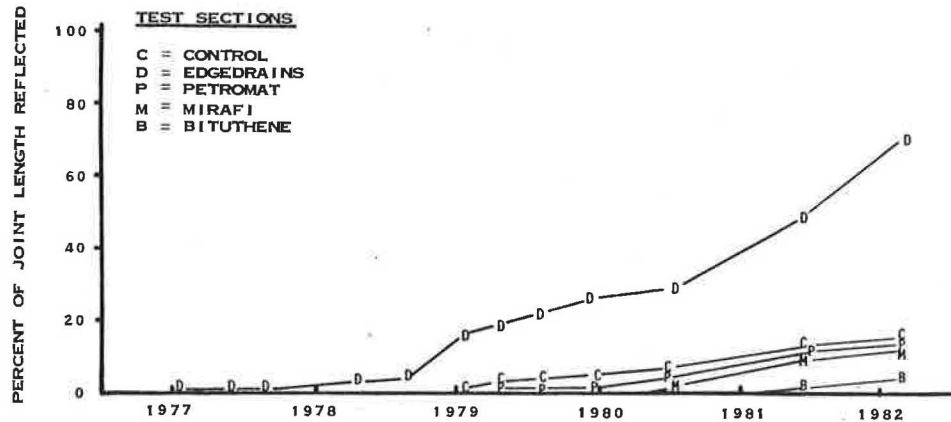


Table 3. Joint reflection into asphalt overlay: I-85, Troup County (March 1982).

Treatment	Joints Re- flected (%) by Overlay Thickness		Joint Length Reflected (%) by Overlay Thickness	
	2 in.	4 in.	2 in.	4 in.
Polyguard	100	70	38	28
Polyguard with 9 percent rubber	95	35	48	8
Heavy-duty Bituthene	95	55	33	18
8-oz Petromat strips	89	75	53	30

during the second and third winters after placement, whereas the treated sections began to show increases after the fifth and sixth winter. The Bituthene and Petromat sections are still significantly lower in reflective cracking than the control sections.

No definite trends can be seen as yet in the 6-in. overlay area because the sections with fabric and the control section are performing equally well. The Bituthene section has the best performance--a lower crack reflection percentage than the other sections. Of interest is the unsatisfactory performance of the area with edge drains.

The section with the Arkansas base as a crack-relief treatment is showing significant reflection cracking. In comparison to the 4-in.-thick overlay section, it is performing well; however, when compared with the 6-in.-thick overlay section, it is not performing as satisfactorily as the other treatments. The Arkansas treatment has a 3.5-in. overlay, but the total thickness of the treatment plus overlay is 7 in., and the performance has generally been gauged against the 6-in.-thick sections in Georgia.

I-85, Troup County

The results of the latest available crack survey are given in Table 3. The data represent the amount of reflective cracking after three winters. Generally the waterproofing membranes have less length of the joints reflected through them for both the 2- and the 4-in. AC overlays. Any differences between the membranes are not clear-cut at this time. The Polyguard, which has a lower rubber content, has the least length of reflective cracking with the 4-in. overlay but has the greatest amount of cracking of the membranes with the 2-in. overlay.

The heavy-duty Bituthene is considered the control section on this project because of its past history on the original research sections on I-85 in Gwinnett County. The reflective cracking that has

occurred is concentrated on the outside lane, with less cracking occurring on the passing lane. This phenomenon could be attributed to the concentration of heavy trucks on the outside lane and to larger vertical movement of the joints. The slabs were test rolled, and slabs that had excessive corner movements were stabilized through pressure grouting.

For comparison purposes, the amount of reflective cracking on the Gwinnett County project was 29 percent on the 2-in. overlay and 10 percent on the 4-in. overlay for the Bituthene sections after three winters. The amount of reflective cracking on the Troup County project is somewhat higher for the same time period. Additional time will be needed to determine if this trend will continue.

IMPLEMENTATION

Georgia's program for rehabilitation of the Interstate system dictated an early decision on the type of joint treatment under asphaltic-concrete overlays. The waterproofing membrane was chosen based on the excellent results that were obtained in the early phases of the project. The use of strips of waterproofing membrane became a standard construction item for treatment of PCC pavement joints before placing an asphalt overlay. Both construction and material specifications were developed by Georgia DOT. The width of the strips used on the experimental sections was 18 in., but this was reduced to 12 in. for all contract projects. The material should only be placed over joints with stable slabs so as to minimize vertical movement. The membrane should also have firm support over the joint, and all joints should be filled flush with the pavement surface.

Traffic is allowed to travel over the waterproofing strips for up to 7 days. It is preferred that traffic travels over the strip at least overnight to tightly bond the material to the concrete. Some problems can be encountered with the strips during the paving operation. Some shoving over the strips has been noticed at times, especially when the roller stops or starts on a strip of waterproofing membrane or during extremely hot weather. Bulging of the asphalt mix over the strips can also occur during placement of the first lift.

The use of fabrics has been limited to the experimental sections. A limited application of heavy fabric strips has recently been made over longitudinal and transverse cracks in asphalt pavement on the Interstate system before placing an asphalt overlay.

CONCLUSIONS

1. The fabrics and waterproofing membranes have

reduced the rate of reflective cracking in both the 2- and 4-in.-thick asphaltic-concrete overlay sections. No conclusions can be drawn at this time with respect to the 6-in.-thick overlay section.

2. The best performance to date has been obtained with the waterproofing membranes.

3. Even when reflective cracking appears over joints with membrane treatment, the cracks appear to stay tighter than cracks over joints without membrane treatment.

4. Proper preparation of the existing concrete pavement and stabilization of slabs with large corner movements must be done in order to obtain maximum benefit from the joint treatment.

5. A minimum of 4-in.-thick asphaltic-concrete overlay should be used on jointed-concrete pavement, and the membrane treatment should be used to control the rate of reflective cracking.

6. The use of waterproofing membranes over concrete pavement joints before placing an asphalt overlay has been adopted as a standard practice in Georgia.

ACKNOWLEDGMENT

The data presented in this paper were obtained as part of Research Study 7502, Overlays for Plain Concrete Pavements, funded by FHWA and Georgia DOT.

The contents of this paper reflect our views, and we are responsible for the facts and accuracy of the data presented. The contents do not necessarily reflect the official views or policies of FHWA or Georgia DOT.

Trade and manufacturers' names appear in this paper only because they are considered essential to the object of the document and do not constitute endorsement of a product by FHWA or Georgia DOT.

This paper does not constitute a standard, specification, or regulation.

Publication of this paper sponsored by Task Force on Engineering Fabrics.

Laboratory Testing of Fabric Interlayers for Asphalt Concrete Paving: Interim Report

ROGER D. SMITH

Because of the proliferation of paving products being presented as reflection crack retarders, the need developed for laboratory tests that can be used as a screening device to avoid the extensive costs and delays associated with full-scale field tests of all of these products. This need resulted in an FHWA-financed research project to generate laboratory tests for estimating the effect of various fabric interlayers on asphalt concrete (AC) overlay properties such as (a) water permeability, (b) susceptibility to flexural fatigue reflection cracking, (c) susceptibility to vertical shear fatigue reflection cracking, and (d) susceptibility to horizontal shear failure (slipping). Testing was also done to characterize popular fabrics in terms of physical and mechanical properties such as tensile strength, elongation, modulus, weight, thickness, and heat resistance. Possible correlations between these fabric properties and the above four overlay properties were investigated. In addition, methods for estimating the optimum asphalt tack-coat application rate for fabrics were developed. These research efforts have led to a more educated and selective use of fabrics in AC paving.

Laboratory test methods can be used to predict the relative in-service performance of fabric interlayers in asphalt concrete (AC) pavement overlays as well as the amount of asphalt tack coat to be used with each fabric type. To better understand the need and use of these test methods, the following items are described in this paper:

1. Basic causes of AC overlay cracking,
2. Popular theories of fabric interlayer effectiveness in reducing overlay cracking,
3. Earlier research efforts to predict interlayer effectiveness by using laboratory tests,
4. Measurement of physical and mechanical properties of 12 commercially produced fabrics,
5. Laboratory testing of AC specimens to investigate the effectiveness of fabric interlayers in thwarting the common causes of overlay reflection cracking, and
6. Attempted correlations between the physical and mechanical properties of the fabrics and their performance in the above tests.

BACKGROUND INFORMATION

The reflection of cracks from old distressed pavement through relatively new AC overlays significantly decreases the service life of these overlays. Numerous fabric materials--primarily polyesters and polypropylenes, as well as rubber-asphalt combinations--are being proposed as interlayers to retard this reflection cracking, but no laboratory procedures have been developed to evaluate the validity of these claims. Simple laboratory tests are therefore needed for the

1. Analysis of the mechanisms by which reflection cracking occurs,
2. Estimation of the benefits of using various interlayers,
3. Definition of which interlayer properties correlate to crack retardation, and
4. Avoidance of the extensive costs and delays that are associated with full-scale field testing of inappropriate materials.

Reflection cracking is the propagation of cracks from an existing surfacing of portland cement concrete (PCC) or AC through the resurfacing layer. This problem is serious. Many different remedies have been tried (with varying degrees of success) to eliminate or deter such cracking.

Reflection cracking develops from movement of the pavement under the overlay (Figure 1). It can be caused by several mechanisms, such as

1. Differential vertical movement at a crack or slab joint in the old pavement, which induces a vertical shear stress in the overlay;
2. Horizontal movement associated with tempera-

reduced the rate of reflective cracking in both the 2- and 4-in.-thick asphaltic-concrete overlay sections. No conclusions can be drawn at this time with respect to the 6-in.-thick overlay section.

2. The best performance to date has been obtained with the waterproofing membranes.

3. Even when reflective cracking appears over joints with membrane treatment, the cracks appear to stay tighter than cracks over joints without membrane treatment.

4. Proper preparation of the existing concrete pavement and stabilization of slabs with large corner movements must be done in order to obtain maximum benefit from the joint treatment.

5. A minimum of 4-in.-thick asphaltic-concrete overlay should be used on jointed-concrete pavement, and the membrane treatment should be used to control the rate of reflective cracking.

6. The use of waterproofing membranes over concrete pavement joints before placing an asphalt overlay has been adopted as a standard practice in Georgia.

ACKNOWLEDGMENT

The data presented in this paper were obtained as part of Research Study 7502, Overlays for Plain Concrete Pavements, funded by FHWA and Georgia DOT.

The contents of this paper reflect our views, and we are responsible for the facts and accuracy of the data presented. The contents do not necessarily reflect the official views or policies of FHWA or Georgia DOT.

Trade and manufacturers' names appear in this paper only because they are considered essential to the object of the document and do not constitute endorsement of a product by FHWA or Georgia DOT.

This paper does not constitute a standard, specification, or regulation.

Publication of this paper sponsored by Task Force on Engineering Fabrics.

Laboratory Testing of Fabric Interlayers for Asphalt Concrete Paving: Interim Report

ROGER D. SMITH

Because of the proliferation of paving products being presented as reflection crack retarders, the need developed for laboratory tests that can be used as a screening device to avoid the extensive costs and delays associated with full-scale field tests of all of these products. This need resulted in an FHWA-financed research project to generate laboratory tests for estimating the effect of various fabric interlayers on asphalt concrete (AC) overlay properties such as (a) water permeability, (b) susceptibility to flexural fatigue reflection cracking, (c) susceptibility to vertical shear fatigue reflection cracking, and (d) susceptibility to horizontal shear failure (slipping). Testing was also done to characterize popular fabrics in terms of physical and mechanical properties such as tensile strength, elongation, modulus, weight, thickness, and heat resistance. Possible correlations between these fabric properties and the above four overlay properties were investigated. In addition, methods for estimating the optimum asphalt tack-coat application rate for fabrics were developed. These research efforts have led to a more educated and selective use of fabrics in AC paving.

Laboratory test methods can be used to predict the relative in-service performance of fabric interlayers in asphalt concrete (AC) pavement overlays as well as the amount of asphalt tack coat to be used with each fabric type. To better understand the need and use of these test methods, the following items are described in this paper:

1. Basic causes of AC overlay cracking,
2. Popular theories of fabric interlayer effectiveness in reducing overlay cracking,
3. Earlier research efforts to predict interlayer effectiveness by using laboratory tests,
4. Measurement of physical and mechanical properties of 12 commercially produced fabrics,
5. Laboratory testing of AC specimens to investigate the effectiveness of fabric interlayers in thwarting the common causes of overlay reflection cracking, and
6. Attempted correlations between the physical and mechanical properties of the fabrics and their performance in the above tests.

BACKGROUND INFORMATION

The reflection of cracks from old distressed pavement through relatively new AC overlays significantly decreases the service life of these overlays. Numerous fabric materials--primarily polyesters and polypropylenes, as well as rubber-asphalt combinations--are being proposed as interlayers to retard this reflection cracking, but no laboratory procedures have been developed to evaluate the validity of these claims. Simple laboratory tests are therefore needed for the

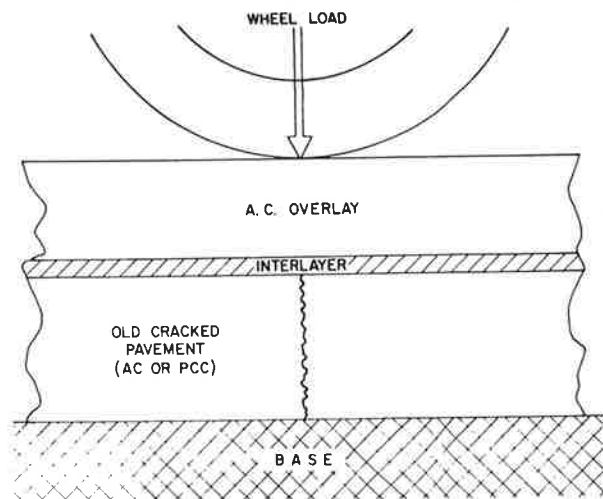
1. Analysis of the mechanisms by which reflection cracking occurs,
2. Estimation of the benefits of using various interlayers,
3. Definition of which interlayer properties correlate to crack retardation, and
4. Avoidance of the extensive costs and delays that are associated with full-scale field testing of inappropriate materials.

Reflection cracking is the propagation of cracks from an existing surfacing of portland cement concrete (PCC) or AC through the resurfacing layer. This problem is serious. Many different remedies have been tried (with varying degrees of success) to eliminate or deter such cracking.

Reflection cracking develops from movement of the pavement under the overlay (Figure 1). It can be caused by several mechanisms, such as

1. Differential vertical movement at a crack or slab joint in the old pavement, which induces a vertical shear stress in the overlay;
2. Horizontal movement associated with tempera-

Figure 1. Pavement overlay components.



ture or moisture changes in the old pavement, which induces tensile stress in the overlay; or

3. Live load flexural stress in the overlay, which tends to concentrate directly over discontinuities.

Since the advent of paving with fabric interlayers in the early 1970s, many claims have been made as to the benefits and problems that might be expected from this relatively new and unconventional paving technique. There were claims of fabric being nothing short of a cure-all for all types of overlay cracking, and many researchers began assigning a structural equivalency (in terms of AC thickness) to fabric for all applications. This meant that thinner overlays could be used, thereby resulting in added benefits where vertical controls existed. However, over the years, as a result of many field test sections, it has become apparent that the use of fabric interlayers in AC overlays is not always cost effective.

To better understand what role fabric might play in AC overlay work, a brief discussion of the mechanics of overlay cracking and the popular theories of how fabric might work are presented below.

Overlay Cracking Mechanisms

Reflection cracking of AC overlays has several primary causes:

1. Flexural fatigue is caused by high wheel load deflections that tend to be concentrated at localized structural inadequacies in the supporting material or at a crack in an underlying pavement structure;

2. Thermal strains that develop in the old pavement, especially PCC slabs during diurnal temperature cycles, can be transmitted to the overlay if the interlayer bond is strong enough; and

3. Various degrees of differential vertical movement (Δ -vert) at discontinuities (such as joints or cracks) in the underlying pavement can occur under heavy wheel loads, especially when the underlying pavement is curled.

Fabric Theory

Several theories have been advanced that support the claim of the ability of fabric to deter reflection cracking.

1. Stress-relieving interlayer theory: This hypothesis is that the fabric simply acts as a containment reservoir for the heavy asphalt tack coat and thereby provides a soft, ductile zone that has a blunting effect on a crack tip advancing into it. The stresses concentrated at the tip of the crack are thereby dissipated and the advance is halted.

2. Slip plane theory: This theory holds that a fabric interlayer system will fail in shear (in the plane of the fabric) before transferring any significant amount of stress from the old pavement (underlayer) to the overlay. This hypothesis applies primarily to overlay cracking that results from tensile stress induced by a cracked or jointed underlayer responding to thermal or moisture changes, such as in the case of a PCC pavement overlaid by AC.

3. Tensile reinforcement theory: This theory holds that the fabric has a reinforcing effect on the AC overlay in a manner similar to the effect of steel tensile reinforcement (rebar) in PCC structures.

4. Waterproofing theory: It is also commonly believed that fabric makes an overlay more impermeable; therefore, base and subbase material are not subject to weakening by hydraulic action. This protection results in the overlay being subjected to less local deflections and an overall less-severe flexural fatigue effect.

Other Research

Before this current study, these four theories had been investigated by controlled laboratory testing in only a limited fashion, as discussed below.

Germann and Lytton (1) of the Texas Transportation Institute investigated the fatigue life of AC that contained a fabric interlayer in the straight (axial) tensile loading mode. Their study dealt with theories 1 and 3, and their research revealed that beams containing fabric exhibited axial tensile fatigue lives several times those with no fabric. Although they recognized that the fabric's contribution to the AC tensile strength was not sufficient to prevent initial cracking, they did claim that the fabric was beneficial in slowing the rate of crack growth by preventing the crack from opening up to those displacements necessary for crack growth. They also reported that the fabrics withstood the strain of crack opening without rupture, which is an important consideration in the waterproofing theory mentioned previously.

Perhaps the earliest laboratory flexural testing of AC beams with fabric was done in 1972 by Draper and Gagle (2) of the Phillips Petroleum Company. Although their investigation dealt with the effects of Petromat on flexural yield strength (as opposed to fatigue life), it did disclose marked improvement (300 to 800 percent) in that property in beams containing Petromat compared to beams with a tack coat only.

Majidzadeh of Ohio State University (3) performed research testing with respect to theory 1. He concluded that, for low-stress situations, a fabric interlayer placed at the lower third point of an AC beam increased its flexural fatigue life by more than 1,000 percent. Also, with respect to theory 2 (the rebar theory), his research revealed that the fabric interlayer was of virtually no value in increasing the fracture toughness of an AC beam specimen, and probably of little value in resisting the high tensile strains associated with thermally induced movements.

The Iowa Department of Transportation (4) attempted some laboratory flexural fatigue testing of sand-asphalt beams with and without various fabric

Table 1. Fabric properties.

Fabric	Weight (oz/yd ²)	Thickness ^a (mils)	Grab Tensile ^b (mils)		Elongation ^b (%)		Secant Modulus ^c (psi)	
			Machine Direction	Cross- Machine Direction	Machine Direction	Cross- Machine Direction	Machine Direction	Cross- Machine Direction
Reepav 376 (Dupont)	3.0	14	110	79	63	64	4,650	3,250
Nicofab B50 (Nicolon)	4.9	68	80	133	100	79	1,339	552
Amoco 4545 (Amoco)	6.6	40	142	147	73	104	1,890	1,480
Trevira 1117 (Hoechst)	4.4	51	162	119	82	111	1,666	810
Petromat (Phillip Fibers)	4.5	40	81	132	85	74	2,294	1,483
Bidim C-22 (Monsanto)	3.2	51	125	98	90	98	1,878	871
Bidim C-34 (Monsanto)	9.6	77	178	151	57	73	1,939	1,731
TrueTex MG75 (True Temper)	6.5	56	170	98	96	97	1,936	666
TrueTex MG100 (True Temper)	6.5	88	174	114	94	116	896	414
Duraglass B-65 (Johns-Manville)	9.8	77	126	116	3	3	^d	^d
Q-Trans-50 (Quline)	7.0	105	93	142	173	107	350	160
Fibretext 200 (Crown-Zellerbach)	6.0	73	183	126	145	175	1,025	368

Note: All values are from Transportation Laboratory (TransLab) testing.

^aASTM 461.

^bASTM 1117; 1-in. grip.

^cAt 50 percent strain, unless tearing occurs.

^dTear.

interlayers. This testing involved four different fabric brands: Petromat, Bidim C-28, TrueTex MG75, and Reepav T-323. This research revealed that the fatigue lives of beams with fabric were from two to four times that of control beams without fabric.

Another laboratory effort in the area of fabric interlayer effects on the flexural fatigue lives of AC beams (0.5 in. maximum) was undertaken by the E.I. DuPont Company (5), the producers of Reepav. This study, in addition to Reepav, also involved Petromat and Bidim. The testing indicated that the fatigue life of fabric was 2 to 22 times greater than the fatigue life of beams without fabric.

With respect to theory 4, a limited amount of permeability testing of cores from new AC pavement containing Petromat interlayers was performed by Bushey (6) of the California Department of Transportation (Caltrans) by using a vacuum pump arrangement. These early tests indicated that a Petromat interlayer could reduce the water permeability of AC. The study also revealed that, in the presence of AC cracking, the Petromat fabric did not appear to rupture, which suggested that even after the overlay has cracked, the fabric can act as a water barrier. More recent field observations by Caltrans personnel suggest that fabric can rupture at crack locations if strains (vertical or horizontal) are sufficient.

Other controlled research in the area of fabric permeability was done by the E.I. DuPont Company (5). This testing, which involved subjecting asphalt-saturated fabric specimens to a hydrostatic head of water, indicated that five test fabrics, with sufficient asphalt saturation, could form an adequate moisture barrier. These results may be of limited significance, however, because no effort was made to simulate the effects of imbedment in an AC pavement structure. However, the results did demonstrate that thin fabrics can provide an impermeable layer by using much less asphalt tack coat than thicker fabrics.

RESEARCH TESTING

Laboratory testing performed as part of this research project involved 12 brands of nonwoven fabric from 10 different manufacturers. These fabrics are listed in Table 1. Also tested were two woven, asphalt-backed membranes--Bituthene and Polyguard. All test specimens of a given fabric brand were cut from the same large parent sample, which represented one roll of production fabric. In all areas of testing, specimens without any interlayer treatment (control specimens) were also tested.

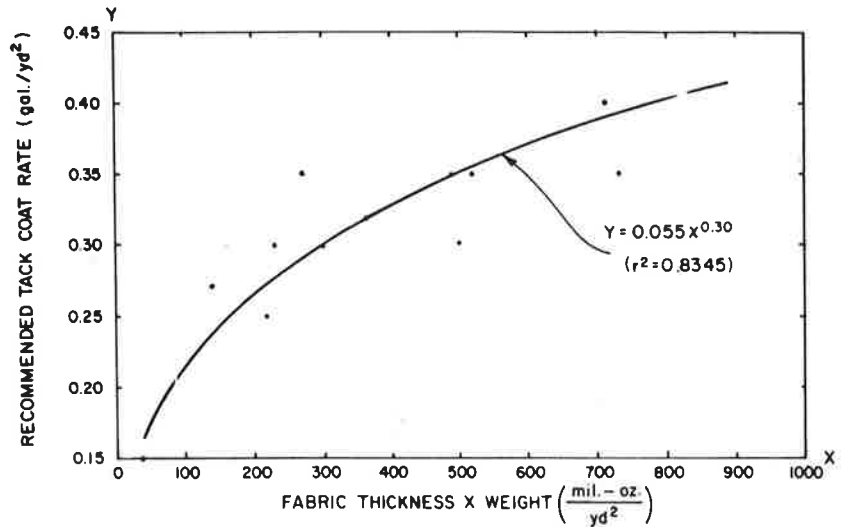
The various test procedures described in this section were designed with the primary objective being to reasonably simulate in-service conditions and mimic some critical behavior or failure mechanism inherent in AC overlays.

Fabric Property Measurements

Measurements of the physical properties of all test fabrics were made by TransLab's Commodities Unit. A total of eight fabric properties were measured, and the results are given in Table 1.

Although most of these fabric property tests are explained by their ASTM test method reference, it is believed that the secant modulus property should be explained further. Secant modulus, as used in this paper, is simply the slope of the stress versus strain plot for tensile loading of a 3x5-in. fabric specimen by using 3x5-in. grips and a 1-in. gauge length. This slope value, for purposes of this paper, is defined as the ratio of stress (pounds per square inch) to strain (percent) at the point of 50 percent strain. Because the 3x5-in. specimens in this study used a gauge length (grip separation) of 1 in., the secant modulus was simply the stress at 0.5-in. elongation divided by 0.50. The values given in Table 1 are the average of three tests at a loading rate of 12 in./min.

Figure 2. Recommended tack-coat rate versus fabric weight x thickness.



Estimation of Tack Coat Requirements

In order for any pavement interlayer system to be successful, it must achieve satisfactory bonding with both the overlay and the existing pavement or underlayer. In the case of a fabric interlayer, this proper bonding should depend on the tack coat that penetrates the fabric from its underside and provides sufficient excess on the fabric's top surface to effect proper bonding with the underside of the overlay. In order for this situation to be realized, three things must occur:

1. The tack coat must be made liquid (melted) enough to enable it to invade the fabric,
2. The tack coat must stay liquid long enough for its migration through the fabric to occur, and
3. External compressive pressure must usually be applied to the system when the tack asphalt is still liquid in order to provide a sponging effect on the fabric.

For this situation to occur, it is apparent that inputs of heat and pressure are necessary. The heat demand must be met by heat from the overlay mix that is adjusted for the overlay thickness, the temperature of the underlayer, and the air temperature and wind speed during paving. The required pressure will be supplied from the deadweight of the overlay and the compactive effort on the overlay.

Testing Discussion

In designing a routine laboratory test for a fabric's asphalt saturation potential (ASP), it is prudent to simulate the probable worst-case field conditions, namely:

1. Low temperature of existing pavement = 40°F;
2. Thin overlay = 0.10 ft;
3. Relatively cool overlay mix = 250°F;
4. Minimal rolling effort = 3 passes of a 12-ton roller; and
5. Heat availability and dwell time = 5 min.

The details of this test cannot be presented here, but basically the test involves placing a 250°F AC briquette (4 in. in diameter) on top of a fabric, under which is an asphalt (AR-4000) film of known thickness (which represents a known tack-coat rate). The briquette is loaded to simulate rolling

forces, and the fabric is inspected for degree of saturation.

Recommended tack coat rates for the fabric's tested are given in the table below:

Fabric	Lightest Tack-Coat Rate Found to be Acceptable (gal/yd²)
Amoco 4545	0.35
Bidim C-22	0.25
Bidim C-34	0.35
TrueTex MG75	0.30
TrueTex MG100	0.35
Trevira 1117	0.30
Nicofab B50	0.30
Petromat	0.25
Reepav 376	0.15
Q-Trans-50	0.35
Fibretext 200	0.30

An investigation was made of possible correlations that might exist between the recommended tack rate (from melt-through testing) and various fabric properties. It was hypothesized that the tack-coat demand of a fabric would depend largely on two fabric properties: weight and thickness. After unsuccessful attempts to establish a meaningful correlation with either of these properties individually, a reasonably valid ($r^2 = 0.8345$) correlation was observed to exist with their product (weight x thickness). This relation is given in Equation 1 and shown in Figure 2:

$$RTC = 0.055 TW^{0.30} \tag{1}$$

where

- RTC = recommended tack-coat rate (gal/yd²),
- T = fabric thickness (mils), and
- W = fabric weight (oz/yd²).

Note that the RTC values calculated from fabric weight and thickness by using Equation 1 should be taken as estimates, and values should be rounded to the nearest 0.05 gal/yd² to be consistent with the accuracies of field application techniques.

Other Tests for Estimating Tack Coat Requirements

Recognizing the need for a simpler test than the one just described, an investigation was made of a test

developed earlier by the Texas State Department of Highways and Public Transportation (7).

The asphalt retention values obtained by using the Texas test had satisfactory correlations with TransLab RTC determinations, as shown in Figure 3. However, the Texas method for determining tack-coat rate, although simple, was not considered an acceptable test method because it did not simulate field conditions. For example, some of the fabric samples shrunk as much as 50 percent in their linear dimensions while in the 285°F oven. This is not comparable to field conditions, where the fabric would be restrained from shrinking. Also, the Texas test did not consider the role of roller pressure or AC mix weight and heat in accomplishing the saturation. It was therefore decided that TransLab should develop its own simple test, with an objective being that any such test should have satisfactory correlation with RTC values obtained from the melt-through test.

The TransLab motor oil retention test was developed to meet this need. In this test, a piece of the fabric is soaked in 20W motor oil at 70°F for 2

min, then removed and placed on an inclined (7.5°) surface. Next, a 3350-g steel cylinder is rolled down the incline 6 times to remove some of the excess oil on the fabric (Figure 4). The weight of the oil retained in the fabric is determined and a recommended tack rate is estimated by using the TransLab correlation shown in Figure 5. (Note that in Figure 5 the tack-coat rate includes 0.05 gal/yd² to fill voids in the surface that receives the tack coat.)

Interlayer Permeability

This study involved the development of a laboratory test for measuring the permeability of AC that contains fabric interlayers and also involved measuring and comparing the permeabilities in AC of 14 paving fabrics. Also measured were permeabilities of an interlayer of asphalt tack coat only (without fabric) and of control specimens (i.e., no interlayer treatment of any kind). Although not yet attempted, permeability tests of pavement cores that contain cracks are also planned.

Another aspect of this study involved determining whether AC aggregate punches through the fabric interlayer during compaction, and whether such punch-through necessarily leads to higher permeability.

In order to make the permeability information obtained in these laboratory tests applicable to field conditions, the specimen was made to model an AC pavement that contains fabric. This model was a 4-in.-diameter DGAC (type A, 0.75-in. maximum aggregate, 5.3 percent AR-4000 asphalt binder) briquette that was 2 in. in height and had a paving fabric sandwiched at middepth (see Figure 6).

The water permeability test apparatus (Figure 7) developed by Chevron was selected for simplicity after trying other less-realistic methods that involved waxed briquettes and vacuum pumps. A

Figure 3. Recommended tack rate versus asphalt retention.

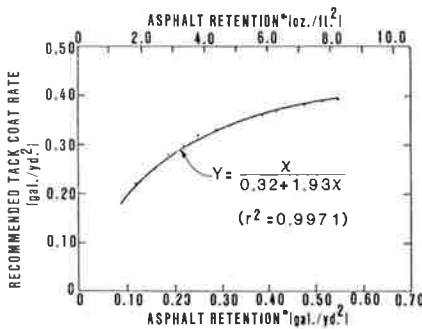


Figure 4. Motor oil retention test setup.

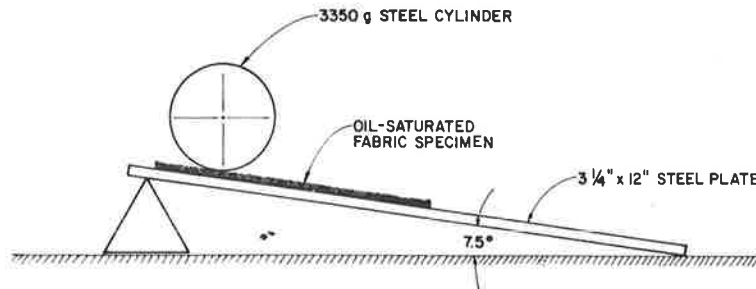
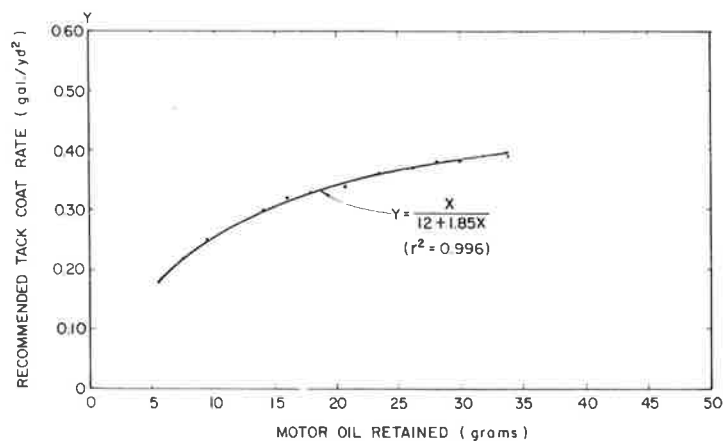


Figure 5. Recommended tack-coat rate versus motor oil retention.



falling-head permeability test was run with an initial head of 8 in. Readings were made in milliliters of the flow at 5, 10, 30, and 60 min. Aerosol was used in the water as a wetting agent at a ratio of 95 mL to 5 gal of water. This minimized the tension of the surface water as it passed through the briquette. This test was repeated at

least twice per specimen; each time the dome-to-briquette joint was retaped. All values are reported in Table 2.

After testing, the briquettes were placed in a 140°F oven and broken down to allow retrieval of the fabric "cookie." The fabric was checked for aggregate punch-through and lack of asphalt saturation.

Correlation between the light transmission and the measured permeability was then investigated based on the assumption that the recovered fabrics that exhibited greater light transmission (aggregate punch-through) would yield higher permeability values, but no such correlation was observed. Small discrete holes, apparently made by sharp edges of aggregate, were noticed on some fabrics, but these fabrics did not necessarily exhibit high permeabilities. This suggests that the openings within the fabric are plugged or otherwise blocked (at least partly) when the fabric is tightly sandwiched in the AC test specimen, and that aggregate punch-through is probably not a major contributor to high permeability.

An investigation was also made into possible correlations between laboratory-measured permeabilities and the following fabric properties: thickness, ultimate strength in weaker direction, and fabric modulus at 50 percent strain. No acceptable correlation(s) was found to exist.

Even though no explanation is offered, note that the following fabrics consistently provided very low interlayer permeability: Reepav 376, Bituthene, and Duraglass B-65.

Although some interlayers performed better than others, note that all interlayer treatments provided a significant reduction in permeability. Even those specimens with only the heavy tack-coat interlayer (no fabric) exhibited, for the most part, very low permeability. This suggests that the primary role of the fabric (from the standpoint of permeability) may be to distribute and secure the tack asphalt as a continuous, uniform membrane within the AC mat. (Note that field experiments by Caltrans have thus far failed to corroborate these laboratory permeability test findings.)

Figure 6. Permeability test specimen.

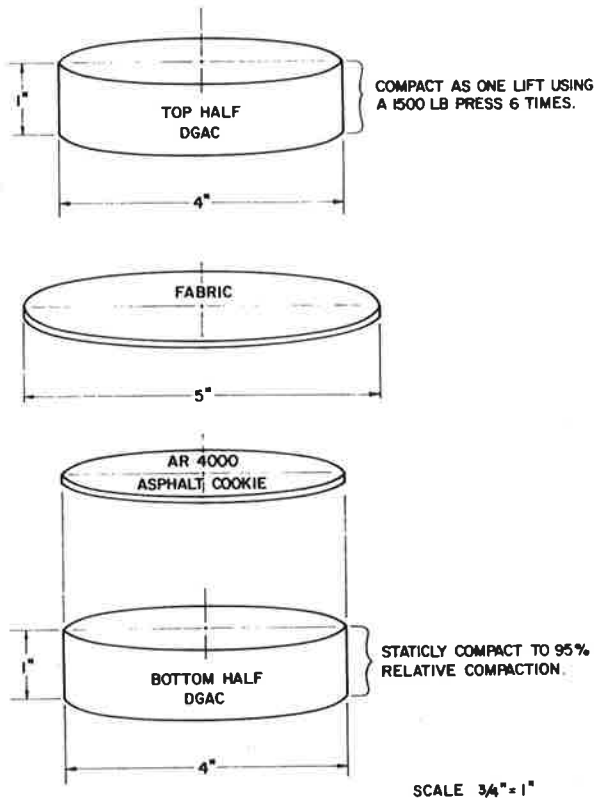


Figure 7. Water permeability apparatus.

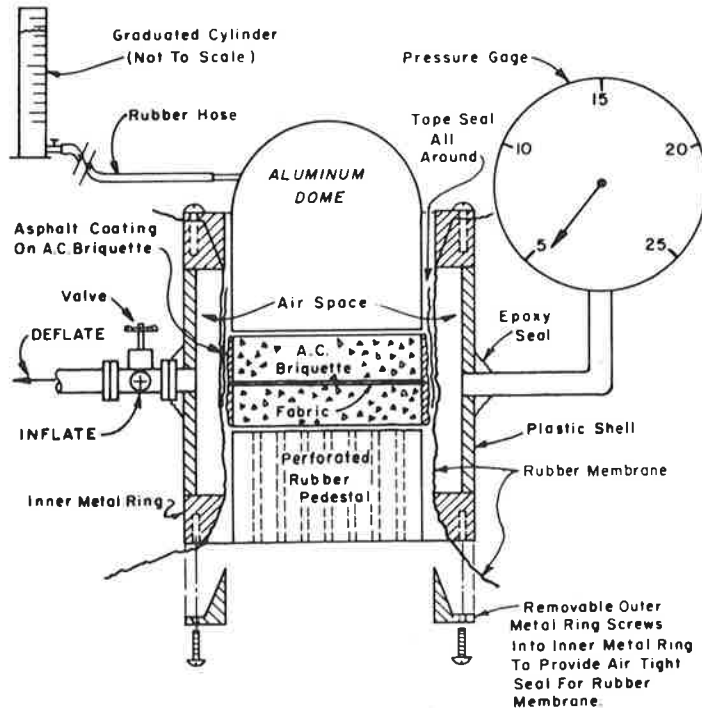


Table 2. Permeability test results.

Interlayer Type	5 Minutes			10 Minutes		
	Specimen A	Specimen B	Specimen C	Specimen A	Specimen B	Specimen C
Petromat	10, 120	100, 60	180, 140	10, 180	140, 110	240, 220
Bidim C-22	125, 90	∞, ∞, ∞	290, 280, ∞ ^a	210, 160	∞, ∞, ∞	350, 380, ∞ ^a
Bidim C-34	130, 70	270, 150	100, 100	200, 120	290, 230	140, 175
TrueTex MG75	20, 20	100, 40, 10 ^a	70, 45	50, 30	200, 70, 20 ^a	100, 80
TrueTex MG100	85, 50	240, 30, 10 ^a	100, 30, 40 ^a	150, 80	350, 60, 20 ^a	150, 60, 70 ^a
Duraglass B-65	15, 20	30, 10	20, 0	30, 30	60, 20	30, 0
Q-Trans-50	70, 80	30, 20	100, 55	130, 130	60, 30	150, 110
Fibretex 200	90, 70	5, 0	230, 50, 120 ^a	160, 110	25, 5	310, 120, 90 ^a
Reepav 376	0, 0	0, 0	20, 5	5, 0	5, 0	30, 10
Nicofab B50	100, 50	110, 60	220, 130, 45 ^a	170, 90	180, 70	300, 95, 200 ^a
Amoco 4545	210, 30, 30 ^a	20, 10	255, 70, 180 ^a	260, 50, 50 ^a	35, 10	320, 135, 290 ^a
Trevira 1117	0, 0	0, 0	100, 220, 130 ^a	0, 0	0, 0	310, 170, 210 ^a
Bituthene	0, 0	0, 0	0, 0	0, 0	0, 0	0, 10
Polyguard	0, 0	0, 10	30, 60	5, 0	10, 10	75, 130
Tack coat only	0, 0	120, 150	20, 0	0, 0	190, 260	30, 0
Control	∞, ∞	∞, ∞	∞, ∞	∞, ∞	∞, ∞	∞, ∞

Note: All values shown are in milliliters of head drop.

^aThird replicate test where repeatability was poor.

^bNot tested in this specimen group.

Flexural Fatigue

Because of the severe stress-concentrating effect of a crack in an underlying pavement, flexural fatigue reflection cracking can occur with the repeated application of normal truck loads. Popular theories that attempt to explain why fabric might delay reflection cracking in these fatigue situations are as follows:

1. The fabric acts as a tensile element (similar to a reinforcing bar in PCC) to resist tensile crack formation and possibly even to reduce wheel load deflection; and
2. The tip of the old crack is effectively blunted by the relatively soft asphalt and fabric interlayer; thus the energy of the crack is dissipated and further growth is curtailed, or at least delayed.

Testing Discussion

To simulate the action of a rolling wheel load, a pneumatic flex-fatigue machine (Figure 8) was designed and built at TransLab to subject an AC beam specimen (Figure 9) to a realistically critical degree of bending. This machine simulates a rolling wheel load by applying the load by a series of four loading feet that "walk" across the beam in sequence (Figure 10).

At the same time that the flexural load is being applied, the beam specimen is subjected to an axial tensile load to simulate thermal-induced stress and create a realistic combined stress condition that should assure crack advancement through the entire beam cross section. The support for the beam specimen consisted of a simply-supported aluminum T-beam, on top of which was a 0.25-in.-thick rubber pad. This pad allowed Δ -vert movement in the specimen between loading feet.

The beam specimen itself (3x3x12 in.) consists of a top and bottom layer each 1.5 in. thick (Figure 9). In an effort to simulate age-hardened asphalt, Chemcrete was used for the top half of the beam. The bottom half was made of conventional AC (0.5-in. maximum aggregate). Fabric interlayers incorporated an appropriate AR-4000 asphalt tack coat.

A 0.125-in.-wide saw cut was then made in the bottom half of the beam specimen to a depth that left a remaining thickness of 1.75 in. This saw cut simulated a crack in an underlying pavement and was positioned between the middle two loading feet in

order to permit differential vertical movement (Δ -vert) and vertical shear stress development in the remaining beam cross section. It is believed that the use of a loading scheme that allowed this vertical shear stress development, in conjunction with flexural and axial tensile stresses, was a big step toward realism in laboratory fatigue testing of AC.

The force exerted by the loading feet on the beam was chosen to produce a maximum radius of curvature in the beam of approximately 125 ft. Early work by Dehlen (8) had found this to be a critical degree of curvature beyond which cracking could be expected in 1- to 2-in.-thick AC pavement. The load cycling frequency was 12 cycles/min (5 sec/cycle), as shown in Figure 11. Degree of curvature in the beam specimen was measured and recorded each time crack length was measured. The device used for measuring curvature is shown in Figure 12.

The axial tensile load applied to the beam specimen during the fatigue loading was 35 lb, which resulted from a machine setting of 5 psi-gauge-pressure (psig). The intent in selecting the magnitude of the tensile load was to use a low-range load that would ensure elimination of any top fiber compressive stress in the beam and promote cracking full-through the beam top half.

Throughout the course of each beam test, continuous autographic plots of flexural and axial loads versus time were compiled. Each specimen's plot provided a complete record of loading history.

Crack length measurements were made on the front and back faces of the specimen at regular intervals of 200 to 400 cycles by using a divider and an engineer's scale. The average of these two values was used in all analyses. Visibility of the crack was enhanced by coating both faces of the specimen with white spackling compound. The test was considered finished when the crack reached the top surface on both faces. All tests were run at room temperature, which varied within a range of 68° to 74°F.

Three beam specimens were tested for each interlayer treatment. Interlayer treatments tested were limited to various fabrics (a total of 12) and a heavy asphalt tack coat without fabric. Several control specimens (no interlayer treatment) were also tested.

Results

For each beam tested, a plot of crack length (c) versus number of loading cycles (N) was con-

structed. An average curve was constructed from the valid tests for each interlayer treatment. These average plots are shown in Figure 13.

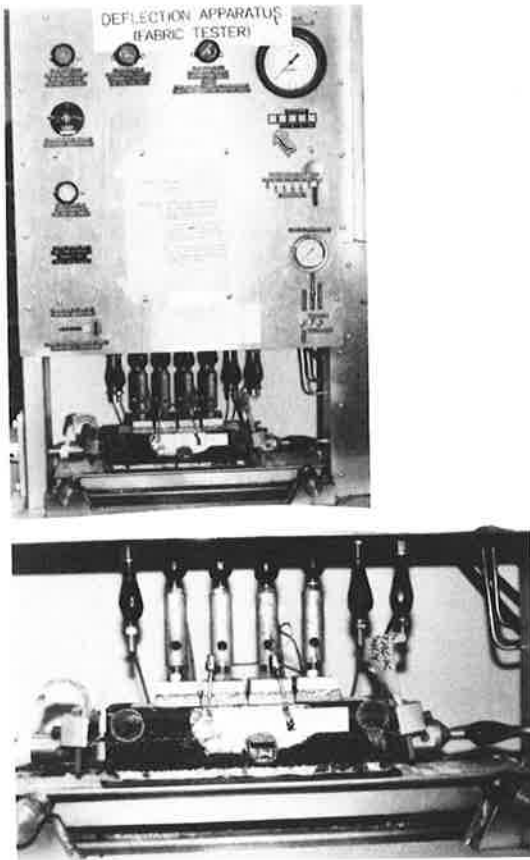
Beam specimen top-half mix properties were considered the most likely cause of the inconsistent fatigue performance. Therefore, a normalization study was undertaken wherein the mix properties (Table 3) of several identical beam specimens without fabric were determined in hope of divulging

normalizing factors that could be used to correct the c versus N curves.

Because none of these normalizing efforts was successful, it was concluded that the error must be random and could possibly have resulted from differences in aggregate arrangement and orientation. For simplicity of presentation, an average c versus N plot was constructed for valid tests of each interlayer treatment. The average plots are presented in Figure 13.

At the start of this project it was considered a top priority to maintain realism in all testing. A conventional AC mix was therefore used with extreme precaution taken to ensure consistency in mix variables and, it was hoped, to minimize this random type of error. It now appears that in order to avoid this error and to enable isolation of interlayer effects on fatigue life, further testing will be required by using a more homogeneous beam specimen. Therefore, a phase 2 fatigue investigation will be undertaken that involves beams made of a homogeneous sand-asphalt mix. In this study, as in phase 1, a hardened Chemcrete binder will be used to simulate aged AC pavement.

Figure 8. Flexural fatigue machine.



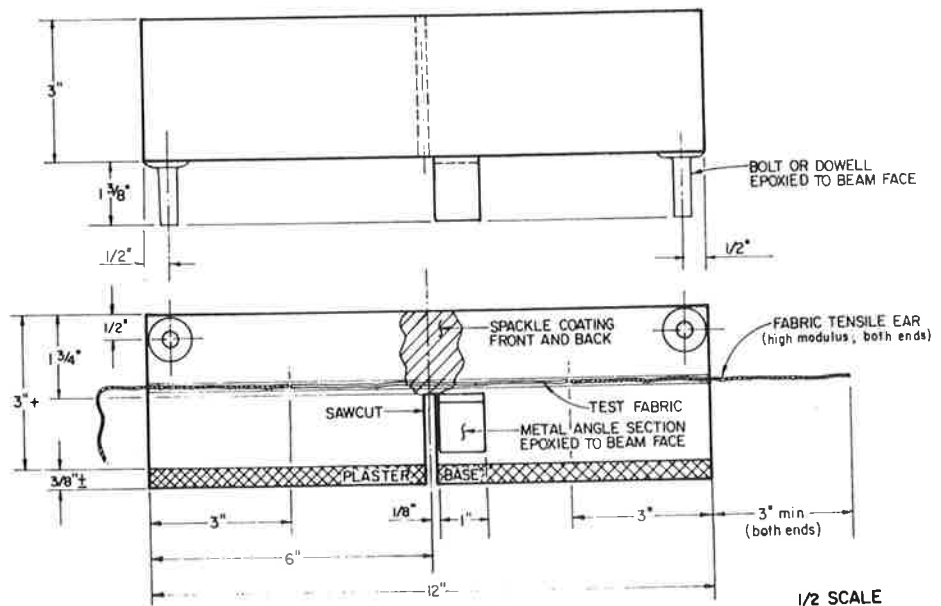
Interlayer Shear Strength

Whenever an AC overlay is placed on a discontinuous existing pavement--especially on PCC slab pavement--it will be subjected to tensile stresses induced by long and short-term thermal strain in the underlying pavement (1). Long-term strains are those associated with the slabs' slow thermal (expansion-contraction) response to seasonal changes, whereas short-term strains are those that result from diurnal slab curling cycles (8). These two effects are additive and time-varying to produce a net stress inducement in an overlay that can often cause reflection cracking.

Axial tensile stress can only be induced in the overlay if it is transferred across the interface between overlay and PCC slab. A condition of tight intimate bonding at this interface would theoretically provide the potential for 100 percent strain transfer. This condition should be realized at low temperatures.

An investigation was undertaken to determine the relation between interlayer shear strength and temperature for AC specimens with and without inter-

Figure 9. Flexural fatigue beam specimen.

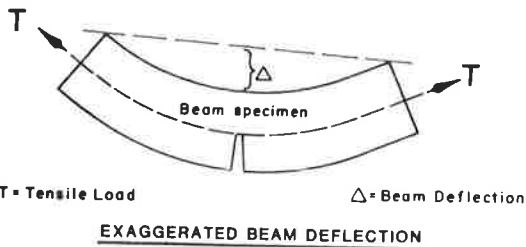
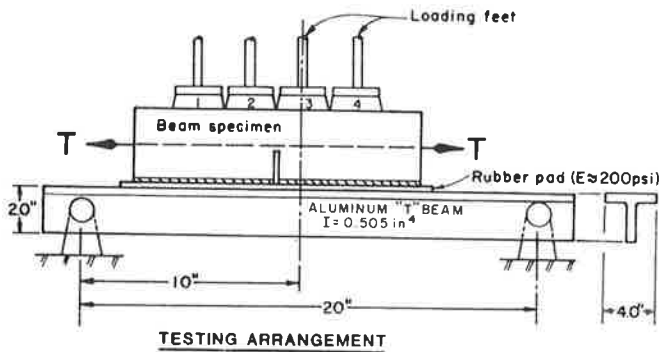


layer treatments. This information could then be used in the

1. Determination of the relative potentials for stress relief in the various interlayers,
2. Assessment of the relative effects of the various interlayers on the horizontal shear strength and slippage potential of the AC, and
3. Indication of the degree that overlay bond is affected by various interlayers.

Also, by using this shear strength information, an

Figure 10. Flexural fatigue testing arrangement.



NOTE :

Beam specimen is positioned so that loading feet 2 and 3 straddle the sawcut. This results in the specimen not being exactly centered on the support beam.

Figure 12. Measurement of degree of bending in beam specimen.

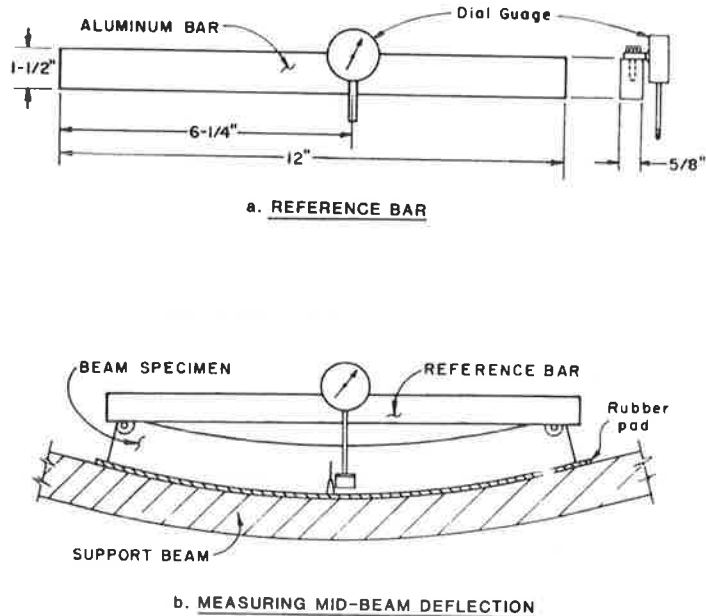
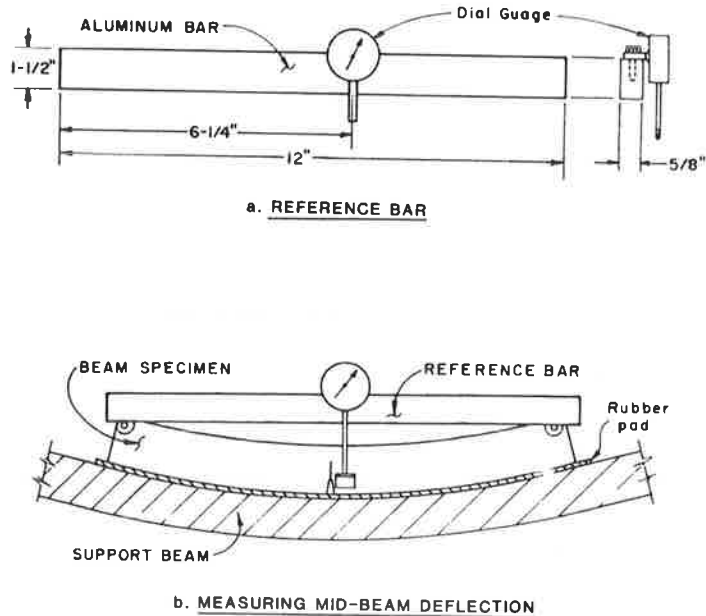


Figure 11. Loading cycle diagram for flexural fatigue test.



analysis can be made of the potential for slipping under wheel loads (9,10).

For the testing procedure of interlayer shear strength, 3x3x12-in. AC beam specimens from the flexural fatigue testing were cut roughly into quarters lengthwise. Two beams of each interlayer type were quartered to produce eight specimens with shear areas approximately 3x2.75 in. All shear tests were done on the apparatus shown in Figure 14, which was used in conjunction with a Baldwin 6,000-lb testing machine.

The bottom half of the specimen was clamped securely so that no rotational movement could take place. A vertical load was applied to the other (top) half of the specimen so that a shear force was created on the interlayer. A plot of head movement versus load was made for each specimen by using an X-Y plotter. The shear test was performed at five temperatures (-20°, 0°, 20°, 60°, and 100°F) at a shear rate of 0.05 in./min.

The ultimate shear load was recorded and divided by the interlayer cross-sectional shear area to obtain the ultimate shear strength. Shear strength versus temperature was then plotted for each interlayer. Finally, the average curve for each interlayer treatment was plotted to facilitate direct comparisons (Figure 15).

The following observations were made from the test results:

Figure 13. Averaged c versus N curves for each interlayer type.

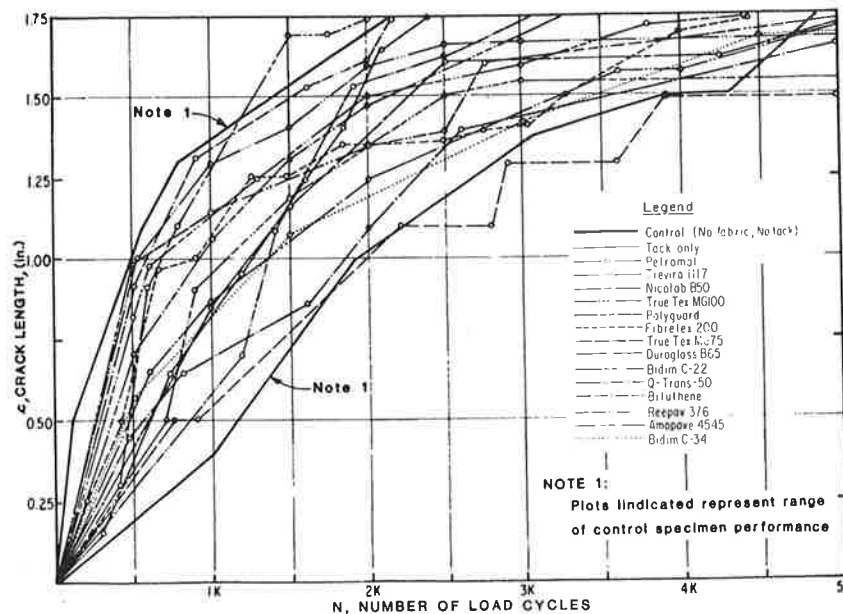


Table 3. Data used in normalization effort.

Specimen No.	Interlayer Treatment	Load Cycles at c = 1.0 in.	Properties of Top Half of Beam Specimen			
			Micro-viscosity ^a (MP)	Shear Susceptibility ^a	Bond Strength ^b (psi)	Air Voids ^c (%)
43	None	1,500	1,020	0.37	940	5
41	None	1,100	178	0.30	1,022	4
42	None	600	265	0.53	898	5
54	None	1,900	670	0.32	980	4
61	None	2,000	186	0.32	850	4
38	None	1,300	1,580	0.21	786	5
69	None	600	225	0.34	841	4
50	None	1,400	1,080	0.33	844	4
78	TrueTex (MG75)	1,900	680	0.42	1,005	6
79	TrueTex (MG75)	4,100	900	0.23	862	4
80	TrueTex (MG75)	600	920	0.32	944	6

^aCalifornia test method 348.
^bAASHTO test T177-68 (1978).
^cCalifornia test method 367.

1. For thin fabrics (Reepav and Petromat), the beam-to-beam difference was minimal, which suggested that 100 percent melt-through always occurred.

2. For thick fabrics (TrueTex MG75, Q-Trans-50, and Bidim C-34), the beam-to-beam shear strength difference was higher, which suggested that partial saturation can occur, thereby resulting in less satisfactory bonding and lower horizontal shear strengths.

3. Fabric interlayers reduced the shear strength of the AC by approximately 50 percent at any temperature (-20° to +100°F).

4. Membranes with a rubberized asphalt backing (Bituthene and Polyguard) did not weaken in shear by embrittling at low temperatures (down to -20°F).

5. Shear strength did not appear to be related to the weight or thickness of the fabric (assuming 100 percent saturation).

6. At temperatures greater than 100°F, all of the fabric interlayers tested had virtually no shear strength.

Differential Vertical Movement

Differential vertical movement (Δ -vert) at underlayer discontinuities (such as joints or cracks in overlaid PCC pavement) has long been known to be a major cause of reflection cracking in AC overlays

(11,12). Therefore an attempt was made to design a laboratory fatigue test whereby an aged AC specimen could be subjected to a vertical shear fatigue mode of loading. Specimens would be tested with and without interlayer treatments in an effort to understand what effect, if any, an interlayer such as fabric will have on an overlay's resistance to this type of reflection cracking.

Developmental testing by using the apparatus in Figure 16 is continuing at this time. Due to the erratic test behavior witnessed thus far, it is suspected that further refinements of the test method will be required, including the use of a specimen more than 2 in. thick.

Fabric Heat Resistance

Claims have been made that polypropylene fabrics, such as Petromat and Fibretex 200, are severely affected by temperatures greater than 300°F. Earlier tests that involved exposing a polypropylene fabric sample to oven temperatures around 300°F showed the fabric to shrink considerably, embrittle, and even disintegrate in some cases. Oven testing, however, does not simulate the true conditions a paving fabric will experience in service. First, soaking the fabric specimen in a hot oven provides a more severe thermal exposure than would be realized by a fabric under a hot overlay mix that is rapidly cool-

ing, at least in the immediate area of contact with the fabric. Second, in the overlay situation, the fabric quickly becomes saturated with the asphalt tack coat, which effectively insulates individual fiber strands from thermal extremes. Finally, the severe shrinkage of the fabric that is observed in oven testing is not realized in an overlay structure where the surrounding AC mat and the fabric's large area create a condition of full restraint. A simple test was therefore devised in an attempt to better simulate in-service conditions that a fabric experiences.

In TransLab's testing, a 6x6x2-in.-thick block of 325°F dense-graded AC (confined in a wood mold) was placed on a fabric specimen approximately 1 ft² resting on a wooden base block. No tack coat was used. A 1,500-lb load was then applied to the top of the hot AC block and held for 1 min. After removing the load and AC block, the fabric specimen was visually inspected for changes.

Petromat and Fibretex 200, the two polypropylene fabrics tested, showed no visible signs of damage or dimensional change. Some additional fusing of the individual fiber strands appears to be the only sign of change. This could possibly lead to a slight change of tensile strength or secant modulus.

Based on these findings, together with field observations, it was concluded that the claims of polypropylene's degradation as a result of heat exposure are not applicable to pavement overlay situations.

INTERIM CONCLUSIONS

Estimating Tack-Coat Requirements

1. The tack-coat application rate required by a paving fabric can be estimated if fabric thickness and weight are known or by using a simple motor oil retention test.

2. Saturation of the fabric by the asphalt tack coat usually requires the presence of heat and pressure.

Flexural Fatigue

1. In closely controlled fatigue testing of AC specimens, the random error associated with aggregate position and orientation is sufficient to mask fabric-related differences in fatigue life.

2. Paving fabrics do not appear to reduce the initial deflection of AC beams in laboratory testing. This suggests that a fabric interlayer is not a significant tensile reinforcing element in an AC pavement.

3. Fatigue crack growth through the AC beam specimens did not appear to be delayed by fabric interlayers.

Interlayer Shear Strength

1. The shear strength of interlayers that involve nonwoven fabrics is maximum in the 0° to +20°F range and virtually zero at more than +100°F.

2. Fabric interlayers reduced the horizontal shear strength of the AC by approximately 50 percent at any test temperature.

3. Membrane interlayers that have a rubber-asphalt backing (Bituthene and Polyguard) do not weaken in shear by embrittlement at low temperatures (down to -20°F).

4. Interlayer shear strength could not be correlated to fabric weight or thickness.

Interlayer Permeability

1. Fabric and asphalt interlayers can provide drastic reductions in the water permeability of AC.

2. An asphalt interlayer without fabric also provides a drastic reduction in the water permeability of AC.

3. Punch-through of the fabric by sharp-edged aggregate does not lead to increased permeability. The fabric interlayers apparently have a self-sealing effect.

4. No correlation was observed between a fabric's permeability as an AC interlayer and its physical and mechanical properties.

Figure 14. Interlayer shear test setup.

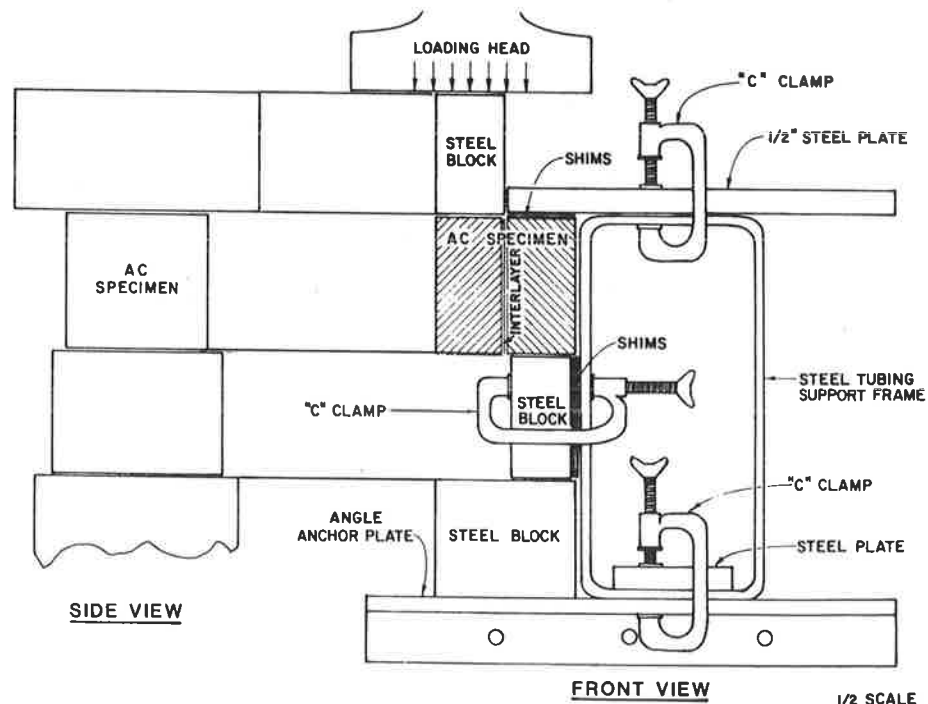


Figure 15. Average interlayer shear strength versus temperature.

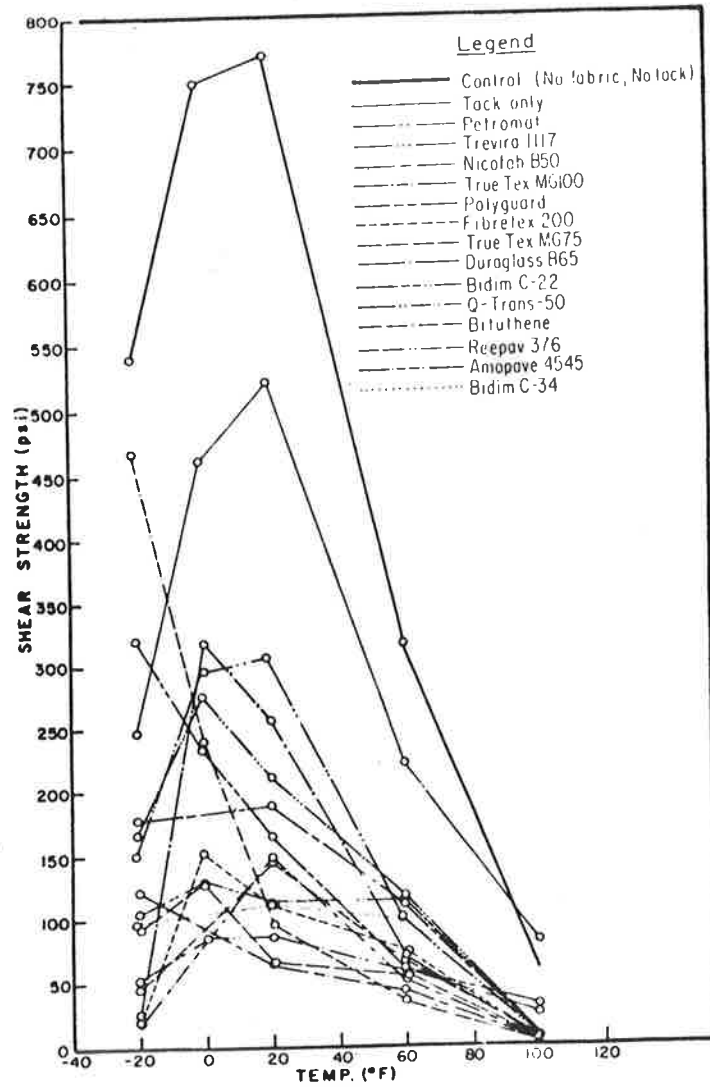
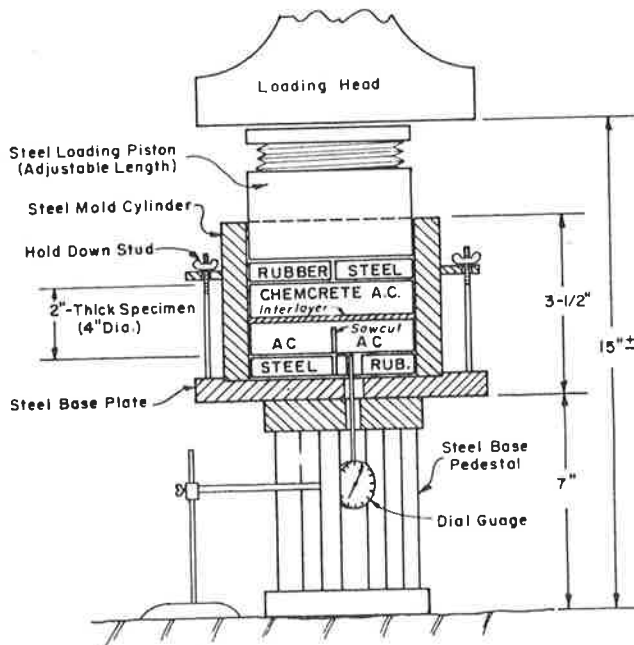


Figure 16. Shear fatigue test setup.



Differential Vertical Movement

Laboratory attempts to test the effect of Δ -vert on AC cracking were not successful. Therefore, a special gauge was developed for field measurement of Δ -vert.

Fabric Heat Resistance

Polypropylene and polyester fabrics do not appear to suffer adverse effects from being in contact with hot (325°F) AC mixes.

ACKNOWLEDGMENT

I wish to acknowledge the efforts of Tom Fellenz, assistant transportation engineer, Caltrans, who performed much of the specimen preparation, testing, and data analyses in connection with this study.

I also wish to acknowledge Brian Murray, associate transportation engineer, and Roy E. Steiner, machinist and instrument maker, for the design and construction of the flexural fatigue testing machine.

This research was funded as part of the Highway Research Program, FHWA.

Note that product brand names were used in this paper because of the comparative nature of the study and in the interest of presenting information meaningful to the reader.

REFERENCES

1. F.P. Germann and R.L. Lytton. Methodology for Predicting the Reflection Cracking Life of Asphalt Concrete Overlays. Texas Transportation Institute, Texas A&M Univ., College Station, Rept. 207-5, March 1979.
2. H.L. Draper and D.W. Gagle. Asphalt Pavement Laminated with Petromat Fabric. Phillips Petroleum Company, Greenville, SC, May 1972.
3. K. Majidzadeh. A Laboratory Investigation of the Use of Petromat for Optimization of Pavement Performance. Ohio State Univ., Columbus, Nov. 1976.
4. J.J. Roland. Beam Tests for Fabrics Used in Reduction of Reflection Cracking. Iowa Department of Transportation, Ames, April 1981.
5. C.D. Murray. Simulation Testing of Geotextile Membranes for Reflection Cracking. E.I. du Pont de Nemours and Company, Wilmington, DE, 1982.
6. R.W. Bushcy. Experimental Overlays to Minimize Reflection Cracking. California Department of Transportation, Sacramento, Sept. 1976.
7. Fabric Underseal Specification. Texas State Department of Highways and Public Transportation, Austin, Item 3099, Feb. 1978.
8. G.L. Dehlen. Flexure of a Road Surfacing, Its Relation to Fatigue Cracking, and Factors Determining its Severity. HRB, Bull. 321, 1962, pp. 26-39.
9. C.L. Monismith and N.F. Coetzee. Reflection Cracking Analyses, Laboratory Studies, and Design Considerations. Univ. of California, Berkeley, 1980.
10. J.A. Epps and J.W. Button. The Slippage Question on Airport Pavements. Texas Transportation Institute, Texas A&M Univ., College Station, Interim Rept. RF 3424-2, 1979.
11. H.J. Treybig and others. Overlay Design and Reflection Cracking Analysis for Rigid Pavements. FHWA, Rept. FHWA-RD-77-66, 1977.
12. K.H. McGhee. Efforts to Reduce Reflective Cracking of Bituminous Concrete Overlays of Portland Cement Concrete Pavements. Virginia Highway and Transportation Council, Charlottesville, 1975.

Publication of this paper sponsored by Task Force on Engineering Fabrics.

Reflection Cracking Models: Review and Laboratory Evaluation of Engineering Fabrics

KAMRAN MAJIDZADEH, GEORGE J. ILVES, AND MICHAEL S. LUTHER

A review of recent theoretical models for analyzing reflection cracking in pavements is presented. Four models are applicable to asphalt overlays of jointed-concrete pavements, and one model deals with asphalt overlays of existing flexible pavements. Both mechanistic and phenomenological models are reviewed, together with a critique of each model's shortcomings. A two-dimensional finite-element analysis of flexible overlay stress for jointed-concrete slabs subjected to seasonal and daily temperature changes is presented. The analysis shows that, contrary to some existing models, curling temperature gradients (cold or slab surface relative to bottom) produce joint openings that induce only tension stress in the overlay. A technique is presented for equating daily (curling) thermal loads to seasonal thermal loads in terms of equivalent maximum overlay stress. The finite-element analysis suggests that a reflection cracking model must consider the ratio of loading and temperature dependency of the asphalt overlay modulus in any stress calculation. Laboratory testing is currently being conducted to verify reflection cracking models and assess performance of geotextiles and stress-absorbing membrane interlayer systems to reduce cracking.

Reflection cracking is the cracking of a resurface or overlay above underlying cracks or joints. It occurs in overlays of both flexible and rigid pavements and is a major cause of distress; it includes spalling, surface water infiltration to underlying layers, and a general reduction in structural stiffness. Reflective cracks require continued future maintenance for crack sealing and patching and thus are a significant expense item.

Reflection cracking is not a new engineering problem. Since the early 1950s many different materials, methods, and techniques have been tried to prevent or at least delay reflection cracking. Most of these efforts have been for an asphalt concrete (AC) overlay on existing portland cement concrete (PCC) slab applications, where existing cracks or

joints are usually reflected through the overlay within a year (1). Early research recognized that the probable cause of reflection cracking was movement of some form in the underlying pavement at existing cracks and joints. This movement can result from both traffic- and environment-induced forces, and includes differential vertical movement, thermal- or moisture-induced expansion, contraction, or distortion (curling) at underlying joints and cracks.

Because the overlay is bonded to the existing pavement, movement at underlying joints or cracks induces stresses in the overlay. Sufficiently high stresses can cause fracture or cracking of the overlay. If the induced stresses do not exceed the yield strength of the overlay material, cracking could still develop as the result of cyclic load applications that produce fatigue fracture of the AC. Bond breakers, cushions, rubber-asphalt stress-absorbing membrane interlayers (SAMIs), fabrics, and stronger overlays modify the existing pavement and are among the methods that have been used in an attempt to mitigate the reflection cracking problem.

The literature indicates that reflection cracking studies and field experiment projects to date have generally been of an empirical nature, with little control or identification of the parameters known to affect cracking. Characterizing the existing pavement in terms of joint width, load transfer, crack spacing, crack and joint opening under known temperatures, and deflection under load are usually not part of such studies. Obviously, certain crack-prevention treatments are sensitive to some of these factors, as demonstrated in numerous field studies.

REFERENCES

1. F.P. Germann and R.L. Lytton. Methodology for Predicting the Reflection Cracking Life of Asphalt Concrete Overlays. Texas Transportation Institute, Texas A&M Univ., College Station, Rept. 207-5, March 1979.
2. H.L. Draper and D.W. Gagle. Asphalt Pavement Laminated with Petromat Fabric. Phillips Petroleum Company, Greenville, SC, May 1972.
3. K. Majidzadeh. A Laboratory Investigation of the Use of Petromat for Optimization of Pavement Performance. Ohio State Univ., Columbus, Nov. 1976.
4. J.J. Roland. Beam Tests for Fabrics Used in Reduction of Reflection Cracking. Iowa Department of Transportation, Ames, April 1981.
5. C.D. Murray. Simulation Testing of Geotextile Membranes for Reflection Cracking. E.I. du Pont de Nemours and Company, Wilmington, DE, 1982.
6. R.W. Bushcy. Experimental Overlays to Minimize Reflection Cracking. California Department of Transportation, Sacramento, Sept. 1976.
7. Fabric Underseal Specification. Texas State Department of Highways and Public Transportation, Austin, Item 3099, Feb. 1978.
8. G.L. Dehlen. Flexure of a Road Surfacing, Its Relation to Fatigue Cracking, and Factors Determining its Severity. HRB, Bull. 321, 1962, pp. 26-39.
9. C.L. Monismith and N.F. Coetzee. Reflection Cracking Analyses, Laboratory Studies, and Design Considerations. Univ. of California, Berkeley, 1980.
10. J.A. Epps and J.W. Button. The Slippage Question on Airport Pavements. Texas Transportation Institute, Texas A&M Univ., College Station, Interim Rept. RF 3424-2, 1979.
11. H.J. Treybig and others. Overlay Design and Reflection Cracking Analysis for Rigid Pavements. FHWA, Rept. FHWA-RD-77-66, 1977.
12. K.H. McGhee. Efforts to Reduce Reflective Cracking of Bituminous Concrete Overlays of Portland Cement Concrete Pavements. Virginia Highway and Transportation Council, Charlottesville, 1975.

Publication of this paper sponsored by Task Force on Engineering Fabrics.

Reflection Cracking Models: Review and Laboratory Evaluation of Engineering Fabrics

KAMRAN MAJIDZADEH, GEORGE J. ILVES, AND MICHAEL S. LUTHER

A review of recent theoretical models for analyzing reflection cracking in pavements is presented. Four models are applicable to asphalt overlays of jointed-concrete pavements, and one model deals with asphalt overlays of existing flexible pavements. Both mechanistic and phenomenological models are reviewed, together with a critique of each model's shortcomings. A two-dimensional finite-element analysis of flexible overlay stress for jointed-concrete slabs subjected to seasonal and daily temperature changes is presented. The analysis shows that, contrary to some existing models, curling temperature gradients (cold or slab surface relative to bottom) produce joint openings that induce only tension stress in the overlay. A technique is presented for equating daily (curling) thermal loads to seasonal thermal loads in terms of equivalent maximum overlay stress. The finite-element analysis suggests that a reflection cracking model must consider the ratio of loading and temperature dependency of the asphalt overlay modulus in any stress calculation. Laboratory testing is currently being conducted to verify reflection cracking models and assess performance of geotextiles and stress-absorbing membrane interlayer systems to reduce cracking.

Reflection cracking is the cracking of a resurface or overlay above underlying cracks or joints. It occurs in overlays of both flexible and rigid pavements and is a major cause of distress; it includes spalling, surface water infiltration to underlying layers, and a general reduction in structural stiffness. Reflective cracks require continued future maintenance for crack sealing and patching and thus are a significant expense item.

Reflection cracking is not a new engineering problem. Since the early 1950s many different materials, methods, and techniques have been tried to prevent or at least delay reflection cracking. Most of these efforts have been for an asphalt concrete (AC) overlay on existing portland cement concrete (PCC) slab applications, where existing cracks or

joints are usually reflected through the overlay within a year (1). Early research recognized that the probable cause of reflection cracking was movement of some form in the underlying pavement at existing cracks and joints. This movement can result from both traffic- and environment-induced forces, and includes differential vertical movement, thermal- or moisture-induced expansion, contraction, or distortion (curling) at underlying joints and cracks.

Because the overlay is bonded to the existing pavement, movement at underlying joints or cracks induces stresses in the overlay. Sufficiently high stresses can cause fracture or cracking of the overlay. If the induced stresses do not exceed the yield strength of the overlay material, cracking could still develop as the result of cyclic load applications that produce fatigue fracture of the AC. Bond breakers, cushions, rubber-asphalt stress-absorbing membrane interlayers (SAMIs), fabrics, and stronger overlays modify the existing pavement and are among the methods that have been used in an attempt to mitigate the reflection cracking problem.

The literature indicates that reflection cracking studies and field experiment projects to date have generally been of an empirical nature, with little control or identification of the parameters known to affect cracking. Characterizing the existing pavement in terms of joint width, load transfer, crack spacing, crack and joint opening under known temperatures, and deflection under load are usually not part of such studies. Obviously, certain crack-prevention treatments are sensitive to some of these factors, as demonstrated in numerous field studies.

Figure 1. Bending of overlay by joint vertical movement.

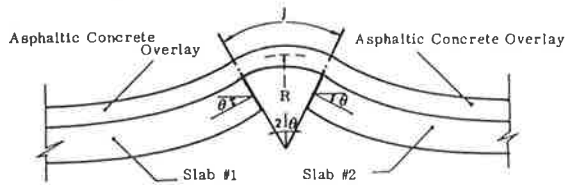
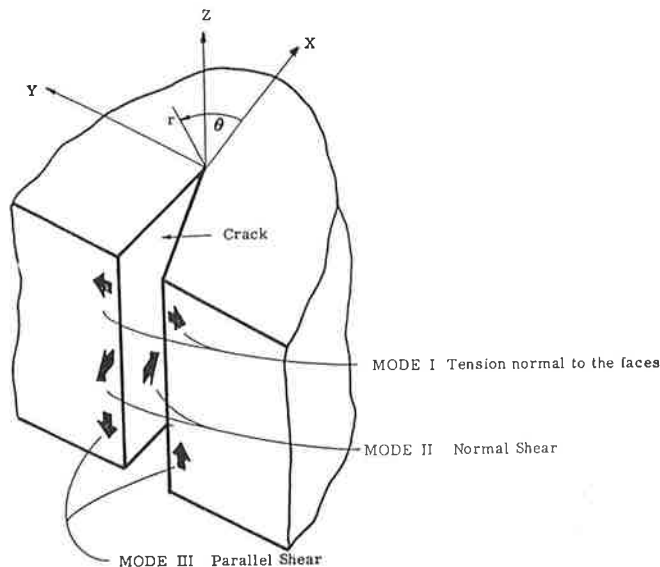


Figure 2. Modes of crack deformation.



Past research, however, has not established quantitative relations between these factors and the success or failure of preventative techniques.

EVALUATION OF EXISTING REFLECTION CRACKING MODELS

Within the past decade several theoretical (mathematical) models have been developed to analyze and predict the occurrence of reflection cracking. All of these models consider the same mechanisms noted above (e.g., reflection cracking is caused by differential horizontal or vertical movements in the underlying layer). The models differ in the methods used to predict the magnitude of underlying layer movements, the magnitude of stresses induced in the overlay by such movements, and the response of the overlay to stress state (sudden failure versus fatigue fracture). Currently existing models are summarized in the following sections, and evaluations of each model's limitations are presented.

Ultimate Strength Model--Ohio State University

The ultimate strength model developed at Ohio State University (OSU) (2) is a nomograph procedure for predicting AC overlay stresses on joints or cracks that result from thermal-induced movements in underlying PCC slabs. Separate stress analyses are performed for horizontal slab movements (i.e., due to seasonal changes in average slab temperature) and vertical slab movements that occur due to slab curling (i.e., the temperature state where the top of the PCC slab is colder than the bottom).

Horizontal movement of the PCC slab (d) for a change in slab temperature [T(°F)] is calculated by using an average value (f) for the friction coefficient, which is similar to calculations for deter-

mining temperature reinforcement in jointed reinforced-concrete pavements. Most importantly, this model neglects the resistance to joint movement provided by the uncracked overlay that is bonded by a tack coat to the underlying slab. The OSU model assumes that this resistance is small and that thin overlays do not affect joint movement due to temperature change. Inputs to a finite-element model to determine overlay stresses are the joint dimension, the thickness and modulus of elasticity of the overlay, and the slabs.

The effect of vertical movements on the overlay due to slab curling is also based on the premise that thin overlays do not significantly affect the curling of slabs. Thus the restraint against curling of the slabs provided by the uncracked overlay is again neglected. This important assumption permits the curved shapes of slabs to be predicted by using a computer simulation (PLATES program) of the Westergaard solution for temperature differentials between the top and bottom of the slab. Curling-induced overlay stresses are estimated on the assumption that the overlay takes the slope shown in Figure 1 (2).

For a joint width (j) and edge slopes (θ) calculated from the PLATES program (radians), the radius of curvature in the overlay can be estimated from

$$R = j/2\theta \tag{1}$$

In turn, overlay stresses can be calculated from

$$\sigma_{ov} = E_{ov}h_{ov}/j \tag{2}$$

where E_{ov} is the overlay stiffness, and h_{ov} is the overlay thickness.

Equation 2 is derived from the basic strength of materials for pure bending, i.e., $\epsilon(u) = u/R$, where $\epsilon(u)$ is the axial strain distance from the neutral axis, and R is the radius of curvature. Because Equation 2 is derived from pure bending, symmetric bending of the overlay, where there is tension at the top and compression at the bottom, is implied.

The OSU ultimate strength model presents an easy nomograph procedure for determining overlay stresses from thermal movements of underlying PCC slabs. However, the accuracy of the stress computation is suspect due to the following factors:

1. Restraint imposed by the uncracked overlay against slab movements (horizontal and curling) is not considered. Thus the calculated force in the overlay at the time of cracking is probably incorrect.
2. Overlay stresses due to horizontal joint movement appear low and should be validated by additional finite-element investigation.
3. The tack-coat bonding-stress values are also low and should be established by a laboratory investigation that considers temperature, tack-coat type and amount, and roughness of the PCC slab.
4. The Westergaard analysis used to predict slab curling neglects the weight of the slab and overlay, which would reduce the curl.
5. The simplistic analysis of overlay stresses due to curling should be verified by finite-element analysis. The fact that curling introduces a horizontal joint opening is neglected by the analyses. This horizontal movement could be significant and change the stress state considerably.
6. The model is incapable of assessing effects of crack-prevention measures on stresses in the overlay.
7. The model does not make recommendations for

selecting design parameters such as temperature change, curling, AC modulus, and AC strength.

Ultimate Strength Model--Austin Research Engineers

Austin Research Engineers (ARE) developed a procedure for reflection crack stress or strain analysis that considers two different failure modes (3). The first is an opening mode [Figure 2 (4)], which is due to horizontal movements of the underlying PCC slab that result from seasonal temperature reduction. Joints or cracks without steel reinforcement, or cracks with steel reinforcement [such as a continuously reinforced-concrete pavement (CRCP)], can be analyzed for horizontal movement. The second mode is a shearing mode (Figure 2) that results from differential deflection across the joint or crack as the traffic load moves across the discontinuity.

In developing the model, a number of assumptions were made, including (a) the materials are elastic in response, (b) temperature variations are uniformly distributed in the existing concrete slab (no curling), (c) concrete movement is continuous with slab length, and (d) movement is uniform with depth in a particular layer.

The ARE ultimate strength model has been computerized in a program called RFLCR to minimize difficulties in using the model. It is the most versatile procedure currently available because it can consider slab or overlay reinforcement, bond breakers, and granular cushions (shear failure analysis only). However, the simplifications in the model that permit strain calculations without the use of analytical computations for stress distribution have not been validated. This is the primary problem with the ARE model. Although force magnitudes may be reasonable, the assumed simplistic distribution of stresses within the overlay for both open and shear failure modes is suspect because no concentration of stresses at the joint tip are considered. Other, less significant problems with the ARE model include the following:

1. Characterization of the existing pavement by joint opening measurements over a certain temperature range cannot necessarily be extrapolated to a different design temperature range. For example, restraint exhibited between 70° and 50°F may not identify the restraint between 70° and 20°F.
2. The assumed value for bonding stress between the overlay and slab is important in the analysis because it establishes the gage length over which the overlay force at the joint is distributed. The suggested values need to be validated experimentally.
3. The concept that a bond breaker reduces overlay strain by merely increasing gage length for force transfer should be validated by analytical investigations of stress distribution.
4. Load transfer is determined from preoverlay measurements, and no adjustment is made for the effect of the overlay, which may be an important consideration. Also, load transfer is probably load and temperature dependent.
5. The temperature for determining dynamic modulus in the shear model is not specified, but according to the model a high temperature would be critical because larger strains would result. However, the allowable strain is likely to be temperature dependent.

Fracture Mechanics Model--OSU

Fracture mechanics has been used to develop a reflection cracking propagation model for asphalt overlays on PCC slabs (4,5). The model considers only traffic-induced fatigue cracking that results

from differential deflection at slab joints or cracks.

The first step in applying fracture mechanics principles was to identify the fracture mode(s) associated with crack initiation and extension (Figure 2). A finite-element stress analysis of full-scale pavements predicted that the asphaltic overlay would be in compression, thus leading to the conclusion that the opening mode (mode 1) type fracture does not occur. The computer analysis also predicted significant relative vertical displacement (mode 2) between the two concrete slabs when loaded at the edge of the load over the center of the crack position. These conclusions led to the hypothesis that load-induced reflection cracking is the result of general or mixed-mode fracture of the bituminous material that occurs under the simultaneous interaction of $-K_1$ (negative σ_x), K_2 , and K_3 . Laboratory testing of two- and three-dimensional model overlay pavements supported this hypothesis.

Sih's theory of fracture (6), which is based on the field strength of the local strain-energy density, was used to analyze mixed-mode crack propagation. The two fundamental hypotheses of crack extension in Sih's theory are

1. The crack will spread in the direction of maximum potential energy density or minimum strain-energy density, and
2. The critical intensity (S_{cr}) of this potential field governs the onset of rapid or brittle crack propagation.

In those cases where a fracture is not a rapid unstable process [i.e., the stress-intensity factor under an applied load condition does not exceed the critical stress-intensity factor, or the strain-energy-density factor (S_{min}) is less than the critical value (S_{cr})], slow, stable fatigue crack growth is presumed. Typically, crack growth laws relate the rate of change of crack length to the stress level or stress-intensity factor, such as

$$dc/dN = A(\Delta K)^n \quad (3)$$

For mixed-mode fracture, the OSU model uses the crack growth law in terms of the strain-energy-density factor along the direction of fracture (S_{min}):

$$dc/dN = B(\Delta S_{min})^n \quad (4)$$

The fatigue life, or number of load applications to produce a crack through the overlay, is given by

$$N_f = \int_{c_0}^{c_f} [1/B(\Delta S_{min})^n]^{dc} \quad (5)$$

where c_0 is the initial starter flow, and c_f is the crack length at which the overlay is considered failed (either the thickness or the length at which the critical $S_{min} = S_{cr}$ is reached, whichever is less). S_{cr} , B , and n are material constants derived from fatigue tests on asphaltic-concrete beams.

The OSU fracture mechanics model is not a complete method for predicting the occurrence of reflection cracking. An analytical method for computing stress-intensity factors and S_{min} (such as in the finite-element model) must be combined with a program that calculates fatigue life in an incremental fashion by using the growth law given in Equation 4. A nomograph procedure could be developed from this model, which would be similar to the nomograph procedure developed by Majidzadeh and others (7) for fracture mechanics predictions of load-associated fatigue cracking in flexible pave-

ments. Thus further development of the OSU fracture mechanics model is necessary before it could be implemented by pavement engineers.

Fracture Mechanics Model--Texas Transportation Institute

The Texas Transportation Institute (TTI) fracture mechanics model also uses fracture mechanics crack-propagation theory to predict cracking. Only mode I fracture and, therefore, the K_I stress-intensity factor induced by horizontal thermal movements of the underlying layer are considered. However, rather than the simple crack growth law given in Equation 3, the TTI model uses Schapery's theory on crack growth in viscoelastic materials to develop the following growth law (8):

$$dc/dN = Bt (\Delta K)^{2(1+1/m)} \quad (6)$$

where

$$B_t = (\pi/6\sigma_m^2 I_1^2) [(1-\nu^2)D_2/2\Gamma]^{1/m} \left[\int_0^{\Delta t} W(t)^{2(1+1/m)} dt \right] \quad (7)$$

where

- ν = Poisson's ratio,
- σ_m = maximum tension strength the AC mixture can sustain,
- I_1 = dimensionless integral between 0 and 2,
- Δt = period of the load cycle,
- $W(t)$ = wave shape of stress-intensity factor,
- m = slope of straight-line portion of tension creep compliance curve for the AC binder,
- D_2 = intercept of straight line with $\log t = 0$ on creep compliance curve, and
- Γ = fracture energy density (force times displacement) to produce a unit area of crack surface.

The TTI model is also not a complete procedure for predicting the occurrence of reflection cracking. It is a technique for obtaining crack growth laws without having to perform fatigue tests. Fatigue life is then obtained by integrating Equation 6 from the limits of c_0 to c_f , which is similar to Equation 5 in the OSU fracture mechanics model. The limitations of the OSU fracture mechanics model are applicable to the TTI model.

Phenomenological Model

Resource International, Inc. (RII) developed a phenomenological model for crack prediction in overlaid flexible pavements that are reinforced by placement of engineering fabrics on the existing surface before placement of the overlay. The model considers only traffic load stresses in predicting the fatigue life of the overlaid pavement, and it has been used in the design of the RII computer program.

This model was established after extensive laboratory testing that established the relation between the fatigue life of reinforced and normal or unreinforced AC beams. All fatigue tests were beams on elastic foundations that were tested at a constant load at 70°F. The performance factor of the fabric in enhancing fatigue or delaying reflective cracking is called the fabric effectiveness factor (FEF), i.e.,

$$FEF = N_f \text{ reinforced} / N_f \text{ unreinforced} \quad (8)$$

where FEF is the ratio of fatigue lives obtained from the beam tests. The range of FEF is generally between 4 and 8, depending on stress level, placement depth within the beam, and fabric type.

The FEF function is expressed as

$$FEF = a_1 (\epsilon_h)^{a_2} \cdot \text{GEO} \quad (9)$$

where

- a_1, a_2 = constants, depending on fabric type;
- ϵ_h = horizontal strain at the bottom of the existing asphalt-bound layer (in./in.); and
- GEO = geometry factor that considers depth of fabric placement relative to neutral axis depth.

The fatigue life of the pavement in the design computer program (HWYPAV) is

$$N_f = N_{f_u}' (\text{FEF}) \quad (10)$$

where N_{f_u}' is a strain-dependent distress function for AC developed from AASHO Road Test data.

Cracking of the existing pavement is accounted for by reducing the elastic modulus of this layer. HWYPAV uses the elastic multilayer program ELSYM5 to calculate pavement strains.

The RII model has the following limitations:

1. Because the model is phenomenological, the mechanics of crack propagation and crack arrest are not identified.
2. FEF values need to be investigated to determine if they are temperature or scale dependent. FEF values were established from small beam tests and may differ from those under full-scale conditions.

DEVELOPMENT OF A LABORATORY MODEL

Simulation of reflective cracking of rigid pavement overlays requires modeling of both thermal and traffic loading conditions. As previously noted, thermal stresses result from both seasonal and daily changes in slab temperature. Thermal loading can be represented by the superposition of two different thermal conditions:

1. Uniform change (ΔT) in slab temperature, which represents seasonal changes in average slab temperature that occur over long time periods, and
2. Pure curling, which represents the daily or short time period temperature variation within the slab. [Pure curling means that the average slab temperature has not changed; however, the top of the slab is colder than the bottom, and the temperature is assumed to be linearly related to slab depth. The curling gradient (CG) is given in degrees Fahrenheit per inch of slab depth.]

A representation of thermal loading by using the above definitions is shown in Figure 3. The reference temperature (T_R) is the zero-stress temperature for the overlay. Slab temperatures less than T_R will transfer stresses to the overlay. The expected monthly average slab temperature and curling gradient for overlaid concrete slabs in Ohio are shown in Figure 4 (2). This figure is based on a computer prediction of pavement temperature developed from field temperature measurements on several pavements in central Ohio (2). Slab thickness varied from 8 to 10 in., and asphalt overlay thickness varied from 2.5 to 5.0 in. for the Ohio study pavements. Figure 4 estimates thermal load magnitudes. Expected CG varied from 0.5°F/in. in spring and fall to about 1.0°F/in. in winter. Mean slab temperature changes by about 40°F from summer to winter, dropping at a rate of about 8°F/month

Figure 3. Example of PCC slab thermal loading.

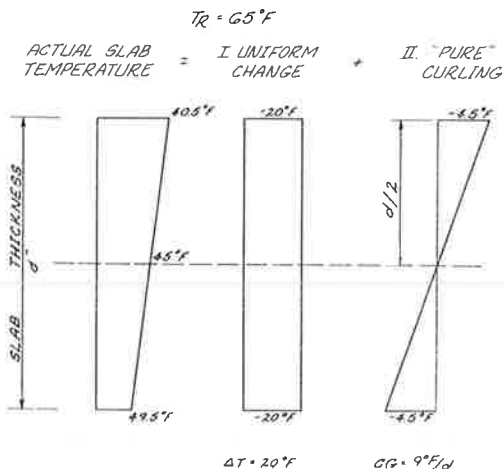
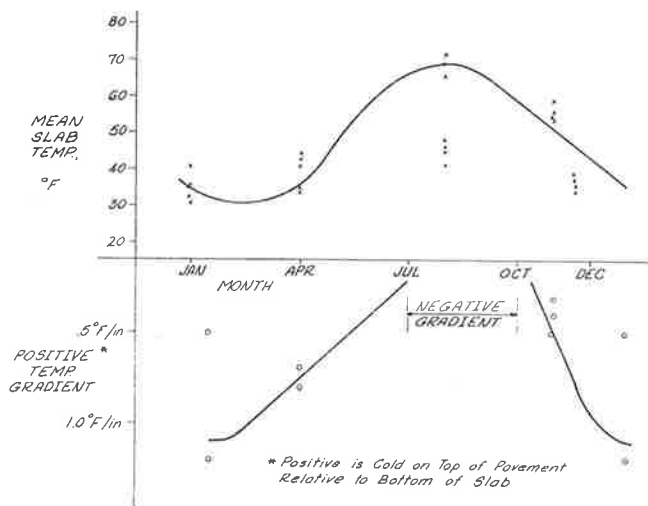


Figure 4. Expected seasonal pavement and CG temperature.



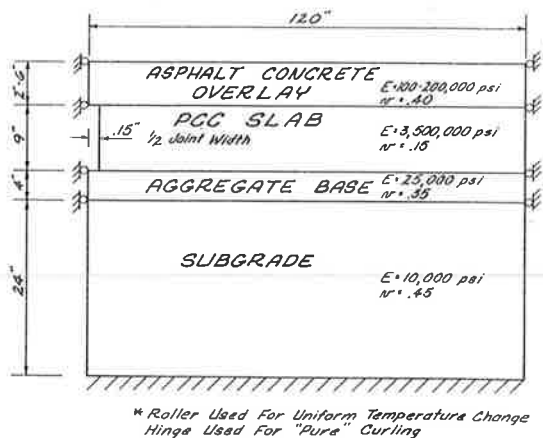
during the fall. This range of thermal loading parameters should be simulated in laboratory testing.

To manufacture and subject full-scale pavement models to actual thermal loads as experienced in the field is not economically feasible in the laboratory. Thus model pavements are used that have external forces applied to produce joint movements equal to those of full-scale pavements under field thermal loading. Uniform or seasonal reductions in slab temperature are simulated by applying horizontal tensile forces to the PCC slabs to produce joint openings similar to those of full-scale pavements. Traffic forces are simulated by applying dynamic vertical loads to the model pavements, with the model supported on elastic foundation, which is similar to previous OSU studies (5,7).

The most difficult simulation is curling of the PCC slab. Recent studies at the University of California and the Portland Cement Association were not successful in inducing temperature curling of model PCC slabs. Thermal gradients are difficult to establish in the laboratory, and the gradients necessary to curl model slabs of short length have to be large in order to produce the same curled shape as full-scale slabs because the curling deformation is directly proportional to slab length squared (L^2).

A theoretical investigation of curling in full-

Figure 5. Schematic of two-dimensional finite-element model.



scale slabs was conducted because of the difficulties in modeling curling and the shortcomings of the OSU ultimate strength model in predicting the significance of overlay stresses that result from slab curling. The purpose of this investigation was to determine the overlay stresses produced by curling and to determine if curling could be equated to uniform temperature change: Does curling produce horizontal joint openings and, if so, could these stresses be equated to joint openings that result from a uniform temperature change (ΔT)?

A two-dimensional finite-element analysis that used the SAP IV program of the full-scale pavement shown in Figure 5 was conducted. As shown in Figure 5, only asphalt overlay modulus and overlay thickness were varied in these analyses. The slab length was 20 ft in all cases. Two separate thermal loading conditions were analyzed: a uniform reduction (ΔT) of 30°F in slab temperature, and a pure CG of 0.5°F/in. Overlay stresses and joint openings were found to be linearly related to ΔT and CG for constant overlay thickness and modulus. Both full friction (no slip) and no friction (slip) between the PCC slab and aggregate base were investigated. Full friction reduced overlay maximum stress by less than 6 percent for a uniform temperature change and 4 percent for curling when compared with the no-friction condition. Full bond was assumed between asphalt overlay and PCC slab in all cases.

Computed stresses in the overlay at the center of the joint as a function of depth (Z) are shown in Figures 6-8. In all cases, for both curling load and uniform temperature change, maximum stress occurs at the bottom of the overlay. The stress distributions are similar for the uniform temperature change and curling loading conditions. The similarities occur throughout the range of overlay thickness and overlay modulus investigated. (Note that a ΔT of 3°F was used to plot Figures 7 and 8b simply to provide stresses of closer magnitude to those of the curling load. Recall that stress is linearly related to ΔT .) Figures 6 and 8a show that, for curling load, the overlay stress at the joint in the horizontal (X) direction is in a tensile state throughout overlay depth and rapidly increases in magnitude below 0.6 times the overlay thickness.

The computed shear stress at the overlay-slab interface is shown in Figure 9. Again, the stress distributions are similar for the two loading conditions. These shear stresses would have to exceed the tack-coat bonding stress to cause slippage between the two layers. The maximum shear stresses are greater than the 6- to 10-psi bonding stress

Figure 6. Overlay stress for curling load.

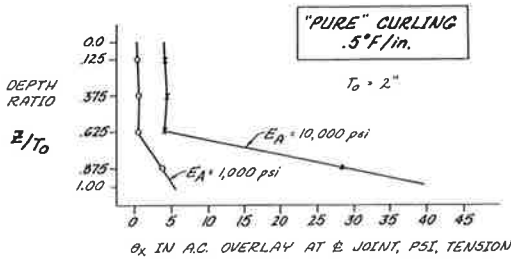


Figure 7. Overlay stress for uniform temperature.

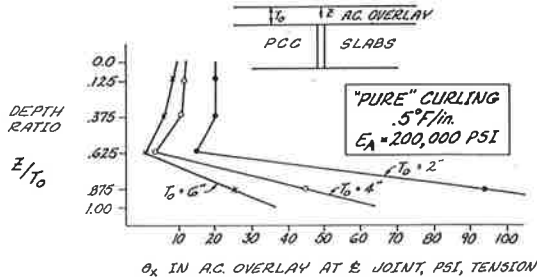


Figure 8. Overlay stress versus modulus.

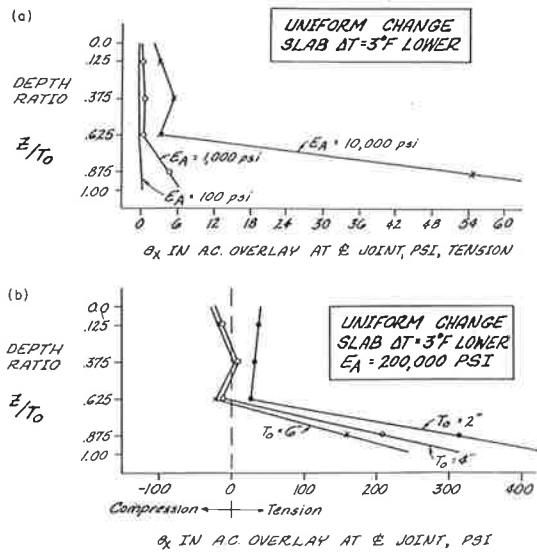


Figure 9. Overlay stress versus distance from joint.

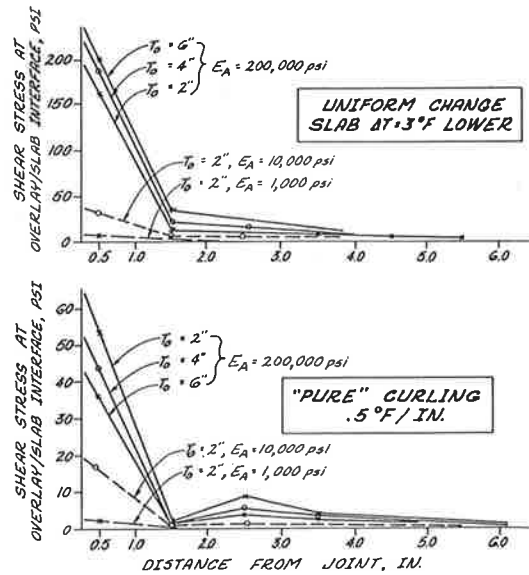
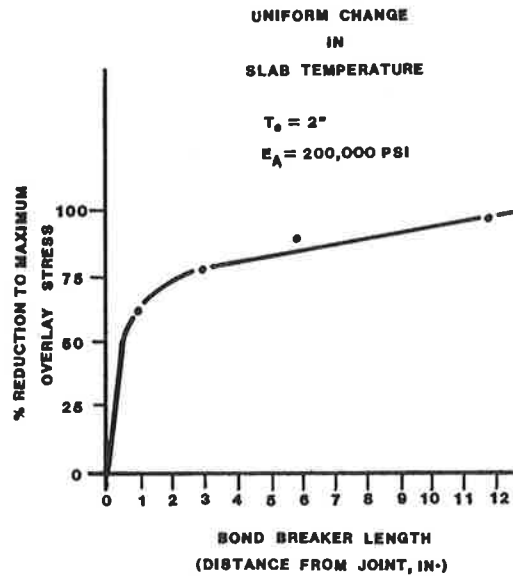


Figure 10. Overlay stress versus bond-breaker length.



suggested by Majidzadeh and Suckarieh (2), but are generally less than those given by ARE (3).

The effect of breaking the bond, either by slip-page or by the introduction of a bond breaker on maximum overlay stress is shown in Figure 10. A dramatic reduction in stress is predicted for bond-breaker lengths as short as 1 in. The data in Figure 10 indicate that the ARE model, which uses the bond-breaker length to increase the gage length for the overlay stress calculation, probably underestimates the stress reduction by a significant amount. Bond between overlay and slab will be an important parameter in laboratory testing. The data in Figure 10 indicate that improper bonding near the joint can significantly affect test results.

The high sensitivity of overlay stress to overlay stiffness is clearly illustrated in Figure 11. As noted earlier, the ARE model suggests that creep

modulus (E_c) be used for stress calculations. However, E_c is both temperature and loading time dependent. Figure 12 presents this dependency for a typical dense-graded AC with E_c calculated by the Heukelom and Klomp (Shell) method (9). This procedure determines the compressive creep modulus.

The tensile creep modulus is needed for reflection cracking analysis, but no procedure for predicting this parameter has been published. If tension creep modulus curves are similar to those in Figure 12, then the implications for thermal reflection cracking analysis and modeling are significant. An incremental analysis that uses the loading time and temperature-dependent creep modulus would be necessary in order to calculate overlay stresses and joint opening. Seasonal changes occur over long periods of time (time required to drop from T_R by a ΔT amount), whereas curling can occur over relatively short time periods (less than half a day) and at all temperatures. The fact that curling oc-

occurs over shorter loading times than seasonal uniform temperature change means that a higher E_c should be used for curling load than for uniform temperature change stress calculations. The higher E_c will result in higher overlay stresses that

should be considered when comparing seasonal and curling-induced loading conditions.

The data in Figure 11 can be used to compare the two thermal loading conditions. The data in Figure 12 indicate that in the fall (50° to 55°F) an E_c of

Figure 11. Overlay stress versus modulus.

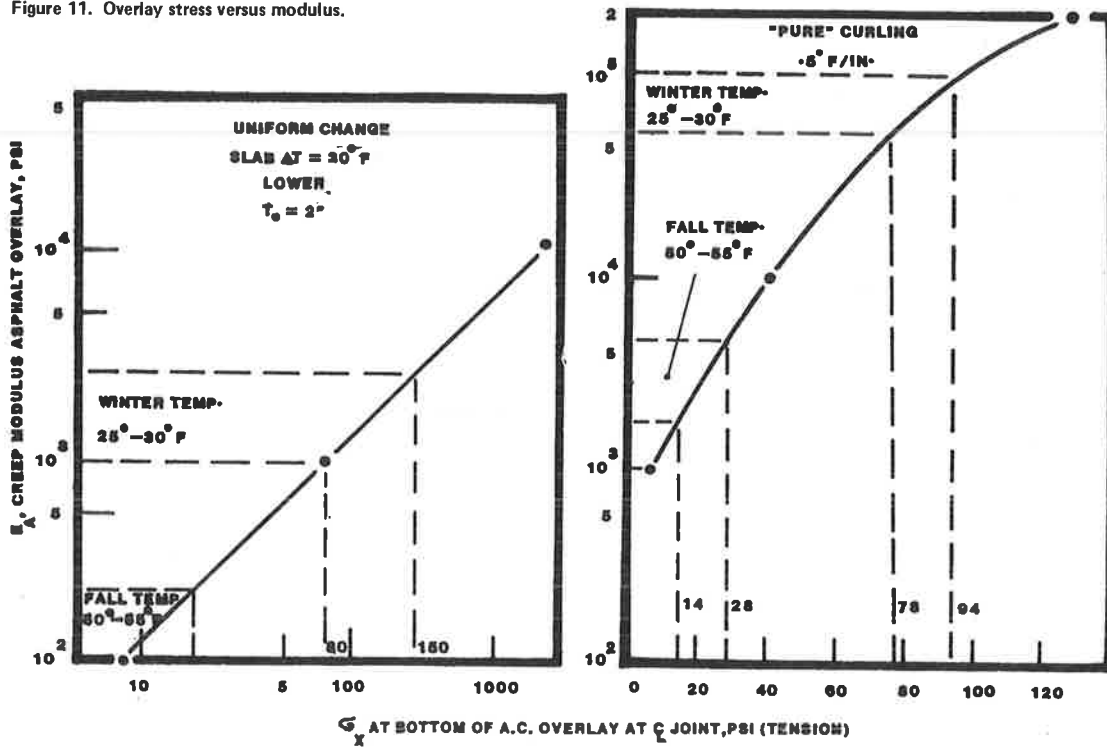


Figure 12. Creep modulus versus time and temperature.

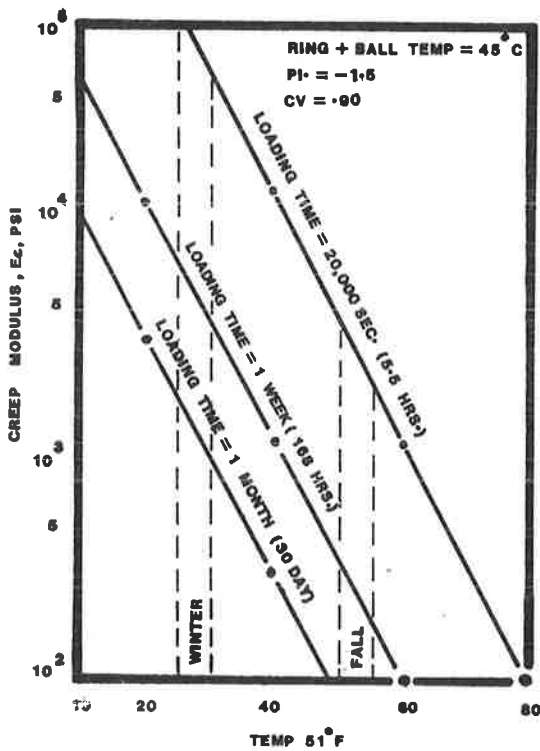


Figure 13. Joint opening versus modulus.

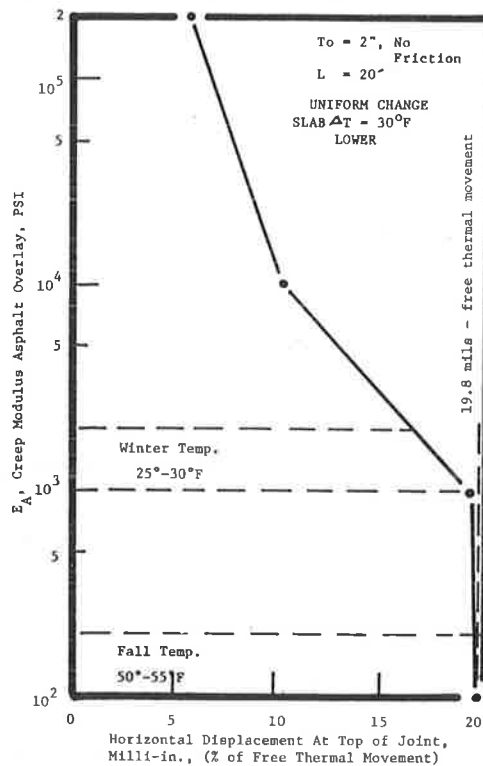
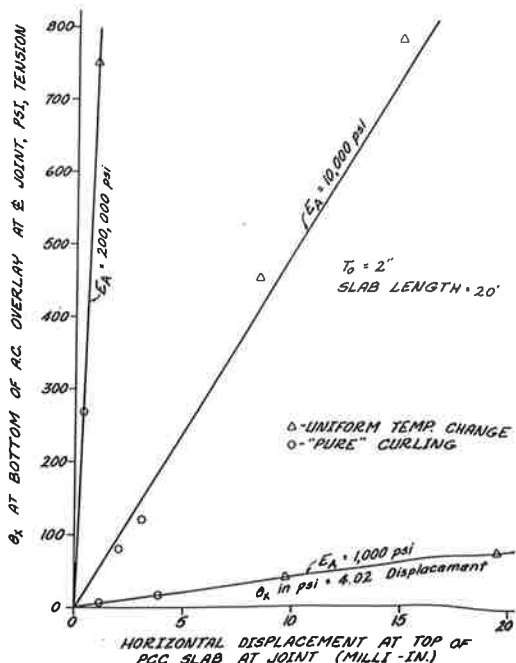


Figure 14. Overlay stress versus joint opening.



100 to 200 psi is obtained for a uniform slab temperature change (1 month loading time) and an E_c of 2,000 to 5,000 psi (5.5-hr loading time) is obtained for curling loading. According to the data in Figure 11, the curling load would produce a stress of about 21 psi, whereas the uniform temperature change ($\Delta T = 30^\circ F$) produces a stress of about 12 psi. On the basis of equal maximum overlay stress, the two loading conditions can be equated by

$$CG = (\sigma_x \text{ curl} / \sigma_x \text{ seasonal}) (\Delta T); 0.5^\circ F/\text{in.} = 21 \div 12 (30) = 52.5^\circ F \tag{11}$$

Therefore a seasonal change of $52.5^\circ F$ would be required to produce the same overlay stress as curling with $CG = 0.5^\circ F/\text{in.}$ Similar analysis for winter temperature ranges (20° to $25^\circ F$) yields

$$0.5^\circ F/\text{in. curl} = 22.4^\circ F \text{ seasonal change} \tag{12}$$

Because both curling and seasonal change produce a joint opening that induces similar overlay stress distributions, it is reasonable to equate the two loading conditions in this manner. The ability to equate curling loads to seasonal changes is important because laboratory tests need not try to induce curling in the PCC slab. Uniform temperature changes will be simulated by applying horizontal tensile forces on the PCC slab to produce the joint opening. The amount of joint opening is a function of the ΔT and slab length (L) being simulated. Seasonal temperature change (ΔT) could be converted to equivalent CG by using equations similar to Equations 11 and 12. Therefore, simulated temperature conditions at the time of failure or cracking of the laboratory model could be expressed as either ΔT or CG at the test temperature for a full-scale slab of length L .

The relation between overlay modulus and predicted joint displacement for the finite-element model is shown in Figure 13. For E_c less than 1,500 psi, movement nearly equals that for free unrestrained thermal movement [$\alpha \cdot \Delta T \cdot (L/2)$]. The data in Figure 12 indicate that the expected modulus

is below 1,500 psi for long loading times (greater than 1 month) for temperatures greater than $25^\circ F$. Laboratory test temperature and loading times are chosen such that the tension creep modulus of the overlay will be less than 1,500 psi. The joint opening can then be calculated by using [$\alpha \cdot \Delta T \cdot (L/2)$]. This will simulate joint openings that occur in real pavements at temperatures greater than about $25^\circ F$.

The data in Figure 14 indicate that overlay stress is linearly related to displacement at the top of the joint. The slope of the stress-joint displacement line is a function of overlay modulus. The overlay stresses are independent of thermal load type. At constant overlay modulus, a horizontal displacement (x) will produce the same overlay stress (σ_x), regardless of whether this displacement was produced by slab curling or uniform temperature change. This is further evidence that curling can be equated to seasonal temperature change.

LABORATORY TESTING

Laboratory testing is currently under way to verify the reflection cracking models presented here. The laboratory test plan includes use of engineering fabrics and SAMI and will quantify the performance of the crack-prevention techniques. The model pavements will be subjected to joint openings commensurate with the thermal loadings that occur in full-scale pavements as described in this paper. This research is being sponsored by the Office of Research and Development, U.S. Department of Transportation. Laboratory results will be reported when available.

REFERENCES

1. F.R. McCullough. Reflection Cracking of Bituminous Overlays on Rigid Pavements. New York State Department of Transportation, Albany, Special Rept. 16, 1973.
2. K. Majidzadeh and G. Suckarieh. The Study of Pavement Overlay Design, Final Report. Ohio State Univ., Columbus, Rept. EES 457, 1977.
3. H.J. Treybig and others. Overlay Design and Reflection Cracking Analysis for Rigid Pavements; Volume 1, Final Report. FHWA, Rept. FHWA-RD-77-66, Aug. 1977.
4. M.S. Luther, K. Majidzadeh, and C.-W. Chang. Mechanistic Investigation of Reflection Cracking of Asphalt Overlays. TRB, Transportation Research Record 572, 1976, pp. 111-122.
5. M.S. Luther. The Fracture Mechanics Approach to Reflection Cracking. Ohio State Univ., Columbus, M.S. thesis, 1974.
6. G.C. Sih. Strain-Energy-Density Factor Applied to Mixed-Mode Crack Extension Problems. Institute of Fracture and Solid Mechanics, Lehigh Univ., Bethlehem, PA, Tech. Rept., 1972.
7. K. Majidzadeh and others. Application of Fracture Mechanics for Improved Design of Bituminous Concrete, Final Report. FHWA, Rept. FHWA-RD-76-91, June 1976.
8. F.P. Germann and R.L. Lytton. Methodology for Predicting the Reflection Cracking Life of Asphalt Concrete Overlays. Texas Transportation Institute, Texas A&M Univ., College Station, Res. Rept. 207-5, March 1979.
9. W. Heukelom and A.J.G. Klomp. Road Design Dynamic Loading. Proc., Association of Asphalt Paving Technologists, Vol. 33, 1964.

Optimum-Depth Method for Design of Fabric-Reinforced Unsurfaced Roads

T. ALLAN HALIBURTON AND JOHN V. BARRON

In recent years, the use of engineering fabric, when placed directly on the subgrade and covered with a single aggregate layer, has been a cost-effective alternative in unsurfaced road construction, especially on soft subgrades. Most fabric-reinforced unsurfaced road design criteria use Boussinesq stress-distribution theory to determine the amount of aggregate cover on the fabric. The research presented in this paper shows that placement of an optimum depth of aggregate on the fabric, when related to the width of the loaded area and independent of subgrade strength and wheel load, will increase strength and deformation resistance of the aggregate cover and produce significant Burmister-type modular ratio stress reductions at the subgrade surface. An alternate method for the design of fabric-reinforced unsurfaced roads, based on the described research, is presented. The method requires significantly less aggregate cover on the engineering fabric than predicted by other current methods of fabric-reinforced road design.

In recent years, engineering fabrics, or permeable artificial fiber textiles, have been widely used in the design and construction of unsurfaced low-volume or temporary unsurfaced roads, usually where soft subgrades are encountered. The fabric is placed directly on the subgrade or on a prepared working table and then covered with a single layer of cohesionless or low-plasticity aggregate base (fabric cover material). Such fabric-reinforced roads can be a cost-effective alternative to other methods of soft subgrade unsurfaced road construction.

Currently available design criteria for fabric-reinforced unsurfaced roads make use of the flexible-pavement-based physical distance separation concept; i.e., increasing the thickness of aggregate cover material with decreasing subgrade strength or increasing wheel load. Based on current research, an alternate design approach is presented in which the aggregate thickness is independent of subgrade strength or wheel load, is a constant, and is controlled by design vehicle tire size.

CONCEPTS IMPORTANT IN FABRIC-REINFORCED ROAD DESIGN

Three concepts are important when considering the use of fabrics in soft subgrade unsurfaced road construction: load-carrying ability of the subgrade and fabric cover material (base) road system, fabric survivability, and field workability of the fabric.

Load-Carrying Performance

Four mechanisms have been found to give improved performance for fabric-reinforced road systems on soft subgrade: material separation, subgrade restraint, lateral restraint reinforcement of cohesionless material placed above the fabric, and membrane-type support. Contributions from these four sources are summarized below.

1. **Material separation:** When placed between soft subgrade and overlying cohesionless material, engineering fabric prevents subgrade intrusion and mixing of the two soils, thus preserving the original design. Although the use of fabric for separation does not in itself strengthen the road system, it does allow dissipation of excess subgrade pore pressures and subgrade consolidation, which will cause long-term subgrade strength improvement. This factor allows the road to improve, rather than degrade, with time and number of load repetitions.

2. **Subgrade restraint:** Steward and others (1) found that the presence of fabric and cover material prevented punching or local shear failure of soft subgrade soils; instead, it caused such subgrades to fail in general shear when overloaded. The net effect of fabric-induced subgrade restraint is to increase allowable cohesive subgrade bearing capacity by a factor of approximately 1.8. This strength gain is available only for weak subgrades that would normally fail in local shear, and, according to Steward and others (1), improvement in load-carrying ability from subgrade restraint will occur only for subgrades with a California bearing ratio (CBR) of 3 or less.

3. **Lateral restraint reinforcement of fabric cover material:** Research by Haliburton and others (2) determined that maximum restraint reinforcement of cohesionless soil placed above a geotextile would occur when the geotextile was located to interfere with normal cover soil (base material) shear failure patterns. Placement of cover material to a depth of 0.33B over the geotextile [where B was the width of the loaded area (tire footprint)] was found to give optimum performance. Placement of the geotextile at shallower or deeper depths was found to cause a decrease in performance. Placement of the geotextile at the optimum depth was found to greatly increase the ultimate strength and deformation modulus of cohesionless material above the fabric, and there was potential for significant Burmister-type stress reduction at the subgrade surface below the geotextile.

4. **Membrane-type support:** If an engineering fabric is strained in place, normally through deformations associated with wheel-path rutting, it must develop tensile stress. The vertical component of such tensile stress will reduce the effective wheel load transmitted to the subgrade (3), with the amount of membrane support developed being proportional to fabric tensile stress-strain modulus.

Improvements in road performance from use of a fabric may accrue from one or all of the above factors, depending on the specific design criteria used.

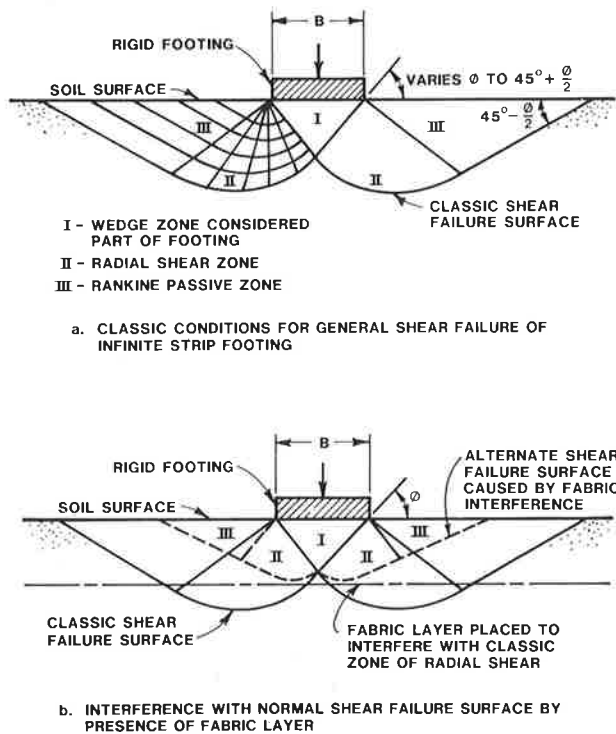
Fabric Survivability

An engineering fabric cannot perform any function unless it survives initial placement and covering. Thus, fabric survivability is defined as resistance of the fabric to the destructive forces imposed during actual road construction and in-service operation. The magnitude of these forces will be dependent on existing subgrade conditions, type of prior site preparation conducted (if any), type and angularity of cover material, and type of equipment used for road construction. More detail is available elsewhere (4).

Field Workability of Fabric

The field workability of fabric is defined as the ability of the fabric to support the contractor's workmen in an uncovered state when laid directly on the subgrade and also support the contractor's equipment during initial placement of the cover

Figure 1. Use of engineering fabric to cause interference with normal soil shear deformation patterns.



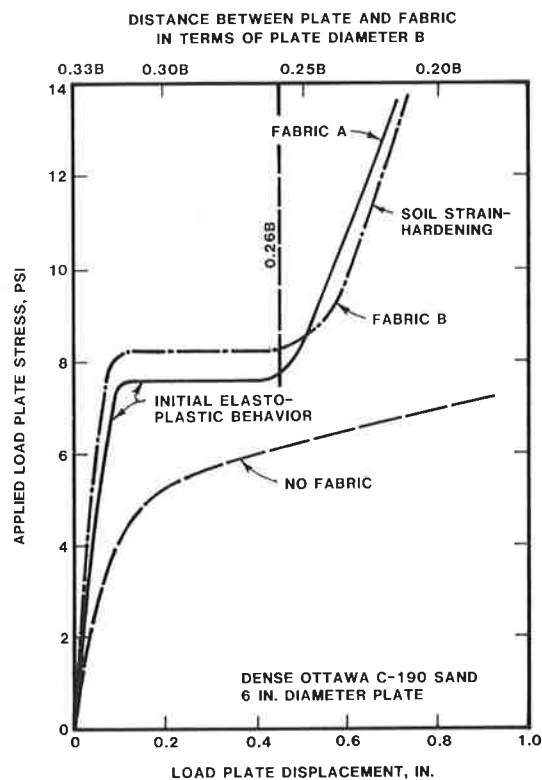
material. When construction on extremely soft soils is contemplated, such that mobility problems are encountered by both workmen and equipment on the existing soil and essentially all construction work must be conducted on the fabric, materials with high field workability or stiffness have been found to allow much more expedient and cost-effective construction. Field workability has been related to ASTM D-1388 fabric stiffness, and requirements increase as subgrade strength decreases. More detail is available elsewhere (4).

PREVIOUS RESEARCH ON OPTIMUM FABRIC DEPTH

In previous laboratory research conducted on model dense Ottawa sand (ASTM C-190) subgrade, Haliburton and Lawmaster (5) determined that covering the fabric with cohesionless material to an optimum depth of $0.5B \tan \phi$ (where B was the width of the loaded area and ϕ the angle of internal friction for the cohesionless fabric cover material) gave a marked increase in the load-deformation resistance of the cover material compared to similar test conditions when the fabric was omitted. They postulated that placement of the fabric [as shown in Figure 1 (5)] to interfere with normal shear deformation patterns for the fabric cover material, which caused increased lateral confinement in the zones of radial shear under the loaded area and forced development of a new shear failure surface above the fabric, was responsible for increased load-deformation resistance, such as that shown in Figure 2 (5). (Note: In Figure 2, there is one order of magnitude difference in strength and modulus of fabric A and B.) Based on experimental measurements, an optimum depth of 0.33B was found to approximate the theoretical $0.5B \tan \phi$ optimum embedment depth.

In other experiments, where the fabric was initially placed at a distance beneath the cover material surface greater than approximately 0.33B, no

Figure 2. Effect of optimum-depth fabric placement on soil mass load-deformation behavior.



improvement in load-deformation behavior (when compared to the no-fabric case) was noted until after cover material shear failure sinkage of the loaded area brought the load to within approximately 0.33B of the fabric. In extrapolating results of greater-than-optimum-depth fabric placement to unsurfaced airfield runway and roadway applications, Haliburton and Lawmaster (5) noted that this effect would cause excessive load sinkage (wheel-path rutting) to mobilize effects of fabric reinforcement.

The optimum-depth concept was verified by using various nonwoven and woven fabrics that had more than two orders of magnitude difference in tensile strength and tensile deformation modulus, with and without fabric prestressing. All load-deformation relations for fabric-reinforced soil were similar, which led to the conclusion that, for reinforcement of material above the fabric, position was more important than fabric type.

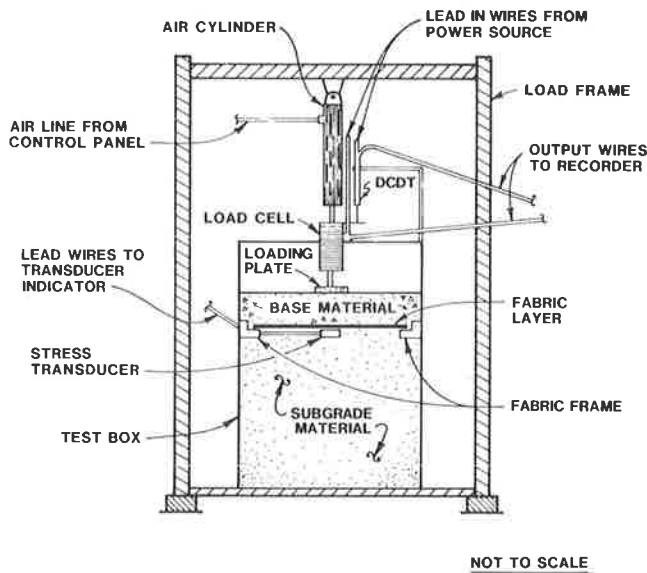
In all experiments, the effects of fabric subgrade restraint were eliminated because of the high-strength model subgrade, and the effects of membrane-type fabric support were eliminated because insignificant fabric deformations occurred during testing. By noting the marked improvement in load-deformation modulus obtained for the fabric-reinforced cover material, Haliburton and Lawmaster (5) postulated that a significant modular ratio might be developed between the fabric-reinforced cover material and softer subgrades, thereby causing a significant stress reduction at the subgrade surface from Burmister effects (6). They also concluded that classic bearing failure per se could not occur in the cohesionless material placed an optimum depth above the fabric. Thus, overload failure of a subgrade and fabric cover material system must occur in the subgrade.

In order to extend the optimum-depth concept to

Table 1. Properties of engineering fabrics evaluated in test program.

Designation	Manufacturer Trade Name	Fabric Description	Fabric Direction Tested ^a	Secant Modulus at 5 Percent Strain ^b (lb/in.)	Ultimate Tensile Strength ^b (lb/in.)	Ultimate Tensile Strain ^b (%)
Fabric M	Geolon 200	Woven polypropylene; slit film	M	460	160	34
Fabric S	Geolon 400	Woven polypropylene; monofilament	CM	1,100	162	22
			M	700	284	36
Fabric VS	Geolon 1250	Woven polypropylene; multifilament	CM	900	185	26
			M	1,700	1,050	20
			CM	460	238	15

^aM = Machine direction and CM = cross-machine direction.
^bResults of wide strip tensile tests (4).

Figure 3. Apparatus used in model subgrade, fabric, and base load testing program.

soft subgrade conditions, verify the significant Burmister stress reduction from optimum-depth reinforcement, and investigate effects of membrane-type support on soil-fabric system load-carrying performance, additional research was conducted.

EXTENSION OF OPTIMUM-DEPTH CONCEPT TO SOFT SUBGRADES

Engineering Fabrics Used in Test Program

Although previous research (5) had indicated that optimum-depth reinforcement effects were essentially independent of fabric type on good subgrades, three moderate to very high strength geotextiles were selected for use in the soft subgrade testing program to reverify the concept and also to facilitate an investigation of potential fabric membrane-type support. Table 1 summarizes data for the three woven engineering fabrics, including tensile strength and secant modulus at 10 percent elongation. Fabrics were supplied by the Nicolon Corporation of Atlanta, Georgia. As may be noted from Table 1, an approximate order of magnitude variation in tensile strength and tensile modulus occurred among the three fabrics, denoted hereafter as fabric M (moderate strength), fabric S (high strength), and fabric VS (very high strength).

Materials Used to Model Base and Subgrade

In order to determine the effect of varying base

(fabric cover) material types on relatively soft subgrade, two soils were used to represent base materials commonly used in the construction of unsurfaced roads on soft subgrade. A well-graded nonplastic crushed limestone, which had 100 percent passing the No. 4 sieve, 100 percent retained on the No. 200 sieve, a uniform coefficient (C_u) of 18.3, and a compacted CBR of approximately 30, was chosen to represent a medium-quality base material. Dense Ottawa 20-30 (ASTM C-190) sand with a CBR of approximately 10 was chosen to represent a low-quality base material used in areas where better material is not available.

Selection of materials to represent soft subgrades was based on the need to obtain mediums that could be prepared with a minimal amount of effort so that many tests could be conducted and repeatable strength of subgrade achieved. The material selected to represent a low-strength subgrade included Perlite, which is a volcanic glass expanded by heat to form a lightweight aggregate that is commonly used in concrete and plaster and frequently mixed with soil for greenhouse applications. After conducting numerous tests, it was found that Perlite could be prepared as a subgrade by using a concrete vibrator, and CBR values of 1 ± 0.1 were consistently measured. Load-deformation behavior of the Perlite model subgrade under plate bearing tests was found markedly similar to that of a soft cohesive soil.

Other materials used as test subgrade included a white Georgia Kaolinite clay that had a liquid limit of 70 and a plastic limit of 33, which was used (at varying water contents) to simulate subgrades with CBR values less than 1, and loose Ottawa C-190 sand, which was used to simulate subgrades with a CBR of approximately 2.

Experimental Design

Figure 3 shows a simplified drawing of the load-testing apparatus used in the soft subgrade test program. Test soil and soil-fabric systems were compacted and placed in 24-in.², 30-in.-deep reinforced Lucite test boxes. Load was supplied to 4- and 6-in.-diameter circular steel loading plates by Schraeder air cylinders with 2- or 6-in.-diameter pistons and 12-in. stroke. The air-loading system was chosen to allow rapid load following when bearing failure of either the fabric cover material or subgrade allowed rapid system deformations. Applied load was monitored with BLH Model U1 strain-gauge load cells of either 2,000- or 5,000-lb capacity, and vertical displacement of the loading plate was monitored by a Hewlett-Packard Model 3000 direct current displacement transducer. Loads and corresponding displacements were continuously recorded on a Sargent-Welch Model DSRG-2 dual-pen strip chart recorder.

Loading was applied by sequential incrementation

of air pressure controlled by a Western Pacific Micromaster Model WP6001 microprocessor controller. Stresses at various locations within the soil-fabric system were measured with Precision Instruments Model 156 miniature pressure transducers and a Model 8 strain indicator.

Test Procedures

Test procedures were designed to isolate the effects of fabric-caused Burmister-type modular ratio stress reduction and fabric membrane-type support. A testing matrix was developed for the three different fabric types (slit-film woven fabric M, monofilament woven fabric S, and multifilament woven fabric VS), three subgrade types (kaolinite, Perlite, and loose Ottawa sand), and the two different geotextile cover materials (well-graded crushed limestone and dense Ottawa sand). In general, three replicate tests were conducted for each cover material, fabric, and subgrade combination, with additional testing conducted if discrepancies were noted among test results.

Miniature pressure transducers were initially placed at various locations in the soil-fabric system, but after evaluation of initial test data, it was determined that the desired information could be obtained by placement of a single pressure transducer on the prepared model subgrade surface immediately beneath the fabric and centered directly under the load plate. Two sizes of circular steel load plate (4 and 6 in. diameter) were used during the initial portions of the test program. However, review of initial data indicated that consistent results were obtained between the two plate diameters; therefore, the majority of testing was conducted with a 6-in.-diameter load plate, which approximated the contact width of a standard passenger car tire.

Two types of testing were conducted sequentially for each model base, fabric, and subgrade system to monitor elastic and plastic behavior. In the elastic range before either subgrade or cover material bearing failure, initial testing was conducted by sequentially increasing the load plate stress while measuring corresponding load plate deformation and stress level at the subgrade surface to evaluate Burmister-type modular ratio effects caused by the three different types of fabrics. These data were compared with data obtained for homogeneous dense sand and similar thickness base and subgrade systems without fabric. Relations among applied load plate stress, load plate deformation, and stress at the subgrade surface were recorded until plastic bearing failure occurred in either the fabric cover material or the subgrade.

In general, and especially for the Perlite and kaolinite subgrades, system failure occurred in the subgrade, with resulting vertical subgrade displacement, elongation of the anchored fabric, and subsidence of the fabric cover material and load plate. Once plastic equilibrium conditions were established, loading was continued until a total deformation of approximately one-half the load plate diameter or more had been obtained. Average fabric elongation caused by plastic subgrade deformation was also estimated.

Test Results and Discussion

Typical modular ratio effects determined for elastic-type system behavior are shown in Figure 4 for low applied stress levels. A 6-in.-diameter load plate was used with a 2-in. fabric cover material thickness of dense Ottawa sand over Perlite (CBR = 1) subgrade. The figure shows the relation between stress applied to the load plate at the sand

surface and stress measured experimentally at the top of the model subgrade (2-in. depth) for homogeneous dense sand, 2 in. of dense sand cover on Perlite without fabric, and 2 in. of dense sand cover with the three different fabrics. The Boussinesq theoretical stress relation calculated at the center of the circular loaded area 2 in. below the surface (of a homogeneous, isotropic material) is also plotted in Figure 4.

As may be noted from Figure 4, theoretical Boussinesq values agree reasonably well with the stress measured in homogeneous dense sand. Because of the difference in the modular ratio between the 2-in. dense sand cover and CBR 1 Perlite subgrade, some Burmister-type stress reduction is noted without fabric; but when the fabric is used to provide interference with cover material deformation patterns and give increased load-deformation resistance, a markedly greater Burmister-type stress reduction (amounting to approximately 50 percent of the Boussinesq theoretical value) is noted. Further, as may be noted in Figure 4, the Burmister-type stress reduction is essentially independent of fabric type. Similar results were obtained when the plate size was decreased to 4 in. diameter and a 1.33-in. dense sand cover was used. At higher stress levels similar results were also obtained, and slightly better than a 50 percent Boussinesq theoretical stress reduction was obtained for crushed limestone fabric cover material, as shown in Figure 5.

Similar results (with an approximate 50 percent Boussinesq theoretical stress reduction) were obtained for the CBR 2 loose sand model subgrade, and somewhat greater than 50 percent stress reduction was obtained for the CBR < 1 kaolinite model subgrade. These results tended to be more erratic because of variations in placement density and water content of the wet clay and the large system deformations measured, even during elastic behavior.

Model system loading was carried out until large deformations, on the order of 3 in. for the 6-in.-diameter plate, had been obtained. As shown in Figure 6, fabric-reinforced behavior was better than no-fabric behavior, but no marked difference was noted among the three fabrics tested, thereby indicating that the membrane-type support component contributed little to the total load-carrying ability of the model base, fabric, and subgrade system. When fabric strains were computed and fabric tensile modulus data from Table 1 used, calculations based on both fabric deformation conditions observed during model testing and the fabric road rutting model developed by Kinney and Barenberg (3) showed that even the highest tensile modulus fabric would offer only a small contribution to total load resistance, hence confirming the experimental data.

DEVELOPMENT OF OPTIMUM-DEPTH ROAD DESIGN CRITERIA

Based on obtained test data and previously known relations concerning fabric-reinforced behavior of unsurfaced roads, optimum-depth fabric-reinforced unsurfaced road design criteria were developed. Procedures used to evaluate expected vehicle performance are given below.

1. Determine the maximum vehicle tire pressure (P) and the wheel load (Q) to which the road will be subjected.
2. Knowing the real or equivalent tire footprint width (B), calculate the approximate length of the loaded area (L) by using the relation

$$L = Q/(PB) \quad (1)$$

3. Apply Boussinesq theory (7) and, by using Q,

B, and L, determine the predicted stress at a depth of $0.5B \tan \phi$ below the wheel load (where ϕ is the angle of internal friction for the cohesionless geotextile cover material). Alternatively, a depth of $0.33B$ may be used.

Figure 4. Burmister-type stress reduction measured at model subgrade surface for optimum-depth fabric-reinforced system with CBR 10 fabric cover material.

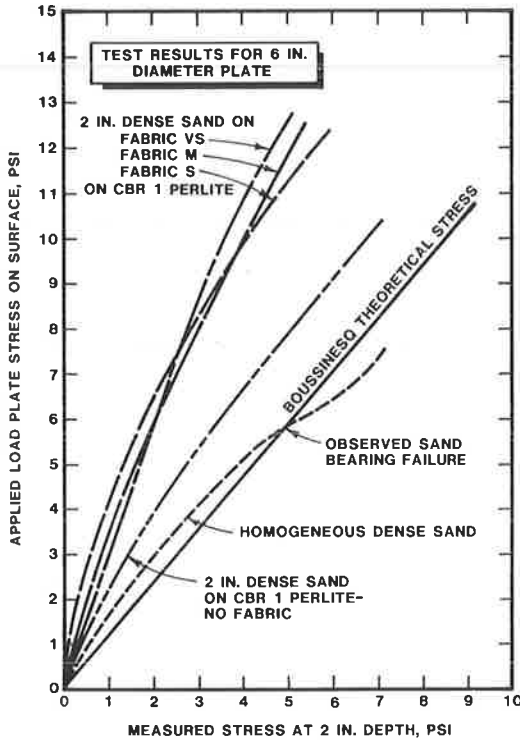
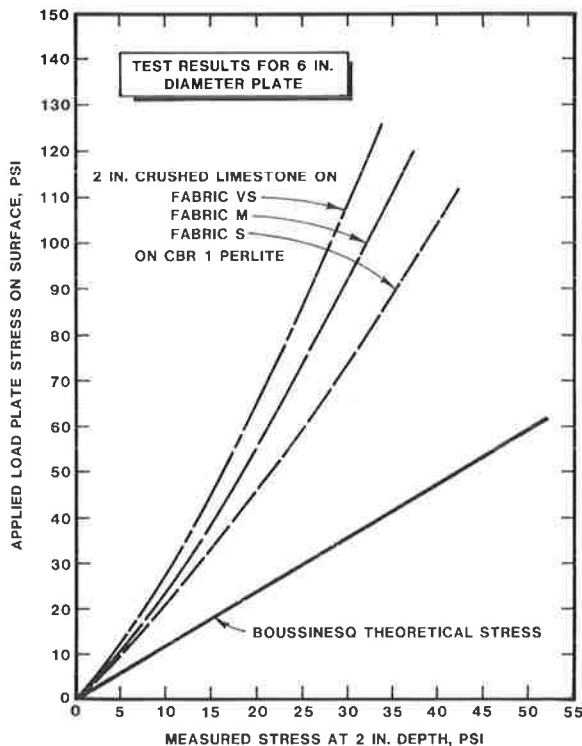


Figure 5. Burmister-type stress reduction measured at model subgrade surface for optimum-depth fabric-reinforced system with CBR 30 fabric cover material.



4. Multiply the predicted stress by 0.5 to obtain the 50 percent Burmister stress reduction from optimum-depth reinforcement, and compare this reduced stress to the allowable bearing capacity at the subgrade surface, based on ultimate bearing capacity considerations and by incorporating whatever factor of safety is desired.

5. If the predicted stress is less than the allowable stress for the subgrade, the optimum-depth road design criteria will perform satisfactorily. In this case, the design thickness of fabric cover material equals approximately $0.33B$.

6. Conversely, if the predicted stress is greater than the allowable stress, unsatisfactory subgrade performance will result and an alternate method of fabric-reinforced unsurfaced road design, based on concepts of physical distance separation, must be used. In this case, use of the U.S. Forest Service road design criteria (3) is recommended. More detailed information on optimum-depth design theory is available elsewhere (4).

As a practical matter, optimum-depth design concepts will work for the majority of reasonable design cases, with subgrade overstress occurring on weak ($CBR < 1$) subgrades and above design or legal load limits for trafficking vehicles.

Road design curves may also be produced by using the methodology. Typical curves are shown in Figure 7 for standard dual-tire, single- and tandem-axle trucks. The curves are used by constructing a vertical line from the horizontal subgrade strength axis (A) and a horizontal line from the vertical axle load axis (B), and then determining the maximum allowable vehicle tire pressure (C) at their intersection. If the maximum allowable tire pressure exceeds the operating pressure in the vehicle tires, the optimum-depth design criteria will provide sat-

Figure 6. Load-deformation behavior for model subgrade, fabric, and base system.

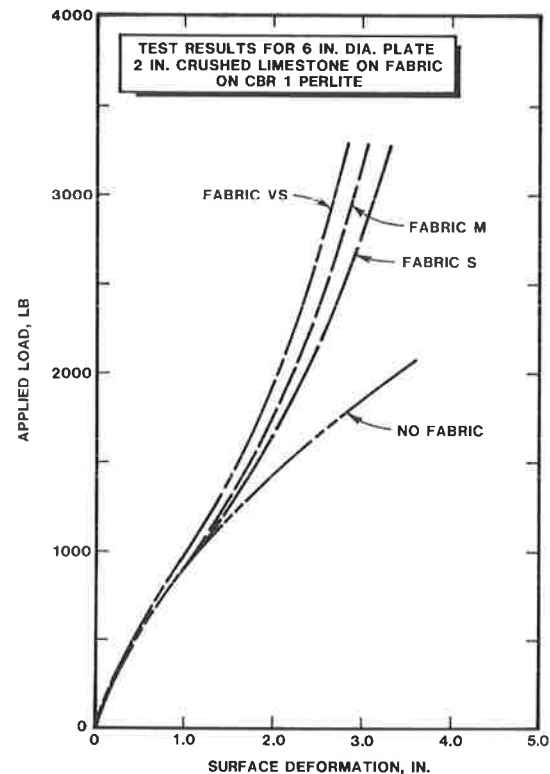
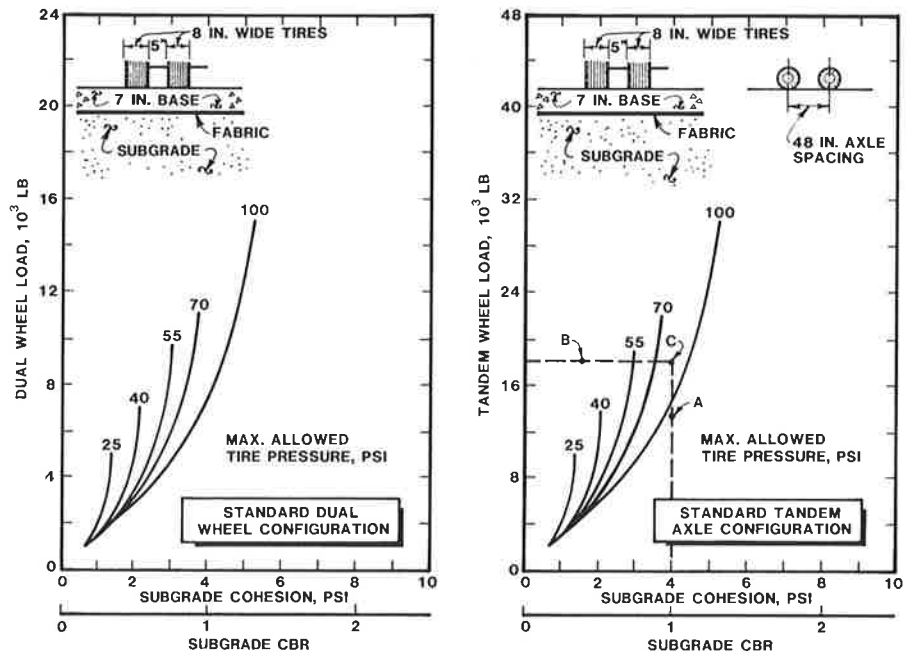


Figure 7. Typical unsurfaced road design curves using optimum-depth concept.



isfactory performance. The required thickness of aggregate cover on the fabric (7 in. of densely compacted cohesionless material) is shown in the upper portions of the figure. Similar curves for other actual or equivalent tire sizes are available elsewhere (4,8), as are data and procedures for fabric cover material selection, road construction procedures, and fabric selection criteria based on site-specific fabric survivability and field workability considerations.

The presented optimum-depth design method for unsurfaced fabric-reinforced roads has two obvious advantages. First, it is simplistic in that the depth of the aggregate cover on the fabric remains at a constant thickness necessary to provide reinforcement and produces a maximum Burmister-type stress reduction. Use of a less-than-optimum thickness will reduce fabric anchorage away from the loaded area and increase stress on the subgrade. Use of a greater-than-optimum thickness will cause loss of the Burmister-type stress reduction and also result in subgrade overstress. Second, for soft subgrades, the optimum-depth thickness of fabric cover is some 30 to 100 percent less than predicted as necessary by other fabric-included unsurfaced road design methods that do not consider Burmister-type effects (4).

CONCLUSIONS

Based on the results of research presented herein, the following may be concluded.

1. Optimum-depth engineering-fabric-reinforcement concepts that were originally developed for strong materials beneath the fabric may be extended to cases where weak materials underlie the fabric.
2. When the fabric is placed on weak material and overlain by an optimum depth of densely compacted cohesionless material, Burmister-type modular ratio effects cause a stress reduction, such that the actual stress immediately beneath the fabric is approximately 50 percent of that predicted by

Boussinesq theory. The optimum depth is approximately one-third the width of the loaded area.

3. Even at large deformations, the amount of membrane-type support obtained from the fabrics tested, including the very high tensile modulus fabric, was small compared to the total load capacity of the model systems.

4. The optimum-depth road design criteria for construction of fabric-reinforced unsurfaced roads on soft subgrade can be developed, where the optimum fabric cover depth is approximately equal to one-third of the real or equivalent vehicle tire footprint width, independent of subgrade strength. This design method requires considerably less aggregate cover over the fabric than other currently available unsurfaced road design criteria that incorporate engineering fabrics.

ACKNOWLEDGMENT

The research described here was supported by Nicolon Corporation, Atlanta, Georgia. This support is gratefully acknowledged.

REFERENCES

1. J. Steward, R. Williamson, and J. Mohney. Guidelines for Use of Fabrics in Construction and Maintenance of Low-Volume Roads. Forest Service, U.S. Department of Agriculture, Pacific Northwest Region, Rept. FHWA-TS-789-205, June 1977.
2. T.A. Haliburton, J.D. Lawmaster, and J.K. King. Potential Use of Fabric in Airfield Runway Design. School of Civil Engineering, Oklahoma State Univ., Stillwater, Oct. 1980.
3. T.C. Kinney and E.J. Barenberg. Mechanisms by which Fabrics Stabilize Aggregate Layers on Soft Subgrades. Geotechnical Laboratory, U.S. Army Corps of Engineers Waterways Experiment Station, Vicksburg, MS, Miscellaneous Paper, Feb. 1978.
4. T.A. Haliburton, J.D. Lawmaster, and V.C. McGuffey. Use of Engineering Fabrics in Trans-

- portation-Related Applications. Haliburton Associates, Stillwater, OK, Dec. 1981.
5. T.A. Haliburton and J.D. Lawmaster. Experiments in Geotechnical Fabric-Reinforced Soil Behavior. *Geotechnical Testing Journal*, ASTM, Vol. 4, No. 4, Dec. 1981, pp. 153-160.
 6. D.M. Burmister. The Theory of Stresses and Displacements in Layered Systems and Applications to the Design of Airport Runways. *Proc.*, HRB, Vol. 23, 1943, pp. 126-144.
 7. E.J. Yoder and M.W. Witczak. Principles of Pavement Design. Wiley, New York, 1975.
 8. Nicolon Corporation Criteria for the Design of Geolon Fabric-Reinforced Unsurfaced Roads. Haliburton Associates, Stillwater, OK, July 1981.

Publication of this paper sponsored by Committee on Low-Volume Roads.

Notice: The Transportation Research Board does not endorse products or manufacturers. Trade and manufacturers' names appear in this paper because they are considered essential to its object.

Dynamic Test to Predict Field Behavior of Filter Fabrics Used in Pavement Subdrains

DONALD J. JANSSEN

A dynamic test that attempts to duplicate field conditions for filter fabrics used in pavement subdrains is described. A filter fabric sample under a saturated silty-sand test soil is subjected to repeated axial loading while water flow is maintained through the sample under a unit hydraulic gradient. Sample permeability is monitored continuously. Results are presented in the form of a plot of sample permeability versus accumulated loads, and plots that show the movement in soil after 1 million loads.

The use of engineering fabrics in filter applications has become widespread in the past 10 years. They can be effective in protecting soil from erosion while permitting water to pass through the fabric to the drain. However, with the large number of filter fabrics available, some means must be found to determine the fabrics best suited for each application. The fabric must not clog or in any way significantly decrease the rate of flow. At the same time, the fabric must not let too much material pass through it because clogging of the drainage material and loss of subgrade support could occur (1).

Various tests have been proposed to help evaluate filter fabrics for various uses. The U.S. Army Corps of Engineers employs a test in which the fabric is used as a dry sieve in order to determine the largest size of glass beads that pass through the fabric (2). The largest size opening that at least 5 percent of the beads pass through the fabric is called the equivalent opening size (EOS) (2).

Calhoun (3) developed a constant-head permeameter test to examine fabric clogging under constant-head water flow. The overall hydraulic gradient across the soil sample could be changed in order to evaluate clogging under differing hydraulic conditions. In addition, piezometric pressure taps were installed at various depths in order to measure the hydraulic gradient throughout the sample. The Corps of Engineers used the ratio of the hydraulic gradient in the 2.5 cm (1 in.) of the sample directly above the fabric to the hydraulic gradient in the next 5 cm (2 in.) of the sample as one criterion for accepting a filter fabric for a given filter application [see Figure 1 (2)].

In the actual soil and filter fabric interaction, a rather complex bridging or arching occurs in the soil next to the fabric that permits particles much smaller than the openings in the fabric to be retained. Copeland (4) provides a good discussion of this process along with results of tests she per-

formed with various fabrics and soils under constant hydraulic gradients. She considers failure of the soil-fabric system as either excessive piping of soil particles through the fabric or as a substantial decrease in permeability through the fabric and adjacent soil. She also identifies the hydraulic gradient through the sample that causes the failure.

The use of filter fabrics in highway subdrains requires the consideration of an additional factor. A highway is subjected to repeated dynamic loading by traffic. Dempsey (5) found that this loading can lead to substantial pore-pressure pulses in a saturated pavement system.

A soil and filter fabric system at the pavement edge may be subjected not only to a possible unit hydraulic gradient during heavy rain, but also to an additional gradient caused by highway traffic loading. The fact that this gradient would be changing in magnitude rather than remaining constant means that any comparison with constant-gradient soil-fabric tests would be difficult. Instead, a test that duplicates the effects of repeated traffic loading would be useful in predicting filter fabric behavior in highway subdrain applications. The conditions to be duplicated should also include continuous water flow (as in a heavy rainfall) and the use of a test soil that would show any soil movement and cause clogging under test conditions.

OBJECTIVES

This study was conducted in order to determine the behavior of filter fabrics to be used in pavement subdrain systems in the field. Specific test objectives were to

1. Develop a repeated triaxial-loading test to simulate truck traffic on the pavement;
2. Develop a continuous water-flow system to provide a unit hydraulic gradient through the soil sample, such as would be caused by heavy rainfall;
3. Select a soil that will cover the size ranges expected to be the most likely to move under water pressures created by the combined water flow and dynamic loading; and
4. Develop a system for the test to permit continuous monitoring of the flow rate in order to evaluate filter performance.

- portation-Related Applications. Haliburton Associates, Stillwater, OK, Dec. 1981.
5. T.A. Haliburton and J.D. Lawmaster. Experiments in Geotechnical Fabric-Reinforced Soil Behavior. *Geotechnical Testing Journal*, ASTM, Vol. 4, No. 4, Dec. 1981, pp. 153-160.
 6. D.M. Burmister. The Theory of Stresses and Displacements in Layered Systems and Applications to the Design of Airport Runways. *Proc.*, HRB, Vol. 23, 1943, pp. 126-144.
 7. E.J. Yoder and M.W. Witzak. Principles of Pavement Design. Wiley, New York, 1975.
 8. Nicolon Corporation Criteria for the Design of Geolon Fabric-Reinforced Unsurfaced Roads. Haliburton Associates, Stillwater, OK, July 1981.

Publication of this paper sponsored by Committee on Low-Volume Roads.

Notice: The Transportation Research Board does not endorse products or manufacturers. Trade and manufacturers' names appear in this paper because they are considered essential to its object.

Dynamic Test to Predict Field Behavior of Filter Fabrics Used in Pavement Subdrains

DONALD J. JANSSEN

A dynamic test that attempts to duplicate field conditions for filter fabrics used in pavement subdrains is described. A filter fabric sample under a saturated silty-sand test soil is subjected to repeated axial loading while water flow is maintained through the sample under a unit hydraulic gradient. Sample permeability is monitored continuously. Results are presented in the form of a plot of sample permeability versus accumulated loads, and plots that show the movement in soil after 1 million loads.

The use of engineering fabrics in filter applications has become widespread in the past 10 years. They can be effective in protecting soil from erosion while permitting water to pass through the fabric to the drain. However, with the large number of filter fabrics available, some means must be found to determine the fabrics best suited for each application. The fabric must not clog or in any way significantly decrease the rate of flow. At the same time, the fabric must not let too much material pass through it because clogging of the drainage material and loss of subgrade support could occur (1).

Various tests have been proposed to help evaluate filter fabrics for various uses. The U.S. Army Corps of Engineers employs a test in which the fabric is used as a dry sieve in order to determine the largest size of glass beads that pass through the fabric (2). The largest size opening that at least 5 percent of the beads pass through the fabric is called the equivalent opening size (EOS) (2).

Calhoun (3) developed a constant-head permeameter test to examine fabric clogging under constant-head water flow. The overall hydraulic gradient across the soil sample could be changed in order to evaluate clogging under differing hydraulic conditions. In addition, piezometric pressure taps were installed at various depths in order to measure the hydraulic gradient throughout the sample. The Corps of Engineers used the ratio of the hydraulic gradient in the 2.5 cm (1 in.) of the sample directly above the fabric to the hydraulic gradient in the next 5 cm (2 in.) of the sample as one criterion for accepting a filter fabric for a given filter application [see Figure 1 (2)].

In the actual soil and filter fabric interaction, a rather complex bridging or arching occurs in the soil next to the fabric that permits particles much smaller than the openings in the fabric to be retained. Copeland (4) provides a good discussion of this process along with results of tests she per-

formed with various fabrics and soils under constant hydraulic gradients. She considers failure of the soil-fabric system as either excessive piping of soil particles through the fabric or as a substantial decrease in permeability through the fabric and adjacent soil. She also identifies the hydraulic gradient through the sample that causes the failure.

The use of filter fabrics in highway subdrains requires the consideration of an additional factor. A highway is subjected to repeated dynamic loading by traffic. Dempsey (5) found that this loading can lead to substantial pore-pressure pulses in a saturated pavement system.

A soil and filter fabric system at the pavement edge may be subjected not only to a possible unit hydraulic gradient during heavy rain, but also to an additional gradient caused by highway traffic loading. The fact that this gradient would be changing in magnitude rather than remaining constant means that any comparison with constant-gradient soil-fabric tests would be difficult. Instead, a test that duplicates the effects of repeated traffic loading would be useful in predicting filter fabric behavior in highway subdrain applications. The conditions to be duplicated should also include continuous water flow (as in a heavy rainfall) and the use of a test soil that would show any soil movement and cause clogging under test conditions.

OBJECTIVES

This study was conducted in order to determine the behavior of filter fabrics to be used in pavement subdrain systems in the field. Specific test objectives were to

1. Develop a repeated triaxial-loading test to simulate truck traffic on the pavement;
2. Develop a continuous water-flow system to provide a unit hydraulic gradient through the soil sample, such as would be caused by heavy rainfall;
3. Select a soil that will cover the size ranges expected to be the most likely to move under water pressures created by the combined water flow and dynamic loading; and
4. Develop a system for the test to permit continuous monitoring of the flow rate in order to evaluate filter performance.

Figure 1. Method of determining Corps of Engineers' gradient ratio with Calhoun-type constant-head apparatus.

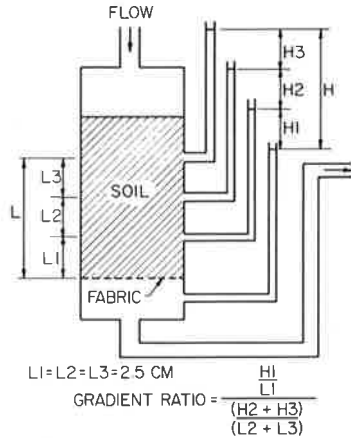


Figure 2. Triaxial cell parts. [Shown (from left to right) are the cell base, loading cap, and porous stone; the cell cap is in the back.]



TESTING EQUIPMENT

Triaxial Cell

The triaxial cell used to hold the sample (Figures 2 and 3) has been used at the University of Illinois for several years. It will hold a 203-mm (8-in.) diameter sample that is 406 mm (16 in.) high (6).

The top of the cell is adapted to allow tube connections to the sample loading head for flushing and to permit water flow through the sample. An additional tube connection is made to allow for a piezometric pressure tap at the base of the soil sample (Figure 4).

Loading

The flexible confining membrane used to contain the sample is made of 0.8-mm (0.03-in.) thick neoprene rubber cut to size and glued with a 7.5-cm (3-in.) overlap to form a cylinder. Two membranes are used: one attached directly to the filter fabric and containing the soil, and a second membrane to contain the entire sample setup. A small hole is cut in the outer membrane below the filter fabric to permit the installation of a piezometric pressure tap.

Porous carborundum stones [20 cm (8 in.) in diameter and 2.5 cm (1 in.) thick] are placed on both ends of the sample to facilitate water flow through the entire sample cross section.

Figure 3. Assembled triaxial cell.



Repeated axial loading is produced by an air-actuated diaphragm air cylinder. The loading rate is approximately once every 2 sec. This rate is slow enough to permit the damping out of residual pressure fluctuations after each load pulse. The magnitude of the load pulse is 17.5 kN/m² (2.5 psi). The confining pressure was maintained at 12.1 kN/m² (1.75 psi). These values were determined from elastic-layer and finite-element analyses as typical stresses in the subgrade from truck loadings on an Interstate pavement. Water is used as the confining medium, and pressure is controlled by a single-stage air-pressure regulator. A mercury manometer is used to read the pressure difference between inside and outside the sample membrane to determine the net confining pressure.

Permeameter

A schematic for the equipment used to maintain water flow through the sample is shown in Figure 5. A similar device for permeability measurement has been in use at the University of Illinois for several years and is reliable (7). The apparatus consists of a water reservoir, manometer tube, bleeder valve, micro-adjust valve, and valves for sample isolation. In practice, there is an additional water reservoir and assorted valves to permit operation while one reservoir is being refilled. The apparatus is shown in Figure 6.

The water used in the system is de-aired under vacuum in order to prevent air bubbles from forming in the system and to dissolve any bubbles already present. The whole system is back-pressured to about 220 kN/m² (32 psi). In order to keep the water de-aired, a layer of mineral oil covers the water in the reservoir tanks, thereby separating the water and air.

Water flow is accomplished by means of the bleeder valve connected to the bottom of the sample. By allowing water to drain from the bottom of the sample, a pressure difference across the sample is created. This pressure difference is read on the manometer connected to the piezometric tap and is

Figure 4. Triaxial cell schematic.

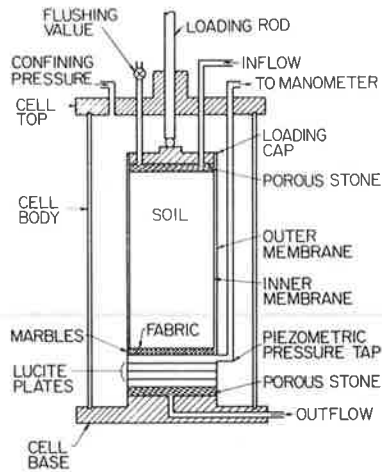
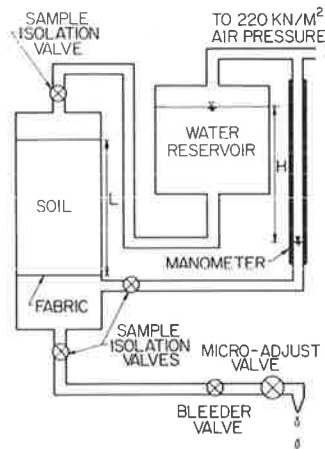


Figure 5. Permeameter schematic.



controlled by adjusting the flow rate with the micro-adjust valve.

The practical range of permeability values for this equipment is from 2×10^{-2} to 1×10^{-6} cm/sec.

Sample

The test sample consists of soil, filter fabric, 1.5-cm (0.625-in.) diameter glass spheres (marbles) for fabric support, confining membranes, and soil collection plates (see Figure 3).

The soil is a mixture of 90 percent class X concrete sand (no material smaller than the No. 200 sieve) and 10 percent Roxana silt, all of which pass the No. 200 sieve. This mixture was chosen to provide a test soil with silt and fine sand that is most likely to move due to hydraulic gradient (8). The coarse sand fraction provides a supporting matrix. The complete gradation is shown in Figure 7.

The fabric is supported on a layer of marbles, and beneath the marbles are four perforated Lucite plates. The faces of the plates are recessed to provide space to collect the soil that passes through the fabric.

SAMPLE PREPARATION

The outer sample membrane is placed on the triaxial cell base and tied with multiple wraps of cotton cord. A watertight seal is ensured by the use of silicone vacuum grease on both the membrane and the cell base. A porous stone and the four Lucite plates are then placed inside the membrane. The

Figure 6. Permeameter apparatus.

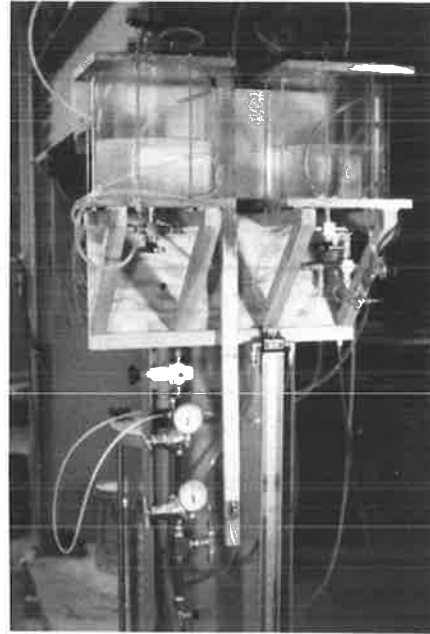
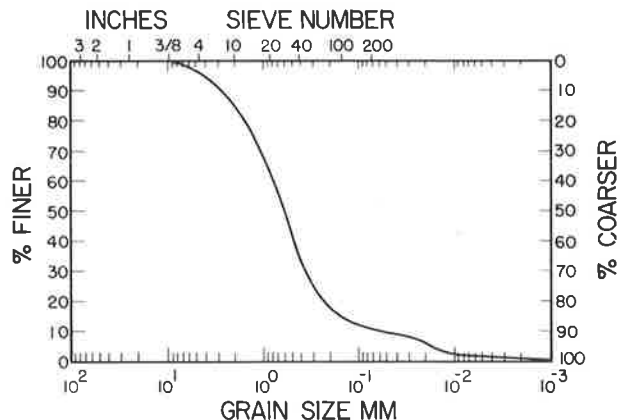


Figure 7. Test soil gradation.



piezometric pressure tap is installed through the membrane just below the top Lucite plate. This is also sealed with a liberal coating of vacuum grease. A single layer of marbles is placed on the top Lucite plate, and a second membrane that has the filter fabric attached is inserted into the confining membrane. A coating of vacuum grease is used to prevent water from flowing between the two membranes.

The bottom of the sample confining membrane is now filled with water to above the filter fabric and then drained so that the water level is at the level of the filter fabric. This filling is done from the bottom with frequent tapping and shaking to loosen any trapped air bubbles.

Dry soil [13.6 kg (30 lb)] is thoroughly mixed with water [2 L (4.4 lb)] to produce a mixture close to 100 percent saturation. This mixture is placed by hand in the sample membrane. Excess water is allowed to drain through the sample and out the piezometric tap, the open end of which is about 1 cm (0.4 in.) above the level of the filter fabric. A dry density of about 1620 kg/m^3 (101 lb/ft^3) is produced by this method and is easily reproducible.

The sample is allowed to sit until any excess water on the top of the sample has drained through the sample. A porous stone and the loading cap are then placed on the sample, and the loading cap is tied in place. Again, vacuum grease is used to ensure a watertight seal.

The Lucite cell body is placed on the cell base. Water tubes are connected from the cell top to the sample. The cell top is then tightened onto the cell body and the loading rod is attached through the cell top onto the loading cap. The cell is then filled to the top of the sample with water, and the remaining water tubes are connected to the cell to complete sample preparation (Figure 3).

TEST PROCEDURE

The sample is saturated from the bottom up, and the system is then closed to permit pressurization. Both the confining pressure and the internal pressure are increased slowly, keeping the confining pressure at least 15-cm (6-in.) mercury greater than the internal pressure. This pressure difference is read on the mercury manometer. Pressure is increased until the internal pressure is 220 kN/m². The final confining pressure is adjusted to 16.5-cm (6.5-in.) mercury greater than the internal pressure. The net confining pressure (P) is computed by the following equation:

$$P = 1.33[H - (Hw/13.6)] \quad (1)$$

where

- P = net confining pressure (kN/m²),
- 1.33 = conversion from centimeters mercury to kilonewtons per square meter,
- H = pressure difference (cm mercury),
- Hw = distance (cm) from middle of reservoir tank to top of confining water in triaxial cell, and
- 13.6 = conversion from centimeters mercury to centimeters water.

Flow is initiated in the sample by opening the bleeder valve. The flow rate is adjusted with the micro-adjust valve to give a pressure difference across the sample in the range of 24 to 26 cm (9.5 to 10.25 in.). Readings of quantity of flow, time for collection, and head difference are taken until the permeability is stabilized, which is usually 10 to 15 min. Loading is then started.

Readings are taken after 1, 10, 100, and 500 loads, and after that as needed, depending on how much the permeability is changing. On long-term tests, readings are generally taken at least every 6 hr. Notes are also made on whether or not the water is cloudy.

At the conclusion of the test, the system is depressurized, keeping the confining pressure at least 15-cm mercury greater than the internal pressure. In addition, the pressure gradient in the sample is kept to less than 25-cm (10-in.) water.

The cell is then taken apart and the sample divided into eight layers [approximately 3 cm (1.2 in.) thick] for grain-size analysis. In addition, the soil that has passed through the fabric is collected for grain-size analysis.

RESULTS

The water bled off is collected and the flow rate is used to calculate the sample permeability by the following equation:

$$K = QL/HAT \quad (2)$$

where

- K = sample permeability (cm/sec);
- Q = measured volume of flow (cm³);
- L = length of soil sample (cm); see Figure 5;
- H = pressure head difference across sample (cm); see Figure 5;
- A = cross-sectional area of sample (cm²); and
- T = time required to collect volume Q (sec).

The sample permeability is then plotted versus the accumulated number of loads (see Figure 8).

Cloudy water was noted from about 300,000 to 320,000 loads. It also occurred at about 650,000 loads and gradually cleared until about 900,000 loads, when it was again clear.

Gradation analysis is run on the soil taken from the sample in 3-cm (1.2-in.) layers. The gradation for each layer can be plotted for comparison with the original retained soil gradation.

Assuming that no movement of materials larger than the No. 10 sieve has occurred, the percentage of the original for each of the smaller-sized fractions can be calculated by the following equation:

$$\%DR = [(wtD)(\% + 10)] / [(\%D)(wt + 10)] \quad (3)$$

where

- %DR = percentage of size range D retained,
- wtD = actual weight of size range D for soil layer being considered,
- %D = percentage of size range D in original gradation,
- % + 10 = percentage of material larger than No. 10 sieve in original gradation, and
- wt + 10 = actual weight of material larger than No. 10 sieve found in layer in question.

The percentage of material retained versus height in the sample can then be plotted for each size range. Figures 9 and 10 show this for material finer than the No. 80 sieve but retained on the No. 200, and for material finer than the No. 200 sieve.

DISCUSSION OF RESULTS

The usefulness of this test for the evaluation of filter fabrics is probably most easily shown by the examination of a set of results for a test run to 1 million loads. The data are for a nonwoven, needle-punched, and heat-bonded fabric with a minimum EOS of 70 (the largest pores are equivalent to the openings in a No. 70 sieve).

Figure 8 shows that the first few loads caused a rapid increase in sample permeability. This is probably due to the washing out of any fines that accumulated in the fabric during sample preparation. Then the permeability gradually dropped until 300,000 loads, where it dropped abruptly. This was accompanied by cloudy water coming through the permeameter. It is believed that a graded soil-filter structure was being built up adjacent to the fabric as fines migrated down through the sample. At 300,000 loads, this structure collapsed, causing a rapid decrease in permeability. From here the permeability again gradually decreased, possibly caused by the accumulation of fines adjacent to the fabric.

At about 675,000 loads, the permeability suddenly increased. Before that, at about 650,000 loads, the water again appeared cloudy. It appears that the high hydraulic gradient right above the filter fabric, along with the stretching of the fabric and fabric pores, caused piping of the fines through the fabric. This gives the appearance of a self-cleaning action. The wide fluctuations in permeability between 675,000 and 700,000 loads may possi-

Figure 8. Sample permeability versus accumulated loads.

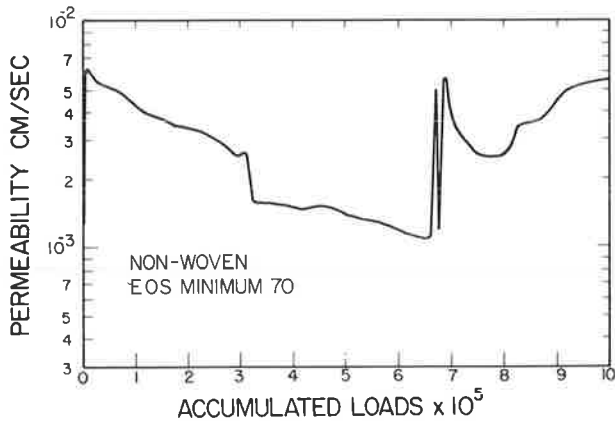


Figure 9. Percentage of material smaller than No. 80 sieve and larger than No. 200 sieve remaining in sample versus position in sample.

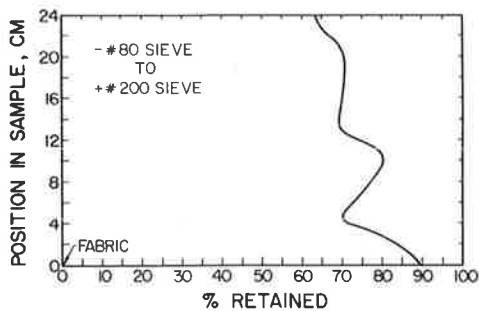
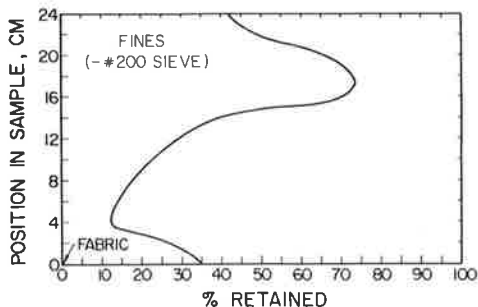


Figure 10. Percentage of fines (smaller than No. 200 sieve) remaining in sample versus position in sample.



bly have been caused by soil structure collapse followed by more soil piping.

The permeability again decreased from 700,000 to about 820,000 loads. The water was still slightly cloudy. Then at 820,000 loads the permeability increased and continued to increase to the end of the test at 1,000,000 loads. It appears that a more stable soil-filter structure had formed by this time that allowed some of the fines to pass through the fabric without clogging behind the fabric, which would have decreased permeability.

The fact that the fabric was able to clean itself is probably due to the nature of the loading. If the total hydraulic gradient in the sample had been constant, plugging of the soil-fabric system and loss of permeability would probably have been irreversible. However, the hydraulic gradient is

pulsed. The accelerating water velocity caused by the changing hydraulic gradient transfers momentum to the soil particles and dislodges them from their existing structure. Each gradient pulse, although short in duration, is able to move the soil particles a bit. This can combine with stretching of the fabric between points of support and enlarging of the fabric pores. Eventually the soil particles are able to pass through the fabric, which assumes that the openings in the fabric are large enough. If the openings in the fabric are too small or too infrequent, soil particles will not pass through and the fabric will not be self-cleaning.

Figures 9 and 10 show the migration of material through the soil and fabric. Much of the material smaller than the No. 200 sieve and some of the material with gradations smaller than the No. 80 sieve larger than the No. 200 sieve have been lost through the fabric. It should be noted that there is a relative accumulation of material right above the fabric. This was also visible when the sample was disassembled.

SUMMARY AND CONCLUSIONS

The test described in this paper provides an important step in the evaluation of filter fabrics when used in highway subdrains because it attempts to duplicate actual field conditions. The parameters of loading, soil, and hydraulic gradient can be varied to attain any type of field condition expected for the evaluation of filter fabrics for use in conjunction with drainage in pavement systems.

Additional tests are being conducted in order to compare the behaviors of various filter fabrics.

ACKNOWLEDGMENT

This paper was prepared from a study conducted by the Department of Civil Engineering, Engineering Experiment Station, University of Illinois at Urbana-Champaign, in cooperation with the Monsanto Plastics and Resins Company. Special thanks are given to Barry Dempsey for consultation in the development of the testing procedure.

The contents of this paper reflect my views, and I am responsible for the facts and the accuracy of the data presented herein. The contents do not necessarily reflect the official views or policies of the Monsanto Plastics and Resins Company. This paper does not constitute a standard, specification, or regulation.

REFERENCES

1. E.J. Barenberg and S.D. Tayabji. Evaluation of Typical Pavement Systems Using Open-Graded Bituminous Aggregate Mixture Drainage Layers. Department of Civil Engineering, Univ. of Illinois, Urbana-Champaign, Transportation Engineering Series 10, May 1974.
2. T.A. Haliburton, J.D. Lawmaster, and V.C. McGuffey. Use of Engineering Fabrics in Transportation-Related Applications. Office of Development, FHWA, Oct. 1981.
3. C.C. Calhoun, Jr. Development of Design Criteria and Acceptance Specifications for Plastic Filter Cloth. U.S. Army Corps of Engineers Waterways Experiment Station, Vicksburg, MS, Tech. Rept. F-72-7, 1972.
4. J.A. Copeland. Fabrics in Subdrains: Mechanisms of Filtration and the Measurement of Permeability. Department of Civil Engineering, Oregon State Univ., Corvallis, Transportation Res. Rept. 80-2, Jan. 1980.

5. B.J. Dempsey. Laboratory and Field Studies of Channeling and Pumping. TRB, Transportation Research Record 849, 1982, pp. 1-12.
6. R.M. Knutson and M.R. Thompson. Permanent-Deformation Behavior of Railway Ballast. TRB, Transportation Research Record 694, 1978, pp. 60-65.
7. D.J. Janssen and B.J. Dempsey. Soil Water Prop-

- erties of Subgrade Soils. Department of Civil Engineering, Univ. of Illinois, Urbana-Champaign, Transportation Engineering Series 184, April 1980.
8. K. Terzaghi and R.B. Peck. Soil Mechanics in Engineering Practice. Wiley, New York, 1967.

Publication of this paper sponsored by Task Force on Engineering Fabrics.

Abridgment

Mechanism of Geotextile Performance in Soil-Fabric Systems for Drainage and Erosion Control

RICHARD D. WEIMAR, JR.

Over the past 15 years, more than 250 000 000 m² (300,000,000 yd²) of geotextiles have been used in drainage and erosion-control systems. Initial geotextile specifications established a decade ago were based on the best-available understanding of fabric function in fabric-soil systems. Considerable research over the past 10 years has significantly changed the understanding of how fabrics function in these systems. As a consequence, fabric specifications now need modification to achieve maximum cost-effective performance. Therefore, a state-of-the-art model of soil-fabric systems is given, and the key physical properties of geotextiles needed for acceptable performance are suggested. Knowing how fabrics function and which properties are important, the designers and contractors of drainage and erosion-control systems can properly specify and install the geotextiles needed in a given system for acceptable performance at minimum cost.

Nonwoven geotextiles account for more than 90 percent of the fabrics used outside of the United States. Within the United States they have only recently reached the same rate of use as wovens because they were introduced 10 years later than wovens. On a worldwide basis, 80 percent of the geotextiles used in erosion control have been nonwoven. The first table gives data on the types of geotextiles installed:

Item	United States		Worldwide	
	No.	Percent	No.	Percent
All fabrics	200		690	
Nonwovens	120	60	590	85
Wovens	80	40	100	15

The second table gives data on the use of geotextiles:

Item	United States		Worldwide	
	Non-woven	Woven	Non-woven	Woven
Drainage	40	10	125	15
Support	65	55	375	65
Erosion Control	15	15	90	20

(Note: In the above tables, geotextiles installed include only those in drainage, support, and erosion control; worldwide figures include U.S. values; and 1 m² = 1.196 yd².)

More than 110 000 000 m² (130,000,000 yd²) of

geotextiles has been installed during the past decade, and these geotextiles have demonstrated acceptable performance in a wide spectrum of erosion-control systems. In drainage systems, 140 000 000 m² (165,000,000 yd²) of fabrics was installed in the past 10 years and have performed satisfactorily.

FUNCTIONS OF GEOTEXTILES IN DRAINAGE AND EROSION CONTROL

In erosion-control systems, geotextiles perform the same functions as in drainage except for some applications, such as protection from wave action, where they are submitted to greater stresses during service than during installation. The three specific functions performed by geotextiles in drainage and erosion-control applications are

1. Prevention of soil movement,
2. Allowing free passage of groundwater, and
3. Prevention of intrusion of the cover material into the protected soil.

In addition, fabrics must be able to withstand installation stresses and must survive in place at least throughout the expected life of the system.

Prevention of Soil Movement

The major function of geotextiles in erosion control and drainage is to prevent the exposed surface soil from being moved by dynamic environmental forces.

To prevent movement of the surface soil, the geotextile must be in intimate contact with the soil (i.e., there must be no space between the fabric and the soil); otherwise the fabric will be forced to act as a true filter at a lower level, where it and the soil come in intimate contact again. Here the fabric actually stops the soil particles from moving and allows water to pass through (Figure 1). However, wherever the geotextile is in intimate contact with the soil, the soil is prevented from moving in the first place (Figure 2). The fabric performs as a permeable constraint, not as a filter. This concept was presented by McGown (1) in 1978 in Europe. Ball and others (2) described this function in 1979 based on their work for the Alabama Department of Highways.

Bell (3) described the constraint function of geotextiles in drainage and erosion control in more

5. B.J. Dempsey. Laboratory and Field Studies of Channeling and Pumping. TRB, Transportation Research Record 849, 1982, pp. 1-12.
 6. R.M. Knutson and M.R. Thompson. Permanent-Deformation Behavior of Railway Ballast. TRB, Transportation Research Record 694, 1978, pp. 60-65.
 7. D.J. Janssen and B.J. Dempsey. Soil Water Prop-

erties of Subgrade Soils. Department of Civil Engineering, Univ. of Illinois, Urbana-Champaign, Transportation Engineering Series 184, April 1980.
 8. K. Terzaghi and R.B. Peck. Soil Mechanics in Engineering Practice. Wiley, New York, 1967.

Publication of this paper sponsored by Task Force on Engineering Fabrics.

Abridgment

Mechanism of Geotextile Performance in Soil-Fabric Systems for Drainage and Erosion Control

RICHARD D. WEIMAR, JR.

Over the past 15 years, more than 250 000 000 m² (300,000,000 yd²) of geotextiles have been used in drainage and erosion-control systems. Initial geotextile specifications established a decade ago were based on the best-available understanding of fabric function in fabric-soil systems. Considerable research over the past 10 years has significantly changed the understanding of how fabrics function in these systems. As a consequence, fabric specifications now need modification to achieve maximum cost-effective performance. Therefore, a state-of-the-art model of soil-fabric systems is given, and the key physical properties of geotextiles needed for acceptable performance are suggested. Knowing how fabrics function and which properties are important, the designers and contractors of drainage and erosion-control systems can properly specify and install the geotextiles needed in a given system for acceptable performance at minimum cost.

Nonwoven geotextiles account for more than 90 percent of the fabrics used outside of the United States. Within the United States they have only recently reached the same rate of use as wovens because they were introduced 10 years later than wovens. On a worldwide basis, 80 percent of the geotextiles used in erosion control have been nonwoven. The first table gives data on the types of geotextiles installed:

Item	United States		Worldwide	
	No.	Percent	No.	Percent
All fabrics	200		690	
Nonwovens	120	60	590	85
Wovens	80	40	100	15

The second table gives data on the use of geotextiles:

Item	United States		Worldwide	
	Non-woven	Woven	Non-woven	Woven
Drainage	40	10	125	15
Support	65	55	375	65
Erosion Control	15	15	90	20

(Note: In the above tables, geotextiles installed include only those in drainage, support, and erosion control; worldwide figures include U.S. values; and 1 m² = 1.196 yd².)

More than 110 000 000 m² (130,000,000 yd²) of

geotextiles has been installed during the past decade, and these geotextiles have demonstrated acceptable performance in a wide spectrum of erosion-control systems. In drainage systems, 140 000 000 m² (165,000,000 yd²) of fabrics was installed in the past 10 years and have performed satisfactorily.

FUNCTIONS OF GEOTEXTILES IN DRAINAGE AND EROSION CONTROL

In erosion-control systems, geotextiles perform the same functions as in drainage except for some applications, such as protection from wave action, where they are submitted to greater stresses during service than during installation. The three specific functions performed by geotextiles in drainage and erosion-control applications are

1. Prevention of soil movement,
2. Allowing free passage of groundwater, and
3. Prevention of intrusion of the cover material into the protected soil.

In addition, fabrics must be able to withstand installation stresses and must survive in place at least throughout the expected life of the system.

Prevention of Soil Movement

The major function of geotextiles in erosion control and drainage is to prevent the exposed surface soil from being moved by dynamic environmental forces.

To prevent movement of the surface soil, the geotextile must be in intimate contact with the soil (i.e., there must be no space between the fabric and the soil); otherwise the fabric will be forced to act as a true filter at a lower level, where it and the soil come in intimate contact again. Here the fabric actually stops the soil particles from moving and allows water to pass through (Figure 1). However, wherever the geotextile is in intimate contact with the soil, the soil is prevented from moving in the first place (Figure 2). The fabric performs as a permeable constraint, not as a filter. This concept was presented by McGown (1) in 1978 in Europe. Ball and others (2) described this function in 1979 based on their work for the Alabama Department of Highways.

Bell (3) described the constraint function of geotextiles in drainage and erosion control in more

Figure 1. Fabric separated from protected soil.

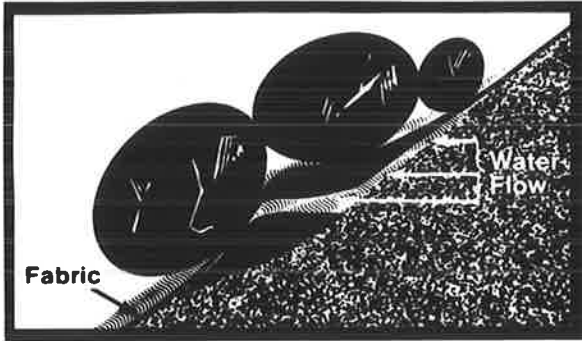


Figure 2. Fabric maintained in intimate contact with protected soil.

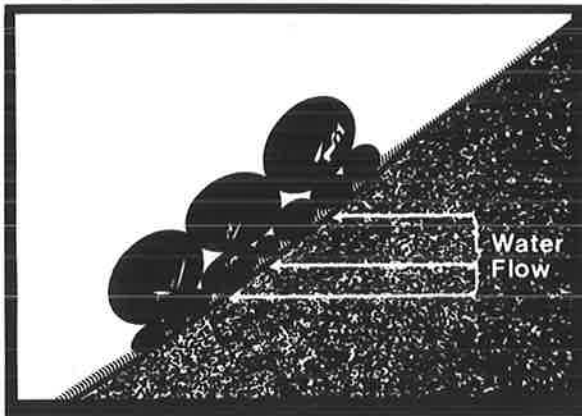
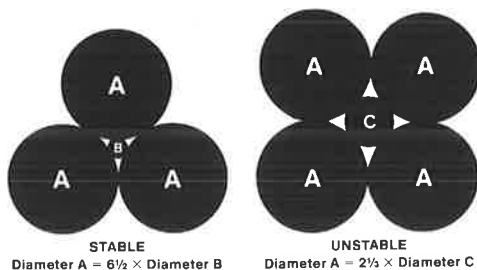


Figure 3. Filter criteria.



The diameter of an opening in a filter medium should be three (3) times greater than the diameter of the particles being separated from a fluid.

detail. His conclusions were based on information gathered from the report on geotextiles prepared for FHWA (4) and from his own studies:

The geotextile is commonly referred to as a filter; however, the real objective is to prevent the geotextile from performing as a true filter. A filter removes suspended particles from a fluid and by this action a filter must plug. Therefore, a geotextile filter application must be designed so that it does not remove large quantities of suspended particles from the pore water. The system must be designed so that, 1) particles do not go into suspension and, therefore, are not filtered by the geotextile; or 2) particles that

are in suspension are allowed to pass through the geotextile so that it does not plug.

Bell (3) summarized the fabric function for constraint purposes and suggested that there were three general objectives of a geotextile filter:

1. To allow the free flow of water from the soil into the drain,
2. To prevent piping of the soil around the drain, and
3. To prevent plugging of the filter (Figure 3).

Allowing Free Passage of Groundwater

A fabric must maintain the ability to allow groundwater seepage to pass freely through the fabric throughout the service life of the system. The principal design uncertainty is how to match the water permeability of the fabric to that of the soil being protected. Marks (5) and Carroll (6) carried out major laboratory studies with nonwovens, which demonstrated that each of several different soil types, not fabric type, controlled the rate of water flow.

Chen and others (7) demonstrated that these results were to be expected. The equation that describes the velocity of water flow (V) through a system of materials that has different permeability coefficients is

$$V = H / \left[\sum_i^n (d_i/k_i) \right] \quad (1)$$

where

V = water flow velocity through the system,
 H = hydrostatic pressure,
 d_i = thickness of a material segment, and
 k_i = permeability coefficient of a material segment.

Therefore, if $k_s = k_f$, and $d_s \gg d_f$ (when s = soil and f = fabric), then $d_s/k_s = (d_s/k_s) + (d_f/k_f)$. Because the protected soil is so much thicker than the geotextile, the soil controls water flow when $k_s \approx k_f$.

Turning from theoretical considerations to practical applications, Table 1 gives water flow rates of soils and fabrics that have the same permeability coefficients.

Because geotextiles have approximately 1,000-fold greater flow capacities than soil at equivalent values of k , a standardized flow index [e.g., permeability = $k_f \div$ (fabric thickness)] is needed to match fabrics to soil.

Prevention of Intrusion of Cover Material into Protected Soil

In fabric-containing erosion-control systems, the aggregate cover material (e.g., gravel, rip-rap, armor stone) serves two main functions:

1. It minimizes the kinetic energy of the water that contacts the fabric from the outside, and
2. It keeps the geotextile in intimate contact with the soil.

The function of the fabric in relation to the cover material is to keep the aggregate separated from the soil below and to prevent the stones from sinking.

To keep the geotextile in continuous intimate contact with the soil throughout the life of the

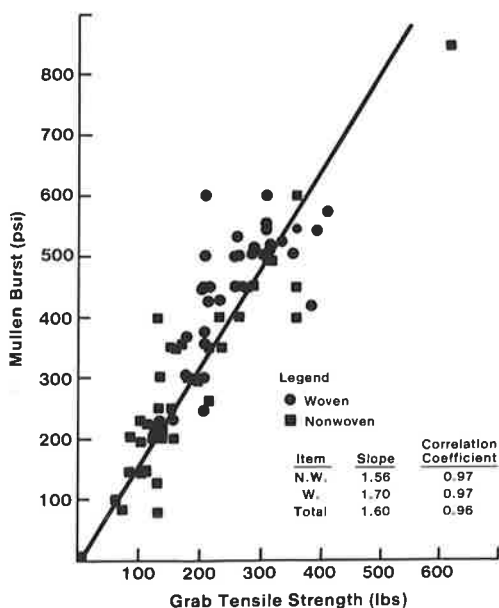
Table 1. Flow rates of soils and fabrics that have the same permeability coefficients under equivalent pressure.

Permeability Coefficient, k (cm/sec)	Soil Flow Rate ^a		Fabric Flow Rate (gal/min/ft ²)
	Type	Rate (gal/min/ft ²)	
0.001	Well-graded silty sand and gravel	0.005	15
0.01	Clean, well-graded sand and gravel	0.05	100
0.1	Uniform, medium sand	0.5	400
1	Uniform, coarse sand	5	
10	Clean, fine to coarse gravel	50	
100	Derrick stone	500	

Note: A hydrostatic pressure of 25 cm (10 in.) was used.

^aA soil thickness of 100 cm (40 in.) was used.

Figure 4. Grab tensile strength versus burst strength for some geotextiles.



erosion-control system, the cover material must be appropriately designed and properly installed to ensure that it will remain in place during the life of the system. A covering aggregate that is too lightweight and placed on a properly selected fabric in a system that is subjected to high wave action may be moved during service.

The stone placed inside a fabric-enclosed drain system should be well compacted to ensure that the geotextile is in intimate contact with the soil for these same reasons.

Another important consideration in designing cover material is to be certain that the material itself is at least as permeable as the soil, and that it will remain so.

Because proper installation methods can prevent premature failure, any new or innovative procedures must be specified by the designers, at least until they become common practice in the construction industry.

DESIGN CRITERIA

Fabric characteristics important in erosion control and drainage are permeability, soil retention abilities, durability, and strength properties. The gen-

erally greater physical property (strength) requirements for erosion-control applications are discussed below. Requirements for drainage fabrics are usually lower than those for erosion control.

Permeability

The ability of nonwoven fabrics to allow water to pass freely is 1,000-fold greater than that of soil of an equal permeability coefficient. To satisfy the immediate need for an acceptable method for matching the flow levels of fabrics to soil with high margins of safety, the recommendation is to allow $k_f = k_s$ for noncritical applications, and $k_f = 10 \times k_s$ for critical applications.

Soil Retention Abilities

Extensive laboratory testing and in-use experience have shown how currently available nonwoven geotextiles that have opening size values of < 0.8 mm ($> \text{No. } 20$ sieve) and wovens with opening size values of < 0.6 mm ($> \text{No. } 30$ sieve), as determined by the U.S. Army Corps of Engineers' equivalent opening size (EOS) test, perform acceptably in erosion-control and drainage applications.

Soil-fabric problems that have occurred to date were not caused by fabrics that have excessively open structures. Problems have occurred from one or both of two causes. Foremost, the fabric was not placed in intimate contact with the soil and it was forced to become a true filter. Second, the fabric openings were too small to allow the usual, initial, short-term passage of suspended fine particles through the fabric.

Currently, no established correlation between EOS values and the performance of geotextiles (5,8) has been found, despite the efforts of many researchers.

Durability

Durability criteria commonly include chemical, biological, thermal, and ultraviolet stability. These properties are addressed by Bell and others (4) and many other researchers.

Strength Properties

There is general agreement among researchers that at least two levels of the strength requirement are needed to differentiate between the general minimum requirements and those fabrics that will be submitted to unusually high stresses during installation or in service.

The majority of drainage applications are satisfied by one set of specifications because there are seldom significant in-use stresses. Where necessary, specifications for erosion control in critical applications may be used.

The lower level of strength requirements was developed to ensure that the fabric will survive construction of the system. Fabrics that have greater strength levels will survive severe in-use stresses. The physical properties generally considered of primary importance are tensile strength, elongation, puncture resistance, tear propagation resistance, and burst strength.

Other properties described by Bell and others (4) that are of secondary importance are bulkiness, weight (dry and wet), specific gravity, flexibility, cutting resistance, and seam strength. Of the specifications on primary properties, burst strength is redundant because it is indexed by fabric tensile strength values, as shown in Figure 4.

SUMMARY

In summary, it should be stressed again that the majority of specifications in place today and the concepts on which they were developed were formulated in the late 1960s and early 1970s. Currently, a rapidly growing body of information demands that these older concepts be modified to accommodate an increased understanding of how fabrics and systems function. Current understanding will change further in this decade. Nevertheless, what is known today must be used as the basis for guidelines and practice. This is the continuing dilemma of working with a dynamic, essential technology.

REFERENCES

1. A. McGown. The Properties of Nonwoven Fabrics Presently Identified as Being Important in Public Works Applications. Presented at INDEX 78 Symposium (EDANA), Amsterdam, Netherlands, 1978.
2. J. Ball and others. Design Parameters for Longitudinal Geotextile Lined Subsurface Pavement Drainage Systems. Department of Civil Engineering, Univ. of Alabama, Huntsville, 1979.
3. J.R. Bell. Design Criteria for Selected Geotextile Installations. Presented at 1st Canadian Symposium on Geotextiles, Calgary, Alberta, Canada, 1980.
4. J.R. Bell and others. Interim Report on Evaluation of Test Methods and Use Criteria for Geotextile Fabrics in Highway Applications. FHWA, Rept. FHWA/RD-80/021, 1979.
5. B.D. Marks. The Behavior of Aggregate and Fabric Filters in Subdrainage Applications. Univ. of Tennessee, Knoxville, 1975.
6. R.G. Carroll. The Behavior of Aggregate and Fabric Filters in Subdrainage Applications. Univ. of Tennessee, Knoxville, M.S. thesis, 1977.
7. Y.H. Chen and others. Laboratory Testing of Plastic Filters. Engineering Research Center, Colorado State Univ., Fort Collins, 1980.
8. J.P. Giroud. Designing with Geotextiles. Matereaux et Constructions, Vol. 14, No. 82, 1981.

Publication of this paper sponsored by Task Force on Engineering Fabrics.

Permeability Tests of Selected Filter Fabrics for Use with a Loess-Derived Alluvium

G.T. WADE, F.W. KLAIBER, AND R.A. LOHNES

Permeability tests on six nonwoven and two woven geotextiles with a silty-clay alluvium indicate that all of the fabrics tested will prevent piping of the soil, regardless of the state of compaction. When a discontinuity (such as a hole) was introduced into the soil, some soils were observed to pipe. The range of permeabilities of soil-fabric systems was observed to be narrow, even though the range of fabric permeability was wide and the soil compaction varied. A theoretical analysis shows that the permeability of the soil is the controlling factor in permeability testing of the soil-fabric system. A piping test similar to the test for dispersive clays is suggested as an alternative to permeability testing of soils and filter fabrics.

Drainage problems have traditionally been solved by using aggregate filters. Loess-derived silty soils (like those in western Iowa) require multilayer filters, which are both expensive to produce and labor intensive to construct. The need for more economical methods of filter construction with silts resulted in a study of geotextile filters for use with these soils. There are currently more than 100 (1) different geotextiles available in the United States, which consist of both woven and nonwoven fabrics.

Several weaving techniques are used, but the products are essentially the same: a relatively thin cloth that has a rectilinear pattern of openings. The sizes of the openings differ, depending on the thickness of the filament and the number of picks per inch, but for any given fabric there is only slight variability in the size of the openings.

Nonwoven fabrics are produced by several techniques, depending on the manufacturer, and may be thin or more than a centimeter thick. Regardless of thickness, the irregular filament pattern produces various pore sizes through the fabric. Thicker non-

woven fabrics are often arbitrarily classified as mats.

LITERATURE REVIEW

Cotton cloth was first used in North Carolina in 1926 to improve subgrade strength, and the U.S. Army Corps of Engineers began using fabrics in the early 1950s to control shore erosion. Increased construction costs and the development of synthetics resulted in the expanded use of geotextiles, including embankment stabilization, grade stabilization for highways and railroads, retaining walls, consolidation of soils, drainage, and silt fences for erosion control. The product technology and availability of geotextiles have progressed ahead of published research results.

The Corps of Engineers used research conducted at the Waterways Experiment Station to develop guidelines for the use of plastic filter cloth (2). Six woven and one nonwoven filter cloths were tested for various chemical and physical properties. Two characterization tests of particular interest for drainage applications are the equivalent size of the openings and the percentage of openings in the fabric. Rounded sand of known gradation was sieved through the fabric, and the percentage retained was used to determine an equivalent opening size (EOS). The percent open area (%OA) was determined by projecting an image of the cloth on a grid and measuring the amount of open area at randomly selected points on the grid.

Filtration and clogging tests were conducted with several gap-graded soils that exhibited a suscepti-

SUMMARY

In summary, it should be stressed again that the majority of specifications in place today and the concepts on which they were developed were formulated in the late 1960s and early 1970s. Currently, a rapidly growing body of information demands that these older concepts be modified to accommodate an increased understanding of how fabrics and systems function. Current understanding will change further in this decade. Nevertheless, what is known today must be used as the basis for guidelines and practice. This is the continuing dilemma of working with a dynamic, essential technology.

REFERENCES

1. A. McGown. The Properties of Nonwoven Fabrics Presently Identified as Being Important in Public Works Applications. Presented at INDEX 78 Symposium (EDANA), Amsterdam, Netherlands, 1978.
2. J. Ball and others. Design Parameters for Longitudinal Geotextile Lined Subsurface Pavement Drainage Systems. Department of Civil Engineering, Univ. of Alabama, Huntsville, 1979.
3. J.R. Bell. Design Criteria for Selected Geotextile Installations. Presented at 1st Canadian Symposium on Geotextiles, Calgary, Alberta, Canada, 1980.
4. J.R. Bell and others. Interim Report on Evaluation of Test Methods and Use Criteria for Geotextile Fabrics in Highway Applications. FHWA, Rept. FHWA/RD-80/021, 1979.
5. B.D. Marks. The Behavior of Aggregate and Fabric Filters in Subdrainage Applications. Univ. of Tennessee, Knoxville, 1975.
6. R.G. Carroll. The Behavior of Aggregate and Fabric Filters in Subdrainage Applications. Univ. of Tennessee, Knoxville, M.S. thesis, 1977.
7. Y.H. Chen and others. Laboratory Testing of Plastic Filters. Engineering Research Center, Colorado State Univ., Fort Collins, 1980.
8. J.P. Giroud. Designing with Geotextiles. Matereaux et Constructions, Vol. 14, No. 82, 1981.

Publication of this paper sponsored by Task Force on Engineering Fabrics.

Permeability Tests of Selected Filter Fabrics for Use with a Loess-Derived Alluvium

G.T. WADE, F.W. KLAIBER, AND R.A. LOHNES

Permeability tests on six nonwoven and two woven geotextiles with a silty-clay alluvium indicate that all of the fabrics tested will prevent piping of the soil, regardless of the state of compaction. When a discontinuity (such as a hole) was introduced into the soil, some soils were observed to pipe. The range of permeabilities of soil-fabric systems was observed to be narrow, even though the range of fabric permeability was wide and the soil compaction varied. A theoretical analysis shows that the permeability of the soil is the controlling factor in permeability testing of the soil-fabric system. A piping test similar to the test for dispersive clays is suggested as an alternative to permeability testing of soils and filter fabrics.

Drainage problems have traditionally been solved by using aggregate filters. Loess-derived silty soils (like those in western Iowa) require multilayer filters, which are both expensive to produce and labor intensive to construct. The need for more economical methods of filter construction with silts resulted in a study of geotextile filters for use with these soils. There are currently more than 100 (1) different geotextiles available in the United States, which consist of both woven and nonwoven fabrics.

Several weaving techniques are used, but the products are essentially the same: a relatively thin cloth that has a rectilinear pattern of openings. The sizes of the openings differ, depending on the thickness of the filament and the number of picks per inch, but for any given fabric there is only slight variability in the size of the openings.

Nonwoven fabrics are produced by several techniques, depending on the manufacturer, and may be thin or more than a centimeter thick. Regardless of thickness, the irregular filament pattern produces various pore sizes through the fabric. Thicker non-

woven fabrics are often arbitrarily classified as mats.

LITERATURE REVIEW

Cotton cloth was first used in North Carolina in 1926 to improve subgrade strength, and the U.S. Army Corps of Engineers began using fabrics in the early 1950s to control shore erosion. Increased construction costs and the development of synthetics resulted in the expanded use of geotextiles, including embankment stabilization, grade stabilization for highways and railroads, retaining walls, consolidation of soils, drainage, and silt fences for erosion control. The product technology and availability of geotextiles have progressed ahead of published research results.

The Corps of Engineers used research conducted at the Waterways Experiment Station to develop guidelines for the use of plastic filter cloth (2). Six woven and one nonwoven filter cloths were tested for various chemical and physical properties. Two characterization tests of particular interest for drainage applications are the equivalent size of the openings and the percentage of openings in the fabric. Rounded sand of known gradation was sieved through the fabric, and the percentage retained was used to determine an equivalent opening size (EOS). The percent open area (%OA) was determined by projecting an image of the cloth on a grid and measuring the amount of open area at randomly selected points on the grid.

Filtration and clogging tests were conducted with several gap-graded soils that exhibited a suscepti-

Table 1. Fabric properties.

Fabric	Type ^a	Thickness (mm)	EOS ^b	%OA	k (cm/sec)
A	N	1.27	140	NA	0.05
B	N	0.76	80-100	NA	0.07
C	N	0.38	70-100 ^c	NA	0.02
D	N	1.27	80-100	4-6	0.02-0.3
E	N	2.80	80-100	NA	0.3
F	W	0.43 ^d	100	4-5	0.05
G	N	0.762	80-100	NA	0.10
H	W	0.61 ^d	40	21-26	∞

Note: NA = not available.

^aN = nonwoven and W = woven.

^bU.S. sieve sizes.

^cPore-size distribution available.

^dMeasurements conducted on specimens.

bility to piping. Silty soils were omitted because permeability was so low that no useful data could be obtained. By using EOS and %OA, the following guidelines for filter fabric selection were accepted. For granular soils that contain less than 50 percent silt, the EOS of the filter fabric should be smaller than the 85 percent size of the protected soil. Filter fabrics should not be used with soils that have more than 50 percent of their particles smaller than the No. 200 sieve (3). These specifications are now frequently used. There is no problem with the specifications as long as a granular material with less than 50 percent fines is being protected with a woven fabric. No additional guidelines are available for silty soils or nonwoven fabrics.

Ogink (4) studied both woven and nonwoven fabrics with sands and proposed that the ratio (O_{90} of the geotextile/ D_{90} of the soil) be ≤ 1.0 for woven and ≤ 1.8 for nonwoven products, where O_{90} and D_{90} are the 90 percent opening and the particle size, respectively. Zitscher (5) recommends that the O_{50} of the geotextile equal $(25 - 37) \times D_{50}$ for silty soils, where O_{50} and D_{50} are the average pore and particle size. ICI Fibres in Great Britain give elaborate design procedures for "terram," a nonwoven geotextile they manufacture, and include the recommendation that $O_{50}/D_{85} \geq 1$. Rankilor (6) summarized these methods and concluded that more research is needed in this field, especially on cohesive soils.

Rosen and Marks (7) evaluated 12 soils against 1 nonwoven fabric (Mirafi 140) by using static head permeability tests of 300-hr duration. They used a conventional aggregate filter as a standard and noted a decrease in permeability with time for all tests. They concluded that, for well-graded soils, a filter cake develops behind the fabric. The fabric then acts as a boundary for the formation of an internal filter cake. Results of their tests also revealed that well-graded soils that possess higher plasticity and cohesion exhibit less piping before complete filter-cake formation. They concluded that Mirafi 140 was acceptable for all the soils tested, including those that contain up to 70 percent silt.

McKeand (8) performed similar permeability tests with several fabrics and testing durations to 3,000 hr. He concluded that filter-cake formation is a function of the pore-size distribution, percent open area, and thickness of the fabric; however, no quantitative relations were given. He also stated that the three nonwoven fabrics tested performed satisfactorily for the wide range of soils, including soils that possess liquid limits up to 40 percent and plasticity indices less than 15 percent.

The data in Table 1 summarize the physical prop-

erties provided for drainage geotextiles produced by several manufacturers and illustrates another problem currently faced by the engineer: inadequate product information that is nonstandardized. This results from the various manufacturing techniques; differing filament composition, texture, and fabric thickness; differing laboratory equipment; and lack of ASTM standards.

The EOS, as measured by Calhoun (2), is generally accepted for woven fabrics; however, values given for nonwoven fabrics, with their wide range of opening sizes, cannot be measured by sieving techniques. The sand is either entrapped in the fabric matrix or passes through the larger openings, thereby yielding an EOS value near the largest size openings. The EOS for nonwoven fabrics is generally equated to the 95 percent opening size.

The %OA is also not directly applicable to nonwoven fabrics, especially mats, because the openings are neither normal to the surface nor lead directly through the fabric.

Permeability, the most often published parameter for geotextile filters, is usually in the range of a fine to coarse sand. This range is sufficiently high enough to avoid flow restriction in silty soils. Permeability appears to be the most popular characteristic for evaluating geotextile acceptability for drainage and erosion control; however, it has been noted that improved tests and a better understanding of this property are needed (9).

PERMEABILITY AND GEOTEXTILE FILTERS

It is a common observation in permeability testing of soils alone, and in testing of soils in conjunction with filter fabrics, that the permeability of the system being tested decreases with increasing time after initiation of the test. Several interpretations have been offered to explain this phenomenon, including exsolution of dissolved air, bacterial growth, and, in the case of soil and filter fabric systems, formation of a filter cake at the fabric-soil interface.

Bertram (10) conducted tests on sand filters and noted a decrease in permeability with time. He concluded that air in the distilled water was being exsolved, thereby creating an air filter that impeded the flow of water. Subsequent tests with de-aired water demonstrated no further decreases in permeability. Note that de-airing the water also removed the mechanism for organism growth and subsequent permeability decrease; therefore, de-airing the water may have a two-fold effect.

Permeability tests conducted on loess at several degrees of compaction revealed a similar decrease in permeability with increasing time after the initial test (11). Bacterial growth was observed after 7 days on all samples tested. Badger (11) hypothesized that the presence of those organisms decreased the permeability. He reported that his samples showed a 75 percent reduction in permeability after 2 days. Chen and others (12) noted a similar permeability decrease when using a permeant that contained 1 to 2 parts per million (ppm) residual chlorine. They concluded that a small amount of residual chlorine was ineffective in retarding bacterial growth during long-term tests. Subsequent tests performed by using 10 ppm residual chlorine revealed no substantial permeability decrease with time, which suggested that higher chlorine concentrations were effective in retarding the bacterial growth that caused the permeability decrease.

Fabric clogging has not been shown to be a direct factor in permeability reduction. Rosen and Marks (7) demonstrated that less than 0.05 percent of the soil particles are entrapped within the fabric; how-

ever, they concluded that a filter cake develops for gap-graded soils next to the geotextile. This filter cake has a lower permeability than either the geotextile or soil matrix and is increased by the restriction on fine particles within the soil. Chen and others (12) concluded that well-graded soils are natural filters and that no migration of fines occurs.

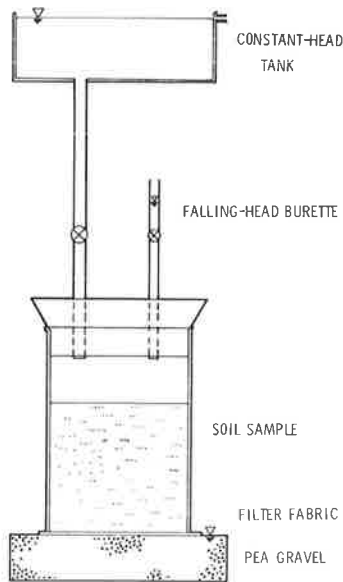
TEST PROCEDURE

To test the acceptability of fabrics that might be used with silty soils, a permeameter was constructed as shown in Figure 1. A constant head of 3 m was applied to induce a continuous flow through the specimen. The soil specimens were placed in 7-cm-diameter Lucite cylinders; the fabric was secured to the bottom of the cylinder; and the samples were allowed to capillary saturate. The 3-m head was then applied to induce flow through the sample. The head was removed periodically and the permeability measured by using the falling-head equation; the static head was then reapplied.

The soil used in the tests was a loess-derived

alluvial material characterized as a silty clay. The soil properties and Atterburg limits are shown in Figure 2. Test conditions were designed to resemble possible field conditions of the soil, including field unit weight, nonuniform compaction, originally saturated unconsolidated soils, and soils with no compaction. Field densities were produced by dynamically compacting air-dried soil in uniform lifts until a density of 1.36 g/cm³ was obtained. These samples were capillary saturated before application of the hydraulic head. The nonuniformly compacted samples were obtained by dynamic compaction of the soil; however, the soil was placed in one layer, and compaction was restricted to the center of the sample. Originally, saturated soils were produced by affixing the geotextile and then pouring a soil-water slurry into the Lucite cylinder. A low density was obtained by pouring the air-dried soil into the cylinders with no mechanical compaction before application of the hydraulic head. Where the aggregate filter was used, approximately 2.5 cm of fine sand was placed in the cylinder below the soil. Where the soil was compacted, the geotextiles were placed after compaction to minimize fabric clogging. Test conditions are summarized in the table below:

Figure 1. Permeameter used for hydraulic testing.

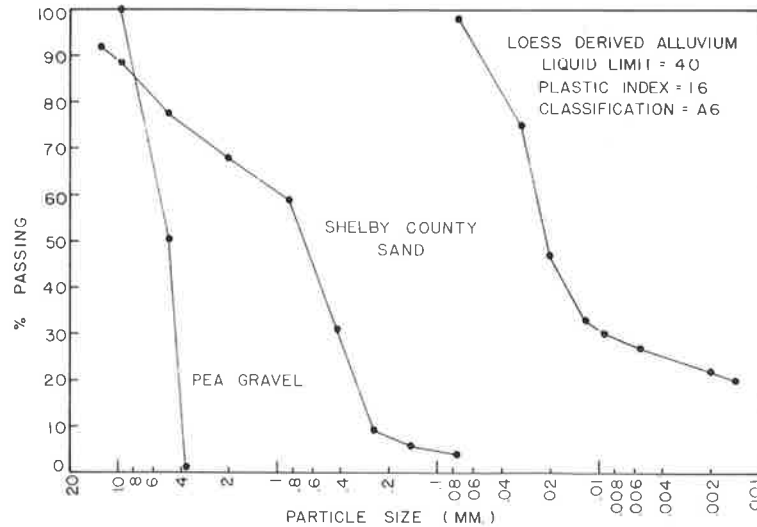


Test	Specimen Thickness (cm)	Filters	Soil Condition
1	5.5	A, B, C, D, F, G, pea gravel, sand	Natural dry unit weight; uniform compaction
2	1.8	A, B, D, G	Soil slurry
3	6.0	E, F, H	No compaction
4	4.0	C, E, F, pea gravel	Nonuniform compaction

Soil specimens in test 4 were intentionally disturbed by placing a 1.5-mm-diameter hole through the soil to the top of the filter. The head was then reapplied and the effect on permeability noted.

The filters selected consisted of one aggregate and eight geotextiles. The fine sand aggregate approximated Terzaghi's (13) piping criteria as a filter for the silty clay. The pea gravel at the base of the apparatus was coarse enough so that negligible head was lost in it. Curves identified as pea gravel reflect the properties of the soil alone. The geotextiles evaluated--two woven and six nonwoven fabrics--are given in Table 1.

Figure 2. Sieve analysis for aggregate filters and loess-derived alluvium.



TEST RESULTS

Test 1 (Figure 3) demonstrated that a wide variety of geotextiles all behaved in essentially the same manner. Each had a decrease in permeability between 35 and 45 percent over the 340-hr test period, and none piped. There was an unexpected 40 percent decrease in the soil alone, whereas the sample with the sand filter had a decrease of only about one-half that experienced by the other samples. The 24-hr permeability of each sample is given in the table below (note that all 24-hr permeabilities are multiplied by 10^{-6} cm/sec, and NA signifies that the test was not conducted with this filter):

Filter	24-hr Permeability		
	Test 1	Test 2	Test 3
A	159	162	NA
B	155	372	NA
C	149	NA	75
D	139	107	NA
E	161	NA	103
F	161	NA </td <td>102</td>	102
G	NA	87	NA
Sand	197	NA	NA
Pea gravel	195	NA	40

In test 2 (Figure 4), all permeabilities decreased from the initial values listed in the table

above and appeared to stabilize at approximately 30×10^{-6} cm/sec. During testing, the soil samples with fabric G showed transverse cracking, thereby giving a nonuniform flow through the samples.

The pattern of decreasing permeability with increasing time was also apparent in test 3. Although the initial permeabilities vary from the other tests, the behavior of these systems is the same as in the other tests.

The results of test 4 (Figure 5) demonstrated that the variation of permeability with time was more erratic than in the previous tests. Fabric E and pea gravel behaved the most erratically in the early portions of the test, whereas fabrics C and F behaved in a manner similar to the previous tests.

The permeabilities of each soil-fabric system decreased with time, regardless of soil preparation or filter type. Also, none of the soils piped, including test 3 where piping was anticipated. However, when a 1-mm hole was punched through the soil, progressive soil piping followed with several of the geotextiles.

DISCUSSION OF RESULTS

The data on initial permeabilities reveal that for each test there is little variation in the permeabilities of the soil-fabric systems. The quantity

Figure 3. Permeability versus time for test 1.

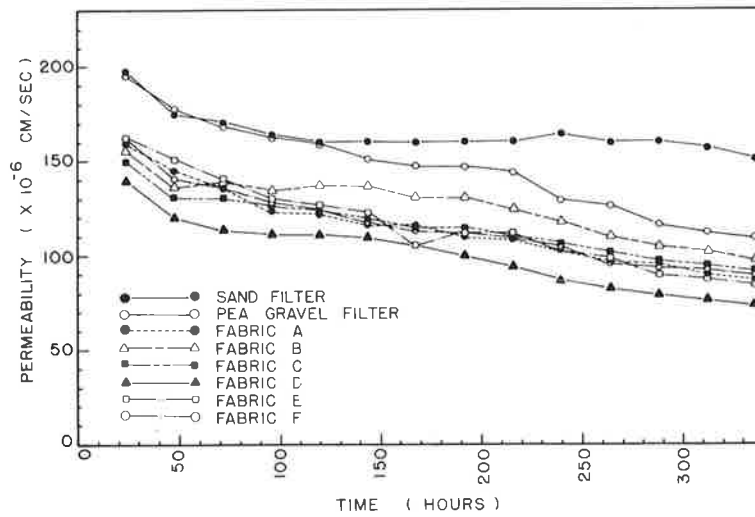


Figure 4. Permeability versus time for test 2.

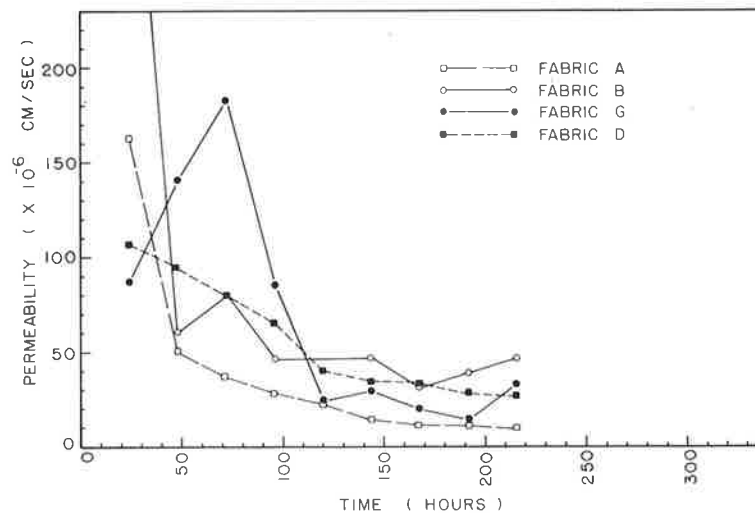
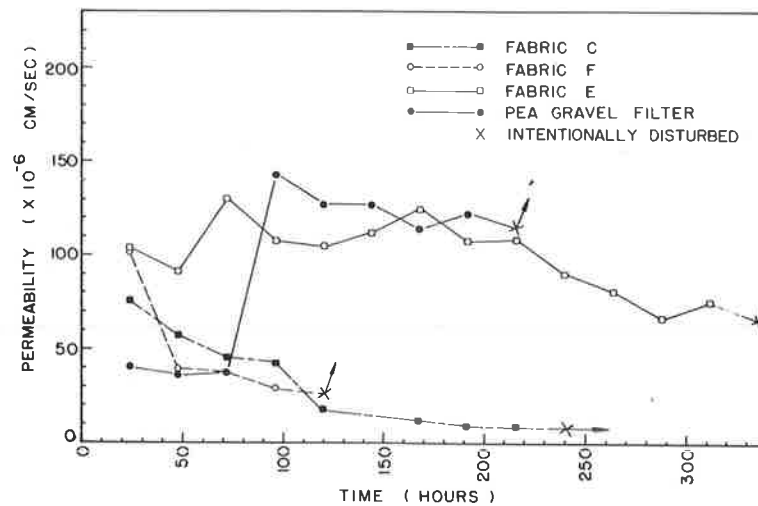


Figure 5. Permeability versus time for test 4.



of water per unit time (Q) flowing through the soil and fabric is described by Darcy's law:

$$Q = Ak_i = Ak(H/t) \text{ or } H = (Q/Ak) \quad (1)$$

where

A = cross-sectional area,
 k = permeability of soil-fabric system,
 i = hydraulic gradient,
 t = combined thickness of fabric and soil, and
 H = head loss in system.

The head loss in the entire system is

$$H = H_s + H_f \text{ or } H_f = H - H_s \quad (2)$$

where H_s is the head loss in the soil and H_f is the head loss in the fabric. Substituting Equation 1 into Equation 2 gives

$$H_f = (Q/Ak) - H_s \quad (3)$$

Because the quantity of flow through the soil and the fabric is the same, and because the cross-sectional areas of both soil and fabric are equal,

$$k_s(H_s/t_s) = k_f(H_f/t_f) = k_f [(Q/Ak) - H_s]/t_f \quad (4)$$

where

k_s, k_f = permeabilities of soil and fabric, respectively;
 t_s = thickness of soil; and
 t_f = thickness of fabric.

Therefore, because

$$Q = k_s(H_s/t_s) A \quad (5)$$

then

$$k_s(H_s/t_s) = (k_f/t_f) \{ [k_s(H_s/t_s)t/k] - H_s \} \quad (6)$$

Equation 6 can be manipulated algebraically, such that H_s cancels out and

$$k = k_f k_s t / (k_s t_f + k_f t_s)$$

Because the product of the permeability of the soil times the thickness of the fabric is very small and the thickness of the fabric is small (relative to

the thickness of the total system), the apparent permeability of the soil-fabric system is approximately equal to the permeability of the soil alone; or by using the symbols above, because $k_s \rightarrow 0$ and $t \sim t_s$, then, $k \sim k_s$.

If Equation 3 (for apparent permeability) is used with the data from Table 1, and a permeability for soil of 0.0002 cm/sec and a thickness of soil at 5.5 cm are also used, then all of the fabrics tested (except fabric A) give a theoretical apparent permeability of about 0.0002 cm/sec. The apparent permeability of fabric A was calculated to be 0.00014 cm/sec. This analysis indicates that the results of permeability tests on soil-fabric systems are of questionable value because they reflect mainly the permeability of the soil, not the soil-fabric system.

All permeability versus time curves show a decrease with time. The nonuniformly compacted samples have the most erratic behavior. This behavior is interpreted to be the result of particle migration as the soil structure is rearranged. Permeabilities of the slurry samples drop to 20 percent of their original value with fabrics A and B, whereas fabrics D and G have less-dramatic decreases. The uniformly compacted samples have a decrease of less than 40 percent. Phenomena that have been used to explain the decrease in permeability with time are consolidation, bacterial growth, fabric clogging, and air entrapment. As discussed in a previous section, evidence exists that clogging of fabric pores is not responsible for a reduction of permeability with time (7,12) with well-graded soils.

The possibility for permeability reduction as a result of consolidation can be evaluated by the following analysis. The flow through the soil creates a seepage force per unit volume (j):

$$j = i \cdot \gamma_w \quad (7)$$

where i is the hydraulic gradient and γ_w is the unit weight of water.

The average effective stress (\bar{s}) created by the seepage force can be shown as

$$\bar{s} = j \cdot t_s \quad (8)$$

where t_s is the soil sample thickness. Combining Equation 8 with Equation 7 gives

$$\bar{s} = i \cdot \gamma_w \cdot t_s \quad (9)$$

or, because $i = H_s/t_s$, where H_s is the head loss,

$$\bar{s} = H_s \cdot \gamma_w \quad (10)$$

In the tests performed in this study, the average effective stress is 29 kN/m². Void ratio versus pressure curves for loess-derived alluvium (14) indicate that a stress increase of this magnitude is negligible; therefore little decrease in permeability can be attributed to consolidation. From the foregoing analyses it appears that the reduction in permeability is the result of bacterial growth, or exsolution of air from the water, or both.

Recognizing that permeability tests on soil-fabric systems may be of limited value, the following analysis suggests an alternate test that may be more useful in evaluating geotextiles for use with various soils.

Hjulström (15) demonstrated that a critical velocity exists below which stream erosion will not occur, and that a minimum velocity of 18 cm/sec is required for erosion, regardless of particle size. Sherard and others (16) have found that nondispersive clays withstand velocities of 300 cm/sec through 1-mm pinholes without erosion. The Corps of Engineers, after performing piping tests with sand filters, concluded that the D₁₅ of the sand filter may be as large as 0.4 mm when protecting medium to highly plastic soils with or without silt partings. Therefore, a critical velocity must exist for erosion through, as well as over, the soil.

Darcy's law states that

$$Q = kiA \quad (11)$$

and because

$$Q = AV - A_v V_s \quad (12)$$

and

$$n = e/(1 + e) = A_v/A \quad (13)$$

then the seepage velocity can be expressed as

$$v_s = [(1 + e)/e] ki \quad (14)$$

where

- n = porosity,
- e = void ratio,
- V = approach velocity,
- V_s = seepage velocity, and
- A_v = area of voids in the cross section.

Typical values for loess-derived alluvium are 0.8 for void ratio (10⁻⁵ cm/sec for permeability). If a minimum velocity for erosion is 18 cm/sec, the minimum hydraulic gradient required of flow through loess-derived alluvium would be more than 800,000. This indicates that the critical velocity will occur only if macrovoids are available.

As reported by Sherard and others (16), the pipe flow relations, which assume that all head is lost in creating fluid flow, are

$$H = (V^2/2g) [K_1 + f(L/d) + K_2] \quad (15)$$

where

- V = velocity through pipe;
- K₁, K₂ = entrance and exit losses, respectively;
- L = pipe length;
- d = pipe diameter;
- f = 64/N_R (assuming laminar flow);

N_R = Reynolds number; and
H = net head loss.

By using values for H, L, and d; values for d of 5 cm, 2.5 cm, and 1 mm, respectively; and values of K₁ = 0.5 and K₂ = 1.0, the velocity (V) will equal 43 cm/sec. Sherard and others (16), while conducting pinhole tests for dispersing soils (by using these values for H, L, and d), obtained velocities of 38 cm/sec, which support the theory.

Theoretically, uniform loess-derived alluvium will not pipe and filters are not required; however, in practice, nonuniformities as small as 1 mm in diameter may exist, which result from incomplete compaction, differential settlement, tunneling of insects or animals, or plant roots. Thus filters are required to avoid piping.

The pinhole test, as explained in detail by Sherard and others (16) for dispersive soils, requires placing a 1-mm-diameter horizontal hole through a 2.5-cm soil sample. After the introduction of a 5-cm hydraulic head, the hole will rapidly erode to 2 or 3 mm in diameter if the soil is dispersive. If the soil is not dispersive, the head can be increased to 100 cm without erosion. This test could be modified to evaluate geotextile performance with dispersive silty soils by placing down a geotextile gradient of a soil that had been previously perforated. The acceptable geotextile would either restrict soil particles, thereby decreasing velocities below critical levels, or sufficiently restrict flow to reduce velocities below critical levels. This test can be conducted rapidly and, if used for other cohesive soils, can also be used to check for dispersive soils.

CONCLUSIONS

Permeability tests on six nonwoven and two woven fabrics with a silty alluvium indicate that all fabrics tested will prevent piping, regardless of whether the soil was noncompacted, uniformly compacted, or in a slurry. However, when a pinhole was introduced, some of the soil-fabric systems were observed to pipe immediately after the disturbance.

Theoretical analyses and the narrow range of observed permeability with a wide range of fabrics tested and varied soil conditions suggest that permeability testing of the soil-fabric systems may be of little value because the data reflect the conditions of the soil, not the soil-fabric system. Theoretical analyses indicate that the ubiquitous reduction in permeability with time is the result of exsolution of air or bacterial growth that clogs the pores of the system. A piping test similar to the test for dispersive clays is suggested as an alternative to permeability testing for selecting geotextiles to be used as filter fabrics with cohesive soils.

ACKNOWLEDGMENT

This research was conducted through the Engineering Research Institute, Iowa State University, and sponsored by the Iowa Highway Research Board, Iowa Department of Transportation. The opinions, findings, and conclusions of this report are ours and not necessarily those of the Highway Division, Iowa Department of Transportation.

REFERENCES

1. R.M. Koerner and J.P. Welsh. Construction and Geotechnical Engineering Using Synthetic Fabrics. Wiley, New York, 1980.
2. C.C. Calhoun, Jr. Development of Design Cri-

- teria and Acceptance Specification for Plastic Filter Cloth. U.S. Army Corps of Engineers Waterways Experiment Station, Vicksburg, MS, Tech. Rept., 1972.
3. Plastic Filter Fabric. Office of the Chief of Engineers, Department of the Army Corps of Engineers, Rept. CW-02215, Nov. 1977.
 4. H.J.M. Ogink. Investigation on the Hydraulic Characteristics of Synthetic Fabrics. Delft Hydraulics Laboratory, Delft Univ. of Technology, Delft, Netherlands, Publ. 146, May 1975.
 5. F.F. Zitscher. Recommendations for the Use of Plastics in Soil and Hydraulic Engineering. *Die Bautechnik*, Vol. 52, No. 12, 1975, pp. 397-402.
 6. P.R. Rankilor. *Membranes in Ground Engineering*. Wiley, New York, 1981.
 7. W.J. Rosen and D.B. Marks. Investigation of Filtration Characteristics of a Nonwoven Fabric Filter. TRB, Transportation Research Record 532, 1975, pp. 87-94.
 8. E. McKeand. The Behavior of Nonwoven Fabric Filters in Subdrain Application. Proc., International Conference on the Use of Fabrics in Geotechnics, Paris, France, 1977.
 9. D. Leschchinsky. AAR Geotextile Testing to Date. *Railway Track and Structures*, June 1980, pp. 18-23.
 10. G.E. Bertram. An Experimental Investigation of Protective Filters. Graduate School of Engineering, Harvard Univ., Cambridge, MA, Soil Mechanics Series 7, Jan. 1940.
 11. W.W. Badger. Structure of Friable Iowa Loess. Iowa State Univ., Ames, Ph.D. dissertation, 1972.
 12. Y.H. Chen, D.B. Simons, and P.M. Demery. Hydraulic Testing of Plastic Filter Fabrics. *Journal of Irrigation and Drainage*, ASCE, Vol. 107, No. IR3, Sept. 1983, pp. 307-324.
 13. K. Terzaghi. *Theoretical Soil Mechanics*. Wiley and Sons, Chichester, Sussex, England, 1943.
 14. F.M. Akiyama. Shear Strength Properties of Western Iowa Loess. Iowa State Univ., Ames, M.S. thesis, 1964.
 15. F. Hjulström. Studies of Morphological Activity of Rivers as Illustrated by the River Fyris. Univ. of Uppsala, Uppsala, Sweden, Geology Institute Bull. 25, 1935, pp. 221-557.
 16. J.L. Sherard, L.P. Dunningan, R.S. Decker, and E.F. Steele. Pinhole Test for Identifying Dispersive Soils. *Journal of the Geotechnical Engineering Division*, ASCE, Vol. 192, No. GT1, Jan. 1976, pp. 69-85.

Publication of this paper sponsored by Task Force on Engineering Fabrics.

Geotextile Filter Criteria

R. G. CARROLL, JR.

In the past decade, drainage fabric performance has been the subject of numerous research projects. Two general conclusions can be drawn from the many research findings: (a) both woven and nonwoven fabrics can provide acceptable filtration performance in drainage applications, and (b) soil and hydraulic conditions influence fabric filter properties necessary for optimum performance. More specific observations are made in this paper concerning the relation between fabric and soil properties versus drain fabric performance. These observations include the following: (a) fabric equivalent opening size (EOS) and permeability coefficients do not indicate clogging potential, (b) fabric EOS provides an indirect indication of retention ability, (c) gap-graded soils and high hydraulic gradient conditions are conducive to soil piping and filter clogging, (d) well-graded soils and low hydraulic gradients are not conducive to soil piping, and (e) fabric clogging potential can be determined by testing soil-fabric systems in simulated drainage tests that model expected use conditions. The state of the art in drainage fabric technology is reviewed, and rational filter criteria for geotextiles based on three performance parameters—retention ability, permeability, and clogging resistance—are recommended.

Geotextiles are rapidly replacing graded aggregates as the approved filter medium in drainage systems. Engineers use the performance and cost benefits of geotextiles in their drain designs, but they are often confused in their efforts to select the appropriate fabric filter. Regardless of the filter medium chosen for drainage applications, it must meet two conflicting requirements to assure optimum performance:

1. Retention--the filter must have a pore structure fine enough to retain erodible soils, and
2. Permeability--the filter must maintain adequate permeability so that seepage can escape freely from the protected soil. (Note that clogging resistance is inherent to this requirement.)

Grain-size distribution of a graded aggregate filter creates its pore structure that, in turn, controls filtration performance. There are universally accepted criteria for specifying the grain-size distribution of aggregate filters that relate the particle size of a graded aggregate to that of the protected soil (1). These criteria, based on theoretical relations among particle size, pore size, and retention ability of granular materials, have proved adequate through decades of use.

There are no well-established filter criteria for geotextiles. Filtration performance of a geotextile is controlled by its fiber structure, which in turn determines pore sizes, pore distribution, and porosity--the major characteristics that control fabric retention ability and permeability. The ideal retention criteria for fabrics should specify the appropriate pore structure in order to eliminate piping through the fabric, provide an adequate fabric seepage rate, and to assure clogging resistance. But an accurate measure of pore structure in porous media is difficult to obtain. Although numerous tests have been developed, no method has been universally accepted. The next-best alternative to an accurate measure of filter pores is an index test(s) that relates pore characteristics to filtration performance. Such index values are the basis for filter media selection in most filtration applications.

Geotextile performance in filtration-drainage applications has been the scope of considerable research over the past 10 years. The state of the art in drain fabric technology contains sufficient information on performance mechanisms and pertinent

- teria and Acceptance Specification for Plastic Filter Cloth. U.S. Army Corps of Engineers Waterways Experiment Station, Vicksburg, MS, Tech. Rept., 1972.
3. Plastic Filter Fabric. Office of the Chief of Engineers, Department of the Army Corps of Engineers, Rept. CW-02215, Nov. 1977.
 4. H.J.M. Ogink. Investigation on the Hydraulic Characteristics of Synthetic Fabrics. Delft Hydraulics Laboratory, Delft Univ. of Technology, Delft, Netherlands, Publ. 146, May 1975.
 5. F.F. Zitscher. Recommendations for the Use of Plastics in Soil and Hydraulic Engineering. *Die Bautechnik*, Vol. 52, No. 12, 1975, pp. 397-402.
 6. P.R. Rankilor. *Membranes in Ground Engineering*. Wiley, New York, 1981.
 7. W.J. Rosen and D.B. Marks. Investigation of Filtration Characteristics of a Nonwoven Fabric Filter. TRB, Transportation Research Record 532, 1975, pp. 87-94.
 8. E. McKeand. The Behavior of Nonwoven Fabric Filters in Subdrain Application. Proc., International Conference on the Use of Fabrics in Geotechnics, Paris, France, 1977.
 9. D. Leschchinsky. AAR Geotextile Testing to Date. *Railway Track and Structures*, June 1980, pp. 18-23.
 10. G.E. Bertram. An Experimental Investigation of Protective Filters. Graduate School of Engineering, Harvard Univ., Cambridge, MA, Soil Mechanics Series 7, Jan. 1940.
 11. W.W. Badger. Structure of Friable Iowa Loess. Iowa State Univ., Ames, Ph.D. dissertation, 1972.
 12. Y.H. Chen, D.B. Simons, and P.M. Demery. Hydraulic Testing of Plastic Filter Fabrics. *Journal of Irrigation and Drainage*, ASCE, Vol. 107, No. IR3, Sept. 1983, pp. 307-324.
 13. K. Terzaghi. *Theoretical Soil Mechanics*. Wiley and Sons, Chichester, Sussex, England, 1943.
 14. F.M. Akiyama. Shear Strength Properties of Western Iowa Loess. Iowa State Univ., Ames, M.S. thesis, 1964.
 15. F. Hjulström. Studies of Morphological Activity of Rivers as Illustrated by the River Fyris. Univ. of Uppsala, Uppsala, Sweden, Geology Institute Bull. 25, 1935, pp. 221-557.
 16. J.L. Sherard, L.P. Dunningan, R.S. Decker, and E.F. Steele. Pinhole Test for Identifying Dispersive Soils. *Journal of the Geotechnical Engineering Division*, ASCE, Vol. 192, No. GT1, Jan. 1976, pp. 69-85.

Publication of this paper sponsored by Task Force on Engineering Fabrics.

Geotextile Filter Criteria

R. G. CARROLL, JR.

In the past decade, drainage fabric performance has been the subject of numerous research projects. Two general conclusions can be drawn from the many research findings: (a) both woven and nonwoven fabrics can provide acceptable filtration performance in drainage applications, and (b) soil and hydraulic conditions influence fabric filter properties necessary for optimum performance. More specific observations are made in this paper concerning the relation between fabric and soil properties versus drain fabric performance. These observations include the following: (a) fabric equivalent opening size (EOS) and permeability coefficients do not indicate clogging potential, (b) fabric EOS provides an indirect indication of retention ability, (c) gap-graded soils and high hydraulic gradient conditions are conducive to soil piping and filter clogging, (d) well-graded soils and low hydraulic gradients are not conducive to soil piping, and (e) fabric clogging potential can be determined by testing soil-fabric systems in simulated drainage tests that model expected use conditions. The state of the art in drainage fabric technology is reviewed, and rational filter criteria for geotextiles based on three performance parameters—retention ability, permeability, and clogging resistance—are recommended.

Geotextiles are rapidly replacing graded aggregates as the approved filter medium in drainage systems. Engineers use the performance and cost benefits of geotextiles in their drain designs, but they are often confused in their efforts to select the appropriate fabric filter. Regardless of the filter medium chosen for drainage applications, it must meet two conflicting requirements to assure optimum performance:

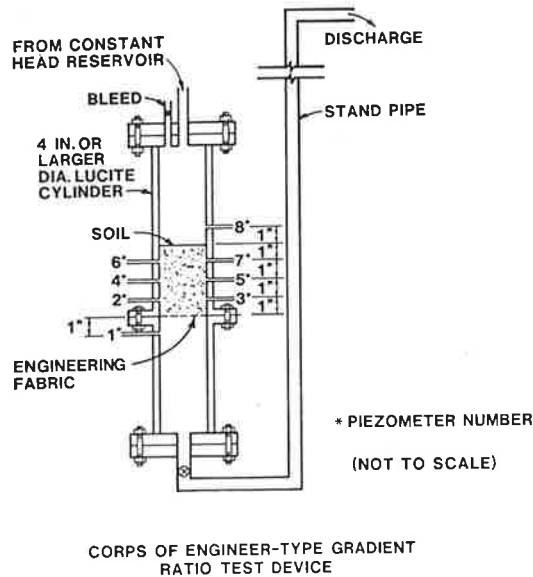
1. Retention--the filter must have a pore structure fine enough to retain erodible soils, and
2. Permeability--the filter must maintain adequate permeability so that seepage can escape freely from the protected soil. (Note that clogging resistance is inherent to this requirement.)

Grain-size distribution of a graded aggregate filter creates its pore structure that, in turn, controls filtration performance. There are universally accepted criteria for specifying the grain-size distribution of aggregate filters that relate the particle size of a graded aggregate to that of the protected soil (1). These criteria, based on theoretical relations among particle size, pore size, and retention ability of granular materials, have proved adequate through decades of use.

There are no well-established filter criteria for geotextiles. Filtration performance of a geotextile is controlled by its fiber structure, which in turn determines pore sizes, pore distribution, and porosity--the major characteristics that control fabric retention ability and permeability. The ideal retention criteria for fabrics should specify the appropriate pore structure in order to eliminate piping through the fabric, provide an adequate fabric seepage rate, and to assure clogging resistance. But an accurate measure of pore structure in porous media is difficult to obtain. Although numerous tests have been developed, no method has been universally accepted. The next-best alternative to an accurate measure of filter pores is an index test(s) that relates pore characteristics to filtration performance. Such index values are the basis for filter media selection in most filtration applications.

Geotextile performance in filtration-drainage applications has been the scope of considerable research over the past 10 years. The state of the art in drain fabric technology contains sufficient information on performance mechanisms and pertinent

Figure 1. COG constant-head permeameter.



fabric properties to support the rational development of geotextile filter criteria. A brief review of that drain fabric technology is provided in this paper, and appropriate geotextile filter criteria based on index and performance testing are recommended.

RETENTION ABILITY AND EQUIVALENT OPENING SIZE

In the late 1960s Calhoun (2) performed research on filter cloths at the U.S. Army Corps of Engineers (COE) Waterways Experiment Station. The objective of the COE project was to develop acceptance specifications and design criteria for plastic filter cloths used in filtration-drainage applications.

Calhoun evaluated several fabrics, most of which were woven monofilament, with one woven multifilament and one nonwoven fabric also included. When the study began woven monofilament fabrics were the only type used in the United States for filtration-drainage applications. These woven monofilament fabrics resembled screen mesh, although their yarn spacing varied somewhat and the pore openings were not square. The woven multifilament and nonwoven fabrics were unlike screen mesh; they had no discrete openings and their pore structures were apparently very fine.

Calhoun developed a test for equivalent opening size (EOS) to characterize the soil particle retention ability of the various fabrics. The test involved sieving rounded sand particles of a specified size through the fabric to determine that fraction of particle sizes for which 5 percent or less, by weight, passed through the cloth. The EOS was defined as the "retained on" size of that fraction expressed as a U.S. standard sieve number (e.g., No. 70 sieve). Assuming that fabrics and screen mesh have comparable retention ability, the EOS was a rational means of correlating fabric pore structure to an equivalent screen mesh size.

The EOS test provided a reasonable comparison between woven monofilament fabrics and screen mesh. EOS results could not be obtained for the woven multifilament or nonwoven fabrics. These fabrics retained even the finest particles (No. 100 to No. 120 sieve); their EOS was apparently finer than a No. 120 sieve.

Calhoun sought to modify the criteria for gran-

ular material adjacent to holes in drain pipes or well screens to accommodate filter fabrics. The filter criterion for drain pipes and well screen holes is

$$85 \text{ percent size of granular material/hole diameter} > 1 \tag{1}$$

By substituting EOS for hole diameter in Equation 1, Calhoun evolved a criterion for fabric retention ability:

$$D_{85 \text{ soil}}/\text{EOS} > 1 \tag{2}$$

where $D_{85 \text{ soil}}$ represents the 85 percent size from a grain-size distribution analysis of the protected soil.

Calhoun performed filtration tests on soil-fabric systems to determine the validity of this filter criterion. Fabric and soil were placed in a specially designed apparatus similar in concept to a laboratory soil permeameter [see Figure 1 (2)]. Water flowed at a constant head down through the soil and fabric. The effluent from the apparatus was carefully monitored to detect any soil loss through the fabric. Surprisingly, test results indicated that a fabric with an EOS equal to a No. 30 sieve would effectively retain and prevent piping of a silty sand with D_{85} equal to 0.008 in. at hydraulic gradients up to 50 (maximum hydraulic gradient tested). These results imply that the retention criterion in Equation 2 is overly conservative. A more appropriate filter criterion for fabrics, based on Calhoun's results, might be stated as

$$\text{EOS}/D_{85 \text{ soil}} < 2 \text{ to } 3 \tag{3}$$

An acceptable ratio of EOS/D_{85} could possibly be greater than 2 to 3, but appropriate combinations of EOS and D_{85} were not tested to establish a maximum limit on retention ability.

EOS VERSUS PORE STRUCTURE

It is imperative to note that EOS values do not accurately define fabric pore sizes, pore structure, or filtration ability. For decades filter media producers and users have adopted various techniques similar to the EOS test for measuring the retention or filtration efficiency of their products. Shoemaker (3) reported that most filter manufacturers have adopted micron-rating techniques, but the method for arriving at the rating varies with the manufacturer and the product. The concept of rating is helpful when developing a relative ranking of retention characteristics of similar products by one manufacturer. A cartridge that has a rating of 5 microns is presumably more retentive than one that has a 50-micron rating. In comparing similar products, such as cartridges from two different manufacturers, the numbers may not be equivalent. When comparing dissimilar products, such as cartridges versus felt versus paper, it is difficult to justify absolute numbers.

The EOS test only provides a crude method for determining the relative size of the maximum straight-through openings in a fabric. EOS values for fabrics of dissimilar construction are not comparable; i.e., a woven monofilament and a nonwoven fabric, both with EOS = No. 70 sieve, will not have the same pore structure or will they provide the same filtration efficiency for all particle sizes.

Visual examination of different fabrics with the same EOS indicates the variety of pore structure and porosity that can exist despite common EOS values. Figures 2 and 3 show a woven monofilament and a nonwoven fabric, both with EOS = No. 70 to No. 80

Figure 2. Woven monofilament fabric with EOS = No. 70 to No. 80 sieve.

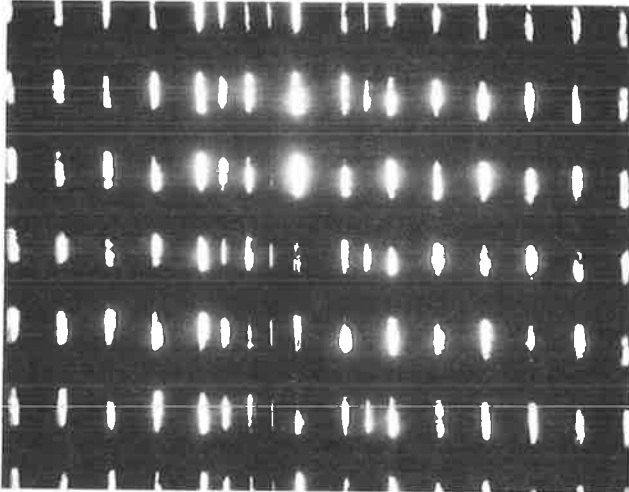


Figure 3. Nonwoven fabric with EOS = No. 70 to No. 80 sieve.

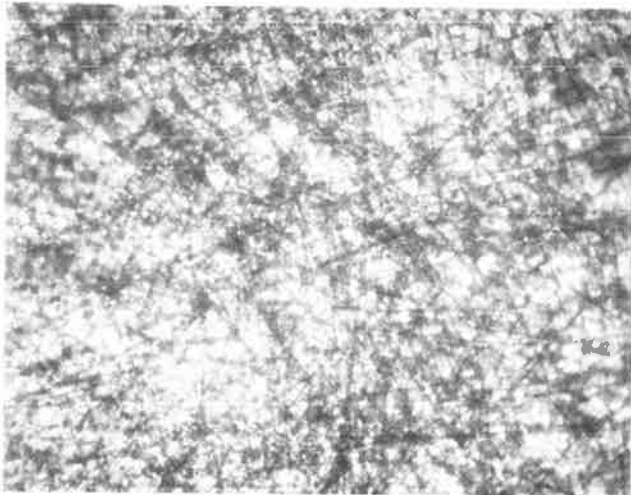


Figure 4. Woven monofilament fabric with EOS = No. 30 to No. 40 sieve.

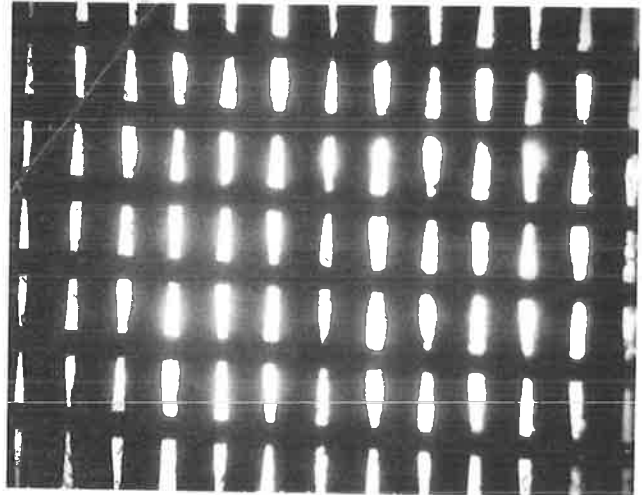
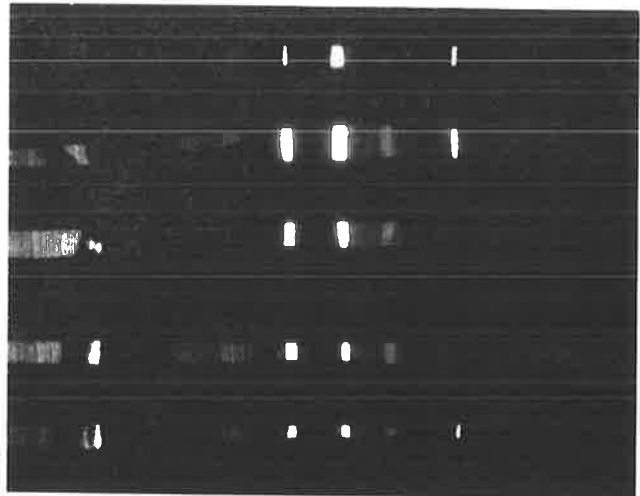


Figure 5. Woven slit film fabric with EOS = No. 30 to No. 40 sieve.



sieve. Figures 4 and 5 show a woven monofilament and a woven slit film fabric, both with EOS = No. 30 to No. 40 sieve. (Note that Figures 2-5 are 7.3 magnifications.)

Filtration tests were run on the woven monofilament and nonwoven fabrics shown in Figures 2 and 3. Fabrics were secured beneath a vertical pipe, and a slurry of soil and water was allowed to flow from the pipe through the fabric as in a falling-head permeameter (see Figure 6). Retention efficiency was measured for each fabric by using several particle size ranges. The results of these slurry filtration tests are shown in Figure 7. Retention efficiency of both the woven and nonwoven fabrics is comparable for the coarsest soil gradation. Note that an EOS of No. 70 to No. 80 sieve is larger than the D_{85} of the coarsest soil. Although the retention efficiency of the nonwoven fabric is greater than the woven fabric, both fabrics provide adequate retention for the No. 100 sieve soil with $D_{85} = 0.10$. This observation further supports the validity of Equation 3. As soil gradation becomes finer, the woven monofilament exhibits a dramatic decrease in retention efficiency, but the retention effi-

ciency of the nonwoven fabric does not change significantly.

Results from this slurry filtration test confirm that EOS values indicate the retention ability of fabrics. But EOS alone does not distinguish the level of retention that a filter fabric can provide. This difference in filtration performance does not discount the validity of a retention criterion that uses EOS. It does indicate that nonwoven fabrics tend to exhibit greater retention ability than woven monofilament fabrics with the same EOS. Therefore, the retention criterion (Equation 3) is more conservative for nonwovens than for woven monofilament fabrics; it should not be restrictive to acceptable fabrics of any type.

Schober and Teindl (4) performed a state-of-the-art review of geotextile filter criteria based on European research. Their conclusions are summarized below:

1. EOS values can be related to the retention ability of geotextiles,
2. EOS values are not comparable between woven and thick needle-felt nonwovens,

3. Uniformity coefficients for protected soils influence the filtration performance of geotextiles, and

4. Woven and thin nonwoven fabrics should have a different retention criterion than thick needle-felt nonwovens.

Figure 6. Slurry filtration test apparatus.

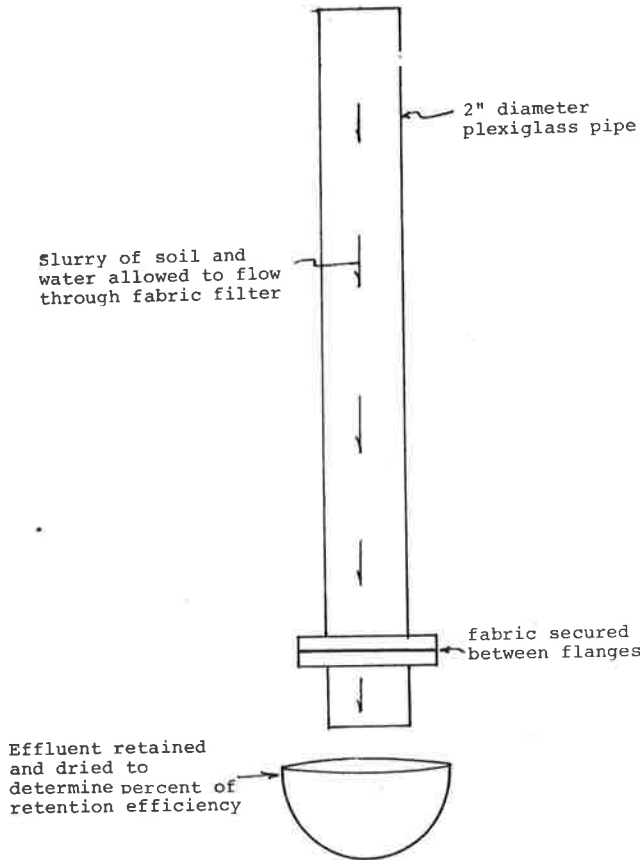


Figure 7. Slurry retention efficiency of woven and nonwoven fabrics.

Fabric	Retention Efficiency (% Particle Weight Retained)		
	Particle Size Ranges*		
	-#80	-#100	-#200
Woven Monofilament (EOS = #70 - #80)	92	82	6
Nonwoven (EOS = #70 - #80)	98	96	94

*Particle Size Ranges: -#80 : 100% passing #80...D₈₅ ~ .15 mm
 -#100 : 100% passing #100...D₈₅ ~ .10 mm
 -#100 : 100% passing #200...D₈₅ ~ .06 mm

Based on these conclusions, Schober and Teindl suggest the following retention criterion for woven and thin nonwoven fabrics:

$$M_w/d_{50} = (O_{90}/d_{50}) < 1.7 \text{ to } 3 \quad (4)$$

where

- M_w = woven mesh width (optically measured),
- O_{90} = particle size for which 90 percent is retained by using a particle sieving test similar to the EOS method, and
- d_{50} = 50 percent size of a protected soil gradation.

For thick needle-felt nonwovens, they suggest the following retention criterion:

$$(O_{90}/d_{50}) > 3 \text{ to } 5 \quad (5)$$

The maximum limit on the ratios of pore to particle size in Equations 4 and 5 include a substantial safety factor.

The ratio of O_{90}/d_{50} varies directly with the uniformity coefficient of the protected soil. The d_{50} value is used in these criteria rather than the D_{85} value used by Calhoun. According to Schober and Teindl, a ratio of 3 for Equations 4 and 5 is comparable to a ratio of 1 for Equation 2. This suggests that Equation 2 is appropriate for wovens and is conservative for nonwovens, especially thick nonwoven fabrics, thereby reinforcing the previously stated conclusions.

PERMEABILITY AND CLOGGING RESISTANCE

Criteria for permeability and clogging resistance of geotextiles must assure that fabric permeability is greater than that of the protected soil throughout the effective life of a drain. Calhoun (2) performed clogging tests to determine the degree of fabric clogging that might be experienced by fabric in contact with a gap-graded soil. The clogging test used a permeameter device similar to the filtration test apparatus previously described (see Figure 1). Hydraulic gradient data from the soil-

Figure 8. Soil-fabric permeameter.

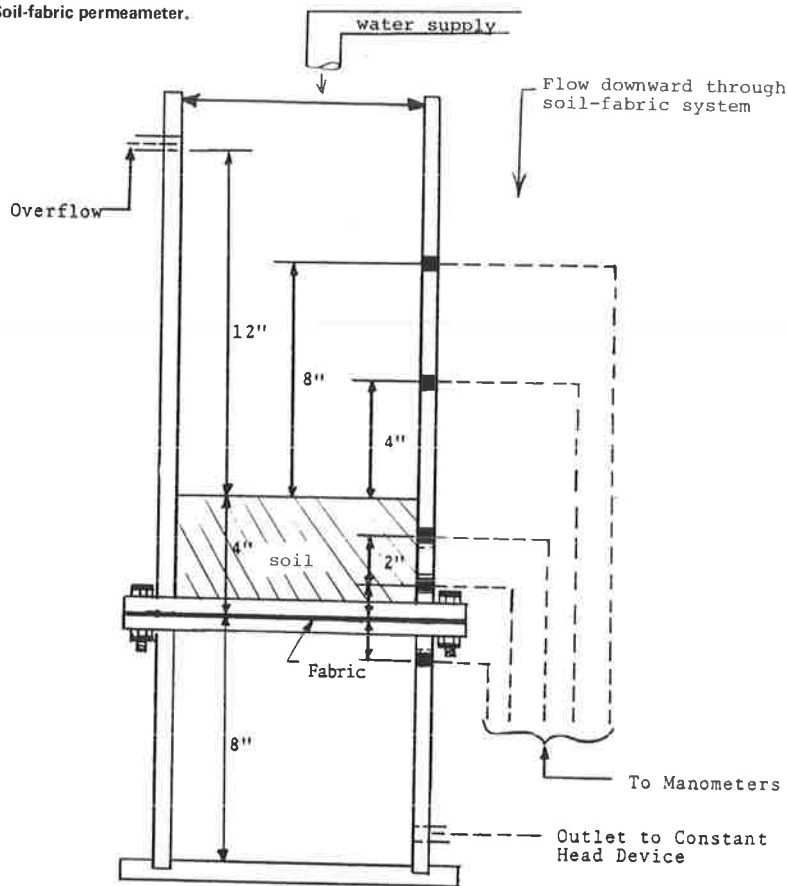


Table 1. Physical properties of protected soils.

Soil Type	LL	PL	PI	D ₁₀	C _u	Soil Classification	
						AASHO	Unified
Natural	28	20	8	0.0100	15	A-2-4(0)	SC
S-0	25	20	5	0.0250	7	A-2-4(0)	SM
S-5	24	18	6	0.200	8	A-2-4(0)	SM
S-15	25	20	5	0.0140	11	A-4(0)	ML
S-25	26	17	9	0.0100	11	A-4(3)	ML-CL
S-35	28	20	8	0.0070	12	A-4(5)	CL
S-50	30	21	9	0.0070	9	A-4(6)	CL
K-0	23	21	2	0.0590	4	A-2-4(0)	ML
K-10	24	18	6	0.0070	27	A-2-4(0)	ML-CL
K-20	26	21	5	0.0006	303	A-2-4(0)	ML-CL
K-30	28	17	11	0.0006	214	A-4(1)	CL
M-2	30	22	8	0.0460	4	A-2-4(0)	CL
M-4	39	24	15	0.0175	11	A-2-4(0)	CL
Soil no. 1	24	20	4	0.0740	2	A-2-4(0)	SM
Soil no. 2	25	15	10	0.0060	33	A-2-4(0)	SC
Soil no. 3	27	21	6	0.0007	308	A-2-4(0)	ML-CL

fabric permeameters were analyzed to determine the clogging potential of a fabric. The analysis made use of a ratio of the hydraulic gradient across the fabric plus an adjacent 1 in. of soil to the hydraulic gradient for the entire system, i.e., the clogging ratio. A clogging ratio greater than 1 signified fabric clogging. Clogging ratios varied, depending on fabric and soil gradation, but no clogging ratios exceeded 2. The COE (5) later established a maximum acceptable clogging ratio of 3.0 based on these and subsequent clogging test evaluations.

Drain fabric research by Marks (6) indicated that nonwoven and woven fabrics performed as satisfactorily as graded aggregate filters under simulated

drainage conditions. The laboratory permeameter used for this evaluation is shown in Figure 8 (6). The fabrics tested had apparent permeability coefficients ranging from 10^{-3} to 10^{-1} cm/sec. Those fabrics were tested with 16 soil gradations ranging from fine sands [SM (Unified Soil Class)] to clayey, silty sands [CL (Unified Soil Class)]. The percentage of fines (passing the No. 200 sieve) for these soils ranged from 10 to 60 percent. Tested soils included both well-graded and gap-graded materials. The properties of the soils used in Marks' test program are given in Table 1 (6).

Permeability performance of graded aggregate and fabric filter systems was found to be essentially the same for comparable soils. All filter media experienced clogging with all soils except one. Filter clogging was attributed to soil infiltration at the soil-filter interface. The poorly graded silty sand (S-0 in Table 1) did not indicate infiltration or clogging with the graded aggregate filter. Fabric permeability had no apparent effect on permeability performance in soil-fabric systems.

Marks' study is significant because it describes the relative performance between fabric filters and conventionally accepted graded aggregate filters with a broad range of soil gradations.

Haliburton and Wood (7) investigated clogging resistance of woven and nonwoven fabrics by using a hydraulic gradient analysis approach similar to Calhoun's. They based clogging performance on a gradient ratio (GR) value, which is the hydraulic gradient through fabric plus the adjacent 1 in. of soil divided by the hydraulic gradient through the adjacent 2 in. of soil [see Figure 9 (7)]. The soil used was gap-graded to provide the maximum potential for soil piping and filter clogging. In addition,

the tests were run under high hydraulic gradients to cause the maximum potential for soil piping. GR results revealed dramatic performance differences between the fabrics tested.

A plot of the GRs for fabrics tested versus silt content in the gap-graded soil is shown in Figure 10 (7). Clogging potential increased for all fabrics as the silt content increased in the protected soil. Results also confirmed that a reasonable limit for a maximum allowable GR is 3. Haliburton and Wood reported that fabric EOS was not related to clogging potential.

The performance results from Marks and Haliburton and Wood appear to be in conflict. Close examination of test conditions, however, reveals that Haliburton and Wood's clogging tests were run at high hydraulic gradients and with gap-graded soils to obtain the maximum effect from soil piping. On the other hand, Marks' soil-fabric systems were evaluated by using a much lower hydraulic gradient with both well-graded and gap-graded soils. As a

result, the potential for soil piping and subsequent filter clogging is much greater in Haliburton and Wood's clogging test than in Marks' permeameter tests. Note that the test conditions have a significant influence over performance.

Soil-fabric clogging tests performed by Carroll revealed a similar performance contrast between high and low hydraulic gradient testing. A permeameter device similar to those in previous clogging studies was used to generate GRs at various system hydraulic gradients (see Figure 11). Woven and nonwoven fabrics and a graded aggregate filter were evaluated by using a well-graded silty sand (15 percent passing the No. 200 sieve) as the protected soil. The filter properties and the GRs measured at various hydraulic gradients are given in Table 2.

Note that the GRs are approximately 1 or less until system hydraulic gradients become >3 . Fabric clogging or soil infiltration is apparently not significant when system hydraulic gradients are 3 or less. Clogging becomes more noticeable as the system hydraulic gradient increases beyond 3. Neither permeability nor EOS of the fabrics tested indicated a relation to soil-fabric system performance.

Several general conclusions can be drawn from the combined results of the clogging studies by Calhoun, Marks, Haliburton and Wood, and Carroll:

1. Fabric EOS and permeability coefficients do not indicate clogging potential;
2. All filter media are likely to experience some degree of clogging due to soil infiltration;

Figure 9. GR permeameter.

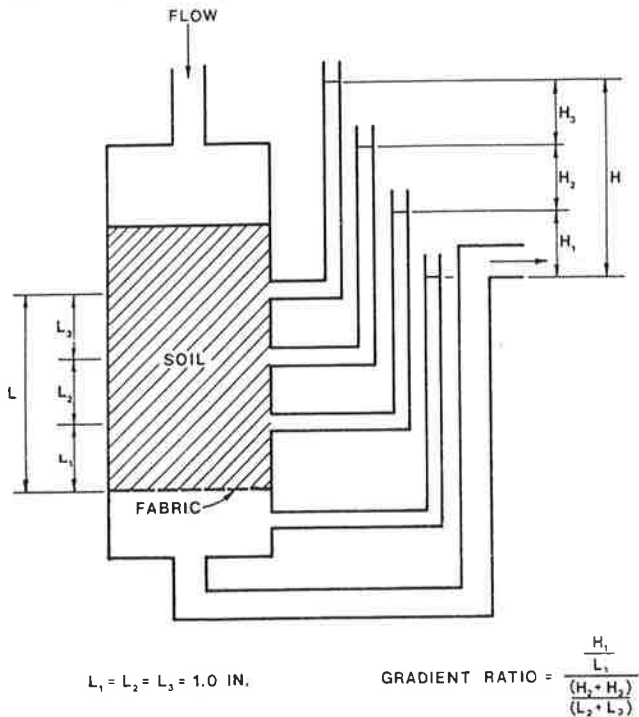


Figure 10. Results of GR testing for various engineering fabrics at different soil silt contents.

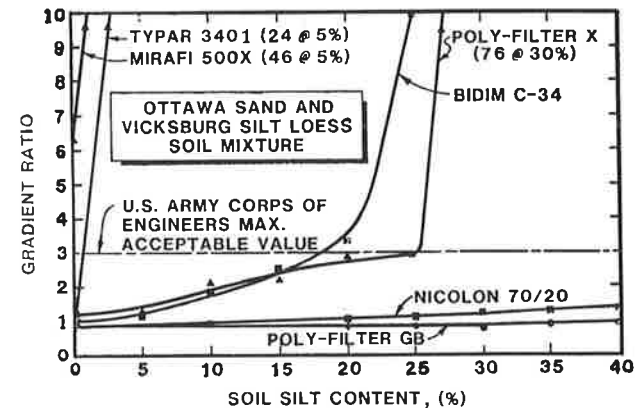
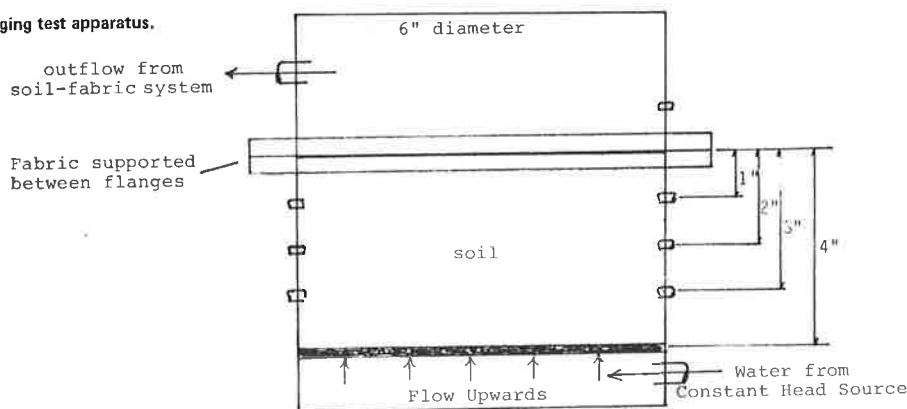


Figure 11. Soil-fabric clogging test apparatus.



Not to Scale

Table 2. Soil-fabric clogging test results.

Filter Identification			Gradient Ratio ^a		
Type	EOS ^b	k (cm/sec)	i _s = 1	i _s = 3	i _s = 5
Graded aggregate	NA	>0.10	0.39	0.66	1.06
Nonwoven					
Heat bonded	100	0.049	0.37	0.84	1.61
Heat bonded	20	0.094	0.12	0.42	0.85
Needle punched	60	0.283	0.52	1.29	2.42
Woven, slit film	50	0.001	0.45	1.05	2.09

Note: NA = not available.

^aGR values listed for system hydraulic gradients of 1, 3, and 5.

^bEOS identified by U.S. standard sieve size.

3. Well-graded soils are not prone to piping; however, high hydraulic gradients may cause infiltration of well-graded soils into a filter media;

4. Gap-graded soils are prone to soil piping and subsequent filter clogging, whereas high hydraulic gradients maximize the potential for piping in gap-graded soils; and

5. A reasonable limit for the maximum allowable GR is 3.

These conclusions provide the basis for developing rational criteria regarding permeability and clogging resistance of fabric filters.

FILTER CRITERIA AND TEST METHODS

Three basic elements are suggested for geotextile filter criteria: retention ability, permeability, and clogging resistance.

Retention Ability

Retention ability can be specified by using the EOS criterion defined in Equation 3 [i.e., $(EOS/D_{85 \text{ soil}}) < 2$ to 3]. Previous discussion has revealed that EOS is an index value that relates indirectly to fabric retention ability. EOS values alone do not indicate relative filtration performance or do they indicate clogging potential. This criterion should only be used to establish a minimum value of fabric EOS for a given soil gradation to be protected. This criterion may be conservative with regard to nonwoven fabrics, but it should not be restrictive to any acceptable fabrics.

There are two methods for determining EOS: (a) the procedure defined by Calhoun (2) that used graded sand particles, and (b) the modified version defined by the COE (5), which used graded glass beads. Testing laboratories have indicated that the sieving process with glass beads typically yields lower EOS values than sieving with sand particles, i.e., $EOS_{\text{glass}} = \text{No. 50 sieve}$ and $EOS_{\text{sand}} = \text{No. 70 sieve}$ for the same fabric. Variability between these tests is attributed to differences between glass beads and sand particles, e.g., particle roundness, static potential.

Equation 3 applies to EOS values determined by sand particle sieving. If glass beads are used to determine EOS, Equation 3 should provide a more conservative assessment of retention ability.

Permeability

Permeability of a geotextile must be substantially greater than that of the protected soil so that partial clogging will not reduce fabric permeability to a critical level, i.e., below that of the protected soil. Accordingly, fabric permeability should be at least 10 times that of the protected soil, i.e.,

$$k_{\text{fabric}} > 10k_{\text{soil}} \quad (6)$$

Darcy coefficients can be calculated for geotextiles by using flow rate and pressure drop across a fabric as measured in both constant- and falling-head permeameters (8).

Researchers have disputed the validity of computing a Darcy coefficient for fabrics from such permeameter testing. The fabrics are very thin (relative to soil thickness used in conventional soil permeameters), and flow through the fabric is likely to be turbulent even with low head pressures. Therefore, Darcy's theory may not apply to these test conditions. Despite these inconsistencies between test conditions and theory, an apparent Darcy coefficient can be determined for fabrics. If turbulent flow conditions are present during testing, then the k value measured for a fabric will be conservative, i.e., lower than the actual k. An apparent Darcy coefficient can also be determined for fabrics by using results from ASTM D-737 (Air Permeability of Textile Fabrics) (9).

The effect of fabric compressibility on fabric permeability is another concern of researchers. Schober and Teindl (4) have reported that a compressive force of 146 psi can reduce the k value of highly compressible needle-felt fabrics by factors ranging between 2 and 8. This compressive force is roughly equal to fabric buried beneath 150 ft of dense soil. Most drains are near the surface, where compressive force on the fabric filter is relatively low and the potential for reduced permeability is insignificant.

Therefore, it is recommended that the fabric permeability criterion stated in Equation 6 be used for shallow drains, with fabric permeability determined by conventional falling- or constant-head permeameters or through air permeability testing. If ground pressures on the fabric filter are expected to be extremely high, then permeability measurements should be determined on a fabric under the appropriate compressive force.

Clogging Resistance

Clogging behavior of a geotextile should be evaluated in a test that simulates in-place conditions. For a filtration-drainage application, this means testing a soil-fabric system in a permeameter apparatus similar to those described previously. The soil and hydraulic gradient conditions used in testing should duplicate expected field conditions. Test parameters that deviate significantly from the use conditions will not provide a useful performance evaluation.

The GR, as defined by Haliburton and Wood (7), provides a rational analysis of fabric clogging potential. As previously indicated, the maximum allowable GR for acceptable performance should be less than 3. The criterion for clogging resistance of geotextiles can be stated in terms of an allowable gradient ratio:

$$GR < 3 \quad (7)$$

IMPLEMENTING FILTER CRITERIA

Drainage projects can be classified in two general categories--noncritical and critical. The following conditions define the noncritical drainage category:

1. Drain failure does not result in either a decrease in structural life or significant structural damage,
2. Evidence of drain clogging appears well in advance of failure,

3. Repair costs are comparable or less than installation costs for the drain,

4. Low hydraulic gradients exist through the soil, and

5. Minimal clogging potential exists (e.g., well-graded or uniform soil to be drained).

Typical applications in the noncritical category are subgrade and pavement drains. Clogging potential for noncritical drains is minimal because of the soil and hydraulic gradient conditions defined. The retention and permeability criteria defined by Equations 3 and 6 provide sufficient filter criteria for filter fabrics in the noncritical category.

In comparison, any or all of the following conditions define the critical drainage category:

1. Drain failure results in either a potential decrease in structural life or significant structural damage,

2. No evidence of drain clogging appears before failure,

3. Repair costs are significantly greater than the installation costs of a drain,

4. High hydraulic gradients exist through the soil, and

5. Protected soils are conducive to piping (e.g., gap-graded soils, fissured clays, dispersive clays, and fractured rock).

Typical critical drain categories include dam chimney drains and coastal erosion-control structures (high risks and high hydraulic gradients, respectively). The consequences of filter clogging in critical drainage applications mandates the evaluation of filter clogging potential. Retention, permeability, and clogging criteria (Equations 3, 6, and 7) should all be used to specify fabric filters for critical drainage conditions.

There is no better proof of performance than actual field use and performance monitoring. Performance testing or trials that simulate conditions of use is certainly the technically preferred approach to filter evaluation and selection. However, the cost of performance testing and trials is often prohibitive to their use for filter media evaluation on individual projects. As a result index values are the basis for filter selection in a majority of filtration applications. The specifier should understand the limits of such index criteria and have experience in filter performance to assure selection of the appropriate filter media.

Geotextiles have been used for filtration-drainage applications for more than a decade. There

are numerous users, researchers, and producers who have a wealth of experience regarding geotextile performance. Whenever available, this first-hand experience should be combined with rational performance criteria in selecting the appropriate geotextile for filtration-drainage use or any other application.

The filter criteria recommended in this paper provide only part of the specification requirements necessary to define an acceptable drainage fabric. Appropriate strength criteria must be established to prevent damage caused by installation and in situ stresses. These strength requirements will vary with application and should be defined according to the conditions of use.

REFERENCES

1. K.P. Karpoff. The Use of Laboratory Tests to Develop Design Criteria for Protective Filters. Proc., ASTM, Vol. 55, 1955.
2. C.C. Calhoun. Development of Design Criteria and Acceptance Specifications for Plastic Filter Cloth. U.S. Army Corps of Engineers Waterways Experiment Station, Vicksburg, MS, Tech. Rept. S-72-7, June 1972, pp. 6-55.
3. W. Shoemaker. The Spectrum of Filter Media. Filtration and Separation, Jan./Feb. 1975.
4. W. Schober and H. Teindl. Filter Criteria for Geotextiles. In Design Parameters in Geotechnical Engineering, BGS, London, England, Vol. 2, 1979, pp. 121-129.
5. Civil Works Construction Guide Specification for Plastic Filter Fabric. Office of Chief Engineer, Corps. of Engineers, Department of the Army, Rept. CW 02215, Nov. 1977, p. ii.
6. B.D. Marks. The Behavior of Aggregate and Fabric Filters in Subdrainage Applications. Department of Civil Engineering, Univ. of Tennessee, Knoxville, Feb. 1975, pp. 36-107.
7. T.A. Haliburton and P.D. Wood. Evaluation of the U.S. Army Corps of Engineers Gradient Ratio Test for Geotextile Performance. Proc., 2nd International Conference on Geotextiles, Las Vegas, Vol. 1, 1982, pp. 97-101.
8. Test Procedure for Falling Head Water Permeability of Geotextiles. Celanese Fibers Marketing Company, New York, Rept. CFMC-FFET-1, Aug. 1981.
9. R.G. Carroll. Determination of Permeability Coefficients for Geotextiles. Geotechnical Testing Journal, ASTM, June 1981, pp. 83-85.

Publication of this paper sponsored by Task Force on Engineering Fabrics.

Use of Fabrics for Improving the Placement of Till on Peat Foundation

C. LUPIEN, G. LEFEBVRE, P. ROSENBERG, J. J. PARE, AND J. G. LAVALLE

Observations made during the construction of test embankments, which were built to investigate the possibility of placing till directly on peat, are reported. The test fills were constructed on two test sites that presented different peat properties. Different uses of fabrics were tested at each experimental site: as a separation and reinforcement between the muskeg and the fill, as slope protection, and as reinforcement at midthickness of the fill. For comparison, a few test fills were constructed without fabrics. The observations made during construction describe the difficulties encountered in fabric handling and the effect of geotechnical fabrics on the behavior of the fill material and the peat foundation. Of particular interest was the use of geotextile (used as a fill material) as reinforcement at midthickness of the fill to prevent a loss in the bearing capacity of the till. The use of fabrics as reinforcement of the peat foundation proved to be of little significance when the peat offers sufficient strength.

The hydroelectric development of the Nottaway, Broadback, and Rupert (NBR) rivers in the southeast part of the James Bay region in Quebec province, Canada, necessitates the construction of several kilometers of roads across muskeg-covered areas. Canadian expertise with respect to highway embankment construction on peat in northern areas is significant and has been reported by many researchers (1-4). They have shown that the construction problems of an embankment on peat are mainly related to the properties of peat and the construction techniques used.

Fills on peat are normally constructed with free-draining granular material. On the NBR project the scarcity of clean granular borrow material required that silty sand with gravel till be used on long sections of the access roads. Because construction difficulties can be expected with the placement of a silty material in wet conditions, an experimental program was initiated in order to investigate the possibility of placing these tills directly on the muskeg.

Two test sites that presented different peat conditions were retained for the experiments, and four different test fills were constructed at each site. Geotechnical fabrics were incorporated in half of the test fills.

The purpose of this paper is to report the observations made on the various uses of fabrics during construction of the test fills.

CONDITIONS OF TEST SITES

The two test sites, NBR-2 and NBR-3, named after the nearest exploration camps, are located about 238 and 148 km north of the city of Matagami along the James Bay access road (Figure 1). At both sites the muskeg surface inside the perimeter of the test fills is covered with moss, hay, and some conifers less than 2 m high (see Figures 2 and 3). The peat layer is about 2.5 to 3.5 m thick, overlaying a clay deposit with a stiff weathered crust. The water level in the peat was found to vary slightly with the seasons; at the time of construction it was mostly at the peat surface at the NBR-3 site and about 25 cm below the muskeg surface at the NBR-2 site.

The peat is fibrous at both sites. According to the von Post (5) classification system, the NBR-3 peat averages H-4 whereas the NBR-2 peat appears more humified, with an average of H-7. Average water content profiles and the range of variation are shown in Figure 4. The water content at the

NBR-2 site increases slightly with depth, and the average value for the whole profile is equal to 1,460 percent. The water content at the NBR-3 site is practically constant with depth, and the average value is 860 percent. Averaged vane profiles shown in Figure 5 also show consistent behaviors for both sites; the average shear strength for NBR-2 is 10 kPa, and for NBR-3 about 20 kPa.

As indicated by these properties, the peat deposits differ significantly at both sites. Compared with the NBR-3 peat, the higher water content and lower strength of the NBR-2 peat reflect a more deformed peat that has a greater potential for failures.

Figure 6 shows the grain-size distribution of the two tills used as fill material at both sites. The percentage passing the 4.75-mm sieve is on the order of 70 percent for the NBR-2 material and 95 percent for the NBR-3 till. The uniformity coefficient is significantly different between the two tills: about 10 at NBR-3 and 40 at NBR-2.

CONSTRUCTION PROGRAM

Four test fills were constructed at each experimental site and different uses of geotextiles were tested. In particular, the geotextiles were used as slope protection membranes (a) to restrain the sloughing of the fill material and (b) for a reinforcement at the top of the peat foundation and in the fill.

Geotextiles used for these experiments were those already available in the James Bay area and are identified by their strength and deformation properties (6) in the following table:

Type	Polymer	Fabric Construction	Grab Tensile Strength (N)	Elongation at Breaking Load (%)
A	Polypropylene	Woven	485	16
B	Polyester	Nonwoven	710	35
C	Polypropylene	Woven	800	22

For comparison purposes, some test fills were constructed directly on muskeg without geotextiles or by means of other approaches. The lengths of the test sections varied between 30 and 40 m.

The following is a description of the NBR-3 test fills.

1. Section A (1.5 m thick) was built with a type B geotextile as reinforcement between the muskeg and the fill. A type A geotextile was used on the same test fill to retain the slope material. Both were installed in the longitudinal direction of the test fill. The fabric layout is shown in Figures 7-9.

2. Section B was built directly on the muskeg surface and had a fill thickness of 2 m.

3. Section C was similar to section B but had a fill thickness of 1.5 m.

4. Section D (1.5 m thick) was built directly on the muskeg surface but incorporated a type A geotextile as reinforcement at midheight of the fill (Figure 9). The width of the test fills was about 13 m at the crest.

Figure 1. Location of NBR-2 and NBR-3 test fill sites.



Figure 2. NBR-3 test site: surface aspect and instrumentation layout.



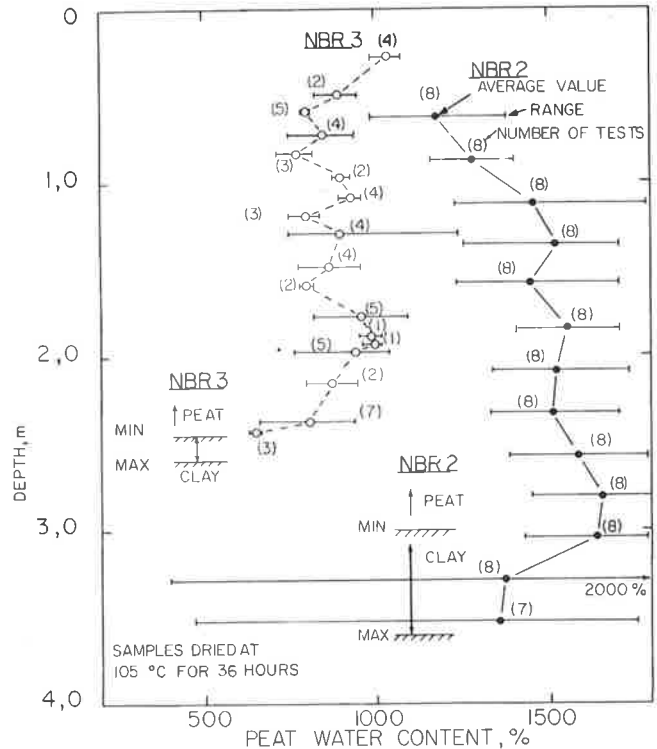
The test fills at NBR-2 were built to a height of 1 m above the muskeg surface. The final thicknesses varied from 2 to 3 m. The following is a description of the NBR-2 test fills.

1. Section A was built by using a clean granular pad with a thickness just sufficient to support construction equipment. The fill was then completed to final grade with till.
2. Section B was built with a type C geotextile wrapped around the first layer of the fill. In this case the geotextile was installed transversally to the fill by using an overlap of about 1 m between layers. This layout is shown in Figures 9 and 10.
3. Section C was built by using an impervious polyethylene membrane between the till and the muskeg surface.

Figure 3. NBR-2 test site: surface aspect and instrumentation layout.



Figure 4. Average water content versus depth, NBR-2 and NBR-3 sites.



4. Section D was built by using till directly on the muskeg.

The width of the test sections was 15 m at the beginning of construction, but it was reduced to 10 m due to construction scheduling constraints.

Instrumentation at both sites consisted of open-tube-type piezometers located in the fill and at various depths in the peat foundation, along with settlement plates on the peat surface. Figure 9 summarizes test fill conditions and instrumentation locations.

BEHAVIOR OF TEST FILLS BUILT WITHOUT FABRICS

Fill Material

Fill materials used at both sites have shown different behaviors. Construction difficulties were

encountered with the NBR-3 till due to a loss of bearing capacity into the fill. After placement of the fill, the increased pore pressure induced into

Figure 5. Average vane profile, NBR-2 and NBR-3 sites.

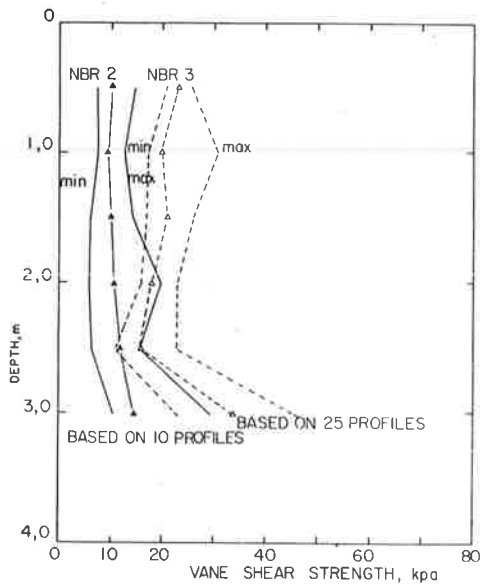


Figure 6. Granulometric ranges of NBR-2 and NBR-3 tills.

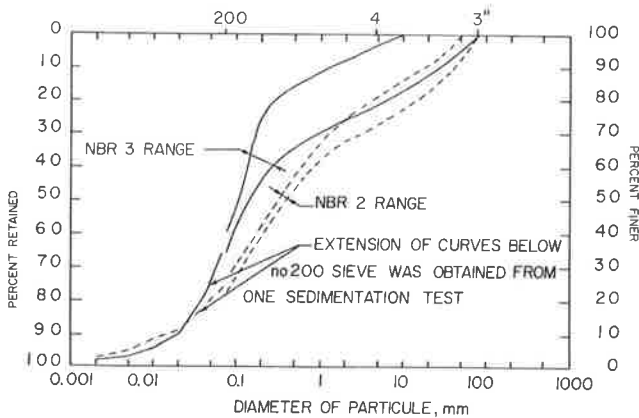


Figure 7. NBR-3 test fill A: type A geotextile as foundation reinforcement and type B geotextile for retaining fill material on slope.



the peat foundation was transmitted to the fill material.

Figure 11 shows typical piezometer elevations observed within a few hours after placement of the fill within the test fill A area. The significant piezometer response into the fill is indicative of pore pressure buildup and the saturation of most of the fill. Under such conditions compaction of the fill material is made difficult. The movement of trucks on the fill increases the problem because a pumping action is created, which results in a rise of water toward the fill surface. This phenomenon became so significant at a few locations on the test fills and the access road that a complete loss of bearing capacity occurred and construction equipment could not operate on these zones. The addition of fill material did not improve the behavior of the weakened zones. Geotextile was used to strengthen the fill in these circumstances (see discussion later in this paper).

Sloughing of the slopes with the NBR-3 till was a generalized phenomenon. The slopes were stable immediately after placement of the fill. Then a rise of water level in the slope material was achieved by pore pressure transmission, capillarity, and precipitation. The poorly compacted till near the slopes became unstable under these new water conditions, and sloughing of the slope material occurred. Material losses were important, with resulting slopes varying from 3:1 to 7:1. This phenomenon was especially significant after severe precipitations. Figure 12 shows a typical case.

These stability problems were not observed with the NBR-2 till, even in the case where the fill material was placed on a more compressible peat foundation that had a higher water content. The NBR-2 till behaved more like a clean granular material.

The differences in the behavior of the two tills are mainly explained by the properties of the fill materials. Both tills were nonplastic, but their grain-size distributions were different. The most significant factor is the uniformity coefficient ($C_u = d_{60}/d_{10}$), which was on the order of 10 and 40 for the NBR-3 and NBR-2 tills, respectively.

Figure 8. NBR-3 test fill B: fill material on slope retained by type B geotextile.



Figure 9. NBR-3 and NBR-2 test fill sections.

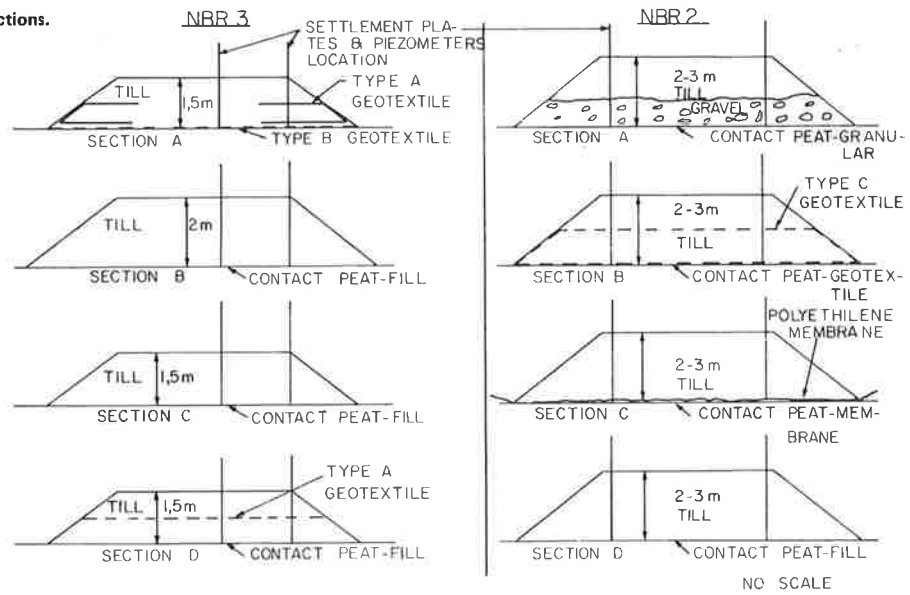


Figure 10. NBR-2, section B: first layer of fill wrapped with type C geotextile.



Figure 12. NBR-3 test site: sloughing of slope material.



Figure 11. NBR-3, test fill A: maximum piezometer readings.

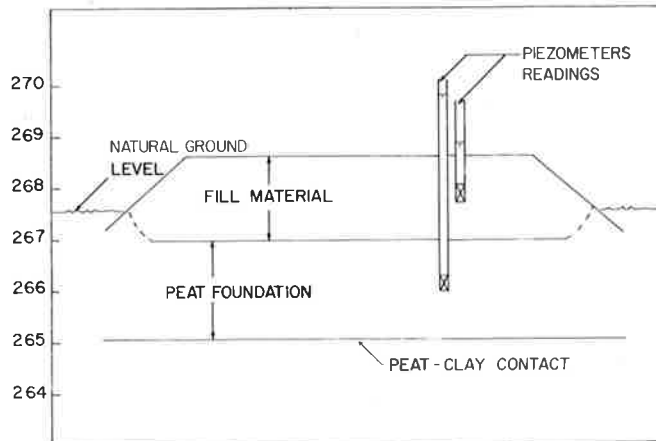


Figure 13. NBR-2, section B: lateral displacement and heave of peat.



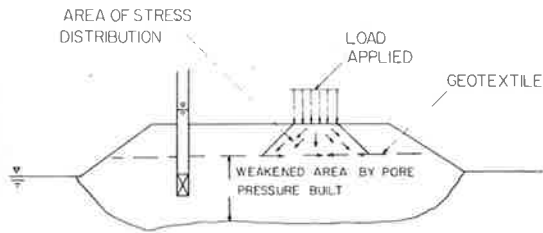
Therefore, the difference in behavior of the two tills is the inherent stability of the material itself.

Peat Foundation

Behaviors of the peat foundations were different at

both sites. Significant lateral displacement of the peat was observed at the NBR-2 site. The difference in measurements between the settlement plates before and after construction indicated a lateral strain of the peat that varied from 20 to 80 percent. Heave of the peat at the toe and front of the advancing fill (Figure 13) was also observed and was on the

Figure 14. Use of geotextile over a locally weakened fill.



order of 0.7 m. A failure in the peat foundation did occur at section B at this site, which will be discussed later.

No lateral displacement or heave was observed at the NBR-3 site. It is believed that here the compression of the peat primarily was achieved uniaxially.

This difference in foundation behavior is related to the properties of these peats. The NBR-2 peat had lower strength and a higher water content than the NBR-3 peat, which indicates a more deformed and less resistant peat.

BEHAVIOR OF TEST FILLS BUILT WITH FABRICS

Observations made during the construction of the test fills built with fabrics are grouped under the three following subjects: geotextile handling, behavior of the peat foundation, and behavior of the fill material.

Difficulties Encountered in Fabric Handling

Some tree cutting was required at the construction sites before the placement of membranes. The resulting muskeg surface was irregular because of dispersed mounds and some vegetation (Figures 2 and 3). The placement of the geotextile on such a surface was especially difficult under wind conditions, and closely spaced stickers had to be used to secure the geotextile to the peat surface. This operation was conducted before the construction period and required a crew of two to three workers, depending on wind conditions. It is believed that this operation would be more easily accomplished in the case of a flat muskeg surface.

When the geotextile was used as a material-retaining membrane on slopes, placement proved to be especially laborious. It is difficult to have control of the geometry at the foot of the slopes of the fill when a till that contains boulders is used, and the material is placed on an irregular surface. The operation required shoveling to achieve some uniformity of slope geometry, and also to secure the membrane at the surface of the embankment before the placement of the upper layer of the fill.

Effect of Geotextiles on Behavior of Peat Foundation

The bearing capacity of the peat foundations was different at both sites. This was shown previously by the difference in peat strength, which was 2 times stronger at the NBR-3 site. Observation of the behavior of the test fills built without fabrics confirmed this difference in peat strength between the two sites. The NBR-3 peat, which has an average strength value of 20 kPa, proved to be resistant; therefore the use of fabrics as reinforcement for these test fills was not advantageous. Thus it may be concluded that where the muskeg is not susceptible to bearing failure displacements, fabric is not useful. Experimental studies reported by Vischer (7) indicate the same conclusion.

With respect to the deformed NBR-2 peat, the behavior of the foundation was different, with the lateral displacement varying from 10 to 80 percent, with an average of 45 percent. For the test fill built with a type C geotextile wrapped around the first layer of the fill material, the lateral deformations registered varied between 40 and 65 percent. The fabric used for this test fill had an elongation at breaking load on the order of 20 percent. Even if there was no evidence of fabric rupture, with the comparison between actual and tolerable elongation as established for this product, it is believed that the geotextile at the peat-fill contact surface was brought to failure.

A foundation failure was observed on this test fill. The rupture was evidenced by a crack at the fill surface and a differential settlement of about 15 cm at the crack level. It was possible to reload the affected area and proceed with construction.

Before the construction period it was not expected that the lateral movement of the peat foundation and the resulting elongation of the peat below the fill would be of that magnitude. It is believed that the use of a nonwoven geotextile with an elongation capability of about 100 percent (with the appropriate strength) would have been more appropriate for this deformed peat.

Improvements in Behavior of Fill Material with Use of Fabrics

The use of geotextiles as a slope protection membrane proved to be of interest at the NBR-3 site where sloughing of the slope material was generalized. In test fill A, which was built by using a type A geotextile for slope protection, the loss of material by sloughing was prevented for the protected material. However, the sloughing of the till over this level occurred.

Test fill D at the NBR-3 site, which was built with a geotextile at midthickness of the fill, was easily constructed because the geotextile prevented the occasional losses in bearing capacity of the fill material as in the other test fills. The inherent stability of the fill material at the NBR-2 site was not improved by the use of fabrics because it was unnecessary, as already explained.

As described earlier, construction difficulties were encountered at the NBR-3 site where softening of the fill material had occurred. In these cases, the addition of fill material over the affected area did not improve the situation. The limited areas so affected were repaired by undercutting the till, placing a geotextile, and refilling with till. This method proved to be efficient and improved the performance of the saturated fill. Both geotextiles--type A and B--have been successfully used for this purpose.

The efficiency of the method can be explained either because the saturated fill did not reach sufficient compaction or because the pore pressure buildup into the fill was so significant that the bearing capacity became weak in relation with the loads applied. In such a situation it becomes impossible to achieve compaction of a new layer because the underlying till does not offer a sufficient reaction (see Figure 14). The use of a geotextile allows certain reactions to occur under the compacted layer so that it acts as a reinforcement inside the fill.

CONCLUSIONS

The experimental program reported allowed comparison of the behaviors of test sections built with and without geotextiles. The test fills were built on

two different sites and presented different peat conditions in terms of strength and deformation.

The following observations were made during construction:

1. The use of a geotextile as reinforcement of the foundation is not necessary when the peat is not susceptible to bearing failure displacement.
2. The use of fabrics on an irregular and tree-covered muskeg surface presents some handling difficulties.
3. The use of a geotextile for retaining fill material on slopes prevented sloughing of the slopes constructed with a susceptible material, but the handling operation was difficult because of a course till fill.
4. Of particular interest was the use of a geotextile at midthickness of the fill, especially when used locally to make repairs when a loss in the bearing capacity of the fill material occurred.
5. The use of a woven geotextile is normally suggested for foundation reinforcement. However, it was shown that when the foundation material is deformed, a nonwoven geotextile may be more suitable because it allows the foundation to develop more strength.

ACKNOWLEDGMENT

We wish to thank the Société d'énergie de la Baie James for permission to publish this paper.

REFERENCES

1. K.O. Anderson and R.A. Hempstock. Relating the Engineering Properties of Muskeg to Some Problems of Fill Construction. Proc., 5th Muskeg Research Conference, National Research Council of Canada, Tech. Memorandum 61, 1959, pp. 16-25.
2. C.O. Brawner and G. Tessier. Road and Railway Construction. In Muskeg Engineering Handbook (I.C. McFarlane, ed.), Univ. of Toronto Press, Toronto, Ontario, Canada, 1969, pp. 150-208.
3. G.P. Raymond. Construction Method and Stability of Embankments on Muskeg. Canadian Geotechnical Journal, Vol. 6, 1969, p. 81.
4. P.A. Brochu and J.J. Paré. Construction de routes sur tourbières dans la province de Québec. Proc., 9th Muskeg Research Conference, National Research Council of Canada, Tech. Memorandum 81, 1963, pp. 74-108.
5. L. von Post. Sveriges Geologiska Undersøknings torvmentering och nogra av dess hittills vunna resultat (SGU Peat Inventory and Some Preliminary Results). Svenska Masskulturörensningens Tedsherift, Jönköping, Sweden, Vol. 36, 1922, pp. 1-27.
6. Engineering Geotextiles. Engineering Materials Office, Ministry of Transportation and Communications, Downsview, Ontario, Canada, Rept. EM-45, 1981, 47 pp.
7. W. Vischer. Use of Synthetic Fabrics on Muskeg Subgrade in Road Construction. Forest Service, U.S. Department of Agriculture, Nov. 1975.

Publication of this paper sponsored by Task Force on Engineering Fabrics.

Geotextile Earth-Reinforced Retaining Wall Tests: Glenwood Canyon, Colorado

J. R. BELL, R. K. BARRETT, AND A. C. RUCKMAN

The Colorado Division of Highways elected to use flexible reinforced-soil retaining structures to meet architectural and environmental constraints in the design of I-70 at sites underlain by compressible soils in Glenwood Canyon. Four wall systems were constructed: Reinforced Earth, Retained Earth, Wire Wall, and geotextile reinforced walls. The geotextile reinforced-soil retaining wall tests are described, and design, construction, and instrumentation details are provided. The test wall is 300 ft long and approximately 15 ft high. The wall incorporates four nonwoven geotextiles (each in two weights) in 10 test segments. Instrumentation is provided to monitor settlements and surface and internal deformation of the reinforced soil. The test wall has a gunnite facing. The wall was designed by conventional methods; however, some segments were assigned lower-than-usual factors of safety to provide a more critical test. Since construction, the wall has settled from 6 to more than 18 in. due to foundation consolidation. Test wall performance, however, has been satisfactory, and none of the segments has exhibited distress. Wall design and performance relative to laboratory geotextile strength and creep test results are analyzed, and it is concluded that safe, economical geotextile walls can be designed by existing methods if certain factors, as discussed in the paper, are appropriately considered. Recommendations are also made. It is concluded that construction methods are appropriate for contractor-constructed projects. Cost data are also presented.

The Colorado Division of Highways (CDOH) designed and constructed a geotextile earth-reinforced retaining wall in conjunction with project I-70-2(90) in Glenwood Canyon, Colorado. This was one of four experimental flexible walls constructed on this

project. The other wall systems were all proprietary and included Wire Wall, Retained Earth, and Reinforced Earth. Construction was completed during spring 1982.

BACKGROUND

Site Description

Glenwood Canyon is a narrow, steep-walled chasm cut by the Colorado River through resistant limestone, quartzite, and granite. The deep slash through the bedrock was formed by a gradual regional uplift, which caused the Colorado River to accelerate downcutting with limited lateral cutting. The 12-mile-long canyon is located about 150 miles west of Denver in west-central Colorado, as shown in Figure 1.

Geologic investigations indicate that bedrock lies up to 150 ft below the river, and that thick lake deposits, which consist of highly compressible silts and clays, are present through the eastern half of the canyon. The lake deposits indicate that, at one time, a temporary dam was formed at some point in the canyon.

two different sites and presented different peat conditions in terms of strength and deformation.

The following observations were made during construction:

1. The use of a geotextile as reinforcement of the foundation is not necessary when the peat is not susceptible to bearing failure displacement.
2. The use of fabrics on an irregular and tree-covered muskeg surface presents some handling difficulties.
3. The use of a geotextile for retaining fill material on slopes prevented sloughing of the slopes constructed with a susceptible material, but the handling operation was difficult because of a course till fill.
4. Of particular interest was the use of a geotextile at midthickness of the fill, especially when used locally to make repairs when a loss in the bearing capacity of the fill material occurred.
5. The use of a woven geotextile is normally suggested for foundation reinforcement. However, it was shown that when the foundation material is deformed, a nonwoven geotextile may be more suitable because it allows the foundation to develop more strength.

ACKNOWLEDGMENT

We wish to thank the Société d'énergie de la Baie James for permission to publish this paper.

REFERENCES

1. K.O. Anderson and R.A. Hempstock. Relating the Engineering Properties of Muskeg to Some Problems of Fill Construction. Proc., 5th Muskeg Research Conference, National Research Council of Canada, Tech. Memorandum 61, 1959, pp. 16-25.
2. C.O. Brawner and G. Tessier. Road and Railway Construction. In Muskeg Engineering Handbook (I.C. McFarlane, ed.), Univ. of Toronto Press, Toronto, Ontario, Canada, 1969, pp. 150-208.
3. G.P. Raymond. Construction Method and Stability of Embankments on Muskeg. Canadian Geotechnical Journal, Vol. 6, 1969, p. 81.
4. P.A. Brochu and J.J. Paré. Construction de routes sur tourbières dans la province de Québec. Proc., 9th Muskeg Research Conference, National Research Council of Canada, Tech. Memorandum 81, 1963, pp. 74-108.
5. L. von Post. Sveriges Geologiska Undersöknings torvmentering och nogra av dess hittills vunna resultat (SGU Peat Inventory and Some Preliminary Results). Svenska Masskulturörensningens Tedsherift, Jönköping, Sweden, Vol. 36, 1922, pp. 1-27.
6. Engineering Geotextiles. Engineering Materials Office, Ministry of Transportation and Communications, Downsview, Ontario, Canada, Rept. EM-45, 1981, 47 pp.
7. W. Vischer. Use of Synthetic Fabrics on Muskeg Subgrade in Road Construction. Forest Service, U.S. Department of Agriculture, Nov. 1975.

Publication of this paper sponsored by Task Force on Engineering Fabrics.

Geotextile Earth-Reinforced Retaining Wall Tests: Glenwood Canyon, Colorado

J. R. BELL, R. K. BARRETT, AND A. C. RUCKMAN

The Colorado Division of Highways elected to use flexible reinforced-soil retaining structures to meet architectural and environmental constraints in the design of I-70 at sites underlain by compressible soils in Glenwood Canyon. Four wall systems were constructed: Reinforced Earth, Retained Earth, Wire Wall, and geotextile reinforced walls. The geotextile reinforced-soil retaining wall tests are described, and design, construction, and instrumentation details are provided. The test wall is 300 ft long and approximately 15 ft high. The wall incorporates four nonwoven geotextiles (each in two weights) in 10 test segments. Instrumentation is provided to monitor settlements and surface and internal deformation of the reinforced soil. The test wall has a gunnite facing. The wall was designed by conventional methods; however, some segments were assigned lower-than-usual factors of safety to provide a more critical test. Since construction, the wall has settled from 6 to more than 18 in. due to foundation consolidation. Test wall performance, however, has been satisfactory, and none of the segments has exhibited distress. Wall design and performance relative to laboratory geotextile strength and creep test results are analyzed, and it is concluded that safe, economical geotextile walls can be designed by existing methods if certain factors, as discussed in the paper, are appropriately considered. Recommendations are also made. It is concluded that construction methods are appropriate for contractor-constructed projects. Cost data are also presented.

The Colorado Division of Highways (CDOH) designed and constructed a geotextile earth-reinforced retaining wall in conjunction with project I-70-2(90) in Glenwood Canyon, Colorado. This was one of four experimental flexible walls constructed on this

project. The other wall systems were all proprietary and included Wire Wall, Retained Earth, and Reinforced Earth. Construction was completed during spring 1982.

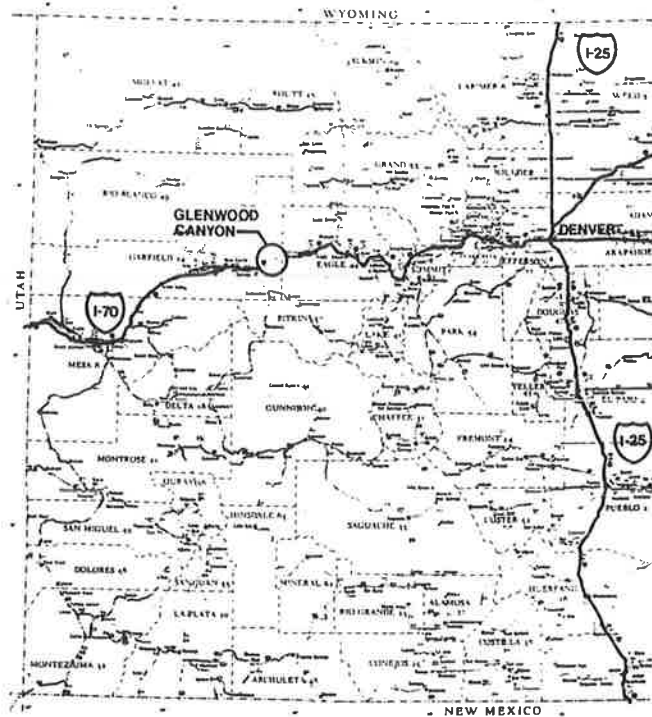
BACKGROUND

Site Description

Glenwood Canyon is a narrow, steep-walled chasm cut by the Colorado River through resistant limestone, quartzite, and granite. The deep slash through the bedrock was formed by a gradual regional uplift, which caused the Colorado River to accelerate downcutting with limited lateral cutting. The 12-mile-long canyon is located about 150 miles west of Denver in west-central Colorado, as shown in Figure 1.

Geologic investigations indicate that bedrock lies up to 150 ft below the river, and that thick lake deposits, which consist of highly compressible silts and clays, are present through the eastern half of the canyon. The lake deposits indicate that, at one time, a temporary dam was formed at some point in the canyon.

Figure 1. Location of Glenwood Canyon.



Problem

The damming of the river was probably the result of a catastrophic event. Based on Carbon-14 dating, lacustrine deposition occurred over an approximate 2,000-year period and ended about 7,000 years ago. This segment of the canyon's history is still a unique and interesting puzzle for project geologists. It has presented unique and difficult problems for foundation designers because it was assumed in the early design phases that bedrock would be found at shallow depths beneath the river and that foundations would not be a problem in the otherwise severely constrained Interstate corridor.

The first project designed for the area where the compressible deposits were found included a rigid, posttensioned cantilever wall with a cantilever pavement section (1). This design was obviously incompatible with the geology. Geologists and engineers could safely predict that significant differential settlements would occur, but predicting the amount of settlement and the time required were beyond the state of the art. Laboratory tests indicated a settlement range of 4 to 40 in., and settlement times of 6 months to 15 years.

Surcharging was not possible due to limited space, and wick drains were deemed prohibitively expensive. Architects and designers finally relented on their insistence for rigid structures and allowed the use of flush-faced flexible walls, but only with the stipulation that the first project be used as a full-scale test to determine the field behavior of the lake deposits.

The only flexible retaining wall system fully approved for use by FHWA on the Colorado Interstate system was the Reinforced Earth Company product. Because extensive reinforcements for flexible walls in the canyon would be needed, it was decided that other systems should be tested to determine if one or more could be approved for competitive bidding. The I-70-2(90) project was designated experimental to allow testing of these other systems and to mon-

itor behavior of the lake deposits. Four wall types were tested: Wire Wall, Retained Earth, Reinforced Earth, and geotextile walls. The design, construction, and performance of the geotextile wall tests are discussed in this paper.

Objectives of Geotextile Wall Tests

Geotextiles have been model tested as earth-reinforcement systems for a number of years (2,3), and several walls have been successfully constructed (4-6). The walls offer an apparently significant economic advantage over most proprietary systems, yet enough questions remain concerning design parameters and long-term stability to cause reluctance on the part of designers to fully accept this type of system.

None of the full-scale geotextile walls reviewed for this research had shown significant creep, and all have performed satisfactorily, even under loadings imposed by heavy logging trucks. However, none of the full-scale tests was designed to determine limiting bounds for geotextile as an earth-reinforcement system. Many of these walls had high live loadings; therefore, dead loads did not produce low factors of safety, and creep resistance was not tested.

A primary objective of the Glenwood Canyon test was to determine lower stability limits for a geotextile earth-reinforcement system. This was investigated by designing at or near equilibrium safety factors on portions of the walls to test the reliability of current design procedures.

A second objective was to demonstrate that the system could be constructed by a major contractor. Most other walls had been the products of special crews, which caused labor and other costs to be disproportionately high.

A third objective was to demonstrate overall cost-effectiveness of the geotextile reinforcement system when directly compared to other systems. A more reliable cost comparison was possible when several systems on the same project were erected by the same contractor.

A fourth objective was to investigate the tolerance to differential settlement, and a fifth objective was to demonstrate a facing system that could perform for the design life expectancy of a wall system.

A final objective was to demonstrate, by reduced fabric embedment lengths in the lower portion of the wall, the stability of this system in side-hill and other situations, where the minimization of initial excavations could save a significant amount of money.

TEST DESCRIPTION

The geotextile test wall is approximately 15 ft high and 300 ft long. The wall is divided into ten 30-ft segments, with a different fabric or fabric strength combination used to construct segments 1-8. Segments 9 and 10 are identical to 1 and 2, except the lower fabric layers are shortened.

The segments were designed with different factors of safety. Six segments had very low computed safety factors and were expected to creep, possibly to failure.

Geotextiles

Four common, readily available nonwoven geotextiles were selected for the tests. Each fabric was used in two weights. These fabrics represent a range of fabric constructions, polymers, and stress-strain characteristics. None of the geotextiles had particularly high strength or other special character-

Table 1. Test geotextiles.

Trade Name, Manufacturer, and CDOH Code No.	Approximate Weight (oz/yd ²)	Filament	Construction
Fibretex, Crown Zellerbach		Continuous, polypropylene	Needle punched
CZ 200	6		
CZ 400	12		
Supac, Phillips Fibers		Staple, polypropylene	Needle punched, heat bonded (one side)
P 4 oz	4		
P 6 oz	6		
Trevira, Hoechst Fibers		Continuous, polyester	Needle punched
H 1115	5		
H 1127	11		
Typar, DuPont		Continuous, polypropylene	Heat bonded
D 3401	4		
D 3601	6		

Table 2. Geotextile strength characteristics.

Geotextile	Ultimate Strength (lb/ft)	Failure Strain (%)	Recommended Working Load	
			No. (lb/ft)	Percent of Ultimate
Fibretex				55
CZ 200	400	140	220	
CZ 400	680	145	375	
Supac				40
P 4 oz	860	65	345	
P 6 oz	1,665	60	670	
Trevira				65
H 1115	455	80	295	
H 1127	1,155	75	750	
Typar				40
D 3401	525	60	210	
D 3601	850	55	340	

istics. The geotextiles tested and some descriptive characteristics are given in Table 1.

The tensile strengths of the geotextiles were determined by a wide-strip tensile test (7). Specimens 8 in. wide and 4 in. long were loaded between grips in simple tension at a constant rate of strain of 10 percent. The specimens were soaked in water before testing. The peak strengths and corresponding elongations as determined by these tests are given in Table 2. Typical load-strain curves are shown in Figure 2.

The recommended working loads in Table 2 are selected to prevent failure by tertiary creep. The various phases of creep are shown in Figure 3. Tertiary creep can be prevented by limiting the applied loads to values less than some critical value, below which tertiary creep will not occur during the design life. Experience and tests indicate that this critical value is controlled, for a given geotextile, by loading and environmental conditions. The recommended values were taken from tests performed at Oregon State University (8).

Backfill Soil

The backfill soil was a free-draining, pit-run, rounded, well-graded, clean sandy gravel. Nearly all particles were less than 6 in. Approximately 50 percent passed the 0.75-in. sieve and approximately 30 percent passed the No. 4 sieve. The backfill soil is shown in Figure 4. Compaction specifications required 95 percent of AASHTO T-180. Conservative values of 35° and 130 lb/ft³ were assumed for the angle of internal friction and unit weight, respectively, for the preliminary design calculations.

Instrumentation

Instrumentation at the site was designed to provide both qualitative and quantitative information on settlement in the vicinity of the wall and to identify specific soil layers or zones of settlement. Information on horizontal deflection in the foundation soils and the vertical deflections of the face of the wall was obtained. Measurements of the deflections of the wall face and the surface above the wall were made to indicate settlement and creep of the fabrics. Movements within the backfill soil mass were also monitored.

These measurements were taken with 5 vertical inclinometer (Sondex) installations spaced evenly in front of the wall 5 ft out from the face; 5 manometers installed evenly along the back edge of the wall; 30 horizontal inclinometer-extensometer casings, with 3/test segment spaced vertically in the center of each segment; direct measurement survey posts at the center of each segment; and several survey points on and in front of the wall for direct measurement of changes in elevation. Many of these installations can be identified in Figure 5.

Test Wall Design

The test wall was designed by assuming the fabric layers had to resist a triangular lateral pressure distribution by friction on the portion of the fabric layer extending beyond the Rankine failure surface. This method was used by Lee and others (9) for Reinforced Earth walls. The method was modified for fabric walls by researchers at Oregon State University (2,10), and it has been used by the U.S. Forest Service (4,5,11) and the New York State Department of Transportation (6) to successfully construct several geotextile walls in the United States.

The geotextile wall section that indicates the fabric layer spacings is shown in Figure 6. The general wall layout is shown in Figure 7, which shows the 10 wall segments and identifies the fabric types in each. This figure also shows the locations of some of the instrumentation installations.

Each test segment is 30 ft long. The fabric layers all extend 12 ft into the fill, except for the lower layers in segments 9 and 10 (Figure 6). All segments incorporate a stronger geotextile (Trevira H 1155) for the lower three layers. Segments 5, 6, and 8 incorporate a lightweight fabric for the upper layers (10-17) and a heavier weight of the same fabric for the lower layers (4-9). All other segments use a one-strength geotextile, except for the cover fabric (layer 18) and the lowest layers (1-3).

To facilitate construction, geotextile layer spacings are the same in all wall segments. Therefore, because the geotextiles have different

strength characteristics, the factors of safety are different for different segments. Design relative loads for each wall segment are given in Table 3. The relative load is the computed load expressed as a percentage of the appropriate ultimate load (strength) given in Table 2.

Safety considerations dictated that the wall should not fail rapidly during construction; therefore, some conservatism was retained in the design method. However, the data in Table 3 indicate that many computed loads are well above the recommended values in Table 2, and in two segments the loads approach the ultimate loads. It was expected from this design that the wall would exhibit significant strains in some fabric layers, and deflections of the wall would be evident. In some segments, failure by tertiary creep was considered a real possibility.

CONSTRUCTION

Construction procedures used on the Glenwood Canyon

wall were modeled after Forest Service guidelines (5). The steps required to complete each lift are shown in detail in Figure 4. Different stages of the actual construction are shown in Figure 5. The partly completed wall with the forms set for the next lift (step 1, Figure 4) and the fabric spread (step 2, Figure 4) is shown in Figure 5a. In Figure 5b the backfill for the new layer is being placed. In Figure 5c the backfill is being spread (step 3, Figure 4) and the windrow built (step 4 Figure 4). In Figure 5d the fabric is folded back over the windrow (step 5, Figure 4) and the backfill lift is completed (step 6, Figure 4).

Based on field observations during construction, few modifications for construction of future walls would be made to the general plan used for the test series. It would be prudent to design thin (6- to 9-in.) lifts for the first 2 to 3 ft to allow the field crew to become familiar with the technique. It takes a new crew 3 or 4 lifts to develop their technique so that they can obtain a uniform wall face.

Figure 2. Geotextile load-strain curves.

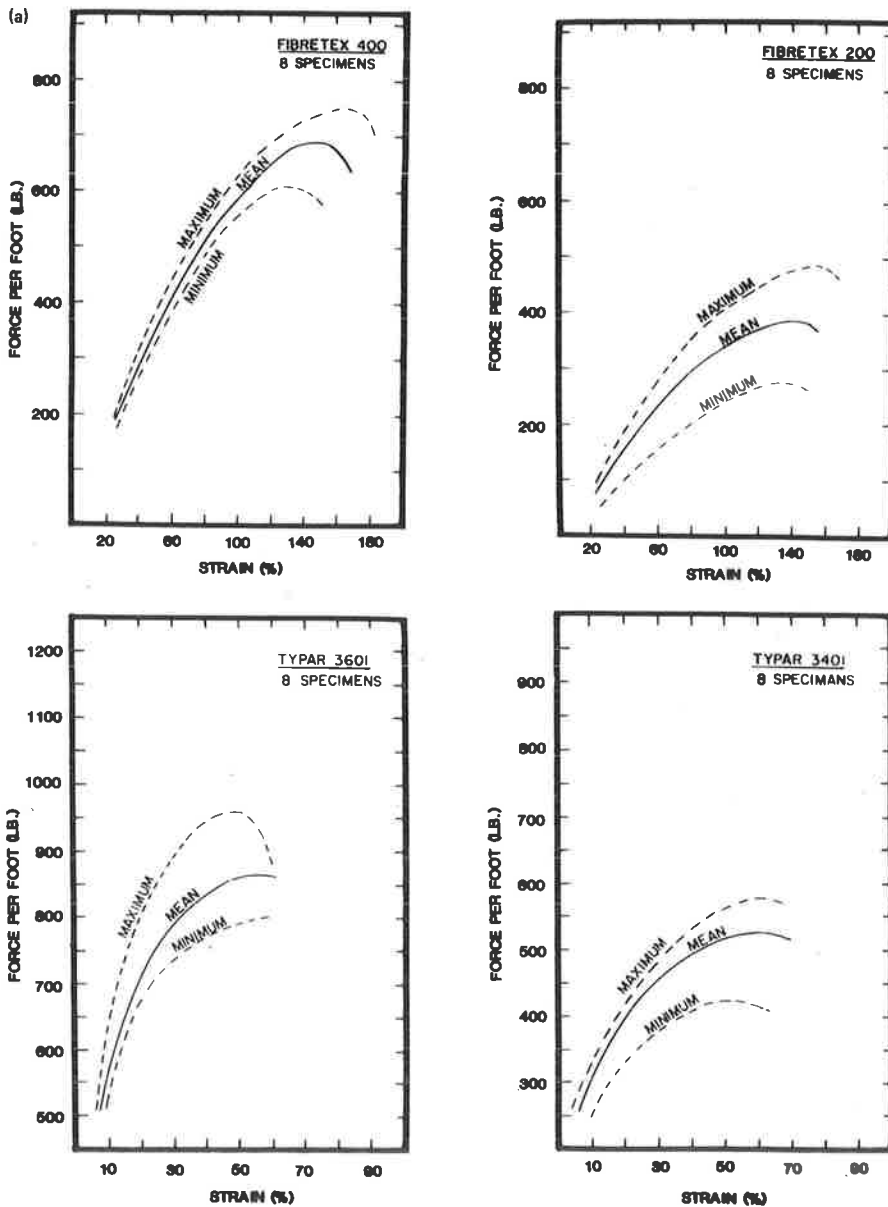


Figure 2. Continued.

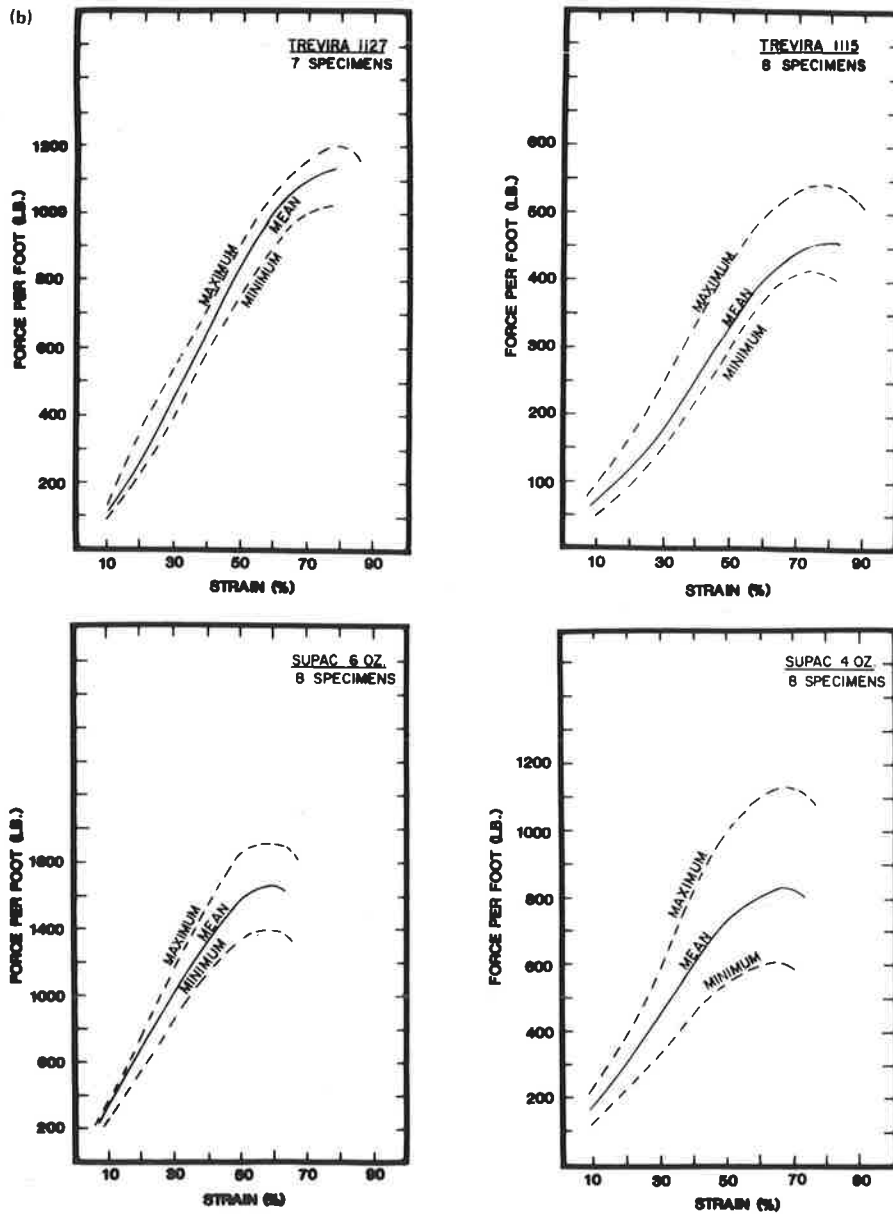
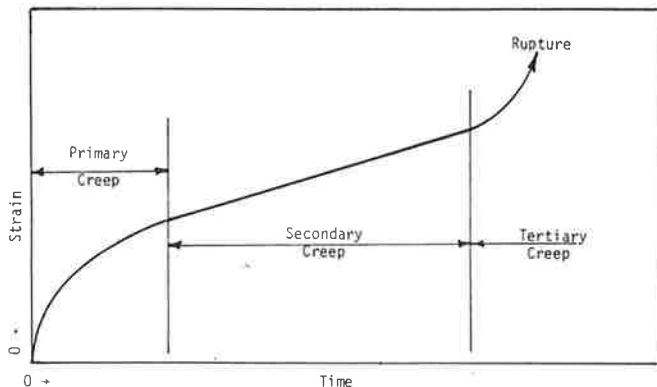


Figure 3. Phases of creep for typical geotextile tested in isolation at constant load and temperature.



The face-forming system used on this project performed satisfactorily. Nevertheless, the experience suggests it is only reasonable for lifts up to about 15 in. Thicker lifts would require a different or modified forming system.

Maintaining design batter, or face slope, requires continual monitoring. The test wall series was planned for a 1-in-10 batter and was constructed with a 1-in-5 batter. This was due to a variety of factors, but the primary one was failure to formally survey each lift.

Many geotextiles must be protected from the sun. Ultraviolet light is the only agent in a typical construction environment that will cause deterioration of either polypropylene or polyester. On this project new lift faces were sprayed within 5 days with a low viscosity water-cement mixture. This fluid penetrated the fabric and set to a brittle

Figure 4. General geotextile wall construction procedure.

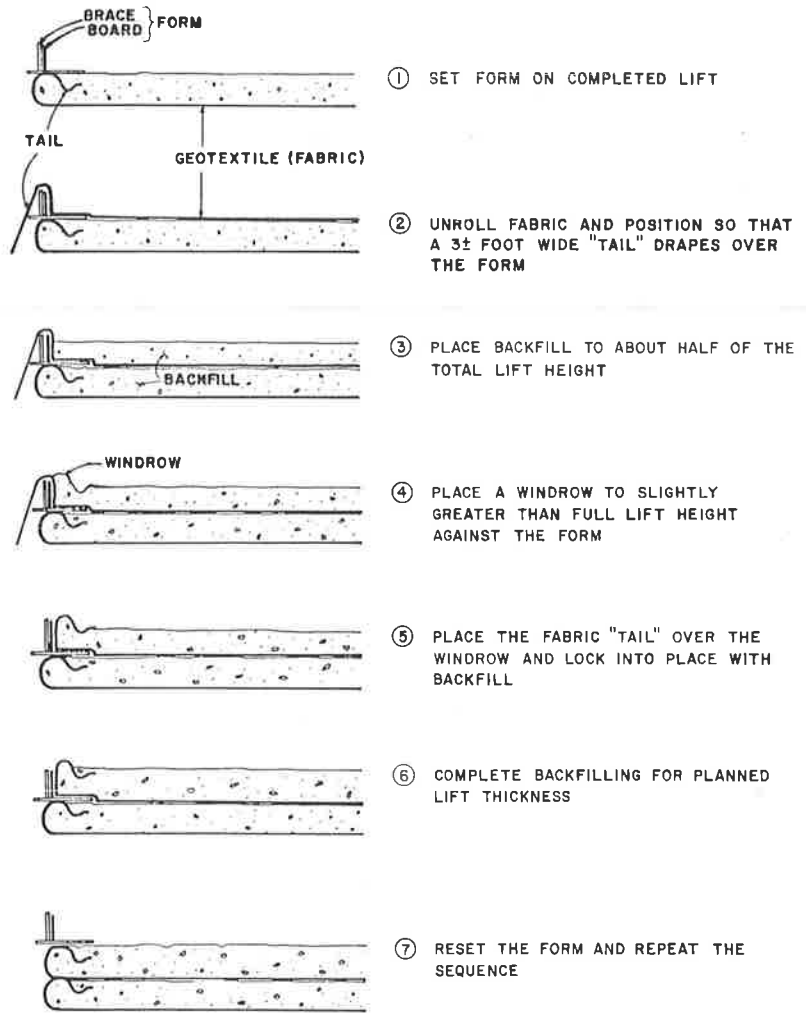


Figure 5. Wall construction.

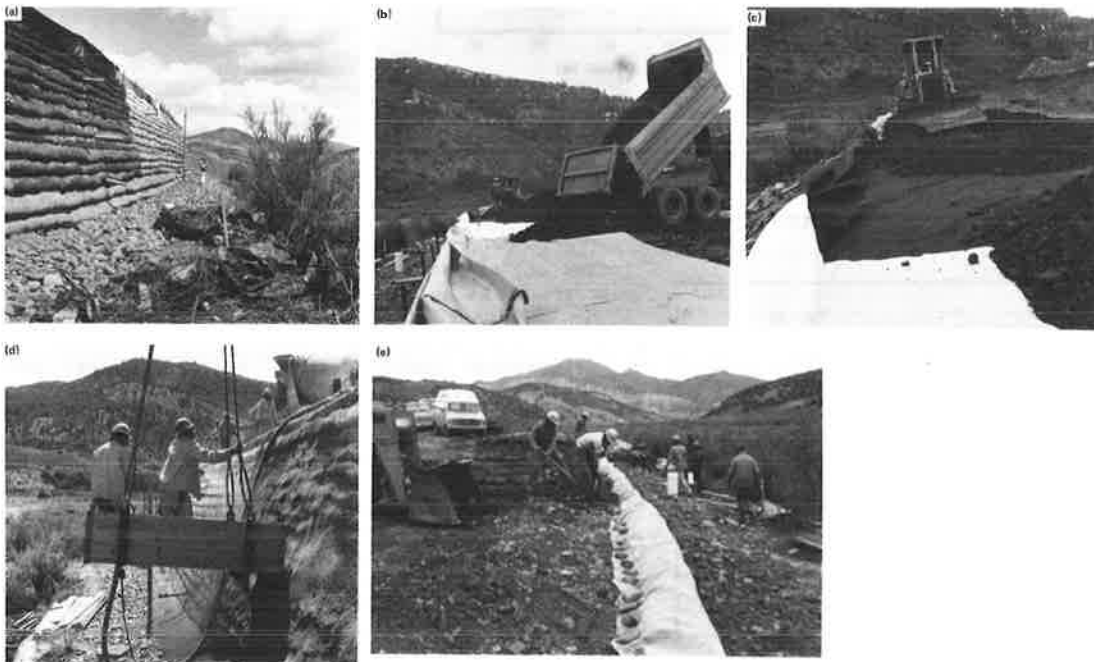


Figure 6. Geotextile wall section.

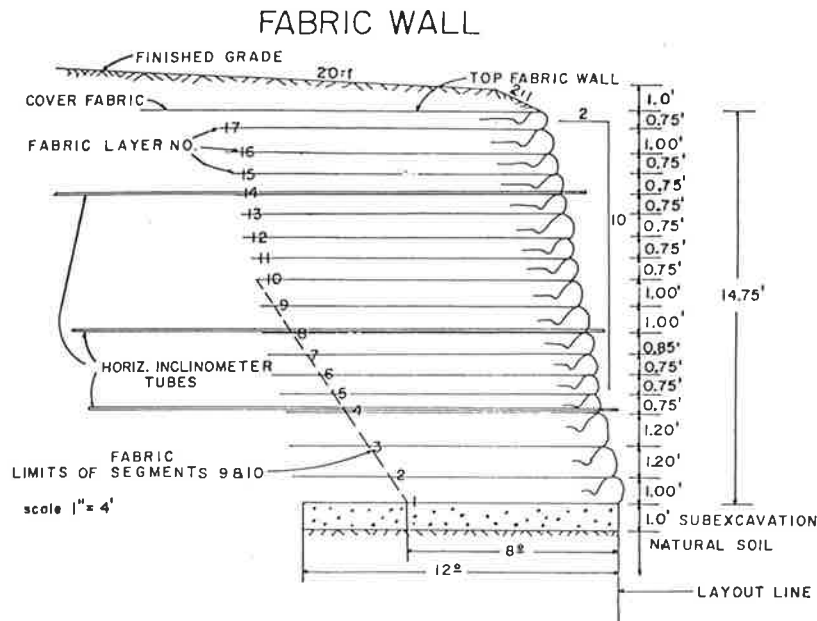


Figure 7. Geotextile wall elevation with test segments and fabric types indicated.

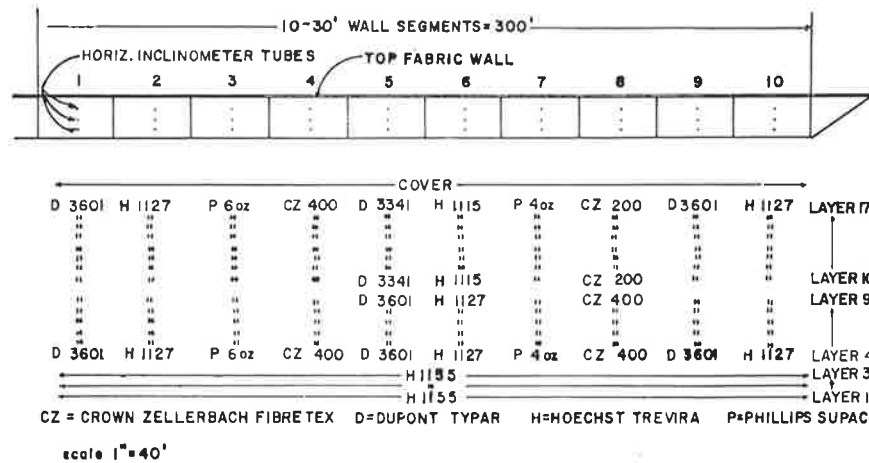


Table 3. Design relative load for test wall segments.

Layer	Relative Load ^a (%) by Wall Segment									
	1	2	3	4	5	6	7	8	9	10
17	10	7	5	13	16	19	10	21	10	7
16	16	12	8	20	26	30	16	34	16	12
15	17	13	9	21	28	32	17	36	17	13
14	21	15	11	26	34	39	21	44	21	15
13	25	18	12	31	40	46	24	52	25	18
12	28	21	14	35	46	53	28	60	28	21
11	32	23	16	40	52	60	32	68	32	23
10	42	31	21	52	68	78	41	89	42	31
9	54	40	28	68	84	94	53	100	54	40
8	56	41	28	70	86	96	55	100	56	41
7	53	39	27	66	82	92	52	98	53	39
6	53	39	27	67	83	93	53	99	53	39
5	57	42	29	71	87	97	56	100	57	42
4	79	58	40	99	100	100	78	100	79	58

^aRelative load is the computed fabric load expressed as a percentage of the geotextile ultimate strength.

stiffness. It bonded well and provided excellent protection, even for the smoother fabrics.

Facing

The wall was faced with gunnite. This facing was easily applied by an experienced crew and has withstood differential settlements of about 12 in. over 300 ft in only 3 months with little cracking of the surface. About 65 yd² of gunnite were required for the approximately 4,700 ft² of wall face.

A number of facades could be adapted for geotextile walls, including logs, treated timber, vertical or horizontal boards, or precast-concrete panels. Any of these systems could be developed cost competitively on a major wall. The wall would be constructed as described previously and the facing attached to the completed wall as a free standing facade tied back to the geotextile wall.

Cost

Costs for the series of geotextile test walls ranged between \$11.00 and \$12.50/ft² of wall face. Variability in the cost figure depended on which items were excluded as special research features and which were included as required for all walls. The cost breakdown in terms of completed square footage of wall face (in 1982 prices) is given in the table below:

Item	Cost (\$)
Geotextiles	2.00 to 2.50
Labor	0.50 to 1.00
Equipment	0.50 to 1.00
Backfill (including haul)	5.00
Gunnite	3.00

DISCUSSION OF RESULTS

In general, the construction procedures, costs, and performances of the wall have been satisfactory. Performance to date has been better than expected in that large strains anticipated in some segments of the walls have not occurred. There are several possible reasons for this fact:

1. The instrumentation does not accurately indicate the strains in the geotextiles,
2. The assumed backfill parameters are incorrect,
3. The theory does not accurately model the true mechanisms, and
4. The laboratory geotextile tests used do not adequately indicate the in-soil behavior of the geotextiles.

Table 4. Computed relative loads and recommended allowable geotextile loads.

Wall Segment	Computed Maximum Relative Load (%)			
	Design	As Built		Allowable Load (%)
		At Rest (K _o)	Active (K _a)	
1	79	63	39	40
2	58	46	29	65
3	40	32	20	40
4	99	79	49	55
5	79	63	39	40
6	78	63	39	65
7	78	62	39	40
8	99	79	49	55
9	79	63	39	40
10	58	46	29	65

Table 5. Computed average relative loads and recommended allowable loads.

Wall Segment	Computed Avg Relative Load (%)						
	Design	As Built		Design	As Built		Allowable Load (%)
		Avg of Layers 5-17	Avg of Layers 4-9		Avg of Layers 5-17	Avg of Layers 4-9	
1	39	59	31	47	19	29	40
2	29	43	23	34	14	21	65
3	20	30	16	24	10	15	40
4	49	74	39	59	24	37	55
5	47	59	38	47	23	29	40
6	44	43	35	34	22	21	65
7	38	59	30	47	19	29	40
8	60	74	48	59	30	37	55
9	39	59	31	47	19	29	40
10	29	43	23	34	14	21	65

Discussions of each of these reasons follows.

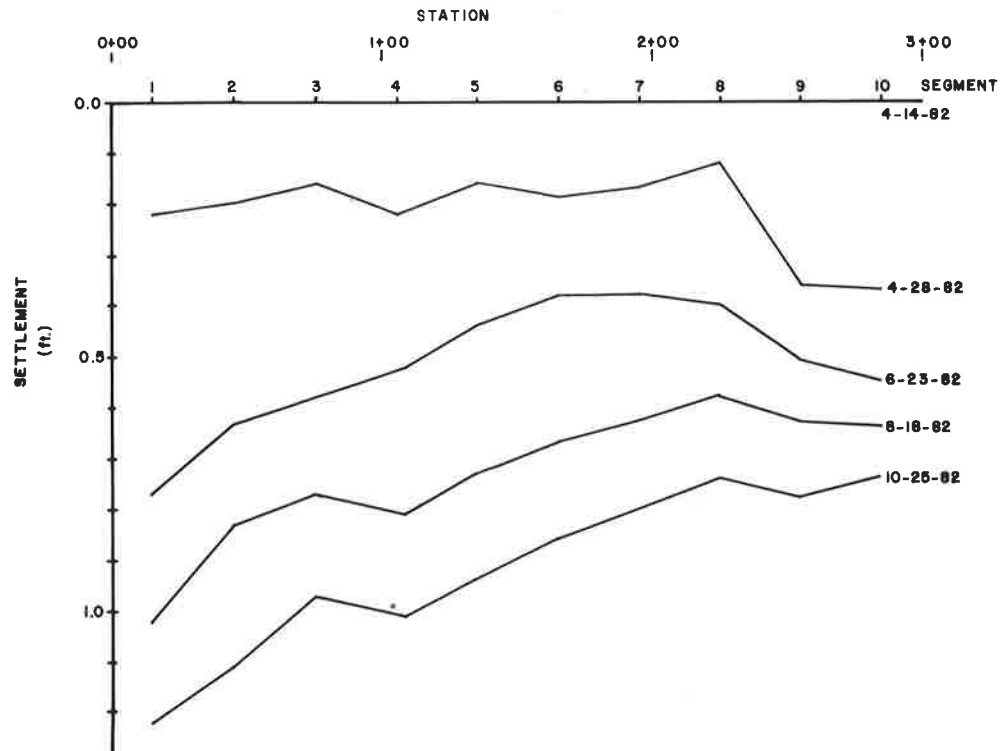
Model tests (2) have indicated that the failure zones in reinforced walls are very narrow. Therefore, the zone of significant strains (initial and creep) in the geotextiles may be narrow. The fabric strains in the test wall may be masked by settlement, at least until strains become large. As of November 1982, the instruments have not indicated fabric strains.

Values of 35° and 130 lb/ft³ were assumed for backfill friction angle (ϕ) and unit weight (γ), respectively. These values were used to calculate the geotextile relative loads given in Table 3. The maximum design load for each wall segment is tabulated in Table 4. These values reveal that, according to the design assumptions for the critical layers in segments 4 and 8, the factors of safety against an immediate failure were 1.0 (a relative load of 100 equals a factor of safety of 1.0). Other segments had immediate factors of safety of 1.25 or higher. With respect to creep failure (rupture by tertiary creep), all but segments 2, 3, and 10 had factors of safety much less than 1.0. Segment 5, for example, only had a factor of safety of 0.5 (ratio of relative load to allowable load). Obviously, the design calculations were conservative, as failure has not occurred.

For the as-built sections, ϕ was about 42° and the average unit weight was about 135 lb/ft³. When these values are used with the other design assumptions, maximum relative loads are as indicated in the third column of Table 4. When these values are considered, the factors of safety against an immediate failure are all greater than 1.0, but factors of safety against creep are still considerably less than 1.0 for 6 of the 10 wall segments. There are apparently more conservative factors than just the assumed backfill parameters.

A major question is the validity of the theory used. The theory does not actually analyze a composite reinforced material. It is actually a pseudo-tie-back analysis. It is known to be conservative (2), but how conservative is not known. The analysis in this design assumed the at-rest earth pressure K_0 rather than the active pressure K_a . The at-rest pressure has also been used for similar analyses by other researchers (5,9,10). The use of the at-rest pressure was reasonable when the heavy traffic loads were expected, but they may be excessively conservative for the actual case with dead loads only. The high-elongation geotextiles may encourage the development of the active state. When the maximum geotextile relative loads are further reduced for active lateral earth pressure, the values in the fourth column of Table 4 are obtained. Currently, none of the computed loads exceeds the allowable loads, and creep failures are not indi-

Figure 8. Average total settlement of fabric wall.



cated; however, creep greater than that indicated by field instrumentation would still be expected.

The distribution of the total load among the geotextile layers is another question. The calculations assume the soil stresses increase linearly with depth, and the load on a given fabric layer is equal to the sum of the soil stresses over an area bounded by the mid-distances to the layers above and below it. Field measurements have revealed that the actual loads were more uniform with depth (12,13). Further, for high-elongation geotextiles, such as those used in this study, the more highly stressed fabric layers may yield sufficiently to transfer parts of their loads to adjacent layers. Thus it might be more realistic to average the geotextile layer loads. Averaging assumes no layer can fail unless all layers fail. This assumes that if the load on any layer exceeds the load on adjacent layers, that layer will creep more than adjacent layers, thereby transferring loads to the adjacent layers.

The average geotextile relative loads are given in Table 5. These values do not indicate possible immediate failure; however, for the at-rest case, when the lower portion of the wall is considered, creep failure is still critical for 6 of the 10 segments. Only when the loads for the active pressure case are averaged are the results consistent with field strain measurements on the test wall. At these stress levels, the fabrics would strain approximately 10 percent or less. This is the maximum strain in a layer, not an average. The instrumentation may not detect this magnitude of movement as being due to fabric creep rather than settlement.

These discussions suggest that the theory greatly overestimates stresses in the geotextiles and that past practices have been excessively conservative. Before accepting this conclusion, however, it is necessary to consider the problem of establishing allowable geotextile loads from simple, in-isolation, tensile testing.

It is known that, when confined in a soil, the load, strain, and time relations of geotextiles are changed (14,15). For needle-punched fabrics, these changes are great. The initial strains at relative loads of 20 to 40 percent may be reduced by one-half or more (14). The ultimate strengths, however, are only slightly increased. There is limited evidence that the critical stress needed to initiate tertiary creep failure is not greatly increased (14,16). However, the creep rate at intermediate relative loads is decreased by orders of magnitude. Therefore, the critical loads assumed in this study may be reasonable, but confinement of the geotextiles in the soil may have reduced the initial strain and delayed the development of time-dependent strain. It may be that the higher computed loads, at least as high as the averages, are realistic and that only time is required to develop the expected high strains.

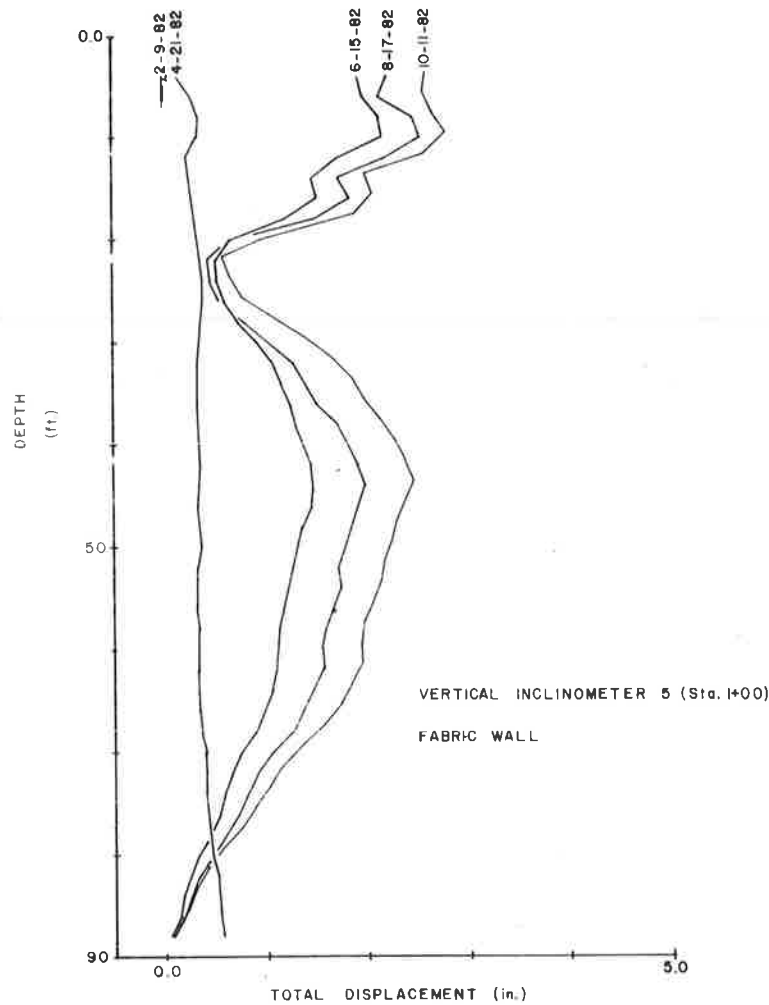
Optical survey measurements for the first 6 months indicate that a relatively large amount of consolidation has taken place in the soils beneath the wall. This settlement has not produced significant cracking in the shotcrete facing to date. The representative settlement data are shown in Figure 8 and the attendant horizontal deflections are shown in Figure 9. All wall instrumentation monitoring will be continued to observe future trends.

Wall segments 5 and 6 have been surcharge loaded. This may help clarify the situation; however, there is a need for full-scale, instrumented walls designed to fail. Only by going all the way to failure with different types of geotextiles for different loadings will it be possible to verify or modify design methods and select appropriate safety factors.

The surcharge load was added too recently to provide data for this paper. These results will be analyzed in a future report.

The use of stronger fabrics will allow building walls with fewer, thicker lifts. This appears to

Figure 9. Horizontal deflections of fabric wall.



offer an economic benefit because of reduced labor. However, experience in these tests suggests that the forming method used is not generally practical for lifts greater than about 15 in. Thicker lifts will require a different method. A more sophisticated method will probably not be economical except on very large jobs. The use of strong geotextiles, therefore, may not offer significant savings except in special cases or for high walls where they would be used in the lower layers.

Some fabrics are stronger in the machine direction than in the cross-machine direction. However, to use this extra strength it is necessary to cut the fabric roll into many short sections and sew them together before installation. This is probably not cost effective. It is probably best to use the cross-machine strength in design. This must be considered when sampling and testing geotextiles.

Although geotextile costs are not to be ignored, the cost data for this wall indicate that geotextile costs are a small percentage of total wall costs. If excavation is required, this percentage cost becomes even smaller. Therefore, the use of conservative allowable loads and other conservative design assumptions does not unduly increase costs.

CONCLUSIONS

The results of this study suggest the following conclusions.

1. Geotextile reinforced walls are economical and practical.
2. Construction procedures are practical for large contractor-constructed projects.
3. Suitable simple, economical, durable facings can be adapted for this system.
4. The mechanisms of geotextile reinforced soil are not well defined. Further, the stress, strain, and creep behaviors of geotextiles embedded in soils are not fully understood, and the ability to evaluate geotextiles and rationally select allowable loads is limited.
5. Designs based on the Rankine model that use at-rest earth pressures as previously published will give economical, safe, practical designs for the following conditions: cohesionless backfill; maximum allowable relative loads, as specified in this paper to limit creep; when allowable loads are applied to the average loads computed, as indicated in this paper for high-elongation geotextiles; and a factor of safety of 1.5.
6. Conservative interpretation of geotextile strengths has a limited effect on economy because the cost of the reinforcing component is a small part of the total cost of the wall.
7. Full-scale wall tests to failure are needed to clarify the theory, develop appropriate factors of safety, and allow more rational, and perhaps more economical, designs.
8. Reduced fabric lengths in the lower portions

of fabric walls may be a safe, effective way of minimizing excavations in side-hill installations.

ACKNOWLEDGMENT

The test walls were constructed during spring 1982 with Task Order funds from FHWA, Federal-Aid Interstate (FAI) funds, and state of Colorado funds. Federal aid was denied for wall test segments that were designed at lower-bound safety factors.

The wall was designed, instrumented, and monitored as a joint venture by Research and Development, Central Laboratory, and District Materials personnel from CDOH.

Dupont Company, Hoechst Fibers, Crown Zellerbach Company, and Phillips Fibers Corporation provided the geotextiles for the test wall.

The wall was constructed by Peter Kiewit and Sons Construction Company.

Note that the use of product, trade, proprietary, and company names in this paper is for clarity and does not imply endorsement or superiority to similar items.

REFERENCES

1. R.J. Trapani and E.A. Beal. Glenwood Canyon I-70 Environmental Concern. ASCE Meeting, Las Vegas, Preprint 82-025, April 1982.
2. J.R. Bell, A.N. Stille, and B. Vandre. Fabric Retained Earth Walls. Proc., 13th Annual Engineering Geology and Soils Engineering Symposium, Moscow, ID, 1975.
3. R.D. Holtz. Laboratory Studies of Reinforced Earth Using a Woven Polyester Fabric. Proc., International Conference on the Use of Fabrics in Geotechnics, Ecole National Des Ponts et Chaussees, Paris, France, Vol. 3, April 1977, pp. 149-154.
4. J.R. Bell and J.E. Steward. Construction and Observations of Fabric Retained Soil Walls. Proc., International Conference on the Use of Fabrics in Geotechnics, Ecole National Des Ponts et Chaussees, Paris, France, Vol. 1, April 1977, pp. 123-138.
5. J.E. Steward, R. Williamson, and J. Mahoney. Guidelines for Use of Fabrics in Construction and Maintenance of Low-Volume Roads. FHWA, Rept. FHWA TW-78-205, 1977.
6. J.E. Steward. Case Histories, Reinforced Earth Walls, Earth-Fabric Wall. Soils Mechanics Bureau, New York State Department of Transportation, Albany, March 1981.
7. S.C. Shrestha and J.R. Bell. A Wide Strip Tensile Test for Geotextiles. Proc., 2nd International Conference on Geotextiles, Las Vegas, Vol. 3, Aug. 1982, pp. 739-744.
8. T. Allen, T.S. Vinson, and J.R. Bell. Tensile Strength and Creep Behavior of Geotextiles in Cold Regions Applications. Proc., 2nd International Conference on Geotextiles, Las Vegas, Vol. 3, Aug. 1982, pp. 775-780.
9. K.L. Lee, B.D. Adams, and J.M.J. Vagneron. Reinforced Earth Retaining Walls. Journal of the Soil Mechanics and Foundations Division, ASCE, Vol. 99, No. SM10, 1973, pp. 745-763.
10. W. Whitcomb and J.R. Bell. Analysis Techniques for Low Reinforced Soil Retaining Wall and Comparison of Strip and Sheet Reinforcements. Proc., 17th Engineering Geology and Soils Engineering Symposium, Moscow, ID, 1979.
11. J. Steward and J. Mahoney. Trial Use Results and Experience Using Geotextiles for Low-Volume Forest Roads. Proc., 2nd International Conference on Geotextiles, Las Vegas, Vol. 2, Aug. 1982, pp. 335-340.
12. N. Jonn, P. Johnson, R. Ritson, and D. Petley. Behavior of Fabric Reinforced Soil Walls. Proc., 2nd International Conference on Geotextiles, Las Vegas, Vol. 3, Aug. 1982, pp. 569-574.
13. M.R. Hausmann. Behavior and Analysis of Reinforced Soil. Univ. of New South Wales, Kensington, Australia, Ph.D. thesis, 1978.
14. A. McGown, K.Z. Andrawes, and M.H. Kabir. Load-Extension Testing of Geotextiles Confined in Soil. Proc., 2nd International Conference on Geotextiles, Las Vegas, Vol. 3, Aug. 1982, pp. 793-798.
15. K.Z. Andrawes, A. McGown, M.M. Mashhour, and R.F. Wilson-Fahmy. Tension Resistant Inclusions in Soils. Journal of the Geotechnical Engineering Division, ASCE, Vol. 106, No. GT12, Dec. 1980.
16. T. Allen. Application of Geotextiles in Cold Regions. Oregon State Univ., Corvallis, M.S. thesis, 1983.

Publication of this paper sponsored by Task Force on Engineering Fabrics.

New York State Department of Transportation's Experience and Guidelines for Use of Geotextiles

ANTHONY MINNITTI, L. DAVID SUITS, AND TODD H. DICKSON

Since the early 1970s, the use of geotextiles by the New York State Department of Transportation has evolved from use as a special item on a job-to-job basis to the establishment of an approved list for use with five application categories. This evolution is described, and a description of each of the five categories is presented. Supporting case histories for each category are also given. The system used to evaluate geotextiles for the approved list is described. Based on the results of laboratory test programs and field experience, a set of design guidelines for the general applications is presented. A discussion of the important steps to follow in using geotextiles, so that improved guidelines and specifications for their use may be developed in the future, is also presented.

During the past 10 years the New York State Department of Transportation (NYSDOT) has been involved in developing technology in order to use filter fabrics for civil engineering applications. During this period the number and varieties of geotextiles have increased to the point whereby the designer and engineer must have a clear understanding as to a geotextile's characteristics in order to specify and use them properly.

The evolution of geotextile use by NYSDOT is described in this paper. Five categories (i.e., underdrain, undercut, bedding, slope protection, and silt fencing) are defined, and supporting case histories are given. Properties (e.g., flow rate, soil retention, strength, and stability) that are important in defining geotextile use for all categories are presented and compared. Minimum acceptance and design guideline values for both general and severe cases are presented along with conclusions and recommendations for future work.

EARLY INVOLVEMENT WITH GEOTEXTILES

The initial use of geotextiles was to solve special problems. During the 1960s and 1970s, NYSDOT was active in constructing new high-quality Interstate roads. The prevention of land and water pollution adjacent to construction sites required building large sedimentation basins to collect water that had suspended solids. The conventional filter criteria design for basin outlets required three filter layers that consisted of sand, pea gravel, and crushed stone, each 1-ft thick. Instead of this configuration, the state recommended the use of an outlet of large crushed stone covered with a woven geotextile that acted as a filter (1).

Geotextiles were selected for use because they would save money and time. If they had not worked, however, it would not have been a major problem to correct the situation by conventional means. These installations were successful because they performed satisfactorily, required less maintenance, and saved approximately \$2,000/outlet installation as compared to the conventional layered-aggregate system.

In the early 1970s a geotextile was used to line a stream channel under NY-85 near Delmar, New York. The geotextile was used to line the bottom and sides of the stream, and to date it has prevented erosion, even though much of the stone has been removed by storms. It is believed that erosion prevention is due to the normal slow velocity of the stream at the site.

Another early use of geotextiles was in the repair of a roadway embankment that was failing into an adjacent stream (2). A berm was to be built at

the toe of the embankment that would extend over an area of active silt boils caused by an artesian water condition. The problem with the berm construction was how to stop the bubbling of the three large silt boils that had developed at the embankment toe. It was decided to sew together sections of a geotextile to form a large sheet, which was then placed over the silt boils and sunk by placing crushed stone directly on the geotextile sheet. This installation was successful because it provided an economical way of filling the silt boils where no conventional remedy was available and because it was easy to install.

These types of successful projects convinced NYSDOT that geotextiles were a viable alternative to conventionally designed solutions for geotechnical problems that otherwise would be expensive or impractical. At the same time, there were many unanswered questions about geotextiles and their use. NYSDOT was not confident that all of the important characteristics for geotextile use were known. Because these construction materials were new, and every manufacturer tested the material by their own special tests, how could the characteristics needed for successful field performance be specified in generic terms?

GEOTEXTILE ACCEPTANCE

NYSDOT procedure for allowing the use of geotextiles has gone through a multiphase development. First, approval was done on a job-to-job basis by specifying a particular brand name geotextile or the equivalent to it. In order for a manufacturer's material to be used for a given application on a construction project, it had to have prior approval, which was obtained by contacting the Soils Mechanics Bureau of NYSDOT. The manufacturers had to demonstrate that the material had performed satisfactorily under similar application and site conditions.

During the mid- to late-1970s, the number of geotextiles on the market increased considerably. Many manufacturers and distributors contacted the Bureau about allowing the use of the geotextiles they provided. Unfortunately, there were no criteria for accepting or rejecting a particular material for the "or equal" alternative in the specifications. Thus it was decided to place part of the burden of proof on the manufacturers and distributors. An acceptance procedure was established whereby the manufacturer and distributor that requested approval would have to show that the material's characteristics had been tested, that the material had been successfully used for the proposed applications, and that a product evaluation form was completed. They also had to provide a 5-yd² sample of the material for evaluation before consideration for acceptance.

This acceptance procedure provided much needed information about geotextiles from both a testing and field installation standpoint. Because of the great number of geotextiles, geotextile properties had to be identified and evaluated for design purposes. The most valid way to do this was to develop and perform the Bureau's own laboratory tests on the geotextiles and to set up trial installations throughout the state.

Unfortunately, none of this work solved the immediate problem of allowing general use of geotextiles in normal construction contracts. As laboratory and field work were being undertaken, a formal approved list was established based on the Bureau's information and on information provided by manufacturers and distributors. This list was issued through the Materials Bureau of NYSDOT. The approved list provides general acceptance of geotextiles separated by application: underdrain, undercut, bedding, slope protection, and silt fencing.

APPLICATIONS, DEFINITIONS, AND EXPERIENCE

Each of the previously mentioned applications may require the performance of a different geotextile characteristic. Therefore, it is important to understand how NYSDOT defines these applications (3). Definitions for each application are given below along with supporting case histories.

Underdrain

The geotextile is used to line a trench adjacent to a highway pavement that collects free water from underground sources, rainfall, and spring melt. It

is intended that the geotextile allow free water entering the trench to pass through, while retaining in situ soil particles in order to prevent clogging or piping of the underdrain system, which could weaken the subgrade and result in substantial damage to the pavement. A typical underdrain section is shown in Figure 1.

In areas where the soil consists of uniform silts or fine sands, piping can be a problem. The use of a geotextile is a practical alternative to constructing the multilayer filter shown in Figure 1. For this application, the soil retention and flow rate (i.e., permeability) characteristics of the geotextile are important to the performance of the underdrain system. The geotextile should also have sufficient strength to withstand the installation process.

Seven underdrain sections were installed in 1975 at Marathon-Willet (near Ithaca) by using combinations of pipe, stone, and various geotextiles. The soils in the area were mixtures of wet gravels, silts, and clays. Plan and section views are shown in Figures 2 and 3. The geotextiles used were all nonwoven and varied greatly in their soil retention and flow characteristics. Seven years after instal-

Figure 1. Typical sections of underdrain system.

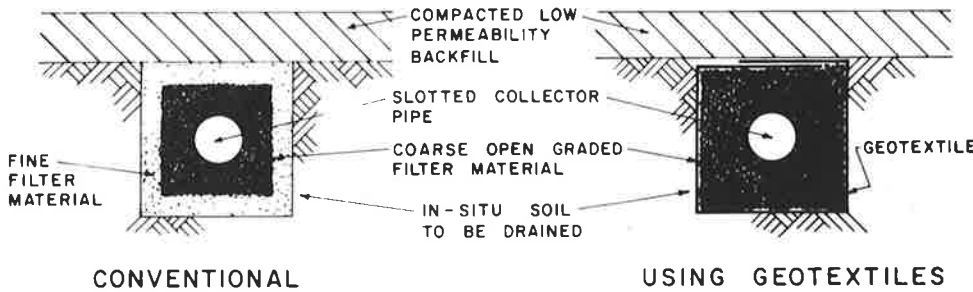


Figure 2. Plan view of underdrain system.

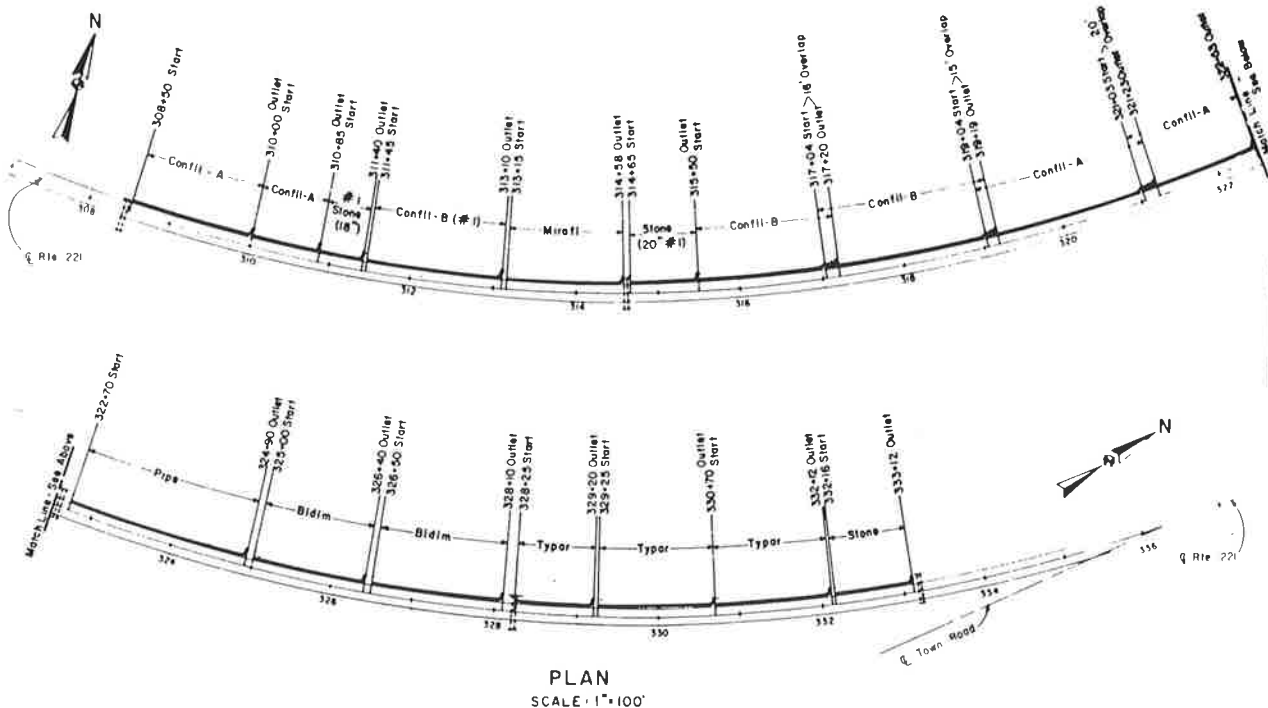


Figure 3. Typical installation details.

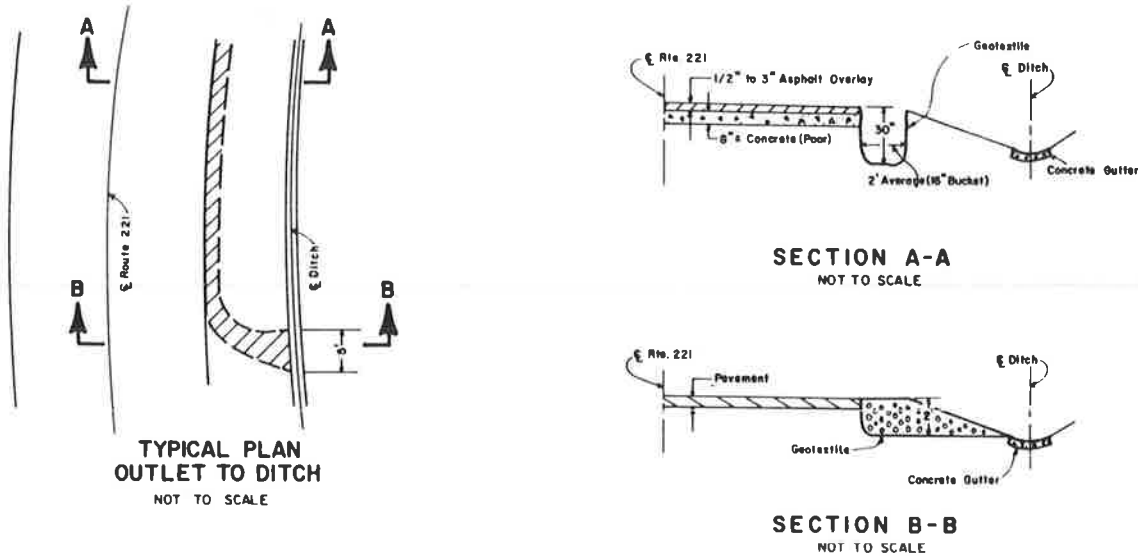
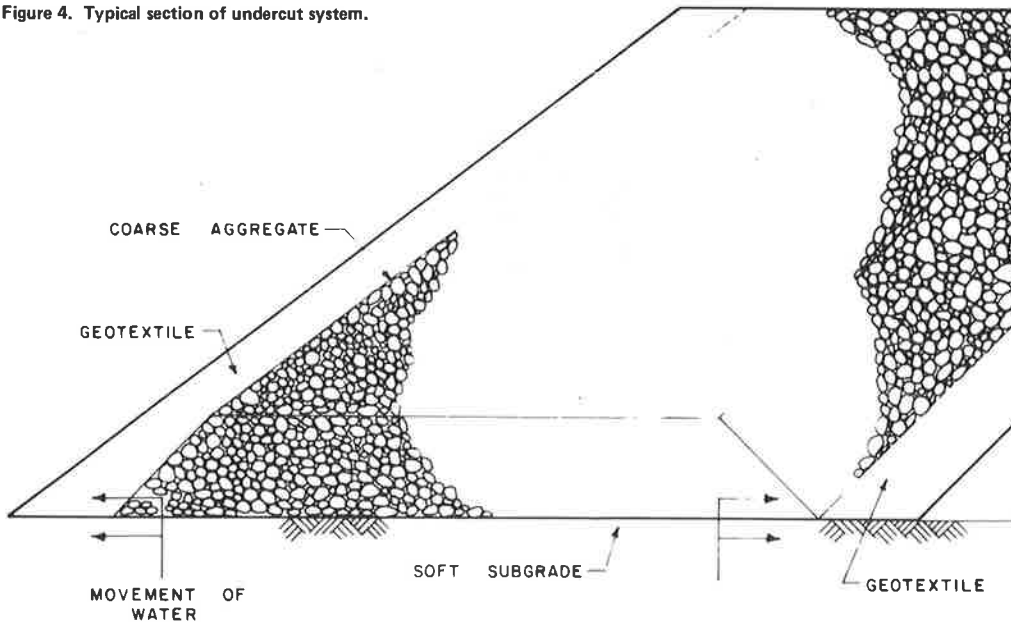


Figure 4. Typical section of undercut system.



lation all underdrains are performing satisfactorily based on observations of water flow at the outlets.

Underdrain sections were installed by the Pennsylvania DOT in 1976. The sections consisted of either (a) an underdrain pipe wrapped with a woven or nonwoven geotextile, which was then placed in a trench and surrounded by stone, or (b) a woven or nonwoven geotextile placed directly in the trench as a lining followed by pipe and stone placement. Typical sections of these installations can be found in Forshey (4,5). In 1977, the Bureau was invited to observe the excavation of these underdrains and to evaluate their performance. Based on the inspection of this site, the following observations were made:

1. All sections had performed satisfactorily. In sections where the underdrain pipe was wrapped with a geotextile, the stone surrounding the pipe was contaminated with soil fines. Although this was not detrimental in this case, it could be for long-term installations. Therefore, in order to prevent contamination, it is recommended that underdrain

trenches be lined with a geotextile rather than wrapping the pipe with the geotextile.

2. Nonwoven geotextiles retain more soil fines than do woven geotextiles. This observation was based on the finding that those trenches lined with nonwoven geotextiles had little or no silt deposition within the underdrain system, whereas the trenches lined with the woven geotextiles did. Therefore, it is recommended that only nonwoven geotextiles be used for underdrain applications.

Undercut (Subgrade Stabilization)

The geotextile is used as a separator between wet, unstable, native soils (i.e., silts and fine sands) and a granular material that is to be placed on the geotextile. It is intended that the geotextile allow drainage of excess water from these unstable soils. Once stabilized, these soils will have sufficient bearing capacity for highway construction. A typical undercut installation is shown in Figure 4. The geotextile must have (a) sufficient perme-

Figure 5. Typical section of bedding system.

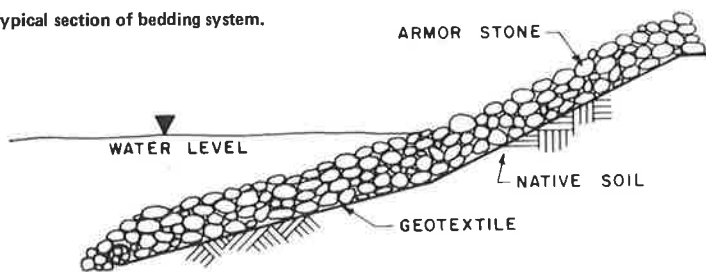
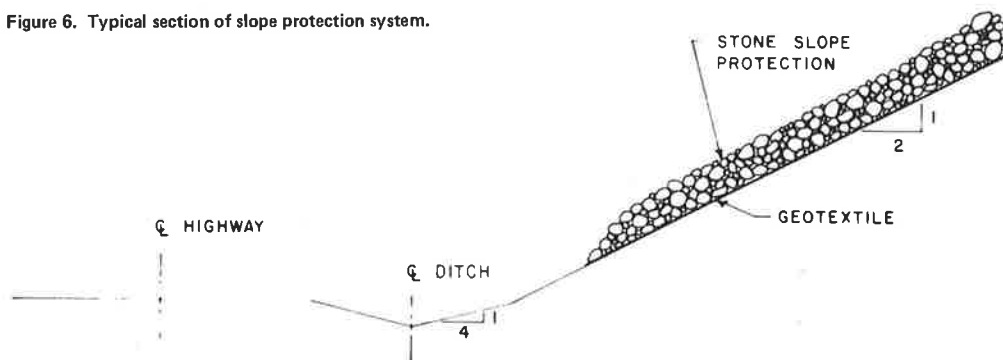


Figure 6. Typical section of slope protection system.



ability to allow drainage, (b) opening sizes that will prevent large amounts of soil from passing through, and (c) sufficient strength to survive installation stresses due to construction equipment.

In 1977 an undercut installation was constructed in Schoharie, New York, where the highway pavement through the village was to be completely replaced. The native soil consisted of a wet, red, fine silt, and when this soil was combined with the traffic loads, cracking in the pavement occurred. It was impossible to raise the final grade of the proposed highway reconstruction because it would disturb the existing road connections, sidewalks, store fronts, and property accesses. The project alternatives were further restricted by the utilities that had been installed at a shallow depth. It would have required a prohibitive expenditure in relocating all existing utilities deeper. To overcome these problems, a nonwoven geotextile was used under 1 ft of granular material. By doing so, the problem area was stabilized, the grade requirements were satisfied, and the utility problems were solved. Therefore, it is recommended that any geotextile that has sufficient strength may be used for undercutting.

Bedding

In shorefront protection, where bedding is used extensively, large rocks are required to withstand wave forces. The larger the rocks, the larger the gaps through which native materials can be lost, thereby reducing or eliminating the protection that the rock affords against the attack of the water.

The geotextile is used to replace the layer(s) of granular materials under the stone filling that is required by conventional filter criteria. The geotextile is intended to prevent the loss of native materials from erosion due to moving water. The geotextile must also allow groundwater in the native soil to drain freely in order to prevent a blow-out due to hydrostatic pressures. A typical bedding installation is shown in Figure 5.

The geotextile must have sufficient permeability, adequate strength to withstand the placement of rock

fill materials, and satisfactory soil retention capabilities, especially for granular materials.

Geotextiles for the bedding application are used almost exclusively under stone in rivers, streams, lakes, and canals. Therefore, the conditions under which the geotextile is being used are less severe than those previously mentioned. To date only woven fabrics are allowed for this application because of the satisfactory performance exhibited by woven geotextiles and because of the lack of knowledge on the performance of nonwoven geotextiles.

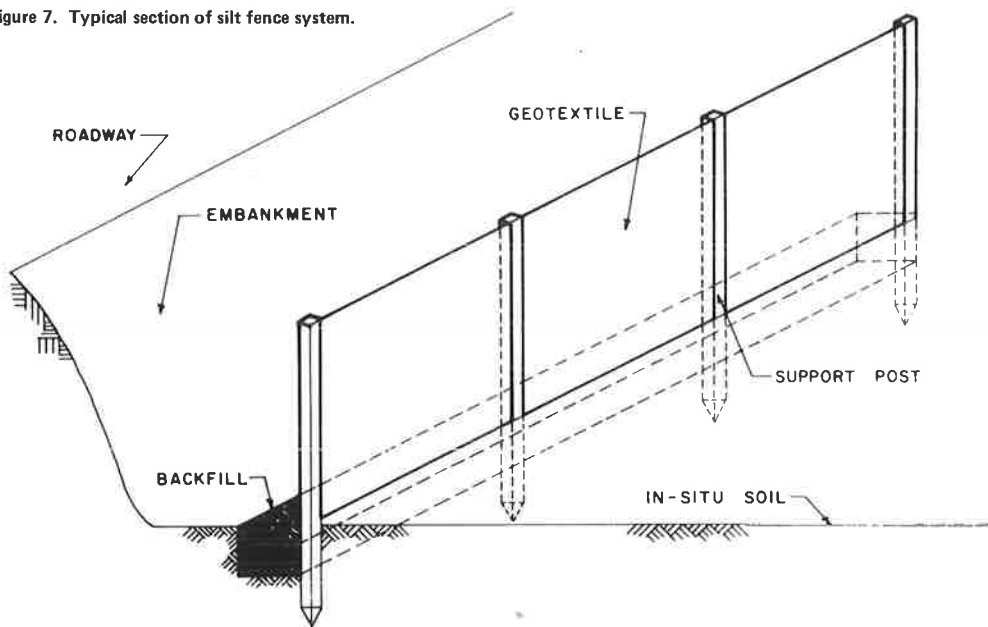
Slope Protection

The geotextile is used as a separator and filter under stone slope protection on highway cut sections. It is intended that the geotextile allow the free drainage of groundwater while holding the in situ fine soil in place. This maintains a stable base on which the stone slope protection can be placed. A typical slope protection installation is shown in Figure 6.

The problem of surface sloughing on a slope is common when the native soil is either wet silts or fine sands. As the water emerges to the exposed face and flows down the slope, it can carry soil particles with it. This will result in a delta soil deposit at the ditch line, with a resulting depression on the slope. Therefore, any soil passing through the geotextile is undesirable.

This problem was initially thought to be due to drainage, and that those geotextiles from the under-drain category could be used. Based on this premise, on one project the geotextile was placed on the high cut slope. A small bulldozer was used to place the 2-ft-thick slope protection blanket. Part way up the slope the entire mass--fabric and stone--failed by sliding into the ditch. It was concluded from this experience that the lack of frictional resistance between the geotextile and the native soil was the cause of the overall failure. It was always apparent that some geotextiles were smoother than others, but it appeared that it would be insignificant to this application.

Figure 7. Typical section of silt fence system.



Consequently, a separate category was established where only needle-punched geotextiles are used for slope protection. These geotextiles must have satisfactory filtration and permeability characteristics and offer satisfactory frictional resistance.

Silt Fencing

The geotextile is used as a barrier to prevent land or water pollution adjacent to a construction site. In NYSDOT contracts, the contractor is responsible for controlling the pollution and contamination of areas adjacent to the construction site. That means, generally, that the contractor is responsible for controlling the runoff waters to minimize erosion of the exposed native materials. This problem has been reasonably met by hay bale check dams and early seeding of slopes.

With the establishment of a silt fence category on the approved list, the contractor is provided another alternative by which to control pollution and contamination. A typical silt fence application is shown in Figure 7.

The contractor must consider three factors when using geotextiles for silt fencing: the flow rate and retention capabilities, the strength, and the resistance to ultraviolet degradation.

LABORATORY TESTING OF GEOTEXTILES

The establishment of the approved list of geotextiles was based on field experience and other information available at that time. As is apparent from the previous discussion, there were certain characteristics common to all five categories that needed to be investigated:

1. Permeability (flow capacity)--(a) geotextile permittivity, and (b) soil and geotextile permeability relation;
2. Soil-retention capabilities--(a) size of openings in geotextiles, and (b) retention in flowing water;
3. Strength characteristics--(a) installation strength, and (b) structural strength; and
4. Geotextile deterioration.

Therefore, laboratory testing was developed to evaluate or model these factors.

Permeability (Flow Capacity)

Geotextile Permittivity

The presence of water and its removal is always a concern in geotechnical design. Therefore, it was only natural to pose the question of how much water could flow through a geotextile. Several different methods of permeability testing were tried. All methods produced erratic results, due mostly to water turbulence and the high air content of the water. After some evaluation and modification, a downward flow device was designed and fabricated that eliminated the turbulent flow previously experienced. It was also found that the use of water de-aired to less than 6 parts per million (ppm) of dissolved oxygen was necessary. As a result of these modifications, more consistent and reproducible results were obtained, which were verified by subsequent testing (6).

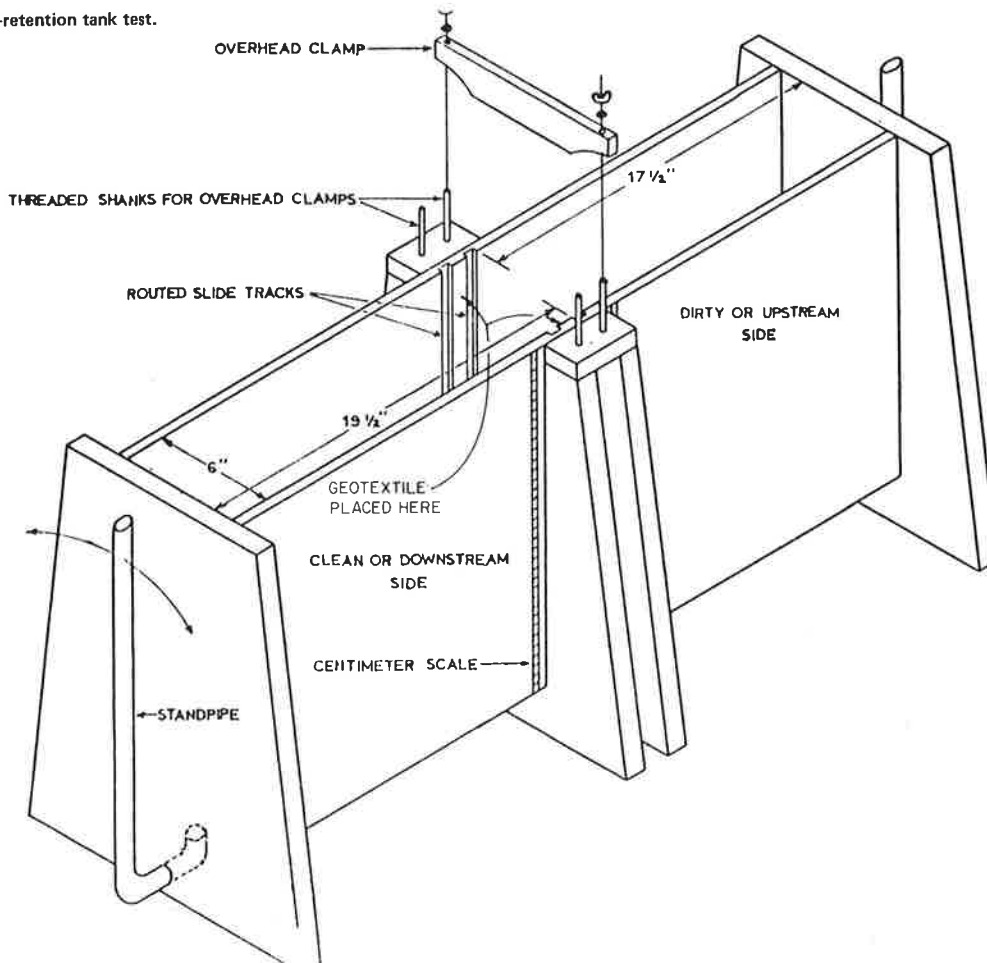
It was also recognized that the use of the value of coefficient of permeability for geotextiles might be misleading due to the varying thicknesses available on the market. It was decided by the ASTM geotextile group to normalize this value, which would give a volumetric flow rate per unit area per unit of head. This term has been defined as the permittivity of a geotextile.

The test provides a means of comparing one geotextile to another. However, it may not necessarily be indicative of its field performance.

Soil and Geotextile Permeability Relation

Once consistent and reproducible results from the permeability tests were obtained, the next logical step was to see what the effects would be on geotextile permeability when soil was placed in contact with it. Several different combinations of geotextiles and soils were tested and compared with the individual geotextile and soil permeabilities. In all cases, it was found that the permeability of the soil, even a coarse sand, controlled the system.

Figure 8. Soil-retention tank test.



Soil-Retention Capabilities

Size of Openings in Geotextiles

The most common method for determining soil particle sizes in soil mechanics is by sieving. It was logical, therefore, to consider this type of test for geotextiles, especially wovens, due to the discrete openings that result from the manufacturing process. The Soil Mechanics Bureau, in conjunction with ASTM, has been investigating the usefulness and appropriateness of the equivalent opening size (EOS) sieving test to determine the maximum opening size in geotextiles. The test consists of shaking various sizes of glass beads through a geotextile. Variables such as shaking time, the order in which glass beads are used (large to small or small to large), the elimination of errors caused by static electricity, and the effects of presoaking the sample before testing have been investigated. In general, the test is appropriate for wovens and thin sheet nonwoven geotextiles. With thicker nonwoven geotextiles, the path of travel for a glass bead is so tortuous that it may become entrapped rather than pass through the geotextile, thus giving a questionable value for the test.

Retention in Flowing Water

A test to study the soil retention capabilities of the geotextiles proposed for use was developed (7). The test apparatus is shown in Figure 8. In one chamber, designated as the upstream side, a predetermined mixture of water and soil was placed. In

the other chamber, designated as the downstream side, clean water was placed. Flow was allowed to take place from the upstream side through the geotextile to the downstream side of the tank, with the outflow being collected. By using hydrometers, the amount of soil that passed through the geotextile was estimated.

Discussion of Permeability and Soil-Retention Characteristics

It is important to emphasize that, in order to correctly evaluate the permeability characteristics of a geotextile, each one of the above properties must be collectively examined to have any meaning as to the flow capacity of a geotextile. As an example, an impermeable membrane with a hole punched in its center may have the same flow capacity characteristics as a geotextile. However, the soil-retention capabilities of the two are quite different. Also, the lower the permittivity of the geotextile, the higher the soil-retention capabilities, and vice versa. Thus it is necessary to specify maximum opening size as well as flow rate to properly select a geotextile for a specific use. It has to be realized that there is a constant trade-off of these properties in any design. It is up to the designer or engineer to determine which characteristic is most important to the design.

Strength Characteristics

Installation Strength

To be installed, all geotextiles must be manipulated

by equipment and people. This manipulation can cause rips and tears that will disrupt the continuity of the geotextile. As a result, a geotextile may not perform as intended. Therefore, it is important that geotextiles have sufficient strength to withstand the installation process. For most of the geotextiles on the market, the ASTM D1682 grab tensile test provides an adequate indication of the installation strength.

Structural Strength

Grab Tensile

Initially, results of ASTM D1682 were used to determine the tensile strength of geotextiles. This test was indicative of the quick, sharp loading that a general textile might undergo. However, it was not indicative of the long-term uniform loading over a wide area that a geotextile might undergo. The test was useful for comparing relative strengths for installation purposes, but it was not potentially useful for design purposes.

Wide Width Tensile Strength

The standard grab tensile test method did not appear suitable for the engineering needs of NYSDOT. Therefore various other methods to measure tensile strength are being investigated. Initially, 1-in.- and 2-in.-wide x 6-in. gauge-length tensile tests were run. Due to the low aspect (width/length) ratio, some of the geotextile specimens underwent severe "neck down." As a result, high elongation values were obtained that gave erroneous strength values.

Further investigation led to the current test method based on an 8-in.-wide by 4-in. gauge-length sample. Because of the higher aspect ratio of the samples tested, this test appears to give the most realistic values for design purposes. The only major problem is the slippage between the jaws experienced with the stronger geotextiles, which will increase the variability of the results obtained. This problem has been minimized by placing four or five pins across the width of the jaws. (Note that details of this new test are from a 1981 unpublished draft report, Wide Width Tensile Strength of Geotextiles, from the Soil Mechanics Bureau, NYSDOT.)

Long-Term Strength (Creep Strength)

The elongation characteristics of a geotextile are important when designing structures such as geotextile-reinforced embankments and retaining walls where the long-term stresses that would be applied to the geotextile may be high. Tests consisted of running a peak strength test on a 2-in.-wide x 4-in. gauge-length specimen. Once this peak strength was determined, the same size specimens were placed in a static loading frame, and loads corresponding to 25, 50, and 75 percent of the peak strength were applied. Deflection data were recorded, and a deflection versus time curve was plotted for either failure or 100 hr. The results obtained are used to determine a geotextile's relative tendency for creep. The results to date have not given numbers that can be used in design.

Geotextile Deterioration

Most plastic polymers used in producing geotextiles are not affected by mild acids, bases, or chemicals encountered in normal highway construction. However, as with most plastics, exposure to sunlight will have a significant effect on the life expect-

tancy of a geotextile. Therefore, the ultraviolet stability characteristics of geotextiles have been investigated. It is generally accepted that geotextiles degraded in a weatherometer do not provide a direct time correlation to what actually takes place in the field. However, plotting a degradation versus time curve for both weatherometer and field exposure results from an ASTM round-robin test program showed that geotextiles degrade in the same pattern for both cases. Therefore, the relative tendency of a geotextile to deteriorate from ultraviolet exposure may be determined from the weatherometer test.

SPECIAL PROJECTS

Although laboratory testing provides NYSDOT with a means of relatively evaluating and accepting geotextiles for general use, it also provides values that may be applied in critical design problems. In such cases, the design criteria for geotextile performance must be carefully evaluated. Two such projects were the design of a geotextile reinforced wall and a pollution containment system.

Geotextile Reinforced Wall

On NY-71 and NY-22 in Columbia County, New York, the existing roadway embankment had been steepened and, as a result, shallow shear failures were occurring. Criteria for treatment of the site were stabilization of the failure areas, low future maintenance, additional shoulder width, and safe traffic control during construction. A geotextile reinforced-earth wall was recommended as an economical alternative to conventional tied-back sheet-pile walls.

Basic geotextile reinforced-earth-wall design consists of alternating layers of crushed stone and horizontal layers of geotextile that are placed a specified distance behind a theoretical failure plane (8). The geotextile provides reinforcement for the wall. Factors such as wall height, geotextile strength, and the friction angle of the crushed-stone fill control the thickness of the crushed-stone layers. Also, as this was intended to be a permanent structure, it was necessary to evaluate the long-term creep behavior of the geotextile used.

The wall height of this project was approximately 17 ft and the geotextile tensile strength was 75 lb/in. Crushed stone was used for its high permeability and frictional characteristics. This resulted in the wall being constructed in 6- and 9-in. lifts, with each lift being formed by the fabric overlapping the face of the wall that retains the crushed-stone fill. On completion, the wall face was shotcreted to prevent possible vandalism and exposure to the elements (see Figure 9).

Instrumentation installed at the site has indicated that the wall was performing satisfactorily.

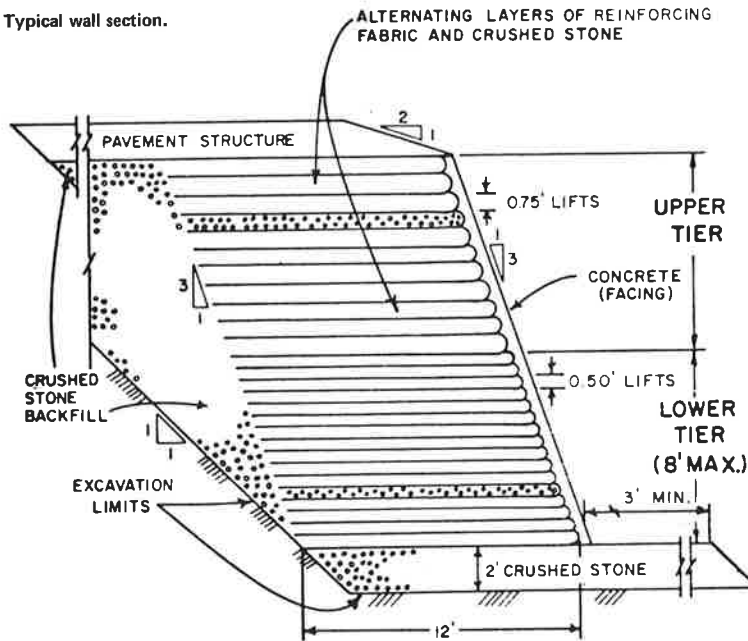
This installation emphasizes the following significant points:

1. Laboratory test values for geotextiles can be used in the design of reinforcement for an earth wall by using conventional analyses, and
2. The design and construction of this geotextile reinforced-earth wall was technically feasible, operationally practical, and cost effective.

Pollution Containment System

The design of the proposed old Westside Highway replacement on Manhattan Island, New York City, calls for extensive construction in the Hudson River. In order for this construction to take place, strict environmental controls must be main-

Figure 9. Typical wall section.



tained. Of primary concern is the control of pollution of the Hudson River.

To control the pollution during construction, it was initially proposed that a nonpermeable barrier (i.e., sheet-pile wall) be used. This proposal proved to be too costly. Further consideration led to the proposal for a permeable curtain system that used geotextiles that were to be placed around the site. To study the feasibility of the system, a prototype curtain was designed and constructed.

The design required knowledge of the soil-retention capability and the long-term strength characteristics of the geotextile because it would be exposed to forces caused by tidal action. The tests previously described were used to quantitatively evaluate the various types of geotextiles available. Based on the results of these tests, a more exact specification was developed than previously described for silt fencing.

The prototype curtain was installed in fall 1981 and remained in place until spring 1982. Monitoring and inspection over this period indicated that the curtain performed satisfactorily.

DESIGN GUIDELINES

The experiences previously described have shown that, to achieve an economical design, there is a constant trade-off of desirable characteristics to achieve the best solution for a particular application. The characteristics of flow capacity, soil retention, strength, ultraviolet stability, and friction have to be constantly balanced by the design engineer. These characteristics are rated in the order of significance in Table 1, with 1 being the most significant and 10 being the least significant.

Based on the concepts of Table 1, the minimum requirements listed in Table 2 were established for placement of geotextiles on NYSDOT's approved list for 1982.

It is emphasized that the values listed in Table 2 are for nonsevere or general applications, as previously described. Conditions that require specific design considerations are

1. Underdrain, where the soil is a fine to

coarse sand (sieve size = No. 10 to No. 100) and there is a constant source of water and potential high flow;

2. Undercut (subgrade stabilization), where a soil has low bearing capacity; and

3. Bedding, where the soil is a coarse sand (sieve size = No. 10 to No. 40) along an ocean front that is subjected to constant erosion due to wave action.

These severe conditions generally occur in approximately 10 percent of NYSDOT's geotextile applications.

SUMMARY

In summary, the establishment of the approved list and general specifications for installation allowed the successful use of geotextiles within New York State.

The Soil Mechanics Bureau has made the following recommendations, which are currently incorporated in the approved list:

1. Only nonwoven geotextiles should be used in drainage applications because they exhibit the best soil-retention characteristics.

2. Soil stabilization requires a geotextile of reasonable strength so as to survive the installation process.

3. Only woven geotextiles should be used for bedding applications.

4. Geotextiles used for slope protection should be needle punched, which will provide frictional resistance between the fabric and native soil.

5. Tests recommended or that are being developed by ASTM should be used.

6. Consideration should be given to the characteristics needed for design, as shown in Table 1. From this, select minimum values for design as shown in Table 2, which have been developed for nonsevere or general applications.

7. For critical or severe applications, special design procedures are required.

GEOTEXTILES IN THE FUTURE

New York has had relative success with the use of

Table 1. Ratings of applications.

Application	Rating by Characteristic ^a				
	Permittivity	Soil Retention	Strength	Ultraviolet Stability	Friction
Underdrain	2	1	5-6	10	10
Undercut	2	3	1	10	10
Bedding	1	3	1	7-8	9
Slope protection	3	2	5-6	7-8	1
Silt fencing	2	1	4	5-6	10

^aThe rating scale is from 1-10, with 1 being the most significant and 10 being the least significant.

Table 2. Minimum requirements for applications.

Application	Permittivity ^d (sec ⁻¹)	Soil Retention	Minimal Grab Tensile (lb)	Minimum Wide Width Tensile Strength (lb/in.)
Underdrain	0.51	Nonwoven	75	35
Undercut	0.02	Nonwoven and low permittivity	75	35
Bedding	0.41	Woven with EOS between No. 70 and No. 100 sieve sizes	100	60
Slope protection ^b	0.51	Needle punched	80	35
Silt fencing	—	—	—	—

^aTo convert to gallons per minute per square foot of area per foot of head, multiply by 454.

^bUsed in high friction situations.

geotextiles. However, there is much need for improvement (9). As manufacturers develop other materials and processes to produce geotextiles, it will become increasingly important and necessary to be able to objectively evaluate geotextiles for potential end use and to be able to restrict the use of products with questionable properties.

More emphasis should be placed on evaluating field performance for the desired end use. This can be accomplished by field instrumentation development for geotextiles and modeling laboratory tests that will simulate field conditions. This type of work will enable a better understanding of how geotextiles will perform in the field and, it is hoped, will upgrade the empirical rules for design.

Yet all of this design work will be wasted if proper construction procedures are not followed. In addition, any problems involved with construction will never be overcome unless monitored in the field. Other questions that need to be asked are as follows: What type of fabric was used? What was the soil type? What was the condition of the site before construction began? What construction and monitoring procedures were used for the job? These are all important questions that should be addressed in the documentation of a project. It is only through documentation that others may share and learn new ideas that can help further develop the appropriate use of geotextiles. This documentation, along with laboratory testing and field instrumentation, should be an all-inclusive process, because it is vital to the understanding of geotextile behavior.

REFERENCES

1. T.J. Novak. 1974 Construction Experience with Item 900 or Item 209. Soil Mechanics Bureau,

New York State Department of Transportation, Albany, Jan. 1975.

2. T.A. Carlo. Embankment Stabilization Utilizing a Nonwoven Filter Cloth at Rte. 55, 55A, Napanoch-Montela, Ulster County, New York. Soil Mechanics Bureau, New York State Department of Transportation, Albany, Dec. 1977.
3. V.C. McGuffey. Filter Fabrics for Highway Construction. Soil Mechanics Bureau, New York State Department of Transportation, Albany, Dec. 23, 1976.
4. A.D. Forshey. Use of Filter Cloths for Subsurface Drainage Systems for Highways. Bureau of Materials Testing and Research, Pennsylvania Department of Transportation, Harrisburg, Title 76-16, Aug. 18, 1976.
5. A.D. Forshey. Use of Filter Cloths for Subsurface Drainage for Highways. Highway Focus, Vol. 9, No. 1, May 1977, pp. 82-87.
6. Standard Method for Testing the Water Permeability of Geotextiles: Permittivity Method. Soil Mechanics Bureau, New York State Department of Transportation, Albany, June 1981.
7. Geotextile Soil-Retention Test Procedure. Soil Mechanics Bureau, New York State Department of Transportation, Albany, Feb. 1981.
8. G.E. Douglas. Design and Construction of Fabric Reinforced Retaining Walls by New York State. Soil Mechanics Bureau, New York State Department of Transportation, Albany, 1981.
9. T.A. Haliburton, J.D. Lawmaster, and V.C. McGuffey. Use of Engineering Fabrics in Transportation-Related Applications, Final Draft. Haliburton Associates, Stillwater, OK, Oct. 1981.

Publication of this paper sponsored by Task Force on Engineering Fabrics.

Evaluation of Two Geotextile Installations in Excess of a Decade Old

BARRY R. CHRISTOPHER

Many erosion-protection installations for roadway embankments were designed and constructed by using geotextiles during the 1960s. Two such installations constructed in 1969 were studied to evaluate the long-term field performance of the facilities and the geotextile material. These projects were the 79th Street Causeway in Miami Beach, Florida, and the Bahia Honda Bridge in Bahia Honda Key, Florida. The 79th Street Causeway was constructed with a woven geotextile as a filter in a rip-rap revetment-type seawall to protect one of the bridge abutments and a segment of the causeway. The geotextile design was used in place of a conventional granular filter design to prevent erosion of the subgrade soils through the rip-rap. The protected section was designed for 3-ft waves and a 3-ft tidal variation. The Bahia Honda Bridge project was constructed with a woven geotextile as a subgrade-protection filter beneath sand-cement rip-rap-constructed bridge abutments, drains, and seawalls at both ends of the bridge. In this system, a geotextile was used to act as a filter between the rip-rap and underlying soil subgrade to prevent loss of soil due to weathering or wave action through cracks and holes in the rip-rap. The abutments and drains at the Bahia Honda Bridge were exposed to weathering conditions, and the seawall was designed to resist wave action and tidal variations. The performance evaluation of these installations consisted of a review of the design, visual observations, and testing of representative rip-rap, fabric, and underlying soil samples. In the laboratory study, the condition of the excavated fabrics was compared with new fabric characteristics. The study included strength and filtration evaluation of the fabric and gradation analysis of the surrounding soils. Field observations of the performance of the structures, evaluation procedures, and the results of laboratory tests are presented. The effects of construction procedures on long-term performance are also reviewed.

One of the most valuable methods of developing design criteria and predictive capabilities is to study the design and performance of existing installations. Field evaluation studies performed in 1979 at two installations constructed in 1969, in which geotextiles were used in erosion-protection systems for roadway embankments, are presented in this paper. The first project reviewed is the 79th Street Causeway in Miami Beach, Florida. A monofilament woven polypropylene geotextile was used in this project as a reverse filter in a stone rip-rap revetment-type seawall to protect one of the bridge abutments and a section of the causeway. The second project is the Bahia Honda Bridge project in which a woven polypropylene geotextile was used as a protection filter beneath sand-cement rip-rap-constructed bridge abutments, drains, and seawalls.

The sites were evaluated by STS Consultants, Ltd. (formerly Soil Testing Services) under contract to Carthage Mills Erosion Control Company, Inc., the manufacturer of the geotextile (Poly-Filter X) that was used in both projects. The studies were performed to evaluate the in-place geotextiles produced by Carthage Mills. The two projects were selected on the basis of their age (10 years or older), type of application, availability of background design information, and performance requirements.

It should be noted that, at the time these projects were constructed, there was little or no design information concerning geotextiles. Also, because only a few geotextiles were in general use in the United States at that time (all of which were monofilament wovens), selection was generally based on intuitive judgment.

79TH STREET CAUSEWAY

The 79th Street Causeway (also referred to as the North Bay Causeway) connects Miami to Miami Beach by traversing Biscayne Bay. In 1969 a bridge was con-

structed over the intracoastal waterway at the westernmost part of the causeway by the Florida Department of Transportation (DOT) to replace the causeway in that section. The bridge extends from Miami to the first island along the 79th Street Causeway, as shown in Figure 1. For construction east of the bridge, a limestone rip-rap placed over a geotextile was used as an erosion-control system to protect the north portion of the bridge abutment and the north part of the causeway.

A geotextile was used as a reverse filter beneath the limestone rip-rap for the design of the seawall. The actual proposed design of the seawall is shown in Figure 2. The original design drawings did not include details for fabric placement or the head or toe of the slope. At that time proper fabric anchorage was not well understood. The actual design was found to be somewhat different than the proposed design, as will be subsequently discussed.

Revetments constructed by using rubble on the upslope of seawalls is a common procedure. The nature of the rubble gives a rough surface, which helps break up on-rushing waves and dissipate the force and energy in the wave. The need for a filter layer beneath the rubble is important in seawall construction because the voids between the pieces of rubble are large, and constant wave action will draw the foundation materials through the rubble, thereby causing the rubble to settle and eventually collapse.

The protected section was designed for 3-ft wave and tidal variation. Several major storms have occurred in the Miami area since construction, periodically exposing the protection system to conditions more severe than design conditions. Florida DOT records indicated that no maintenance had been performed on the abutment section since construction was completed.

Field Study

A field study of the site was performed in October 1979. A photographic and visual survey of the site indicated that the seawall was functioning as designed, as no apparent erosion problems were observed. Several visually different sections along the length of the seawall were observed. From the north end of the bridge abutment to an area just beyond the northwestern corner of the site, several inches of geotextile material protruded from beneath the rip-rap in the uppermost part of the slope. The surface rip-rap in that section was 2 to 3 ft in diameter. The seawall appeared to be constructed as proposed.

To the east of the northwestern corner of the site the geotextile was visible at the surface through the seawall. The fabric was placed over the rip-rap with one boulder layer at the surface. Apparently a lack of knowledge of protecting these materials from ultraviolet rays from the sun and improper construction control were responsible for this condition. However, a majority of the fabric was intact, even though sections of the material have been exposed to the sun and wave action possibly throughout the 10-year life of the project.

The next part of the seawall, which was east of where the fabric was exposed, appeared to be con-

Figure 1. Location diagram for 79th Street Causeway.

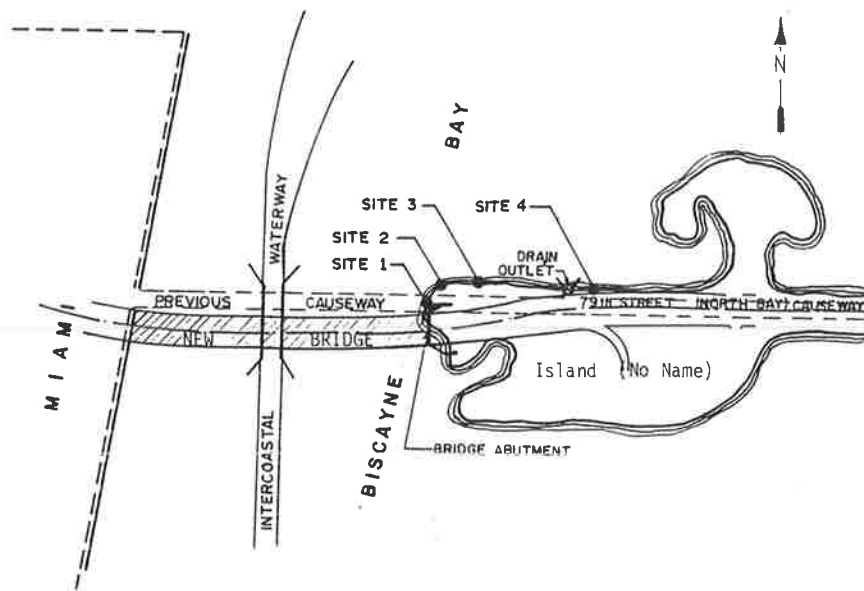
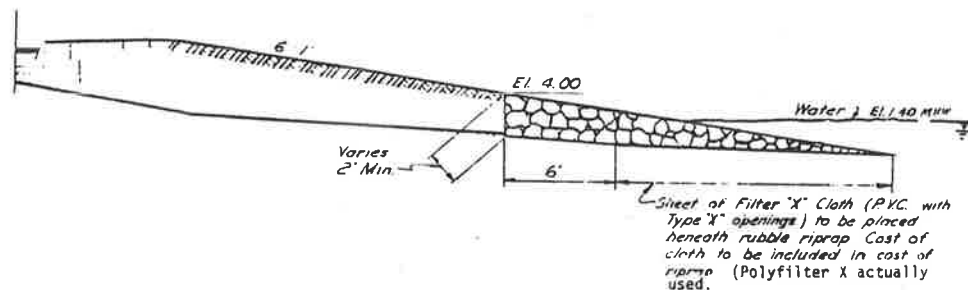


Figure 2. Proposed design of seawall.



structed as designed and was similar to the first section. Fabric was only observed at the top of the seawall where the rip-rap ended. This section continued eastward several hundred feet to a drainage outlet in the seawall.

To the east of the drainage outlet the surface rip-rap was smaller than the surface rip-rap observed in the western portion of the site. The rip-rap was approximately 1 ft in mean diameter. Subsequent evaluation of that section indicated that no fabric had been used.

The morning and afternoon high tides covered most of the seawall, which had approximately 6 ft of the face of the upper slope exposed. The morning low tide was approximately 3 ft lower than the high tide and exposed approximately 15 ft of the slope. The afternoon low tide was about 1.0 to 1.5 ft lower than high tide and exposed approximately 9 ft of the slope. Wave action during the visit was generally on the order of 6 in. to 1 ft in height, with up to 2-ft waves observed when boat traffic was present. This appears to coincide with the normal conditions for which the structure was designed.

Other areas of the causeway were observed where erosion-control systems were not in use. At the southern part of the east bridge abutment, opposite the rip-rap fabric-protected section, erosion problems were evident. Concrete that had little aggregate had been poured against the abutment and over the exposed soil, apparently to check erosion. However large voids (up to 1 ft in diameter) were present in the concrete mat and beneath the mat where the soil and concrete had eroded. Eroded areas south of the causeway on the island shore were also

observed. It appeared that rip-rap with no filter layer was placed in these areas following the erosion to check the erosion process. The areas appeared to still be washing out, which indicated that the minimal amount of erosion control was not successful. It was reported by Florida DOT that maintenance had been required for several other unprotected sections of the causeway during the past 10 years as a result of erosion damage during storms.

Excavation of Soil-Fabric System

Four sites were selected for further examination of the soil-geotextile system, as indicated in Figure 1. Site 1 was located approximately 3 ft north of the north corner of the causeway bridge abutment. The north corner of the concrete abutment and the location of site 1 are shown in Figures 3 and 4. This area was selected due to the relatively smaller size of rip-rap covering the area and the location in reference to protection of the bridge abutment. Also, due to a relatively flat slope in this section, the majority of the excavation could be performed above the water level at low tide.

Site 2 was located at the northwest corner of the causeway approximately 55 ft north and 18 ft east of the north corner of the bridge abutment. This section appeared to be exposed to more direct wave action than the other sections of the causeway.

A third site (site 3) was selected in the area where the fabric was improperly placed and exposed to the sun. This site was located approximately 70 ft north and 110 ft east of the bridge abutment.

The fourth site was located in the eastern sec-

Figure 3. Limestone rip-rap covering fabric at site 1.



Figure 4. Excavated section at bridge abutment corner at site 1.



tion of the causeway where it appeared that no geotextile had been placed. Subsequent excavation of site 4 indicated that geotextiles were not present and, therefore, this site will not be discussed further.

At site 1 an area approximately 3x12 ft was excavated with the limestone rip-rap and other materials removed by hand down to the fabric. Figures 3 and 4 show the area excavated. The surface rip-rap consisted of fossiliferous limestone boulders that had a mean diameter of 12 to 18 in. The surface rip-rap used throughout the site was highly weathered limestone, which was rough and had many sharp edges. (As an example of the abrasiveness of the rip-rap, the subsequent excavation of the rip-rap for this project resulted in the destruction of several pairs of work gloves due to abrasion.)

Beneath the large surface rip-rap a 1-ft layer of 6- to 12-in.-diameter rip-rap was encountered. Beneath the total depth of rip-rap a 3-in. layer of coarse sand and gravel was underlain by approximately 0.25 to 0.50 in. of fine to medium sand. Note that the 3-in. cushion layer of sand and gravel was not shown in the proposed design (Figure 2). The sand was located directly on the surface of the geotextile and was probably the result of sand being washed down from the upper slope above the protec-

tion system or as a result of landward sediment transport (normal shore nourishment process). Samples of all materials over the fabric were collected. Thin-walled 2-in.-diameter Shelby tubes were driven into the fabric at several locations to obtain intact samples of the soil-fabric interface.

The exposed surface of the fabric was gently washed with water to remove the sand from the surface. The fabric appeared to be in excellent condition, and no large tears or punctures were observed. Small perforations and punctures were present, which probably resulted from the placement of the rip-rap during construction. On average, two to three 0.125- to 0.25-in.-diameter holes were noted for each square foot of material. Some smaller holes were also observed. Little abrasion from sliding of the rip-rap was apparent, even though the relatively light wave action during the visit was sufficient to move rip-rap as large as 6 in. in diameter.

The geotextile was cut and carefully peeled off the underlying soils. Light was readily seen through a section of the fabric. Some particle retention was noted in the fabric; however, water was observed to readily flow through the fabric. Samples of the fabric were returned to the STS laboratory for testing.

Directly beneath the exposed section, very fine sand to silt-sized particles were noted, with grain size of the sand increasing with depth. Fine sand with less silt was observed approximately 0.5 to 1.0 in. beneath the fabric. At the lower part of the slope, gravel-sized material mixed with sand was found directly beneath the fabric. Samples of the soils encountered above and below the fabric were returned to the laboratory for further examination and testing.

New fabric was placed over the excavated area with an overlap in excess of 1 ft over the old fabric. Then gravel and rip-rap were replaced in the proper order.

The rip-rap from site 2 was then removed. An area of approximately 3x3 ft was excavated. The rip-rap consisted of larger boulders at the surface that had a mean fragment diameter of 1 to 3 ft. At site 2, 6- to 12-in.-diameter rip-rap was also encountered beneath the surface rip-rap. Gravel to medium-sized (2- to 6-in.) rip-rap was encountered beneath the surface rip-rap and directly over the geotextile. The geotextile itself was then encountered. The fabric was located several inches below the water level at low tide.

A 2-ft² section of the geotextile was cut and removed. As at site 1, no abrasion of the material was apparent. Only one small tear was noted. The same magnitude and size of small perforations that were encountered at site 1 were present. Some fines were retained by the fabric, and it was observed that gentle washing would remove some of these materials. Fine sand and silt-sized particles mixed with gravel and cobbles were encountered directly beneath the fabric. Samples of these materials were collected, and then new fabric was placed over the entire area and the rip-rap was replaced.

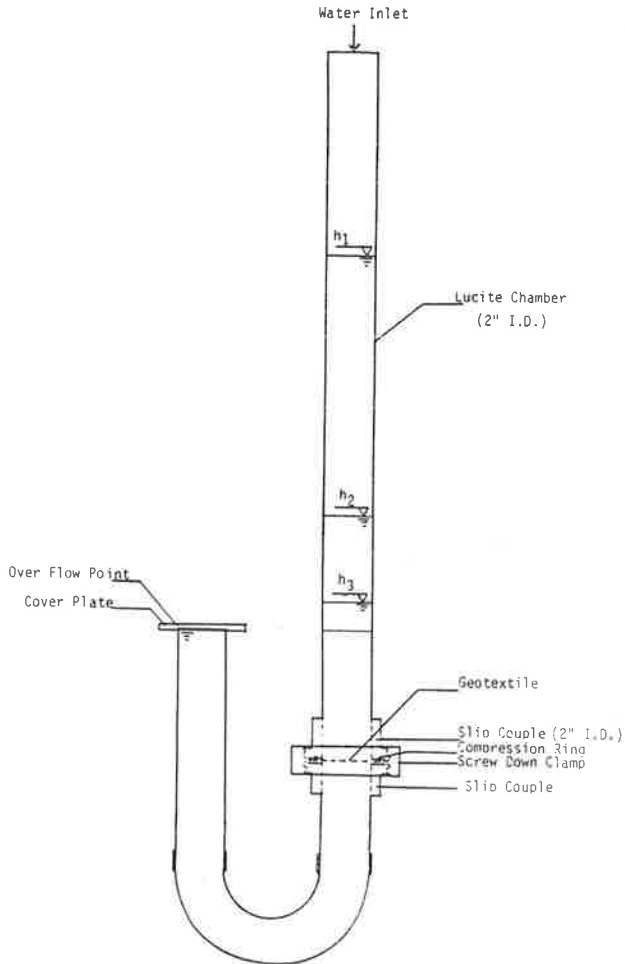
The excavation at site 3 consisted of removing two boulders approximately 0.5 and 2.0 ft in diameter. The geotextile was marked to note the location of the boulders and the location of areas exposed to the sun. A 1.5-ft² section of the fabric was removed. Cobbles and up to 6-in.-diameter rip-rap were noted beneath the fabric. No fines were present. Observations of the fabric after removal indicated several tears and punctures. However, considering the exposed condition and the one-boulder cover (which moved visibly under wave action), the material was in satisfactory condition. The fabric was replaced with new fabric and covered

with the removed boulders. All soil and fabric samples were returned to the STS laboratory for further examination and testing.

Laboratory Testing Program

A series of laboratory tests were performed to determine the physical properties of the exhumed geotextile samples. These tests provided results that could then be compared with the manufacturer's specifications for new samples of the fabric. In this way the performance of the fabric under field conditions could be evaluated.

Figure 5. STS geotextile permeameter.



Tests to determine strength and permeability, and tests to evaluate the particle retention of the geotextile, were performed. In addition, grain-size analyses were performed on soil samples taken from above and below the fabric. The tests followed the procedures recommended by the U.S. Army Corps of Engineers and ASTM (1). Tests were also performed on samples of new geotextiles by using the same equipment and procedures to obtain comparison values.

Two strength tests were performed following the procedures detailed in ASTM D-1682 (Breaking Load and Elongation of Textile Fabrics); these tests were used in the initial evaluation of fabric strength at the time of construction. These test methods are currently being evaluated by ASTM as to their reliability in determining the strength of geotextiles.

Permeability of the geotextile specimens was determined by using the STS U-tube geotextile permeameter. A falling-head technique, from a head of 10 cm to a head of 3.7 cm, was used. This equipment is shown in Figure 5.

The particle retention of the fabric was evaluated by using the Corps of Engineers Waterways Experiment Station AD-745-085 procedure for determining the open area of a geotextile. The number of openings that contained particles was compared to the total number of openings in the fabric. Several samples were flushed with water continuously for several hours at a head of 3 ft to simulate water-flow action on the fabric. The percent open area was again determined to assess how many of the openings were permanently closed.

Grain-size analyses were performed on soil samples taken above and below the fabric in order to evaluate the segregating functions of the fabric. These tests were performed in accordance with ASTM D-422 (Particle-Size Analysis of Soils) and used both sieve and hydrometer methods.

Test Results

In general, the geotextile maintained a high degree of strength. Variations in strength results observed for each site are given in Table 1. The data in the table also present comparisons of field data with tests performed on new fabric at the time of the study. The strength test results on new fabrics were in accordance with the manufacturer's published values. Laboratory strength evaluation indicated a strength reduction of properly installed fabric (sites 1 and 2) ranging from 5 to 40 percent from that of new fabric. Elongation of the 10-year-old material at failure was no more than 5 percent greater than elongation of new fabric at failure. Tests on samples of the geotextile material that were partly exposed to sunlight at site 3 indicated a strength loss of approximately 40 to 50 percent,

Table 1. Summary of grab strength test results.

Specimen	Weaker			Stronger		
	Principal Direction (kg)	Apparent Elongation at Failure (%)	Percentage of Original Strength (% of 100 kg)	Principal Direction (kg)	Apparent Elongation at Failure (%)	Percentage of Original Strength (% of 170 kg)
Site 1						
Section 1	89	37	89	130	38	76
Section 2	96	40	96	144	38	84
Section 3	100	40	100	136	39	80
Section 4	96	37	96	161	38	95
Site 2	67	38	67	104	25	61
Site 3	51	25	51	111	47	65
New 1 ^a	97	50	—	171	30	—
New 2 ^a	101	43	—	163	35	—

^aTwo lots tested.

Figure 6. Strength of fabric versus position on slope at site 1.

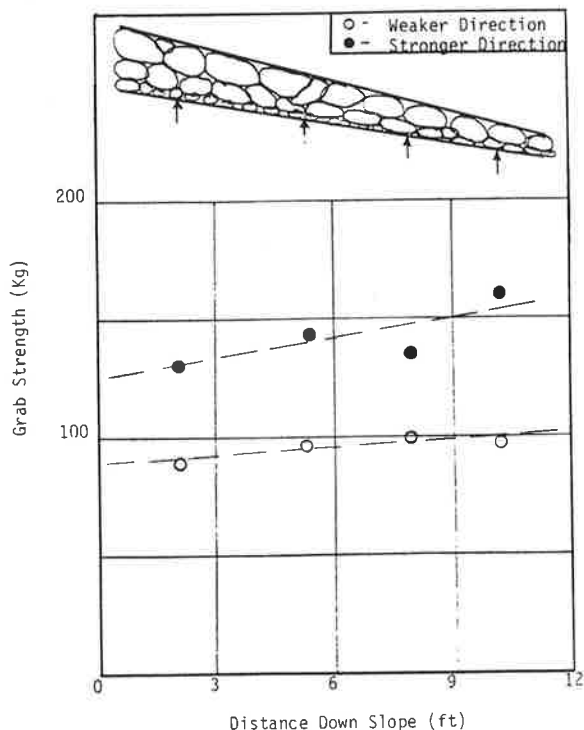


Table 2. Filtration test results.

Specimen	Permeability (cm/sec)	Percent Open Area	Percentage of Openings Containing Particles	Percent Open Area Completely Closed
Site 1				
Section 1	2.6×10^{-2}	5.5	29	6
Section 2	2.2×10^{-2}	5.7	20; 19.5 ^a	4
Section 3	1.8×10^{-2}	5.4	29	6
Section 4	1.9×10^{-2}	4.8	44; 44 ^a	9
Site 2	2.3×10^{-2}	5.0	40 to 48	8 to 10
		5.1	35 to 42 ^b	
New	$3 \text{ to } 4 \times 10^{-2}$	6		

^aWashed with 3-ft head of water.

which was probably partly due to ultraviolet exposure.

As indicated by the data in Table 1, the strength of the geotextile from site 2 was found to be about 30 percent less than the fabric from site 1. As previously mentioned, site 2 received more direct waves and had a steeper slope than site 1. Abrasion potential at site 2 was also increased due to the absence of the cushion layer of sand and gravel observed directly over the fabric at site 1. Either of these factors may have resulted in strength differences.

The data in Figure 6 indicate that strength variations at site 1 may exist due to the location of the test specimens at the site. These data are based on limited testing and may be influenced by nonuniformities in the test specimens (such as perforations). Product variation may also have contributed to the relatively small variations observed. Nevertheless, the grab strength appears to increase with location in the downslope direction. The relation appears to occur for both mutually perpendicular test directions. This general pattern indicates that the observed strength differences are due to tidal fluctuations, which result in differences in exposure to water, air, and temperature.

The fabric has been exposed to more than 7,000 saltwater tide cycles and various degrees of wetting and drying, depending on the location of the materials and the installation (top of slope versus bottom of slope). The fabric at the base of the rip-rap slope (section 4), which was probably under water during most of the 10-year history, had the greatest strength. The data in Figure 6 also show a difference in the change in strength with stronger and weaker principal directions. These differences may be due to the effects of pull from wave action and the direction of pull. Cyclic loading from waves may affect one direction more than the other.

The filtration studies consisted of both permeability and particle-retention evaluations of the fabric. The results of the permeability tests and corresponding particle retention for the same section of fabric are given in Table 2. There was a slight reduction in permeability of 4×10^{-2} cm/sec for new fabric and 2×10^{-2} cm/sec for the excavated fabric.

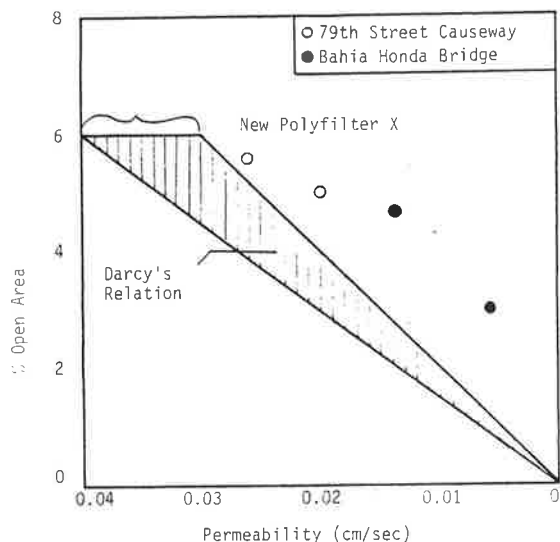
Figure 7 was developed from Darcy's relation among permeability, porosity, and seepage:

$$k = v_s n_e / i \tag{1}$$

where

- k = coefficient of permeability,
- v_s = seepage velocity,
- n_e = porosity = percent open area for woven fabrics, and
- i = gradient.

Figure 7. Relation between permeability and percent open area.



The data in Figure 7 indicate the theoretical decrease in permeability of the fabric with a decrease in the percent open area for a gradient of 1. Percent open area is defined as the area of the openings (times 100) divided by the total surface area of the unit of fabric; it is equivalent to the porosity of the soil. Note that the data in the figure are only applicable to the particular material tested; other fabrics may react in a different manner. Permeability values obtained from the field study are included on the graph. (Also included in this graph are the test values obtained from a similar fabric-exhuming project at Bahia Honda Key, which will be subsequently discussed.) Note that the decrease in permeability due to particle retention in the fabric generally follows the relation of

decrease in porosity for a soil filter. The test results do not fall within the theoretical curve, probably because actual tests were performed under a gradient much higher than 1 (10 to 3.7 cm of water over the thickness of the fabric), which probably resulted in turbulent flow.

The data on the laboratory particle-retention analysis given in Table 2 indicate that less than 40 percent of the openings in the fabric were partly closed with particles. The percent open area was reduced from approximately 5.8 to approximately 5.2 percent, which is within the range of error in determining percent open area. The net results were a decrease of less than 10 percent in the open area of the fabric.

Grain-size distribution curves for the soil from 0 to 0.25 in. below the fabric and soils several inches below the fabric for sites 1 and 2 are shown in Figures 8 and 9. The fabric retained medium to fine sand and silt-sized particles, with up to 20 percent passing a No. 200 mesh sieve. Up to 50 percent of the soil particles directly against the fabric were smaller than the fabric opening. This is in agreement with the work on filter media done by Calhoun (2) and Cedergren (3).

Summary

The project indicates excellent long-term stability of the monofilament woven geotextiles used in this type of rip-rap revetment for the soil and design conditions encountered. The geotextile retained a significant amount of strength after 10 years. No maintenance was required for this erosion-control structure in areas where geotextiles were used. Laboratory studies of the fabric indicated that the filtration characteristics have not been significantly reduced from the filtration capabilities of new fabric. Therefore, it can be concluded that the filtration characteristics of the fabric were functioning according to the design requirements.

BAHIA HONDA BRIDGE

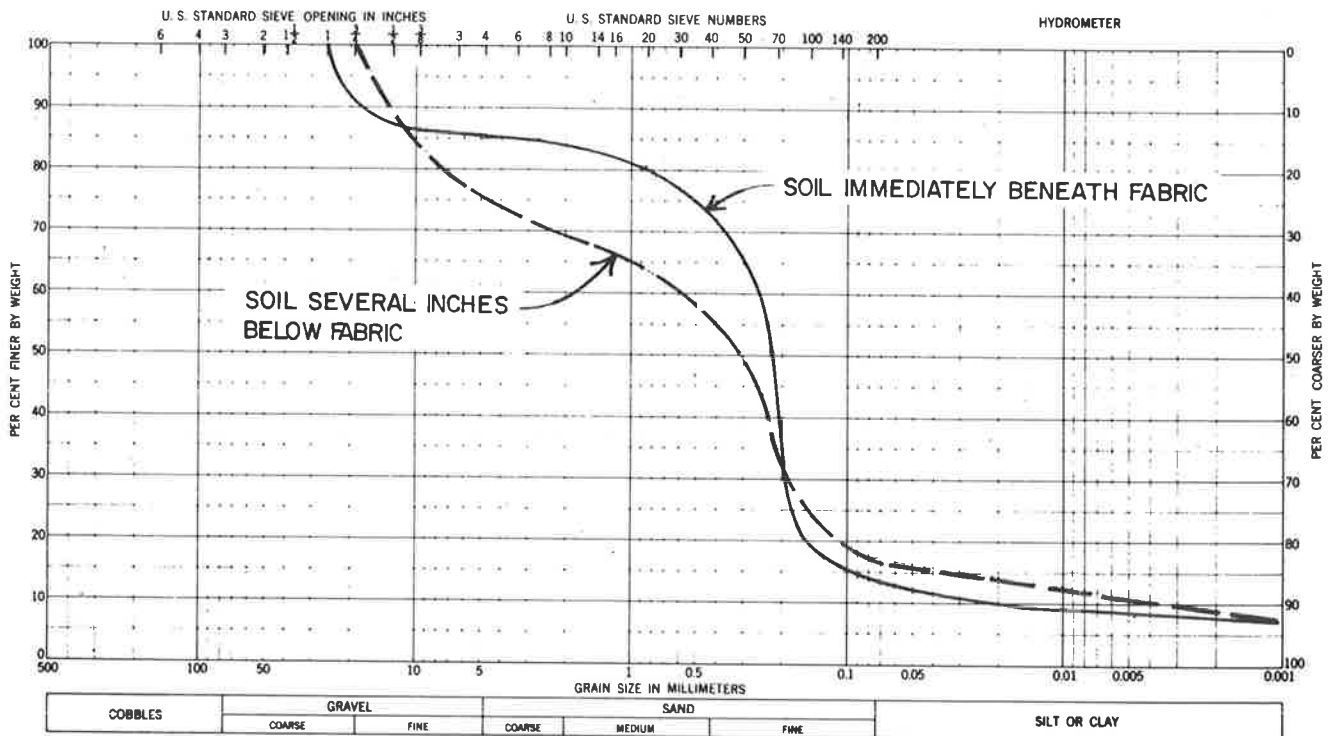
The Bahia Honda Bridge was constructed in 1969 to replace an older bridge between Bahia Honda Key and Spanish Harbor Key in Florida. The older bridge still exists; however, it is no longer used. The location of the new bridge is shown in Figure 10.

Both bridge abutments of the new bridge were constructed with a monofilament geotextile (Poly-Filter X) as a protection filter beneath sand-cement rip-rap-constructed abutment slopes, drains, and seawalls. The proposed designs for each of these sections are shown in Figure 11. The fabric in this system acts as a filter between the erosion-control armoring and the underlying soil to prevent loss of soil due to weathering or wave action through cracks or holes in the rip-rap. Sand-cement armoring construction consists of laying successive courses of burlap or jute sacks, which generally contain a mixture of one part cement to five parts sand. The sandbags are placed with broken joints. Header courses are used to tie the units together. The sacks are rammed or packed against each other so as to form a molded contact after the cement and sand mixture has set up.

The need for a filter layer beneath the armoring is important to prevent the loss of soil on which the construction rests. Erosion of soil can occur through the face of the structure or from beneath the structure due to wave action and weathering. These types of construction have little strength by themselves and rely entirely on the underlying soil for stability. They are surface treatments and are designed to be supported by the soils that they protect.

The design elevation of the top of the bulkhead that protects the toe of the bridge abutments is located approximately 5 ft above the normal water level. The 100-year water level in the area of the Bahia Honda Bridge, which occurred in 1960, was more than 4 ft higher than the bulkhead design eleva-

Figure 8. Grain-size distributions for soil immediately beneath and several inches below bridge abutment protection fabric from site 1.



tion. Such an extreme condition would place the wave action directly against the bridge abutments. Several major storms have occurred in the Florida Keys in the past 10 years, which have exposed the bridge abutments to gale and hurricane-type storm conditions, but Florida DOT reported that maintenance had not been required for any section of the project area.

Field Study

A site visit was made in October 1979. The intent was to make visual observations of the site, observe the fabric performance, and, if possible, collect samples of the fabric to perform a laboratory evaluation of its condition. A photographic and visual survey of the site indicated excellent long-term

Figure 9. Grain-size distributions for soil immediately beneath and several inches below slope protection fabric from site 2.

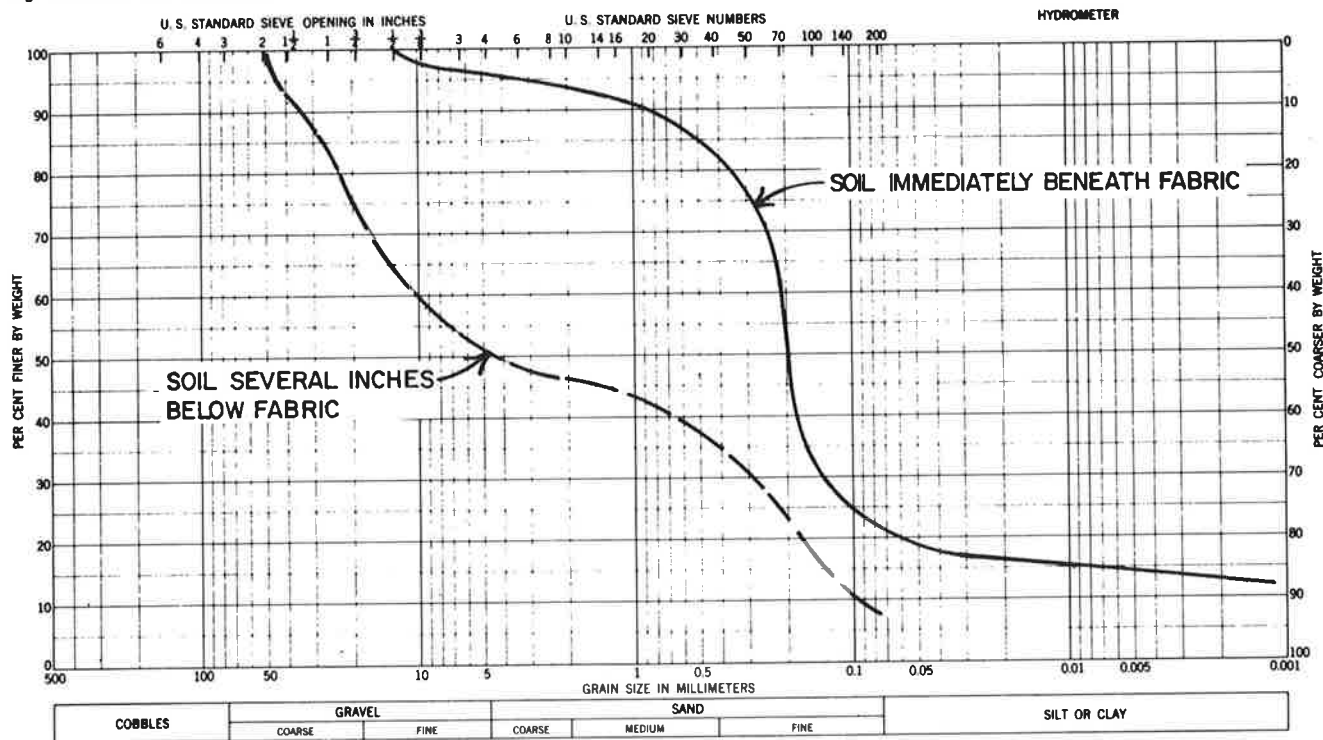


Figure 10. Location diagram of Bahia Honda Bridge.

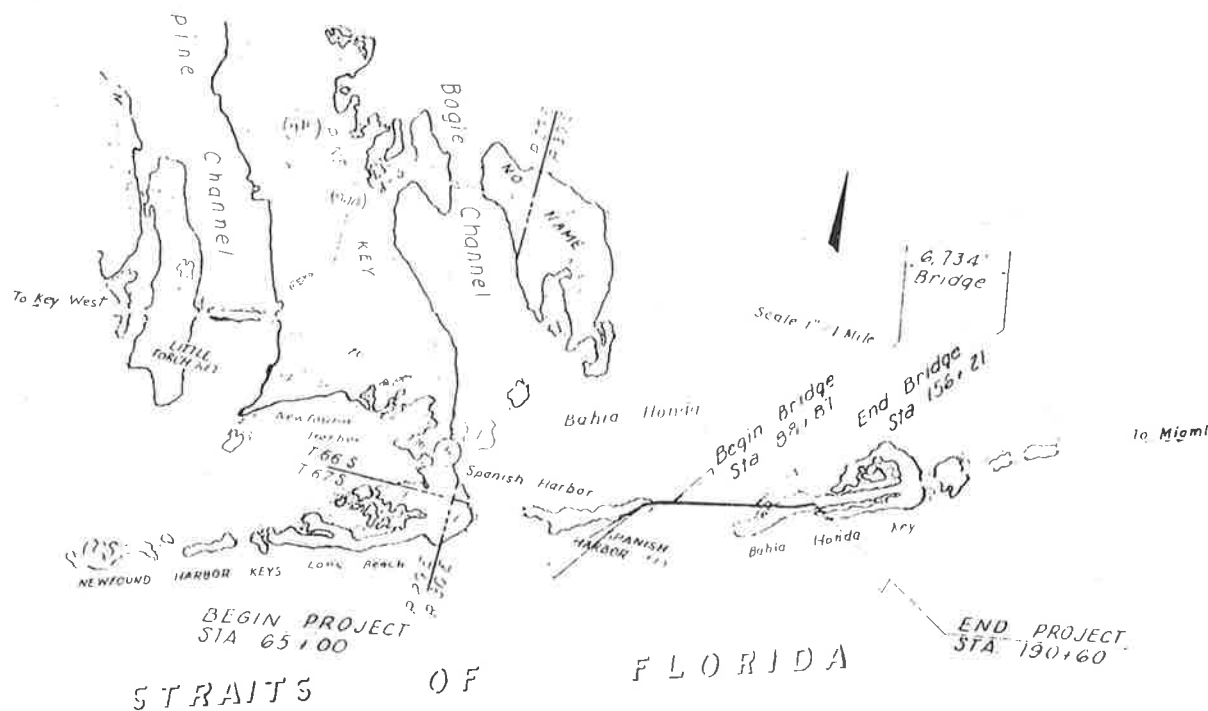


Figure 11. Proposed design of bridge abutments.

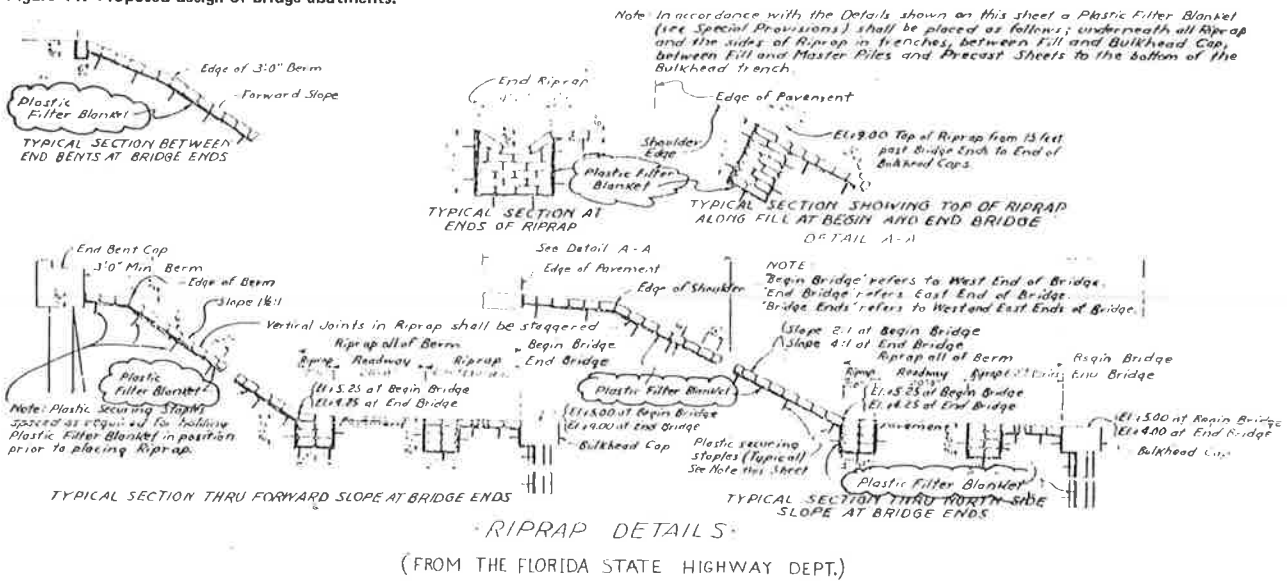


Figure 12. Armoring system: bridge abutment and drain, Bahia Honda Bridge.



Figure 13. Armoring system: bridge side slopes and top of seawall, Bahia Honda Bridge.



stability of the sand-cement constructed facilities, as shown in Figures 12 and 13. No erosion problems were apparent at any of the drains, slopes, and seawalls protected by the sand-cement armoring system, which indicated that the installation was functioning as designed. The armoring, in most cases, has held up completely. Some surface wear was noticeable; however, no washouts of the rip-rap were observed.

Fabric could be seen in several sections protruding from beneath the rip-rap at the edge of the structures. The rip-rap, and in two cases the underlying fabric, had been removed in several areas. Two sections of rip-rap, one at each end of the bridge between the two lanes of the bridge, were recently removed for construction of a future pipeline. Other areas that had been removed were possibly the result of vandalism. Exposed fabric was observed in the abutments, drains, and seawall. In all cases, the fabric appeared to be in excellent condition and could not be distinguished from new fabric.

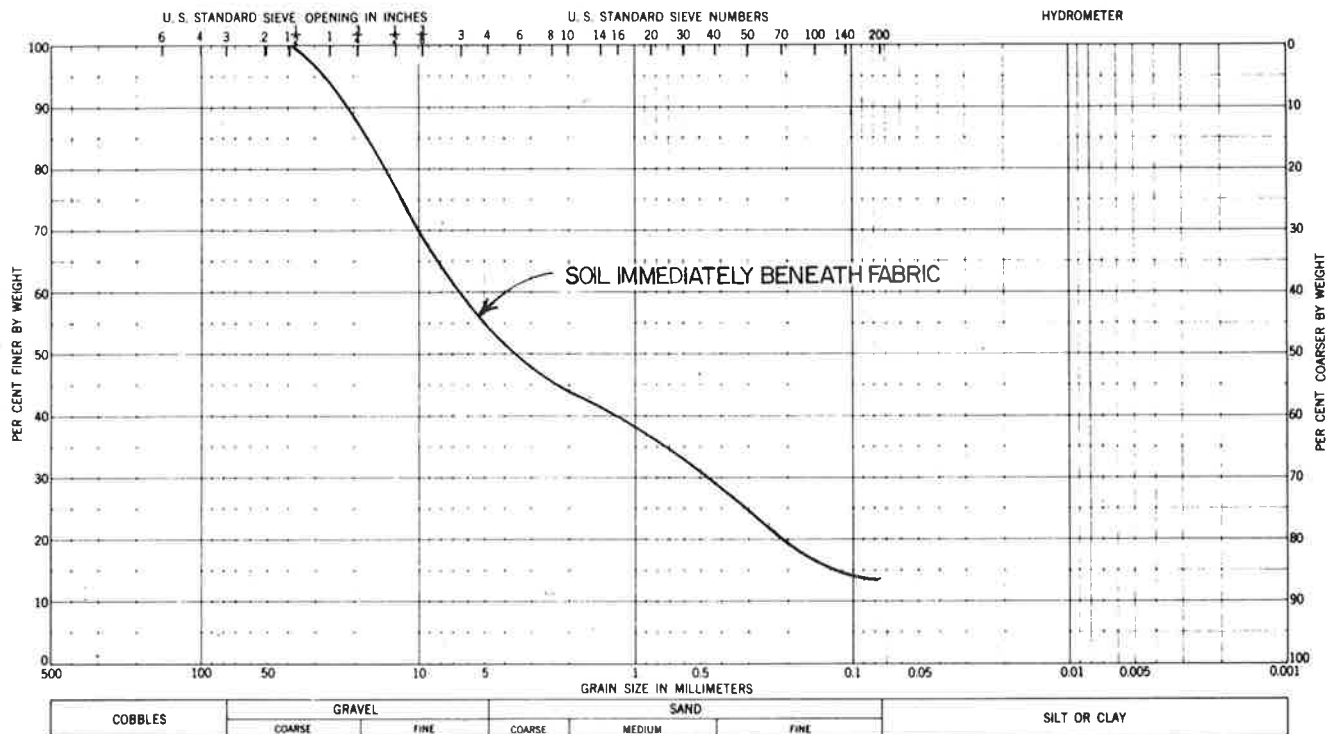
Other areas near the bridge were also examined. Visual observation of the old bridge abutment found signs of severe erosion problems. Large deformations of the steps and abutment slopes adjacent to the seawall had occurred. At the north end of the bridge, adjacent to the north end of the filter-protected rip-rap seawall, boulders had been placed to protect the slope. This area showed obvious signs of erosion; holes and washouts were present in the bank. The rip-rap seawall and the filter-protected drain adjacent to this area have been exposed to the same wave action and weathering conditions; however, they showed no signs of erosion.

The installation of a utility pipe at the time of the site visit allowed the removal of several sandbags from the bridge abutments. This enabled samples of fabric and soil beneath the fabric from the bridge abutment areas to be collected for laboratory analysis. Samples of the fabric and soil beneath the drains and seawalls could not be collected. All soil and fabric samples were returned to the STS laboratory for further examination and testing.

Laboratory Testing Program

Laboratory tests similar to those performed in the

Figure 14. Grain-size distribution of soil immediately beneath fabric in bridge abutment.



previous 79th Street Causeway study were performed on the fabric samples removed from the abutments. Tests to determine strength and permeability, and tests to evaluate particle retention of the filter fabric, were performed. Results were compared to tests on new samples of the fabric. In addition, a grain-size analysis was performed on soil samples taken directly beneath the fabric. Note that the abutment had not been exposed to wave action as had the seawall; therefore, the laboratory results may not reflect the condition of the fabric in the seawall.

Grab strength and elongation and strip tensile strength and elongation tests were performed in accordance with ASTM D-1682 in order to evaluate the strength of the fabric. Permeability of the fabric specimen was determined with the STS geotextile permeameter (Figure 5) by using a falling-head procedure. (The test procedure and equipment were described in the 79th Street Causeway study.) The particle retention of the fabric was evaluated by the Corps of Engineers procedure for the open area of a geotextile. One of the test specimens was flushed with water continuously for several hours under a head of 3 ft to crudely simulate wave action. The percent open area was then repeated to assess how many of the openings were permanently closed.

A grain-size analysis was performed on the soil sample taken from below the fabric in order to evaluate the particle-retention capability of the fabric. This test was performed in accordance with ASTM D-422 (Particle-Size Analysis of Soils) and used both sieve and hydrometer methodologies.

Test Results

The strength evaluation tests indicated that the fabric had a grab strength of 167 kg in the stronger principal direction and 111 kg in the weaker principal direction. This strength is equivalent to the strength of the new fabric, which had a strength of

170 kg in the stronger principal direction and 100 kg in the weaker principal direction. The material had a strip tensile breaking load of 115 kg in the stronger principal direction. Elongation of the material at failure was approximately 43 percent for both stronger and weaker principal directions in the grab tests and approximately 49 percent for the strip tensile tests. The elongation of the material at failure was approximately 10 percent greater than elongation of new fabric.

Permeability and particle-retention evaluations were performed for the filtration studies. The permeability and corresponding particle retention for particular fabric specimens are shown in Figure 7. The fabric between the sandbags had an average permeability of 1.2×10^{-2} cm/sec, and the fabric located directly beneath the sandbags had a permeability of 5.7×10^{-3} cm/sec. This corresponds with the particle-retention analysis, which indicates that the particle retention of the fabric was different, depending on the location of the test specimen.

The fabric between the sandbags had less than 10 percent of the openings closed by particles (an open area of 5 percent). Conversely, fabric beneath the sandbags had up to 50 percent of the space closed by particles (open area of 3 percent). It appears that the large amount of clogging found beneath the sandbags resulted from construction of the armor system. The particles contained in the pore spaces consisted of sand and cement, which indicated that, at the time of construction, cement washed into and closed some of the pore spaces. The reduction in permeability and corresponding particle retention appears to be related to Darcy's relation among permeability, porosity, and seepage, as previously shown in Figure 7. The graph indicates that the decrease in permeability due to particle retention generally follows Darcy's law.

The grain-size curve for the material retained by the fabric is shown in Figure 14. The fabric was generally found to retain medium- to fine-sand-sized particles, with up to 15 percent silt. The Poly-

Filter X used in the installation had an opening size equivalent to a No. 70 mesh sieve. The data in the figure reveal that 20 percent of the soil particles directly behind the fabric were smaller than the fabric openings. When used in drainage applications the fabric has been able to retain particles in which the equivalent opening size of the fabric is less than or equal to the D85 (mean particle diameter of 85 percent of the material) size of the protected soil. However, for wave action problems, model studies should be performed to analyze cyclic gradients.

Summary

No maintenance was required for the structure in any area where geotextiles were used. The lack of maintenance, combined with the visual observation and laboratory test results, indicates that filtration characteristics of the fabric were functioning according to design requirements. The properties of the geotextiles collected from the installation in the abutment area indicated that the material has the strength characteristics of new fabric. Also, the filtration characteristics have not been significantly altered except directly below the sandbags where drainage was not required.

CONCLUSIONS

Both projects indicated the excellent long-term stability of properly designed geotextiles when used in the roadway and bridge abutment erosion-control designs reviewed. Case histories indicated that the filtration characteristics of the fabric and the armoring systems were functioning according to the design requirements and, as such, no maintenance had been required for either structure. A review of the design criteria established by Calhoun (2) for using monofilament woven geotextiles for filtering sand, in conjunction with the soils data presented for both projects, indicated that the geotextile in both projects satisfied the requirements for fabric suitability. Geotextiles that were not exposed to sunlight retained a significant amount of strength after a 10-year period. In most cases, less than a 20 percent decrease from the strength of the new fabric was found, and in some cases only a 5 percent decrease or less was noted. There are indications that the strength of the fabric may be affected by cyclic wetting and drying or repeated loading from

wave and tidal variations. In the specific installations, abrasion was not a problem.

The incorrect placement of the fabric in a section of the 79th Street Causeway reflects the need for construction review by the design engineer, especially because many contractors are still inexperienced in placing these materials. The effects of construction procedures can have a pronounced effect on the long-term performance of a geotextile.

As a closing comment, it was noted during the site visits that the causeways extending through the Florida Keys were being rehabilitated by using rip-rap over fabric armoring systems. The Florida DOT should be commended for their extended use of these design concepts over the past 10 years. It is hoped that the case histories included in this paper, combined with other studies, will provide a useful information base for modifying and improving design criteria and predicted capabilities of geotextiles.

ACKNOWLEDGMENT

Many thanks to the Florida DOT for their assistance in providing design and performance information for these projects, and to Carthage Mills Erosion Control Company for their sponsorship, which made this study possible.

The field study of the 79th Street Causeway was performed by Ed Bennett of Carthage Mills and myself, and I made the field study of the Bahia Honda Bridge.

REFERENCES

1. Natural Building Stones; Soil and Rock; Peats, Mosses, and Humus. In Annual Book of ASTM Standards, ASTM, Philadelphia, Part 19, 1978.
2. C.C. Calhoun, Jr. Development of Design Criteria and Acceptance Specifications for Plastic Filter Cloths. U.S. Army Corps of Engineers Waterways Experiment Station, Vicksburg, MS, Tech. Rept. S-72-7, 1972.
3. H. Cedergren. Seepage Drainage and Flow Nets. Wiley, New York, 1967.

Notice: The Transportation Research Board does not endorse products or manufacturers. Trade and manufacturers' names appear in this paper because they are considered essential to its object.

Publication of this paper sponsored by Task Force on Engineering Fabrics.

Long-Term In Situ Properties of Geotextiles

GARY L. HOFFMAN AND ROBERT TURGEON

Although substantial research of geotextiles (e.g., physical properties, testing procedures, specification requirements) has been accomplished, the majority of this work dealt with original fabric properties (i.e., before installation). The Pennsylvania Department of Transportation (PennDOT) foresaw the potential usefulness of fabrics and undertook one of the earliest field evaluations aimed specifically at monitoring the characteristics of the in-place fabrics over a period of years. Initial fabric properties were well documented before installation in a longitudinal pavement edge drain system. Fabrics were exhumed and tested for permeability and strength properties at 1-, 2-, and 6-year intervals after placement. Results indicated that, even though some reductions in fabric permeabilities and strengths were evident, all fabrics were still substantial enough to perform the intended drainage and filtration functions better than the standard control section without fabric. Permeabilities of each of the six fabric types were still at least 10^{-2} cm/sec after 6 years. The minimum average tensile strength in the weakest direction was still 82 lb after 6 years of service. This work partly influenced PennDOT's recent inclusion of geotextiles in their general specifications and standard drawings for subsurface drainage.

The use of geotextiles (engineering fabrics) as a standard item in the construction of transportation facilities is increasing in Pennsylvania and in many other states. Some agencies have realized significant initial cost and performance benefits by using geotextiles. Although substantial research on the physical properties, testing procedures, and specification requirements has been done by manufacturers, public agencies, and academicians, the bulk of this

work dealt with the original properties of the geotextiles (i.e., before installation). Insufficient data are available on the characteristics and performance of various types of fabrics after they have functioned in a facility or system for a number of years. This lack of performance data is understandable because fabrics have only gained acceptance and use in engineering applications over the past decade. The long-term in situ characteristics of geotextiles are of primary interest to the user because the fabrics must perform adequately throughout the design life of the system in which they are being used.

The Pennsylvania Department of Transportation (PennDOT) foresaw the potential usefulness of fabrics and undertook one of the earliest field evaluations aimed specifically at monitoring the characteristics of in-place fabrics over a number of years. Initial fabric properties were well documented (1) before they were installed in a longitudinal pavement drain system. Fabrics were exhumed and tested for permeability and strength properties at 1-, 2-, and 6-year intervals after placement. Results of this testing and the performance of the installation are reported in this paper.

PROJECT INSTALLATION

The project site is located in the northwestern section of Pennsylvania on Traffic Route 321 in the village of Wilcox in Elk County [Figure 1 (1)]. The site was a two-lane reinforced-concrete pavement with flexible shoulders that was completed in fall 1974. The typical pavement cross section is shown in Figure 2. The project was showing shoulder and joint distress in less than 2 years because no pavement drainage was included in the construction. The shoulders were soft and wet, and obvious differential frost-heave-induced cracking had occurred in the flexible shoulder. The reinforced-concrete (RCC) pavement also showed distress; there was pumping along the centerline, shoulder, and transverse joints; and there was occasional transverse cracking. An investigation revealed that the problem was caused by infiltrated surface water and not groundwater. When the decision was made to retrofit longitudinal pavement base drains to correct the water problem, 12 experimental drainage sections that incorporated various types of fabric were included.

The 12 experimental sites were constructed in September 1976 by Department maintenance personnel

Figure 1. Location map.

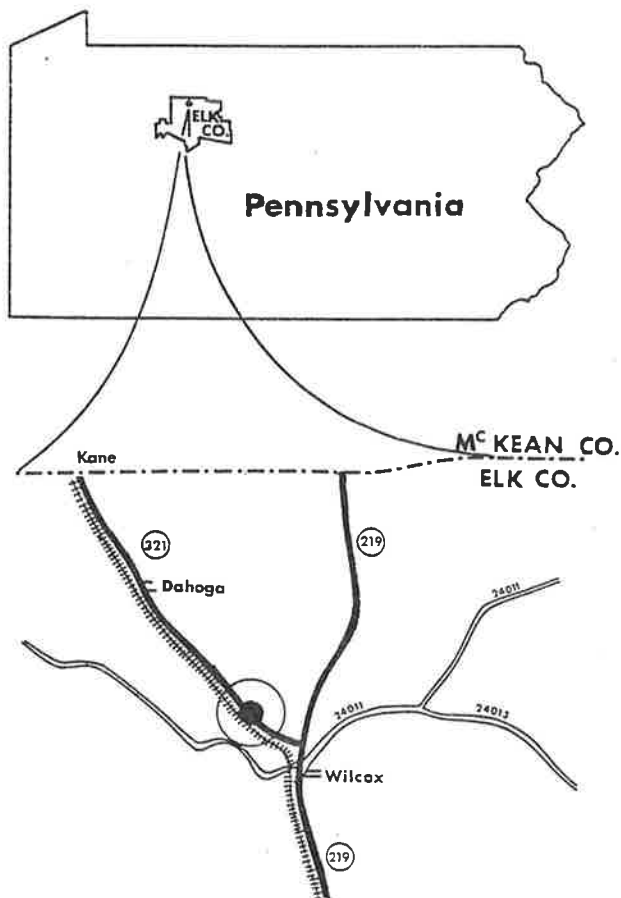


Figure 2. Typical pavement cross section.

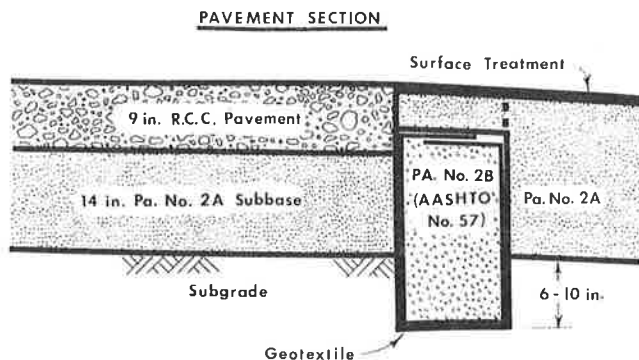


Figure 3. Typical drain cross section and plan section.

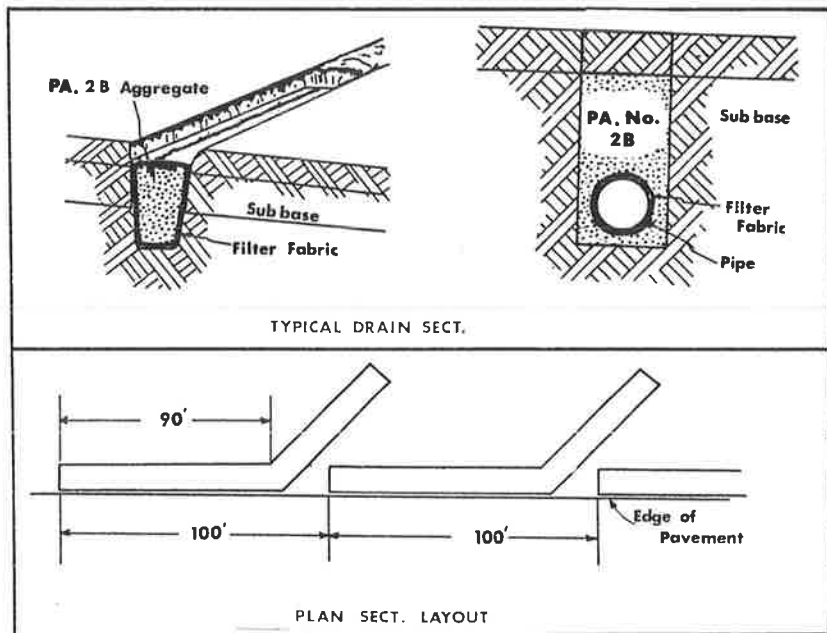


Table 1. Construction details of 12 sites.

Site	Trench Width (in.)	Construction Details
1	24	6-in. porous concrete pipe; 2B aggregate backfill
2	24	Trench lined with Typar 3401; 2B aggregate backfill
3	24	Trench lined with Mirafi 140; 2B aggregate backfill
4	24	Trench lined with Phillips Duon; 2B aggregate backfill
5	24	Trench lined with Bidim C-22; 2B aggregate backfill
6	15	Trench lined with Poly-Filter X; 2B aggregate backfill
7	15	4-in. fiber pipe wrapped with Duon; 2B aggregate backfill
8	15	6-in. corrugated metal pipe (cmp) wrapped with Typar-3401; 2B aggregate backfill
9	15	6-in. cmp wrapped with Bidim C-22; 2B aggregate backfill
10	15	6-in. porous concrete pipe wrapped with Mirafi 140; 2B aggregate backfill
11	15	4-in. fiber pipe; 2B aggregate backfill
12	15	Trench lined with International Paper Company (IPC) 502; 2B aggregate backfill

Table 2. General descriptions of fabrics used in project.

Fabric Type	Sites	General Description
Typar 3401 (cloth type)	2 and 8	Gray, nonwoven, heat-bonded polypropylene monofilament; 4.0 oz/yd ² weight; 15-mil thickness
Mirafi 140 (cloth type)	3 and 10	White, nonwoven polypropylene and nylon random-oriented monofilament; 4.1 oz/yd ² weight; 30-mil thickness
Supac (felt type)	4 and 7	Gray, nonwoven entangled olefin monofilament; 4.0 oz/yd ² weight; 60-mil thickness
Bidim C-22 (felt type)	5 and 9	Gray, nonwoven, mechanically entangled continuous filament polyester; 4.5 oz/yd ² weight; 75-mil thickness
Poly-Filter X (woven)	6	Black, woven polypropylene monofilament; 7.2 oz/yd ² weight; 16-mil thickness
IPC 503 (cloth type)	12	White, nonwoven, bonded polypropylene monofilament; 3.4 oz/yd ² weight; 27-mil thickness

from Elk County. Typical cross-section and plan-section details of the experimental drainage sites are shown in Figure 3 (1). These sites were all located in a tangent section in 3 to 6 ft of fill. The trenches were excavated with a backhoe immedi-

Figure 4. Physical properties of subgrade soil and pH's of water samples.

SUBGRADE SOIL		
Sieve Size	% Passing	
2 1/2 in.	100	
1 in.	90	Class. A-4 (3)
3/8 in.	84	gravelly clay loam
No. 4	79	
No. 20	66	LL-30; P.I.-10
No. 60	60	
No. 200	51	pH-5.3
0.02 mm	38	resistivity - 4460 ohm-cm
0.002 mm	20	

WATER SAMPLES												
Site	1	2	3	4	5	6	7	8	9	10	11	12
pH	9.3	7.8	7.8	7.2	7.5	7.9	7.7	7.1	7.0	8.5	9.3	7.9

ately adjacent to the edge of the RCC pavement to a depth that varied from 6 to 10 in. below the bottom of the subbase. Each of the 12 sites was about 100 ft long and terminated with an outlet pipe through the embankment slope. Site 1 was the Department's standard section at that time and was the control section. Sites 2-6 and 12 had fabric wrapped around the stone backfill in the trench, and no pipe was included. Sites 7-11 had the same fabric types that were used in sites 2-6, but the fabric was wrapped directly around a perforated pipe and then the sites were backfilled with PA No. 2B (AASHTO No. 57) crushed stone. The construction details of the 12 sites are given in Table 1 (1).

Six different fabrics were included in the experiment. A general description of each of these six fabrics is given in Table 2 (1,2). Five nonwoven fabrics were used; three were heat-bonded cloth type and two were needle-punched felt type. One woven fabric was also used. As each type of fabric was installed, random samples were obtained for laboratory testing.

Both the subbase and subgrade were unsatisfactory draining materials. The PA No. 2A dense-graded subbase material was a crushed gravel with AASHTO A-1-b(0) classification and typically had a permeability of 10⁻⁴ cm/sec. The subgrade material was

Table 3. Typical drain cross section and plan section.

Fabric Type	Site	After 6 Years in Service							
		As Supplied		t_{soiled}^a		t_{orig}^b		Change from Original ^c (%)	
		Permeability (cm/sec x 10 ⁻²)	Permittivity (sec ⁻¹)	Permeability (cm/sec x 10 ⁻²)	Permittivity (sec ⁻¹)	Permeability (cm/sec x 10 ⁻²)	Permittivity (sec ⁻¹)	Permeability	Permittivity
Tyvar 3401	2	4.6	1.13	1.4	0.16	0.7	0.16	-70	-86
Mirafi 140	3	4.1	0.65	2.5	0.27	1.7	0.27	-39	-58
Supac	4	7.8	0.48	6.4	0.44	7.9	0.44	-18	+2
Bidim C-22	5	5.0	0.24	51.6	2.22	46.3	2.22	+930	+825
Poly-Filter X	6	1.5	0.37	2.0	0.27	1.1	2.27	+33	-27
IPC 503	12	1.8	0.30	2.7	0.30	1.8	0.30	+50	0

Note: All results are from a minimum of five measurements.

^a Calculated by using respective thicknesses of soiled fabric from Table 4.

^b Calculated by using respective thicknesses of original, clean fabric from Table 4.

^c Percentage change is the difference between the as supplied and 6-year figures divided by the as supplied figures.

classified as an AASHTO A-4(3) with a permeability of 10⁻⁵ cm/sec. The physical properties of this subgrade soil along with the pH's of water samples taken from the outlet pipe of each of the 12 sites are shown in Figure 4.

OBSERVATIONS AND PERFORMANCE

Portions of the 12 sites were exhumed and visually inspected in September 1977, 1978, and 1982--1, 2, and 6 years after installation. Samples of the fabrics from sites 2-6 and 12 were also obtained at these times and retested in the laboratory.

Care was taken not to alter the in situ condition of the fabric before testing. The samples were removed with the built-up layer of soil intact and immediately placed in plastic bags. They were then placed in a sealed container to maintain the in-place moisture condition.

All drainage sites were still functioning after 6 years, as evidenced by positive outflow and the reduction of the aforementioned water-related distress along the shoulder and the outside edge of the pavements. Pumping still existed along the centerline joint because the dense-graded subbase was draining too slow to transmit the water laterally from beneath the pavement in a reasonably short time.

All of the exhumed fabrics, except the Bidim C-22, appeared intact and did not have tears or holes. Pea-sized holes were noted in some of the lapped portions (top of trench) of the Bidim C-22 fabric. The visual appearance of the Bidim C-22 indicated manufacturing inconsistencies of spinnerette and spin-beam placement, which resulted in thin areas. It was concluded that these holes were the result of puncture in these thin areas by the PA No. 2A aggregate that was on top of the fabric. In areas where traffic had eroded the surface of the shoulder along the pavement edge as little as 2 in. of the aggregate existed on top of the fabric. The puncture failure mechanism was also substantiated by studying the filament breaks under 50X magnification.

At control site 1 the unprotected crushed-gravel backfill was becoming progressively more contaminated with fines throughout its entire depth. Although this trench backfill still appeared more permeable than the adjacent subbase and subgrade, it can be projected that at some point the unprotected backfill will approach the slow permeability of these adjacent materials.

In sites 2-6, where the trench backfill was wrapped with fabric and no pipes were installed, minimal contamination of the backfill with fines existed. A discoloration of the aggregate surfaces in the lower 4 to 5 in. of the trench was noted, but substantial filling of the voids with fines was not present. A

layer of colloidal-sized sediments about 0.1 in. thick existed on the inside of the fabric on the bottom of the trench. A buildup of migrated soil was present on all of the outside surfaces of the fabrics, which indicated filtering effectiveness. It was evident from the visual inspection that more fines had been allowed to pass through the woven Poly-Filter X fabric and into the backfill material than through the nonwovens. Also, the retained layer of migrated soil on the outside of the Poly-Filter X was not as pronounced as with the nonwovens.

In sites 7-11, where the pipes were wrapped with the fabric, the backfill contamination appeared similar to control site 1. Again the migrated soil buildup was evident on the outside of the fabric. Some colloidal-sized sediments were present in the bottom of the pipe, but these had little effect on the pipe hydraulics.

FABRIC PROPERTIES

Permeability

Permeabilities were determined before installation of the fabrics with the prototype permeameter from the Celonese Fibers Marketing Company (test method FFET-2). All permeabilities were calculated by using Darcy's equation for laminar flow conditions. All six fabrics had an initial permeability on the order of 10² cm/sec (see Table 3). The AASHTO T-215 constant-head permeability test equipment was used to test the permeability of the 1-, 2-, and 6-year-old fabric samples because the Celanese equipment was not available.

During the initial testing phases of the 6-year-old fabric with the T-215 equipment it became evident that the inflow and outflow capabilities of this equipment were insufficient to measure the relatively high permeabilities of the fabric, even when working with relatively low heads. Thus previously developed permeabilities on the 1- and 2-year-old fabrics were discounted as being incorrect and were not presented. The AASHTO T-215 equipment was then modified by removing the top and bottom of the 4-in.-diameter mold, and PA No. 2B crushed stone was placed below and in contact with the fabric (Figure 5). The fabric was clamped between the mold and its collar in such a way that leaks did not occur. The test was then performed with a 4-in. constant head. The flow capabilities of the various components of the equipment were checked to assure that the permeability of the fabric was actually being measured. The resulting permeabilities on the soiled 6-year-old fabric are also presented in Table 3.

The permeabilities for all of the 6-year-old fabrics were still on the order of 10⁻² cm/sec and

were high enough to function satisfactorily in most soil conditions that might be encountered in Pennsylvania. The Department's specifications on geotextiles require fabric permeability to be one order of magnitude greater than that of the soil to be drained. A comparison of the permeabilities for the 6-year-old fabrics to the respective original permeabilities can be made on a relative basis with the consideration that two different types of testing equipment were used. The cloth-type fabrics (Tytar 3401 and Mirafi 140) apparently had the greatest reduction in permeability. The reason for the order-of-magnitude increase in the permeability of the Bidim C-22 fabric might be related to the previously discussed holes, although care was taken to select intact samples for permeability testing.

The fabric permittivities (i.e., the coefficients of permeability divided by the thicknesses) are also presented for comparison purposes. Thicknesses of the soiled fabric (Table 4) were, for the most part, greater than the original, clean fabric thicknesses. The soiled fabric thicknesses (t_{soiled}) were used to compute 6-year permeabilities because the head losses occurred over these total, actual thicknesses during testing.

Strength

A constant-rate-of-extension (CRE) tensile testing machine was used to perform grab tensile testing. Some modifications to the current ASTM D-1682 procedure were made when testing the 6-year-old samples

Figure 5. Permeability test apparatus.

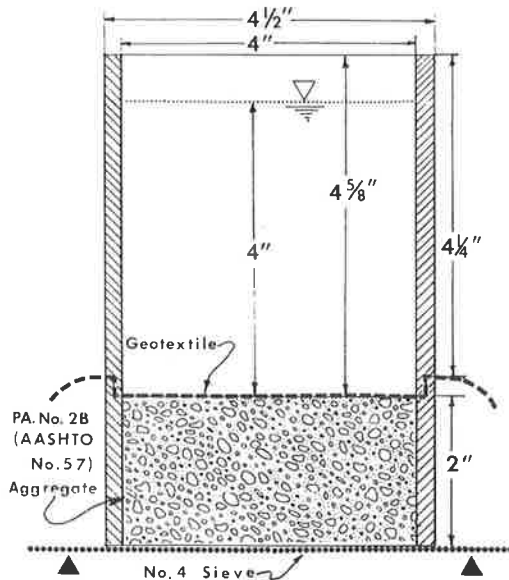


Table 4. Thicknesses of fabrics.

Fabric Type	Site	Avg Fabric Thickness ^a (in.)				Change from Original (%)
		As Supplied	1 Year in Service	2 Years in Service	6 Years in Service ^b	
Tytar 3401	2	0.016	0.015	0.014	0.034	+113
Mirafi 140	3	0.025	0.025	0.023	0.037	+48
Supac	4	0.071	0.043	0.038	0.056	-21
Bidim C-22	5	0.082	0.043	0.064	0.091	+11
Poly-Filter X	6	0.016	0.017	0.017	0.030	+88
IPC 503	12	0.024	0.029	0.030	0.036	+50

^a From a minimum of 10 measurements.

^b The soiled 6 year samples were hand brushed lightly to remove loose soil before measurements were made.

in order to exactly duplicate the procedures used to test the initial and the 1- and 2-year-old samples. The modifications along with the specified items are shown in Figure 6. Essentially, the differences were

1. A CRE of 12 in./min was used for all fabrics instead of an adjusted rate that would cause failure in 20 ± 3 sec,
2. A 5x8-in. fabric sample was used instead of a 4x8-in. sample, and
3. Grips 2.125 in. perpendicular to the direction of pull and 1.75 in. parallel to the direction of pull were used instead of the specified 1x2- or 1x1-in. grips.

The average strengths for the initial and the 1-, 2-, and 6-year-old fabrics are given in Table 5. Elongations for these same tests are given in Table 6. All fabrics experienced some decrease in maximum strength; the Mirafi 140 exhibited the greatest decrease (40 to 45 percent). A sample of the Poly-Filter X that had been exposed to direct sunlight also decreased in strength by about 45 percent, whereas the buried Poly-Filter X only decreased in strength from 20 to 33 percent.

The average elongations at failure decreased for all fabrics except the IPC 503. This indicates that most of the fabrics either became less plastic with age because of environmental conditions or had flaws induced from installation that caused them to break at lower strains.

All of these strengths and elongations still met the Department's minimum specification criteria for new fabrics of 90 lb and 20 percent. However, these specifications referred to the ASTM D-1682 procedure.

Figure 6. Modifications to grab tensile test as compared with specified procedure.

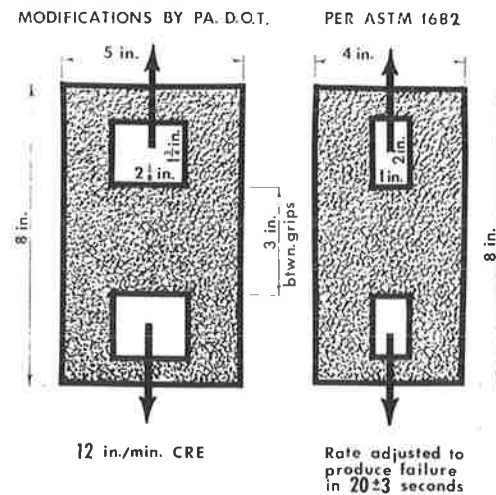


Table 5. Average strength of fabrics.

		Avg Strength (lb) of Fabrics Used on Projects ^a									
		As Supplied		1 Year in Service		2 Years in Service		6 Years in Service		Change from Original (%)	
Fabric Type	Site	MD	CD	MD	CD	MD	CD	MD	CD	MD	CD
Typar 3401	2	193	192	208	129	164	173	150	161	-22	-16
Mirafi 140	3	205	188	208	129	163	165	112	111	-45	-41
Supac	4	266	131	216	130	162	138	217	124	-18	-5
Bidim C-22	5	185	177	235	115	154	99	185	131	0	-26
Poly-Filter X	6	752	468	632	377	360	348	598	313	-20	-33
Poly-Filter X ^b	6	752	468	- ^c	- ^c	- ^c	- ^c	411	269	-45	-43
IPC 503	12	93	112	138	174	- ^c	- ^c	91	117	-2	+4

Note: MD = machine direction and CD = cross direction.

^aAll values are the average of a minimum of three tests in each direction.

^bFabric was not properly covered and therefore was exposed to the environment for the entire test period.

^cNo test.

Table 6. Average elongation of fabrics.

		Avg Elongation (%) of Fabric Used on Project ^a									
		As Supplied		1 Year in Service		2 Years in Service		6 Years in Service		Change from Original (%)	
Fabric Type	Site	MD	CD	MD	CD	MD	CD	MD	CD	MD	CD
Typar 3401	2	63	60	68	60	50	60	61	61	-3	+2
Mirafi 140	3	125	129	104	76	93	105	85	106	-32	-18
Supac	4	79	102	83	81	67	85	73	95	-8	-14
Bidim C-22	5	78	75	62	101	65	64	67	74	-14	-1
Poly-Filter X	6	37	35	36	34	28	27	38	28	+3	-23
Poly-Filter X ^b	6	37	35	- ^c	- ^c	- ^c	- ^c	30	20	-19	-43
IPC 503	12	29	23	30	28	- ^c	- ^c	42	26	+45	+13

Note: MD = machine direction and CD = cross direction.

^aAll values are the average of a minimum of three tests in each direction.

^bFabric was not properly covered and therefore was exposed to the environment for the entire period.

^cNo test.

Table 7. Comparison of strength and elongation results for PennDOT modified grab tensile test with results for ASTM D-1682 procedure.

		Avg Strength (lb) on 6-Year-Old Fabric ^a				Avg Elongation (%) on 6-Year-Old Fabric ^a			
		PennDOT Modifications		ASTM D-1682 Procedure		PennDOT Modifications		ASTM D-1682 Procedure	
Fabric Type	Site	MD	CD	MD	CD	MD	CD	MD	CD
Typar 3401	2	150	161	145	110	61	61	80	80
Mirafi 140	3	112	111	123	108	85	106	118	116
Supac	4	217	124	121	85	73	95	47	84
Bidim C-22	5	185	131	123	101	67	74	82	79
Poly-Filter X	6	598	313	343	242	38	28	24	26
IPC 503	12	91	117	82	88	42	26	54	37

Note: MD = machine direction and CD = cross direction.

^aAll values are the average of a minimum of three tests in each direction.

Because data in Tables 5 and 6 were developed with the modified procedures, a new set of test data was developed in strict compliance with the methods of ASTM D-1682. These latter results on the 6-year-old fabrics are presented in Table 7 along with the respective results obtained with the modified procedures.

A review of the data in Table 7 indicates that the slower elongation rates and narrower test specimens and grips used in the ASTM D-1682 procedure had a noticeable effect on the results. In fact, all but one of the strength values were lower; the majority of the elongations at failure were greater. According to the ASTM D-1682 data, Supac and IPC 503 minimum strengths were below the specified minimum requirement of 90 lb for the new fabric. These two fabrics would still meet the minimum average roll value (weakest direction) for drainage specifications of 80 lb, which was proposed by the Geotextile Com-

mittee of the International Nonwovens and Disposables Association (INDA) as part of their revisions to the FHWA "Fabric Workshop Manual."

Even though strength losses have occurred, sufficient strength to satisfactorily perform the intended function after installation still exists. Specification requirements for this drainage application may require adjustments as manufacturers develop more uniformity in determining and presenting fabric properties, and as more information becomes available on the effects that installation stresses and long-term contact with the environment have on these properties.

CONCLUSIONS

1. All sites with various fabrics were still performing satisfactorily after 6 years.
2. The standard (control) trench section without

fabric was still draining the adjacent soil; however, progressive contamination of the aggregate backfill with migrating fines was evident.

3. All of the exhumed fabrics were intact and without blemish, except for the Bidim C-22. The Bidim C-22 apparently had manufacturing irregularities and was punctured through the lapped portion on top of the trench in areas where insufficient cover material thicknesses existed.

4. Laboratory permeability tests on the 6-year-old soiled fabric indicated that, although some decreases had occurred, all fabrics had permeabilities of 10^2 cm/sec or greater. These permeabilities met PennDOT criteria that the fabrics be 10 times more permeable than the adjacent soils being drained.

5. All of the fabrics experienced strength reductions, which varied from a few percent to about 45 percent. However, all of the fabrics still met the Department's minimum strength requirement of 90 lb for new fabric, except Supac and IPC 503. The Supac and IPC 503 would still meet the minimum average roll value of 80 lb proposed by INDA. All of the fabrics exhibited sufficient strength and satisfactorily performed the intended drainage function in the field.

6. Engineering fabrics can be expected to effectively function as a filter and separator in a drainage trench application for years. These fabrics should be included as a standard part of the drainage system design where open-graded aggregate backfill requires protection from adjacent, low-plasticity fine soils that are prone to migrate.

7. The recent inclusion of geotextiles in the PennDOT standard drawings for subsurface drains (RC-30) was influenced, in part, by this work. The trench backfill, instead of only the pipe, is wrapped with fabric to protect the high-quality aggregate from contamination.

ACKNOWLEDGMENT

We wish to acknowledge the Office of Research and Special Studies and the Materials and Testing Division of PennDOT and Region 3 of FHWA, whose approval and financial sponsorship made this work possible.

Allen D. Forshey is acknowledged for the significant work he did in coordinating the installation and the evaluations at 1 and 2 years after installation. Henry Lahr, Dennis Leahy, and Lori Stewart are thanked for their field assistance in retrieving fabric samples from the field. Thanks are also expressed to Dean Riland, Soil and Foundations Laboratory supervisor, and to Thomas Green, Physical Testing Laboratory supervisor, for their respective efforts in permeability and strength testing. Karen Ford is acknowledged for her skill and patience in typing this manuscript.

REFERENCES

1. A.D. Forshey. Use of Filter Fabrics for Subgrade Drainage Systems for Highways. Pennsylvania Department of Transportation, Harrisburg, Res. Rept. 76-16, May 1979.
2. T.A. Haliburton. Testing of Geotechnical Fabric for Use as Reinforcement. Geotechnical Testing Journal, GTJODJ, Vol. 1, Dec. 1978, pp. 203-212.

Notice: The Transportation Research Board does not endorse products or manufacturers. Trade and manufacturers' names appear in this paper because they are considered essential to its object.

Publication of this paper sponsored by Task Force on Engineering Fabrics.